The Role of a Cyclin D2 Splice Variant in the Regulation of the Cell Cycle: Connecting Cell Cycle to Cancer Biology

by

Karim Fathi Wafa

Submitted in partial fulfillment of the requirements
for the degree of Doctor of Philosophy

at

Dalhousie University
Halifax, Nova Scotia
April 2012

DALHOUSIE UNIVERSITY

DEPARTMENT OF PHARMACOLOGY

The undersigned hereby certify that they have read and recommend to the Faculty of Graduate Studies for acceptance a thesis entitled "The Role of a Cyclin D2 Splice Variant in the Regulation of the Cell Cycle: Connecting Cell Cycle to Cancer Biology" by Karim Fathi Wafa in partial fulfillment of the requirements for the degree of Doctor of Philosophy.

Dated: April 17th, 2012

External Examiner: _____

Research Supervisor: _____

Examining Committee: _____

_____

Departmental Representative: _____

DALHOUSIE UNIVERSITY

DATE: April 17th, 2012

AUTHOR: Karim Fathi Wafa

TITLE: The Role of a Cyclin D2 Splice Variant in the Regulation of the Cell Cycle: Connecting Cell Cycle to Cancer Biology

DEPARTMENT OR SCHOOL: Department of Pharmacology

DEGREE: PhD CONVOCATION: October YEAR: 2012

_____

Signature of Author

This thesis is dedicated to my family, especially…

My parents, my sisters Dina, Reem & Nadine, my beloved, my grandmother, and in loving memory of my grandfather;

Thank you for your love, endless support, patience and encouragement. Your guidance, self-sacrifice and strength are a testament to my success. This triumph is as much yours as it is mine.

Table of Contents

List of Tables

List of Figures

Abstract

CycD2SV is a splice variant of cyclin D2 (cycD2) which has been implicated in cell cycle exit in embryonic cardiomyocytes. To further characterize the role of this splice variant, we overexpressed cycD2SV in a multitude of immortalized and transformed cell lines. We also monitored the expression profile of cycD2SV during cell confluence and serum deprivation, two states of growth arrest. Overexpression of cycD2SV resulted in a marked decrease in cell proliferation as determined by [^{3}H]-thymidine S-phase labeling. TUNEL staining analysis indicated that cycD2SV overexpression does not induce apoptotic cell death. However, compared to control cells, cycD2SV expressing cells were more sensitive to cell death induced by external stressors, such as trypsinization. Deletion experiments identified the 54-136 amino acid sequence of cycD2SV as the cell cycle inhibitory domain while immunoprecipitation and immunofluorescence co-localization experiments elucidate a mechanism for cycD2SV mediated cell cycle exit where by the splice variant sequesters endogenous cell cycle proteins, such as CDK4 and cycD2, into aggresomal structures and targets them to autophagy mediated degradation. Cell cycle arrays completed for cycD2SV transfected cells associated the splice variant with changes in transcriptional profile of G2/M regulatory genes. During cell confluence and serum deprivation, we observed a significant increase in cycD2SV protein levels (2.5 fold) accompanied by a decrease in cycD1, D2 and D3 protein levels. Interestingly, while D-type cyclin mRNA levels decreased, cycD2SV mRNA levels did not change. Knock down of cycD2SV during confluence rescued cycD2 levels but not cycD1 or cycD3 levels suggesting that cycD2SV upregulation is responsible for cycD2 protein downregulation. Furthermore, knockdown of cycD2SV increased the percentage of cells entering S-phase suggesting that endogenous cycD2SV might be responsible for arresting cells at the G1 phase of the cell cycle. Collectively, our results are consistent with a universal negative cell cycle regulatory role for cycD2SV in both non-cardiac and cardiac cell types. Additionally, for the first time we provide evidence that cycD2SV is expressed endogenously and plays a role in cell cycle exit during states of growth arrest. Further studies on cycD2SV structure, function and regulation may facilitate development of novel anticancer strategies.

List of Abbreviations and Symbols Used

4E-BPs	Eukaryotic translation initiation factor (eIF) 4E-binding proteins
5'TOP	5' transcriptional start site
53BP1	p53-binding protein 1
aa	amino acid
AB/AM	antimycotic-antibiotic
ACTB	beta actin
AMPK	AMP-activated protein kinase
ANOVA	analysis of variance
APC/C	anaphase-promoting complex/cyclosome
ATCC	American Type Culture Collection
ATM	ataxia telangiectasia mutated
ATR	ATM and Rad3-related
B2M	beta-2-microglobulin
BSA	bovine serum albumin
CAK	CDK-activating kinase
CAMs	cell adhesion molecules
CBsv	cyclin B splice variant
CCI	cell cycle inhibitory
CDC20	cell division cycle 20
CDKs	cyclin dependent kinases
CKI	CDK inhibitor
CT	Carboxy-terminus
Ct	threshold cycle
Cyc	cyclin
Cyclin D2SV	cyclin D2 splice variant
DMEM	Dulbecco modified Eagle's medium
DMF	N, N-Dimethyl Formamide
DNA	deoxyribonucleic acid
dRn	threshold fluorescence
DSB	DNA double strand break

ER	endoplasmic reticulum
ERAD	ER-associated degradation
ERK	extracellular signal-regulated kinase
Ets	E-twenty six transcription factor family
FACS	fluorescence activated cell sorting
FBS	fetal bovine serum
FSC	forward scatter
FSH	follicle-stimulating hormone
GADD45α	growth arrest and DNA damage-45α
GAPDH	glyceraldehyde-3-phosphate dehydrogenase
GAPs	GTPase activating proteins
gDNA	genomic DNA
GDP	guanine diphosphate
GEFs	guanine-nucleotide exchange factors
GRB2	growth factor receptor-bound protein 2
Gris1	Graffi integration site 1
GSK-3β	glycogen synthase kinase 3 beta
GTP	guanine triphosphate
Ha-MuSV	Harvey murine sarcoma virus
HA-Ubq	Human influenza hemagglutinin tagged ubiquitin
HDAC6	histone deacetylase 6
HEK293	human embryonic kidney cell line
HER2	human epidermal growth factor receptor 2
Hi-DMEM	serum free DMEM
HIV	human immunodeficiency virus
Hoechst 33342	bisBenzimide H 33342 trihydrochloride
HPRT1	hypoxanthine phosphoribosyltransferase 1
HRP	horse radish peroxidase
HSP	heat shock protein
IgH	immunoglobulin heavy chain locus
IKK	IκB kinase

IP	immunoprecipitation
KAP	CDK-associated protein phosphatase
Ki-MuSV	Kirsten murine sarcoma virus
KIR	KEAP1 interacting region
KPC	kip1 ubiquitination-promoting complex
LC3	light chain 3
LI	labeling index
LiCl	lithium chloride
LIR	LC3 interacting region
MAPK	mitogen-activated protein kinase
MAT1	ménage a trios
MCL	mantle cell lymphoma
Mcm	minichromosome maintenance
MEFs	mouse embryonic fibroblasts
MI	mitotic index
MPF	mitosis promoting factor
mRNA	messenger ribonucleic acid
MTOC	microtubule organizing center
mTOR	mammalian target of rapamycin
Myt1	myelin transcription factor 1
NBR1	neighbor of Brca1 gene
NECL	nectins and nectin-like
NES	nuclear export signal
NIH-3T3	murine fibroblast cell line
NLS	nuclear localization signal
NT	amino-terminus
OIS	oncogene-induced senescence
PBS	phosphate buffered saline
PCNA	proliferating cell nuclear antigen
PI3K	phosphoinositide 3-kinase
PKB	protein kinase B

pRb	retinoblastoma protein
propyl gallate	propyl 3,4,5-trihydroxybenzoate
P-TEFb	positive-transcription elongation factor
QPCR	quantitative real time polymerase chain reaction
Rheb	Ras homolog enriched in brain
RNA	ribonucleic acid
RNAPII	RNA polymerase II
RP	restriction point
RPL13a	ribosomal protein L13a
rRNA	ribosomal RNA
RT	reverse transcriptase
RTKs	receptor tyrosine kinases
S6K	S6 kinase
SAC	spindle assembly checkpoint
SCF	SKP1-CUL1-F-box protein
SCID	severe combined immunodeficient mice
SOS	Son of sevenless homolog
SQSTM1	sequestosome1
SSC	side scatter
TEMED	tetramethylethylenediamine
TFIIH	transcription initiation factor IIH
TGFβ	transforming growth factor-β
TUNEL	terminal deoxynucleotidyl transferase mediated dUTP nick end labeling
UBA	ubiquitin-associated domain
UPR	unfolded protein response
UPS	ubiquitin-proteasome system
X-GAL	5-bromo-4-chloro-3-indlyl-β-D-galactopyranoside
α	alpha
β	beta
β-TRCP	β-transducin repeat-containing protein

γ	gamma
δ	delta
ε	epsilon
λ	lambda

Acknowledgments

It is with great honor that I take this time to thank the many people who made this doctoral thesis possible.

I would like to extend my sincerest gratitude to my supervisor, Dr. Kishore Pasumarthi, whose patience, expertise, and enthusiasm tremendously added to my experience as a graduate student, and helped me grow into the researcher I am today. Your endless support, optimism and guidance have been paramount in my success. You are truly the best supervisor and role model a graduate student could ever dream of having; your accomplishments and successes as a researcher and my mentor are attributes I aspire to attain in the next chapter of my life. The ample support and encouragement of my lab members has been imperative, and in particular, I would like to acknowledge the indispensible contributions of Sarita Chini, Feixiong Zhang, Jessica Maclean, Adam Hotchkiss, Jessica Robinson, and Tiam Feridooni.

I would like to thank Dr. Jonathan Blay and his lab, especially Emiley Lefort and Julia Tufts for their informal and scientific support. I would also like to thank Dr. Chris Sinal and his lab for their assistance with some data analysis. The greatest appreciation goes out to Dr. Jonathan Blay, Dr. Eileen Denovan-Wright and Dr. Jana Sawynok for truly making a difference throughout my graduate studies. It was through their kindness, direction, technical support and mentorship that allowed them to far surpass the role of professors, especially with their guidance during the completion of my teaching requirement.

It would not have been possible to write this doctoral thesis without the help, and support of my supervisory committee (Dr. Kishore Pasumarthi, Dr. John Downie, Dr.

James Fawcett and Dr. Eileen Denovan-Wright). Your mentoring and guidance throughout the last four years has truly been invaluable, and for that I am extremely grateful. In turn, I would also like to extend my sincerest appreciation to my examining committee; your support, patience, and time has been invaluable on both a personal and academic level, and for that I am thankful.

Great appreciation and acknowledgement also goes out to the office staff of the Pharmacology Department, Louisa Vaughan, Sandi Leaf and Janet Murphy; your kindness and patience (especially with the photocopier machine) knows no bounds. Luisa, thank you for all the reminders, from registration, to submitting progress reports. God knows I would have gotten myself in a lot more trouble without your constant reminders. Sandi, thank you for all your office related technical assistance and support. Janet, thank you for all the assistance with financial matters. I would also like to take this opportunity to thank the entire department of pharmacology for their encouragement, kindness and support. You have all been wonderful to work with throughout the last four years.

In closing, I would like to acknowledge my family members, who have been a constant source of emotional and moral support throughout my studies. This thesis would not have existed without them. I am indebted to my mother, father, my sisters Dina, Reem, and Nadine, my beloved, my grandmother, and my late grandfather, for serving as my pillars, and my guidance throughout all my struggles and feats. It is to you that this thesis is dedicated.

Chapter 1: Introduction[1]

1.1 The Mammalian Cell Cycle

The term "cell cycle" refers to the sequence of events whereby cells duplicate their genetic material and divide into two identical daughter cells (Vermeulen et al., 2003).The cell cycle is subdivided into 4 distinct phases: G1, S-phase, G2 and M-phase. "The S-phase refers to the DNA synthesis phase where the genetic material is duplicated, and the M-phase (mitosis) is the phase where the duplicated chromosomes are divided equally between the two daughter cells."(Hotchkiss, 2012) Mitosis is further subdivided into five stages based on the physical state of the chromosomes and spindle apparatus: prophase, prometaphase, metaphase, anaphase and telophase (O'Connor, 2008). During these stages many events occur which are necessary for successful segregation of the duplicated genetic material between the newly generated daughter cells. During prophase, chromosome condensation occurs. This event is subsequently accompanied by nuclear envelope breakdown and Golgi disassembly. During prometaphase and metaphase, bipolar spindle assembly occurs and the chromosomes are aligned at the center of the spindle. During anaphase, chromosomes are segregated towards the spindle poles on either end of the dividing cells. Golgi reassembly, nuclear envelope reassembly and

[1] Contains exerts from "Hotchkiss, A., Robinson, J., MacLean, J., Feridooni, T., **WAFA, K.** and Pasumarthi, K.B. Role of D-type cyclins in heart development and disease". Accepted Feb 8th, 2012 in the Canadian Journal of Physiology and Pharmacology (Manuscript ID: 2011-0453). In support of authors who wish or need to sponsor open access to their published research articles, NRC Research Press also offers an OpenArticle option.

chromosome decondensation occurs during telophase. Finally, the physical division of the two genetically identical cells is complete by cytokinesis (O'Connor, 2008; Wurzenberger and Gerlich, 2011). The G1 and G2 phases refer to the gap times preceding the S- and M-phases respectively. During both the G1 and G2 phases, important regulatory events necessary for successful cell division take place. Cells which are not actively dividing enter a quiescent or resting stage termed G0. Usually, cells which are terminally differentiated enter G0 phase. Similarly, cells which do not receive either proliferation signals or anti-mitogenic signals can effectively withdraw from the cell cycle and enter G0 (Vermeulen et al., 2003).

The transition from one cell cycle phase to another is tightly regulated by a number of cellular proteins (Tessema et al., 2004; Vermeulen et al., 2003). Cyclin dependent kinases (CDKs) are a family of serine/threonine protein kinases which are activated at different stages of the cell cycle and play a key role in cell cycle progression (Fig. 1). CDKs are activated by binding to regulatory subunits named cyclins. In mammals, there are at least 15 cyclins, however, not all members of the cyclin family play a direct role in cell cycle regulation (Gopinathan et al., 2011). Cyclins C, K, L and T play a role in the regulation of transcription, whereas cyclin A, B, D and E play a direct role in CDK regulation. Cyclin H plays a role in both transcriptional and CDK regulation. Transcriptional events as well as ubiquitin mediated degradation of cyclins regulate their cyclic appearance and disappearance during various phases of the cell cycle. In contrast to cyclins, CDK protein levels remain stable during the cell cycle. This mechanism ensures that the required CDKs are activated during the correct phase of the cell cycle. For example, upregulation of D-type (cycD1, D2 and D3) cyclins during G1 allows for

Figure 1. The cell cycle phases, CDK/cyclin complexes and the role they play in mammalian cell cycle regulation. CDK3/cycC, CDK4/cycD and CDK6/cycD regulate G0/G1 phase transition in quiescent cells and early G1 phase progression in proliferating cells. CDK2/cycE complexes are responsible for G1/S transition. In early S-phase, cycA complexes with CDK2 promoting the progression of S-phase. Later, cycA complexes with CDK2 where it promotes S/G2 transition. During G2 phase cycB1 starts to accumulate binding to CDK1 where it promotes M-phase entry and completion. CycF is possibly required for G1 entry and cycG is thought to play a role in the DNA damage response pathway at the G2/M transition point. CDK11/cycL function is not yet fully understood, but they are thought to play a role in M-phase. Solid arrows depict the role of the classical CDK/cyclin complexes in the cell cycle. CDK-activating kinase (CAK) is a protein complex which activates CDK/cyclin complexes by phosphorylation and consists of three subunits, CDK7, cycH and Mat1. The asterix (*) denotes complexes subject to CDK activating kinase (CAK) regulation. Dotted arrows depict cyclin or CDK/cyclin complexes for which only preliminary data has been produced. Figure modified from (Malumbres and Barbacid, 2005).

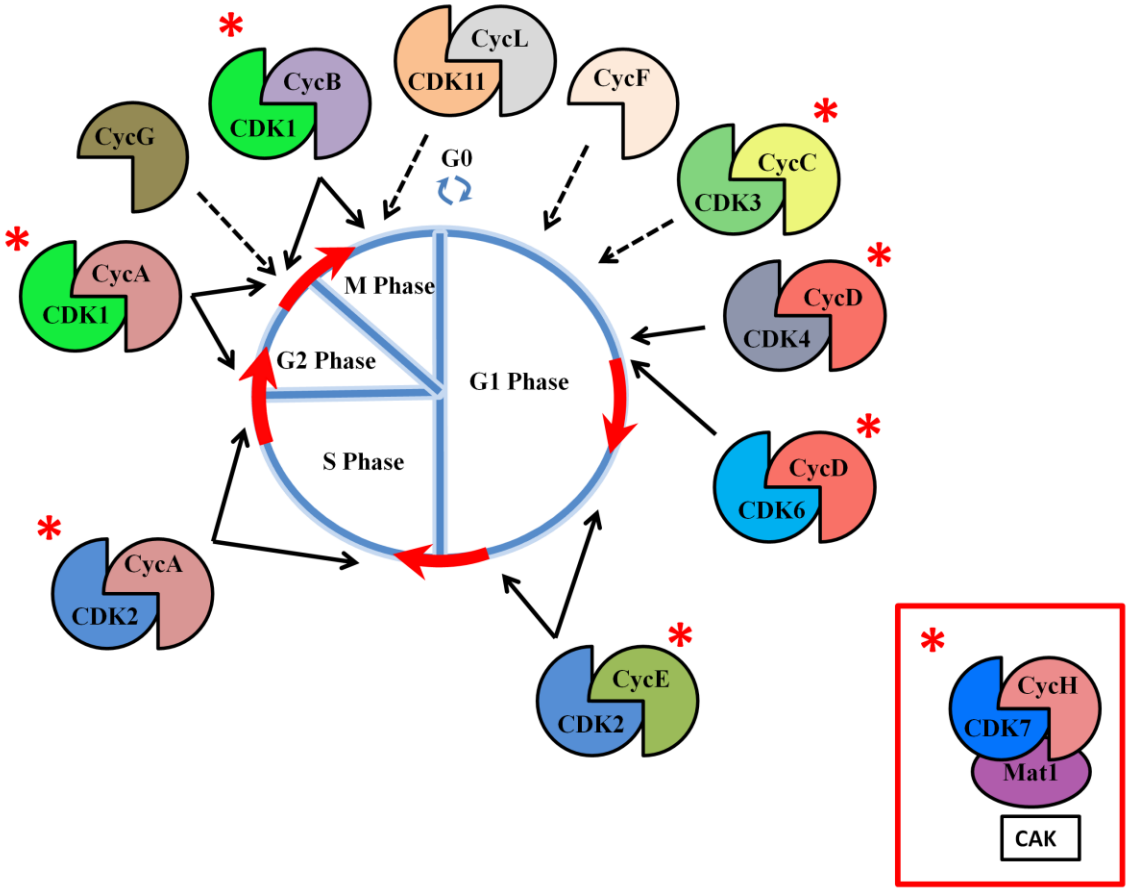
CycB
CDK1
CycL
CDK11
CycF
CycG
G0
CycC
CDK3
CycA
CDK1
M Phase
G2 Phase
G1 Phase
S Phase
CycD
CDK4
CycD
CDK6
CycA
CDK2
CycE
CDK2
CycH
CDK7
Mat1
CAK

the specific activation of CDK4 and CDK6 which are necessary for G1/S transit. Similarly, upregulation of B-type cyclins during G2/M allows for the formation of the CDK1/cycB complex necessary for entry and completion of mitosis (Fig. 2) (Gopinathan et al., 2011; Tessema et al., 2004; Vermeulen et al., 2003).

To date, eleven CDKs and nine CDK-like proteins have been reported. Of the eleven CDKs, five have been shown to play a direct role in cell cycle progression (CDK1, 2, 3, 4 and 6), five in transcriptional control (CDK 7, 8, 9, 10 and 11), and one in neuronal cell function (CDK5, Table 1) (Satyanarayana and Kaldis, 2009). CDK4/cycD and CDK6/cycD complexes are responsible for G0/G1 and G1/S transition. CDK2/cycE complexes are responsible for G1/S transition. CDK2 can also bind cycA, and CDK2/cycA complexes are necessary for S-phase entry and completion. CycA binds CDK1 and plays a role in S/G2 transition. CDK1 binding to cycB is required for G2/M transition and M-phase completion (Gopinathan et al., 2011; Malumbres and Barbacid, 2005).

CDK3 interacts with cycE, A and C (Malumbres and Barbacid, 2005). The CDK3/cycC complex has been implicated in the phosphorylation of the retinoblastoma protein (pRb), a step necessary for G0/G1 and G1/S-phase transition, however, further studies are needed to determine the exact role CDK3 plays in cell cycle progression (Ren and Rollins, 2004). CDK5 is an atypical CDK which has no cyclin binding partner and is instead activated by p35 and p39 proteins (cyclin analogues). CDK5 is mostly abundant in neuronal cells in the brain and is implicated in the regulation of cell survival,

Figure 2. Cyclin protein levels during the various phases of the cell cycle. Generally cyclin levels are induced during specific phases of the cell cycle and decrease shortly thereafter once the phase or phase transition is complete. D-type cyclin expression is initiated in response to external mitogenic signals prompting the cell to initiate the cell cycle. D-type cyclins activate CDK4/6 and are necessary in G1 for overcoming the restriction point (RP), committing cells to dividing, and G1/S transit. Once cells transition to S phase D-type cyclins are no longer required and are downregulated. CycE is upregulated in late G1 where it complexes with CDK2 and is also required for G1/S transition. CycE is downregulated in late S phase. CycA is upregulated during S phase, where it activates CDK2/CDK1 and is necessary for S phase completion. CycB1 is a mitotic cyclin which is responsible for M-phase completion. CycB1 is rapidly upregulated during G2 phase where it binds to and activates CDK1. CycB1 is rapidly degraded upon the completion of M phase. Figure modified from (Roberti, 2009).

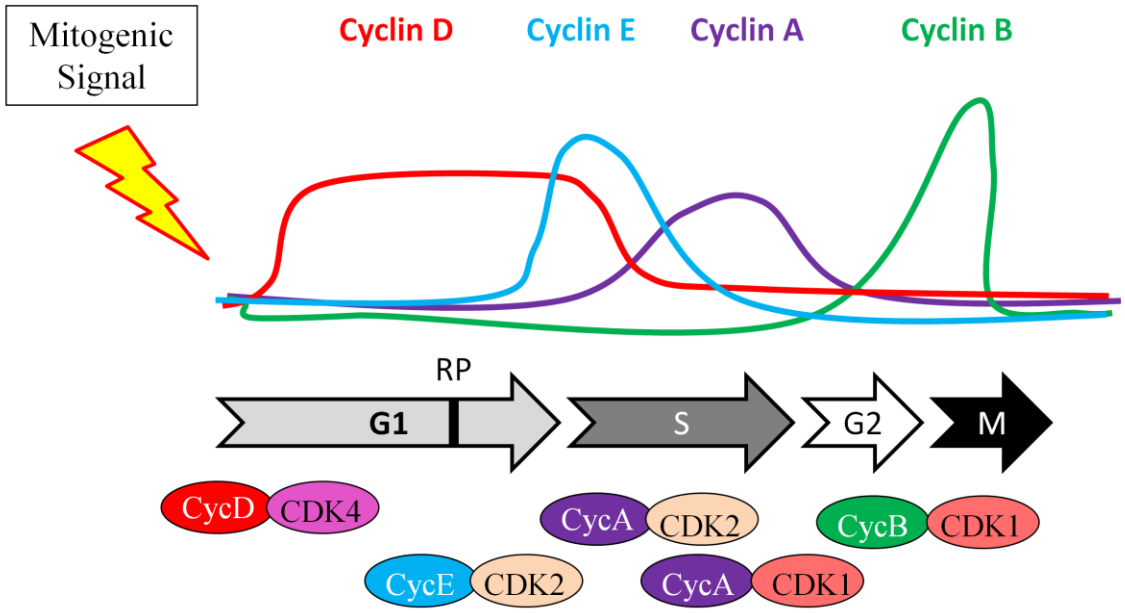
Mitogenic Signal
Cyclin D
Cyclin E
Cyclin A
Cyclin B
RP
G1
S
G2
M
CycD
CDK4
CycE
CDK2
CycA
CDK2
CycA
CDK1
CycB
CDK1

Table 1. The mammalian cyclin dependent kinase (CDK) family members, their cyclin activating partners and their cellular function. Cyclins present in parenthesis denote non-typical cyclin partners for the corresponding CDK.

CDK	Main Cyclin Partners	Cellular Function
CDK1	A1, A2,, B1, B2 (D, E, F, J)	G2/M transition and S phase entry and transition
CDK2	A1, A2, E1, E2 (B1, B2, D1, D2)	G1/S transition, S phase entry and transition
CDK3	A1, A2, E1, E2, C	G0/S transition, transcriptional regulation.
CDK4	D1, D2, D3	G1/S transition
CDK5	p35, p39 (D, E, G-type cyclins, I)	DNA damage response, G1/S transition in the brain
CDK6	D1, D2, D3	G1/S transition
CDK7	H	CDK activation, DNA repair, transcriptional regulation
CDK8	C, K	Transcriptional regulation, G0/S transition
CDK9	T1, T2, K	Transcriptional regulation
CDK10	Unknown	Transcriptional regulation (G2/M transition)
CDK11	L1, L2 (D3)	G1/S transition

transcription, migration and membrane transport (Cruz and Tsai, 2004; Dhariwala and Rajadhyaksha, 2008; Kesavapany et al., 2004). CDK 7-11 are involved in transcriptional regulation of distinct targets some of which play a role in cell cycle progression. CDK7 is part of the CDK-activating kinase (CAK, Fig. 1) enzyme which plays a role in the activation of CDK1, CDK2, CDK4 and CDK6 (Kaldis, 1999). CDK7 also plays a role in promoter clearance and progression of transcription as part of the multi-subunit general transcription initiation factor IIH (TFIIH) (Fisher, 2005; Lolli and Johnson, 2005). CDK8 is activated by cycC and is a part of the RNA polymerase II (RNAPII) holoenzyme complex responsible for phosphorylating the caboxy-terminal (CT) domain of the largest subunit of the RNAPII complex. Furthermore, CDK8/cycC complexes are capable of inhibiting TFIIH by phosphorylating cycH (Akoulitchev et al., 2000). CDK9 binds to both cycT and cycK forming the Positive-Transcription Elongation Factor (P-TEFb). P-TEFb phosphorylates the CT domain of RNAPII positively regulating transcription elongation (Garriga and Grana, 2004). CDK10 has been linked to the regulation of the G2/M-phase of the cell cycle, by inhibiting the transactivation of the E-twenty six transcription factor family (Ets), which is necessary for CDK1 expression. There has been no cyclin partner identified for CDK10 (Bagella et al., 2006). CDK11 is activated by cycL and is implicated in mRNA splicing (Loyer et al., 2008). CDK11 has also been shown to interact with cycD3, thereby inhibiting cell proliferation and inducing apoptosis (Duan et al., 2010).

1.1.1 G0, G1 and Cell Cycle Initiation

During G0 and early G1 phases of the cell cycle, CDKs are maintained in an inactive state by high levels of CDK inhibitors (CKIs) and low levels of cyclins. Cells respond to extracellular proliferative signals only during G0 and G1 phases of the cell cycle. As such, exogenous mitogenic (proliferation) or antiproliferative signals can only effect a cell's decision to commit or withdraw from the cell cycle during these two stages. The "restriction point", also known as the point of no return, is located at the end of the G1 phase and is the point which if passed commits the cell to division. Once the restriction point is passed, the cell no longer responds to exogenous signals (mitogenic or antiproliferative) (Satyanarayana and Kaldis, 2009; Tessema et al., 2004).

Cell division is initiated by mitogenic signals which stimulate the expression of D-type cyclins (Musgrove et al., 2011). The most important signaling pathways involved in cell cycle initiation are the Akt/mammalian target of rapamycin (mTOR) and the Raf/mitogen-activated protein kinase (MAPK) pathways, both of which are activated through receptor tyrosine kinases (Fig. 3) (Raught, 2007). The Akt/mTOR pathway is activated by a multitude of growth stimulating factors like growth hormones, cytokines and nutrients. Upon stimulation, the Akt and phosphoinositide 3-kinase (PI3K) are activated suppressing the activity of TSC1/TSC2. In the absence of Akt and PI3K activation, TSC1/TSC2 bind to, and inhibit the activation of the GTPase Ras homolog enriched in brain (Rheb). Akt and PI3K activation increases the levels of active Rheb GTPase available for stimulating mTOR signaling (Long et al., 2005). The mTOR signaling pathway promotes cell cycle entry and progression by targeting many

Figure 3. Signaling pathways involved in cell cycle initiation. External mitogenic signals initiate the cell cycle by signaling through receptor tyrosine kinases (RTKs). Upon activation, RTKs form receptor dimers and autophosphorylation of the subunits occurs. Once autophosphorylation occurs, the adaptor molecule GRB2 (Growth factor receptor-bound protein 2) is recruited to the receptor where it docks at the phosphorylation sites via an SH2 domain. GRB2 interacts with Son of sevenless homolog (SOS) 1 and 2 via the SH3 protein interaction domain. Once recruited, SOS 1 and 2 are capable of enhancing GEF activity resulting in the activation of Ras which signals through the AKT/phosphoinositide 3-kinase (PI3K) and the Raf/mitogen-activated protein kinase (MAPK) pathways. Signaling through the AKT/PI3K pathway leads to the activation of GTPase Ras homolog enriched in brain (Rheb) GTPase, which, in turn activates mTOR. mTOR upregulates S6 kinase (S6K), which is involved in the translation of cycD1 and c-myc. In addition, mTOR activates the eIF4F complex, which is involved in cap-dependent translation. Once activated the eIF4F complex promotes the translation of positive cell cycle proteins, such as cycD1 and c-myc. Signaling through the Raf/MEK/extracellular signal-regulated kinase (ERK) pathway also promotes the transcription of cycD1 by activating the ETS (E-twenty six) transcription factors.

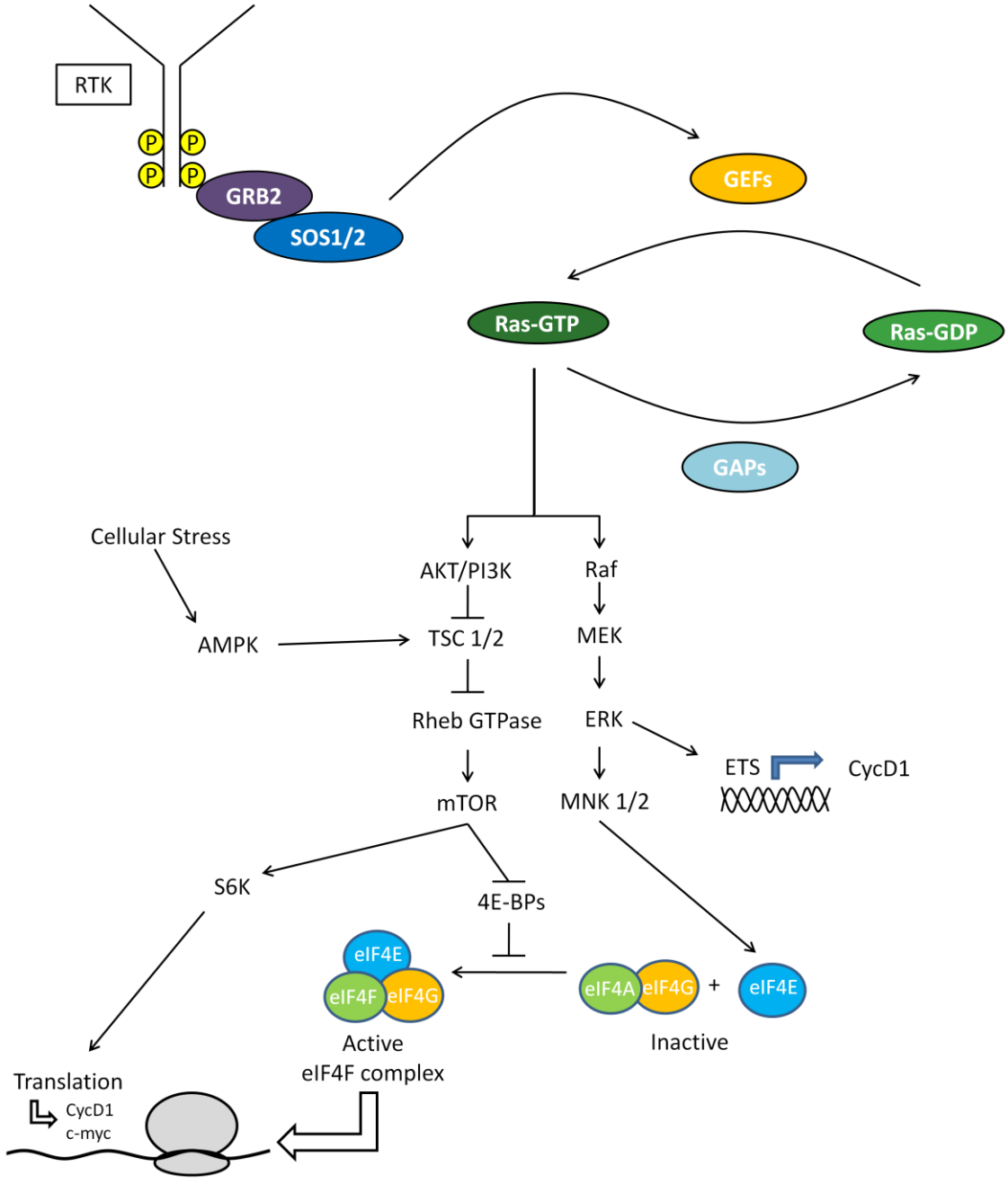
RTK
P
P
P
P
GRB2
SOS1/2
GEFs
Ras-GTP
Ras-GDP
GAPs
Cellular Stress
AMPK
AKT/PI3K
Raf
TSC 1/2
MEK
Rheb GTPase
ERK
ETS
CycD1
mTOR
MNK 1/2
S6K
4E-BPs
eIF4E
eIF4F
eIF4G
eIF4A
eIF4G
+
eIF4E
Active
eIF4F complex
Inactive
Translation
CycD1
c-myc

translational factors, such as eIF4E-binding proteins (4E-BPs). 4E-BPs, regulate the activity of the eIF4F complex, which is involved in cap-dependent translation. The eIF4F complex is composed of the cap-binding protein eIF4E and two other initiation factors, eIF4G and eIF4A (Stevenson and McCarthy, 2008). Hyperphosphorylated 4E-BPs are able to strongly bind to eIF4E preventing the formation of the eIF4F complex (Long et al., 2005). As such, signaling through the mTOR pathway upregulates the production of specific G1/S cyclins, like cycD1, and stimulates G1/S progression by promoting the activity of key translational factors like eIF4E (Averous et al., 2008). Due to the important role mTOR signaling plays in G1/S transition, it comes as no surprise that cells utilize mTOR inhibition to exit the cell cycle when cell division is unfavorable (Pyronnet and Sonenberg, 2001). An example of such, is during cellular stress; growth inhibition signals activate the AMP-activated protein kinase (AMPK), which activates TSC1/TSC2 by phosphorylation effectively inhibiting mTOR signaling (Fig. 3) (Tee and Blenis, 2005).

In addition to upregulating the expression of important G1/S proteins, such as cycD1, mTOR signaling plays a role in determining cell size. Cell size is a major determinant of whether or not cells commit to cell division. In most cells, cell growth is tightly regulated to ensure dividing cells do not subsequently become smaller and smaller eventually losing their capacity to function. As such, cell size co-ordinatation with cell division ensures the viability of daughter cells. Given that protein levels are determined by the number of ribosomes present in the cell, cell size is mostly attributed to the amount of ribosomal RNA (rRNA) and ribosome biogenesis (Jorgensen et al., 2002). mTOR signaling leads to the phosphorylation of the 40S ribosomal protein S6, by the S6

kinase (S6K). The phosphorylation of S6 stimulates the translation of a specific subset of mRNA containing oligopyrimidine tract at their 5' transcriptional start site (5'TOP). Members of the 5'TOP mRNA family encode many of the components of the translational machinery, such as ribosomal proteins and translational elongation factors, thus increasing ribosomal biosynthesis (Dufner and Thomas, 1999). Once the necessary number of ribosomes are synthesized, further synthesis is inhibited by either negative regulators of S6K or by the number of ribosomes present (Fig. 3) (Malumbres and Barbacid, 2001).

Cytokines and growth factors are also known to activate the Raf/MEK/extracellular signal-regulated kinase (ERK) signaling pathway (Chang and Karin, 2001). Phosphorylation of Mnk1 and Mnk2 by ERK leads to the phosphorylation of eIF4E translation factor, which as mentioned earlier, is involved in the translation of transcripts for proteins involved in cell cycle progression, such as, myc and cycD1 (Fig. 3) (Rosenwald et al., 1993; Silvera et al.).

The D-type cyclins are known to activate CDK4 and CDK6 by directly interacting with them. Upon binding, the newly formed complex is recognized by cycH/CDK7/ ménage a trios (MAT1) complex and is phosphorylated on a threonine present in a flexible extended loop of the CDK, termed the T-loop, inducing a conformational change which is necessary for full activation (Lolli and Johnson, 2005). The cycD/CDK activated complex then translocates to the nucleus where it phosphorylates pRb. In an unphosphorylated state, the pRb protein binds and inactivates the transcription factor E2F, however, once phosphorylated, pRb dissociates from E2F allowing E2F to upregulate genes necessary for S-phase entry and cell cycle progression. These genes

include cycE, cycA, and CDK1. CycE mediates the transition from G1 to S-phase by binding to CDK2. One of the functions of the cycE/CDK2 complex is to maintain pRb in a hyperphosphorylated state. The cycE/CDK2 complex is also responsible for phosphorylating histone H1, a function which is important for chromatin rearrangement required for genome replication (Fig. 4) (Malumbres and Barbacid, 2009).

In addition to sequestering the transcription factor E2F, pRb has been demonstrated to bind to the RNA polymerase III specific transcription factor TFIIIB and inhibit its function during G0 and early G1 phases of the cell cycle (Larminie et al., 1997). TFIIIB is necessary for the transcription of all genes regulated by RNA polymerase III some of which are tRNA and rRNA, which play a vital role in cell growth. In the presence of mitogenic signaling, pRb hyperphosphorylation by cycD/CDK4 or 6 and cycE/CDK2 results in the release of the TFIIIB transcription factor upregulating genes required for cell growth in preparation for G1/S transit (Scott et al., 2001). This further highlights the co-ordinated effort between cell cycle initiation and cell growth.

1.1.2 DNA Synthesis Phase

The expression of A-type cyclins (cycA1 and A2) is mediated by E2F and is required for entry into S-phase, completion of S-phase, and subsequent entry into M-phase (Girard et al., 1991; Lehner and O'Farrell, 1989; Malumbres and Barbacid, 2005; Walker and Maller, 1991). CycA associates with CDK2 earlier in the cell cycle followed by CDK1 association in late S-phase (Fig. 4). CycA has also been reported to co-localize with sites of DNA replication indicating that it might play a direct role in DNA synthesis or the prevention of excess DNA replication. One of the unique features of cycA is its

Figure 4. Roles of classical cyclins and CDKs in phase transition and cell cycle progression. Cellular division is initiated by mitogenic signals which stimulate the expression of D-type cyclins. CycD is the regulatory subunit responsible for binding to and activating CDK4/CDK6, and is responsible for G1/S transition and overcoming the restriction point. Once formed, the cycD/CDK4 or CDK6 complex translocates to the nucleus where it upregulates genes necessary for G1/S transit, such as cycE and cycA. Once cycE is expressed it binds to and activates CDK2 mediating the G1/S transition. The cycE/CDK2 complex maintains pRb in a hyperphosphorylated state. CycA binds to and activates CDK2 during early S phase and CDK1 in late S phase. CycB accumulates during G2 phase and competes with cycA for CDK1 binding. CycB/CDK1 complexes are kept inactive by phosphorylation (Myt1 and Wee1) until M phase where they promote M phase progression and completion. When cells are ready to enter M-phase cycB/CDK1 complexes are activated by the phosphatase CDC25. In early M phase cycB1/CDK1 complexes phosphorylate APC/C which induces a conformational change allowing for the association with its co-activator CDC20. To prevent premature mitotic exit, APC/C^{CDC20} activity is inhibited by the spindle assembly checkpoint (SAC). Once cells are ready to exit mitosis APC/C^{CDC20} E3 ubiquitin ligase is activated resulting in the degradation of many mitotic proteins one of which is cycB which allows for mitotic exit.

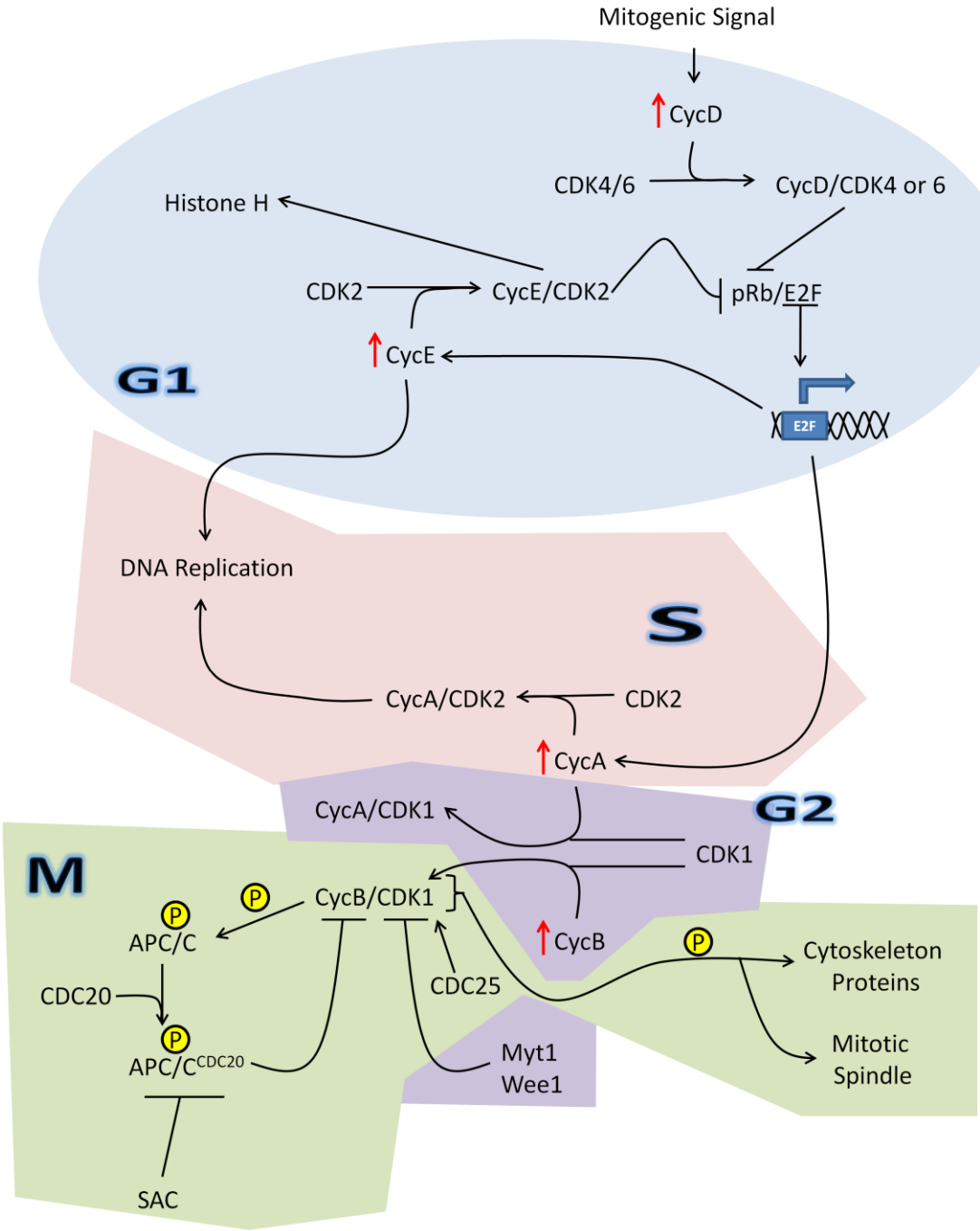
Mitogenic Signal
CycD
CDK4/6
CycD/CDK4 or 6
Histone H
CDK2
CycE/CDK2
pRb/E2F
CycE
G1
E2F
DNA Replication
S
CycA/CDK2
CDK2
CycA
CycA/CDK1
G2
CDK1
M
P
CycB/CDK1
APC/C
CycB
P
Cytoskeleton Proteins
CDC20
CDC25
P
APC/C^CDC20
Myt1
Wee1
Mitotic Spindle
SAC

ability to bind to some of the E2F members (E2F1, E2F2, and E2F3) and negatively regulate their function. CycA/CDK2 complexes inhibit the activity of E2F by phosphorylating the E2F heterodimerization partner DP1. This enables cycA- associated kinases to negatively regulate the transcriptional activity of E2F to counter increased E2F activity mediated by CDK2/cycE phosphorylation of pRb (Johnson and Walker, 1999; Malumbres and Barbacid, 2005).

During S-phase, DNA replication leading to chromosomal duplication occurs. One of the critical components of this phase is to ensure the correct and accurate duplication of the chromosomes. In addition, cells must ensure that DNA replication is not initiated before all the required proteins are available (Tessema et al., 2004). Given the size of the eukaryotic genome, many simultaneous replication sites per chromosome are initiated (hundreds to thousands) in order to complete DNA replication in the most efficient manner (Kelly and Brown, 2000).The replication licensing system ensures cells do not re-initiate another round of DNA replication prior to completion of the cell cycle. This system creates a pre-replicative complex at every replication site which is first composed of an origin recognition complex. Cdc6/18, cdt1 and the Mcm (minichromosome maintenance) proteins are then recruited to the "origin recognition complex". Mcm proteins perform as DNA helicases which unwind DNA, a step necessary for accessing the DNA strands for replication (Blow and Hodgson, 2002). CycA/CDK2 activity is responsible for the initiation of DNA replication by phosphorylating key components of the DNA replication machinery (Tessema et al., 2004). CycA/CDK2 plays a role in the binding of Cdc45 to the Mcm complex and unwinding of the origin of replication (Kelly and Brown, 2000; Nishitani and Lygerou,

2002). Displacement of the Mcm proteins during DNA replication prevents re-initiation of replication of a strand which has been already copied (Blow and Hodgson, 2002).

1.1.3 G2 Phase

In the G2 phase, cells check the integrity of the duplicated genetic material and for the presence of necessary cellular structures in preparation for entry into M-phase. Incomplete duplication of the genetic material or DNA damage during DNA synthesis triggers checkpoint pathways which effectively induce cell cycle arrest. DNA damage induced by ultraviolet light or ionizing radiation stimulates ATM (ataxia telangiectasia mutated) and ATR (ATM and Rad3-related) signaling pathways. ATM and ATR signaling results in the activation, via phosphorylation, of human checkpoint kinases, Chk1 and Chk2 (Chaturvedi et al., 1999). Once activated, Chk1 and Chk2 phosphorylate the phosphatase CDC25, one of the proteins involved in CDK1 activation, inhibiting its function. By inhibiting CDK1 function, cells are unable to enter mitosis and the cell cycle is effectively inhibited. This allows cells to assess the extent of DNA damage and to repair it if possible (Sanchez et al., 1997).

In addition to Chk1/2 activation, ATM and ATR also activate p53, a tumor suppressor protein, which plays an important role in arresting the cell cycle as a response to DNA damage and other cell stressors (Niida and Nakanishi, 2006). In normal cells, p53 levels are tightly regulated by mdm2, an E3 ubiquitin ligase. In the absence of DNA damage or cellular stress, mdm2 binds to p53 and targets it for ubiquitin mediated degradation (Brooks and Gu, 2011). In the presence of DNA damage, p53 is phosphorylated at Ser15 and Ser20 by the DNA damage sensors ATM and ATR kinases.

Phosphorylation of p53 by ATM and ATR inhibits mdm2 association allowing for p53 accumulation and activation (Liang et al., 2009). Once activated, p53 plays a role in G1 arrest in response to DNA damage by upregulating the transcription of the CKI $p21^{Cip1}$ (el-Deiry et al., 1993). p53 also mediates the expression and activation of the growth arrest and DNA damage-45α (GADD45α) protein which has been shown to induce G2/M arrest (Hollander and Fornace, 2002; Zerbini et al., 2005). GADD45α inhibits CDK1 by binding to cycB interfering with cycB/CDK1 association and is involved in nucleotide excision repair (Hollander and Fornace, 2002; Zerbini et al., 2005).

CycB accumulates during G2 phase of the cell cycle until it effectively competes with cycA replacing it as the regulatory partner of CDK1. The newly formed cycB/CDK1 complex is known as the mitosis promoting factor (MPF) (Tessema et al., 2004; Wurzenberger and Gerlich, 2011). The activity of the MPF is regulated by phosphorylation. Phosphorylation of the complex by myelin transcription factor 1 (Myt1) and Wee1 on Thr14 and Tyr15 of CDK1 deactivates the complex, whereas de-phosphorylation of the complex by CDC25B and CDC25C activates it. CDK1/cycB complexes start to accumulate during G2 phase in preparation for mitotic entry, however, CDK1/cycB activation is delayed until preparation for mitotic entry by phosphorylation on Thr14 and Tyr15 by Myt1 and Wee1. Once cells are ready to enter mitosis, Wee1 and Myt1 are inhibited and the CDC25 phosphatase is activated removing the Thr14 and Tyr15 phosphorylations. This allows for the activation of the CDK1/cycB complex and ushers mitotic entry (Fig. 4) (Coulonval et al., 2011; Lindqvist et al., 2009; Potapova et al., 2011).

1.1.4 Mitosis

The entry of mitosis is defined by various cellular events, such as cell rounding (Stewart et al., 2011), nuclear envelope breakdown (Stewart et al., 2009), chromosome condensation (Belmont, 2006) and mitotic spindle assembly (Walczak et al., 2010). In addition, activation of MPF via dephosphorylation is the rate limiting step for entry into mitosis. Once activated, the MPF phosphorylates many substrates necessary for M-phase progression and completion. Some of these substrates include, but are not limited to, motor and microtubule-binding proteins important for chromosome condensation, nuclear envelope breakdown, spindle assembly and centrosome separation (Tessema et al., 2004). Other events include the reorganization of organelles, such as the Golgi apparatus (Zaal et al., 1999) and the endoplasmic reticulum (Lu et al., 2009) to create space for the mitotic spindle and segregation of the genetic material to the two daughter cells.

CDK1/cycB activity drives mitosis up until metaphase, where the chromosomes align at the metaphase plate of the mitotic spindle (Wurzenberger and Gerlich, 2011). Early in mitosis CDK1/cycB complexes phosphorylate the APC/C (anaphase-promoting complex) enabling it to bind to its co-activator cell division cycle 20 (CDC20) creating the APC/C^{CDC20} E3 ubiquitin ligase. The newly formed APC/C^{CDC20} complex is the E3 ligase responsible for the ubiquitin mediated degradation of many mitotic proteins, one of which is cycB (Pines, 2011). To prevent premature mitotic exit, APC/C^{CDC20} activity is inhibited by the spindle assembly checkpoint (SAC). SAC is responsible for ensuring the correct chromosome segregation by prolonging prometaphase to allow for proper chromosome alignment at the metaphase plate (Musacchio and Salmon, 2007). Once

chromosomal alignment and orientation is complete, inhibition of the APC/C^{CDC20} is alleviated, thereby allowing for the degradation of cycB1 and mitotic exit (Fig. 4).

1.2 Mechanism of Cell Cycle Regulation

1.2.1 Ubiquitination, phosphorylation and subcellular localization

"Due to the important role cyclins play in activating CDKs and driving the progression of the cell cycle, cyclin levels are tightly regulated during cell division. Cyclin levels are regulated mainly by two post translational protein modifications: ubiquitination and phosphorylation. The ubiquitin-proteasome system (UPS) involves the covalent addition of multiple ubiquitin molecules to proteins destined for degradation. The polyubiquitinated proteins are then recognized and targeted for degradation by the 26S proteasome complex. The addition of ubiquitin to a target substrate is mediated by three enzymes: the E1 ubiquitin-activating enzyme, the E2 ubiquitin-conjugating enzyme and the E3 ligase catalyst. The E1 enzyme activates the ubiquitin molecule by forming a thioester bond with the carboxyl group of Gly76 of the ubiquitin molecule. Once the ubiquitin molecule is activated the E1 enzyme transfers the ubiquitin to the E2 ubiquitin-conjugating enzyme, which carries the activated molecule as a thioester. Finally, the E3 ligase transfers the activated ubiquitin molecule from the E2 ubiquitin-conjugating enzyme to a lysine residue on the target substrate (Hoeller and Dikic, 2009; Nakayama and Nakayama, 2006; Pickart, 2001)." (Hotchkiss, 2012)

The E3 ligase is thought to be responsible for the specificity of the ubiquitination process (Hershko, 1983). E3 ligases are divided into four major classes based on their

structural motifs: HECT-type, RING-finger-type, U-box-type or PHD-finger-type. Cullin-based E3 subfamily belongs to the RING-finger type E3 ligase family and is one of the largest single class of E3 ligases (Nakayama and Nakayama, 2006). Within the cullin-based E3 subfamily, there are two ligases responsible for the ubiquitin mediated degradation of cell cycle proteins, the SKP1-CUL1-F-box protein (SCF) complex (Nakayama and Nakayama, 2005) and APC/C (Castro et al., 2005; Harper et al., 2002).

The SCF complex is composed of three subunits: RBX1 (RING-finger protein), CUL1 (scaffold protein), and SKP1 (adaptor protein). In addition to these subunits there is a variable F-box protein which associates with SKP1 through its F-box motif and is responsible for substrate specificity. To date, 70 F-box proteins have been identified in humans and belong to one of three groups based on protein motifs those containing WD40 repeats (FBXW), leucine-rich repeats (FBXL) or other domains (FBXO) (Jin et al., 2004). Three F-box-proteins have been associated with the regulation of cell cycle proteins: SKP2 (FBXL1), FBW7 (FBXW7) and β-transducin repeat-containing protein (β-TRCP and FBXW1/11) (Nakayama and Nakayama, 2006).

The APC, like the SCF complex is a multi-subunit complex with variable and invariable components. The APC11 (RBX1-related RING-finger protein), APC2 (CUL1-related scaffold protein) and an additional 11 other proteins with undefined roles make up the invariable core of the APC. In addition to the core proteins there are activator proteins present in mitotically cycling cells of which two are known: CDC20 and CDH1 (also known as HCT1) (Castro et al., 2005; Harper et al., 2002). Activator proteins determine substrate specificity and function during meiosis and in non dividing cells (Nakayama

and Nakayama, 2006). G1 cyclins are ubiquitinated by SCF complex, whereas mitotic cyclins are ubiquitinated by APC/C (Gopinathan et al., 2011).

In addition to regulation through cyclin binding, CDKs are regulated by phosphorylation. Subsequent phosphorylation of the cyclin/CDK complex by the CAK complex on the T-loop threonine (e.g., CDK1 Thr161, CDK4 Thr172, CDK2 Thr160) induces a conformational change which is necessary for full activation. CDK7, cycH and the assembly factor MAT1 make up the CAK complex and is responsible for the activation of CDK1, CDK2, CDK4 and CDK6 (Fesquet et al., 1993; Fisher and Morgan, 1994; Kato et al., 1994; Poon et al., 1993; Solomon et al., 1992). Based on the CDK2 crystal structure, there are two structural restraints which maintain the protein in an inactive state: 1) the T-loop which blocks the substrate binding site and 2) the orientation of the side chains in the ATP site are not optimal, interfering with the efficient phosphotransfer by ATP phosphates. (De Bondt et al., 1993; Morgan, 1995; Morgan and De Bondt, 1994). CycA binding to CDK2 alters the conformation of the CDK allowing access to the T-loop which is otherwise inaccessible (Jeffrey et al., 1995). Phosphorylation of the CDK2 T-loop on Thr160 by CAK further stabilizes the T-loop and allows for the correct amino acid orientation in the substrate binding site (Russo et al., 1996). When CDKs are unbound to a cyclin subunit, the T-loop region of the protein is inaccessible to CAK, thus, monomeric CDKs are not phosphorylated by CAK (Fesquet et al., 1993; Fisher and Morgan, 1994; Kato et al., 1994; Poon et al., 1993; Solomon et al., 1992).

CDK7 is also subjected to regulation by phosphorylation on Thr170 and Ser164 both present in the activation segment of the protein. Phosphorylation on Thr170 is not

required for CAK activity since MAT1 association with unphosphorylated CDK and cycH is capable of activating CAK (Devault et al., 1995; Fisher et al., 1995). However, phosphorylation on Ser164 improves CDK7/cycH association and CAK activity (Lolli et al., 2004).

Dephosphorylation of the CDK T-loop threonine by CDK-associated protein phosphatase (KAP) deactivates cyclin/CDK complexes (Hannon et al., 1994; Poon and Hunter, 1995). Furthermore, the activity of CDK1 can be regulated by the phosphorylation of threonine 14/tyrosine 15 residues (Krek and Nigg, 1991; Parker and Piwnica-Worms, 1992). WEE1-like kinases inactivate the CDK1 upon phosphorylation of these residues whereas dephosphorylation by the dual-specificity phosphatase CDC25 activates the CDK1 (Gautier et al., 1991). CDK are also regulated by CKIs which can bind to and inhibit CDK in complex with cyclins or out of complex (Fig. 5).

In addition to phosphorylation/dephosphorylation and synthesis/degradation, protein intracellular localization also plays a major role in cell cycle regulation. For example, cycB contains a nuclear exclusion signal and is sequestered in the cytoplasm until the beginning of prophase. In addition, the intracellular localization of the CDK inactivating kinases Wee1 (nucleus) and Myt1 (Golgi complex) play an important role in making sure cells do not enter mitosis prematurely. Furthermore, the 14-3-3 group of proteins regulate the intracellular localization of many proteins one of which is CDC25. During interphase, 14-3-3 proteins maintain CDC25 in the cytoplasm. 14-3-3 proteins also play a role in sequestering cycB/CDK1 complexes in the cytoplasm in response to DNA damage preventing them from promoting M-phase (Vermeulen et al., 2003).

Figure 5. CDK regulation by phosphorylation, de-phosphorylation and cyclin dependent kinase inhibitors (CKI). The first step required for CDK activation is the binding of the cyclin regulatory subunit. Upon cyclin binding, a conformational change occurs allowing for the complex to be recognized by the cyclin activating kinase (CAK) complex. The CAK complex is composed of cycH, CDK7 and Mat1. Phosphorylation by CAK is required for the activation of the CDK. Activated cyclin/CDK complexes by CAK can be reversed by CDK-associated protein phosphatase (KAP) mediated dephosphorylation. In addition to regulation by CAK, CDK1/cycB complexes are negatively regulated by Wee1 and Myt1 phosphorylation. When CDK1 in complex with cycB is phosphorylated it is rendered inactive. De-phosphorylation of CDK1 by the phosphatase CDC25 reverses Wee1 and Myt1 inhibition. The additional regulation of CDK1/cycB1 is essential for controlling the precise timing of M-phase entry. CDK activity is inhibited by the CKIs, INK4 and CIP/KIP protein family. CIP/KIP family members interfere with CDK kinase activity by binding to cyclin/CDK complexes forming an inactive trimeric complex whereas INK4 family members bind to the CDK subunit physically interfering with the formation of cyclin/CDK complex. Figure modified from (Malumbres and Barbacid, 2005).

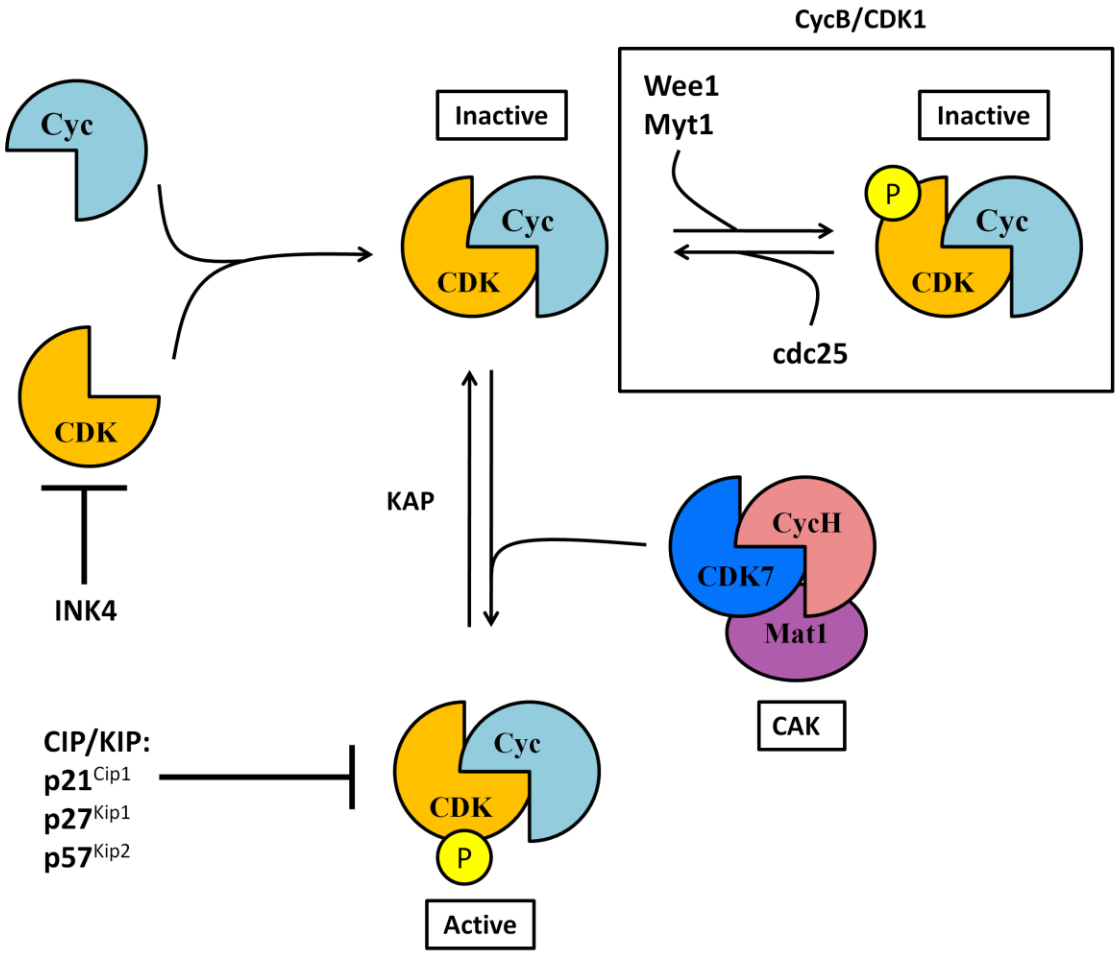
CycB/CDK1
Cyc
CDK
Inactive
Wee1
Myt1
Inactive
P
Cyc
CDK
cdc25
KAP
CycH
CDK7
Mat1
CAK
INK4
CIP/KIP:
p21Cip1
p27Kip1
p57Kip2
Cyc
CDK
P
Active

1.2.2 Cyclin Dependent Kinase Inhibitors: Cip/Kip and INK4 Families

CKIs are divided into two families: the Cip/Kip family and the INK4 family. The Cip/Kip family is composed of three proteins: $p21^{Cip1}$, $p27^{Kip1}$ and $p57^{Kip2}$. Members of the Cip/Kip family share a homologous inhibitory domain which allows for these proteins to both bind and inhibit CDK4 and CDK2 containing complexes (Fig. 5) (Polyak et al., 1994b; Sheaff, 1997; Toyoshima and Hunter, 1994; Vervoorts and Luscher, 2008; Waga et al., 1994). The first member of the Cip/Kip family to be isolated was $p21^{Cip1}$ also known as Cip1, WAF1, SD11, CAP20, PIC1 and mda-6 (Harper et al., 1993; Johnson and Walker, 1999; Vidal and Koff, 2000). $p21^{Cip1}$ was found to be upregulated in wild type cells in response to DNA damaging agents indicating that $p21^{Cip1}$ might play a role in p53-activated cells. As part of the DNA damage response, p53 is stabilized and activated as a transcription factor. Once activated, p53 binds to a p53-binding site in the $p21^{Cip1}$ gene promoter region upregulating $p21^{Cip1}$ gene expression. Upon expression, $p21^{Cip1}$ is thought to inhibit the cell cycle by binding to CDK complexes necessary for G1 cell cycle progression and inhibiting their kinase activity (Johnson and Walker, 1999; Vidal and Koff, 2000). In addition to playing a role in p53 dependent cell cycle inhibition, $p21^{Cip1}$ was also observed to play a role in cell cycle exit mediated by cellular senescence. It was observed that $p21^{Cip1}$ levels accumulated in ageing cells as they approach senescence (Noda et al., 1994).

An alternate mechanism by which $p21^{Cip1}$ inhibits cell cycle is by interacting with proliferating cell nuclear antigen (PCNA), an elongation factor for DNA polymerase δ, which is also part of the DNA repair machinery (Flores-Rozas et al., 1994; Pan et al., 1995; Waga et al., 1994; Warbrick et al., 1995). PCNA is a member of the DNA sliding

clamps (β clamps) family and is an essential cofactor for DNA replication (Bowman et al., 2004; Moldovan et al., 2007). PCNA has been demonstrated to play a role in both the initiation of the leading- strand DNA replication and the discontinuous lagging-strand synthesis by providing a platform for DNA polymerases and other necessary proteins to gain access to the sites of DNA replication (Hubscher, 2009; Moldovan et al., 2007). Binding of $p21^{Cip1}$ to PCNA was reported to inhibit the DNA replication but not repair function of PCNA. Currently, $p21^{Cip1}$ cell cycle inhibition is thought to be mediated by two mechanisms: 1) binding to and inhibiting the activity of various CDK/cyclin complexes and 2) by inhibiting PCNA activity (Johnson and Walker, 1999). $P21^{Cip1}$ function is not limited to inhibiting cell cycle but it has also been implicated in promoting cell cycle by binding to and assisting with the assembly of CDK/cyclin complexes. Currently, $p21^{Cip1}$ function is thought to be controlled by phosphorylation (Scott et al., 2000). Unphosphorylated $p21^{Cip1}$ has been reported to localize to the nucleus where it functions as an anti-proliferative protein by binding to CDK/cyclin complexes and PCNA inhibiting their function. Upon phosphorylation by Akt or protein kinase B (PKB), on Thr145 and Ser146 residues, $p21^{Cip1}$ loses its ability to interact with PCNA and is transported to the cytoplasm (Li et al., 2002; Rossig et al., 2001). Once in the cytoplasm, $p21^{Cip1}$ can interact with cytoplasmic proteins where it plays a role in alternate cellular processes, such as the inhibition of Fas-mediated apoptosis (Suzuki et al., 1998). In addition, it has been reported that cytosolic $p21^{Cip1}$ assists in the assembly of CDK 4/cycD complexes and helps the complex translocate to the nucleus where it can promote G1/S transition (Alt et al., 2002; Cheng et al., 1999; LaBaer et al., 1997).

$p27^{Kip1}$ mediated cell cycle inhibition was first detected in contact inhibited cells and TGF-beta treated cells. The cell cycle inhibitory function of $p27^{Kip1}$ was reported to be due to its ability to bind and inhibit CDK2 (Koff et al., 1993; Vidal and Koff, 2000). $p27^{Kip1}$ was also reported to interact with CDK4/cycD complexes by a tri-hybrid screen (Toyoshima and Hunter, 1994). Like $p21^{Cip1}$, $p27^{Kip1}$ cell cycle mediated inhibition has been demonstrated to be mostly due to inhibition of CDK/cyclin kinase activity preventing the phosphorylation of pRb. $p27^{Kip1}$ has been shown to associate with cycD1-D3/CDK4 or CDK6 and cycE or cycA/CDK2. This inhibits the cells from transitioning from the G1 to S-phase of the cell cycle (Denicourt and Dowdy, 2004; Polyak et al., 1994a; Toyoshima and Hunter, 1994). However, $p27^{Kip1}$ has also been reported to play a role in other cellular processes, such as apoptosis and cell motility. Since $p27^{Kip1}$ has 6-8 phosphorylation sites, it is thought that based on the phosphorylation pattern of $p27^{Kip1}$ the cellular localization of the protein, folding and metabolism are affected dictating the cellular function of the protein. When $p27^{Kip1}$ is localized to the nucleus it is believed to mediate cell cycle inhibition by binding to CDK/cyclin complexes and deactivating them. $p27^{Kip1}$ phosphorylation is thought to promote the transport of $p27^{Kip1}$ into the cytoplasm where it can participate in other cellular functions, such as assisting in cellular motility (Borriello et al., 2007). Cytoplasmic $p27^{Kip1}$, like $p21^{Cip1}$, has been demonstrated to assist in the formation and nuclear translocation of CDK4/cycD complexes where they effect gene transcription to promote G1/S transition (Cheng et al., 1999; LaBaer et al., 1997).

As part of the Cip/Kip, family $p57^{Kip2}$ also has the ability to bind and inhibit CDKs. $p57^{Kip2}$ can bind and regulate the function of the following CDK/cyclin complexes: CDK2/cycE, CDK2/cycA, CDK3/cycE, CDK4/cycD1, CDK4/cycD2,

CDK1/cycB and CDK6/cycD2 (Lee et al., 1995; Matsuoka et al., 1995; Reynaud et al., 2000). The amino-terminus (NT) of $p57^{Kip2}$ contains three sites, a cyclin binding region, a CDK binding site, and a 3_{10} helix, which are necessary for the inhibition of CDK/cyclin activity. $p57^{Kip2}$ inhibits CDK/cyclin complexes by binding to them and inactivating their kinase activity. Like $p21^{Cip1}$, $p57^{Kip2}$ is thought to have the ability to assist with the assembly of CDK/cyclin complexes (Vidal and Koff, 2000). At low levels it is thought that $p57^{Kip2}$ assists with CDK/cyclin complexes and helps them translocate to the nucleus whereas at higher levels it binds to the CDK/cyclin complexes inhibiting their kinase activity (LaBaer et al., 1997). The exact effects of phosphorylation on $p57^{Kip2}$ function have not yet been reported, however, it is known that $p57^{Kip2}$ degradation is regulated by phosphorylation (Pateras et al., 2009).

The INK4 family is composed of four proteins: $p16^{INK4a}$ (p16), $p15^{INK4b}$ (p15), $p18^{INK4c}$ (p18) and $p19^{INK4d}$ (p19). These proteins share a common repeating ankyrin motif which is necessary for CDK4 and CDK6 inhibition. INK4 binds specifically to either CDK4 or CDK6 competing with the association of D-type cyclins (Fig. 5) (Carnero and Hannon, 1998). As a result, INK4 cell cycle inhibition depends on the presence of pRb in the cell. In cells lacking pRb, there is an elevated level of cycE which allows the cells to overcome cell cycle regulation mediated by INK4 proteins (Koh et al., 1995; Lukas et al., 1997; Medema et al., 1995).

1.3 D-type Cyclins

The D-type cyclin family is composed of cycD1, D2 and D3. The D-type cyclins share a high sequence similarity including some conserved protein domains. When

compared with cycD1, cycD2 and cycD3 exhibit a 62% and 51% amino acid sequence homology, respectively (Musgrove et al., 2011). When compared to each other cycD2 and cycD3 exhibit 62% amino acid sequence similarity. All three D-type cyclins contain the cyclin box, a well characterized unique protein sequence that is highly conserved among cyclin family members. The cyclin box is responsible for CDK binding as well as interaction with CKIs $p21^{Cip1}$, $p27^{Kip1}$ and $p57^{Kip2}$. In addition to the cyclin box, D-type cyclins share an RB-binding LXCXE motif, a PEST domain, and a CT conserved threonine responsible for targeting the cyclins for ubiquitin-mediated degradation upon phosphorylation (Zwicker et al., 1999) (Fig. 6). The PEST domain is a peptide sequence rich in proline, glutamic acid, serine and threonine. Most proteins containing a PEST domain have a short half-life thus associating the domain with rapid protein degradation (Rogers et al., 1986). Furthermore, the region between the cyclin box and the CT PEST domain contain the least conserved sequences between the three D-type cyclins. These sequences are thought to give each D-type cyclin unique cellular functions other than binding to and activating cyclin dependent kinase 4 or 6. The LLXXXL motif is unique to cycD1 and is responsible for the binding of the LXXL motif, present in the estrogen receptor co-activator SRC1. CycD1 interaction with SRC1 enhances estrogen receptor activation which plays an important role in breast tissue development (Fig. 6) (Musgrove et al., 2011; Zwijsen et al., 1998).

1.3.1 Functions of D-type Cyclins

In addition to influencing the transcription of genes necessary for S-phase transition, cycD/CDK4 complexes have been demonstrated to sequester proteins of the

Figure 6. Comparisons of functional domains of D-type cyclins (cycD1, D2, D3) and their splice variants (cycD1b, cycD2SV). One of the defining aspects of the cyclin protein family is the cyclin box domain which is responsible for CDK association. The LXCXE motif is shared among the D-type cyclins and is responsible for pRb protein interaction. The LLXXXL motif is unique to cycD1 and is responsible for binding to the LXXL motif, present in the estrogen receptor co-activator SRC1. The PEST domain is responsible for D-type cyclin degradation and contains the conserved threonine residue implicated in D-type cyclin ubiquitin mediated degradation. Other sequences, such as the p21 and p27 binding domain, the cycD2SV CT sequence and the cycD1b CT sequence are depicted in the schematic. Figure modified from (Musgrove et al., 2011).

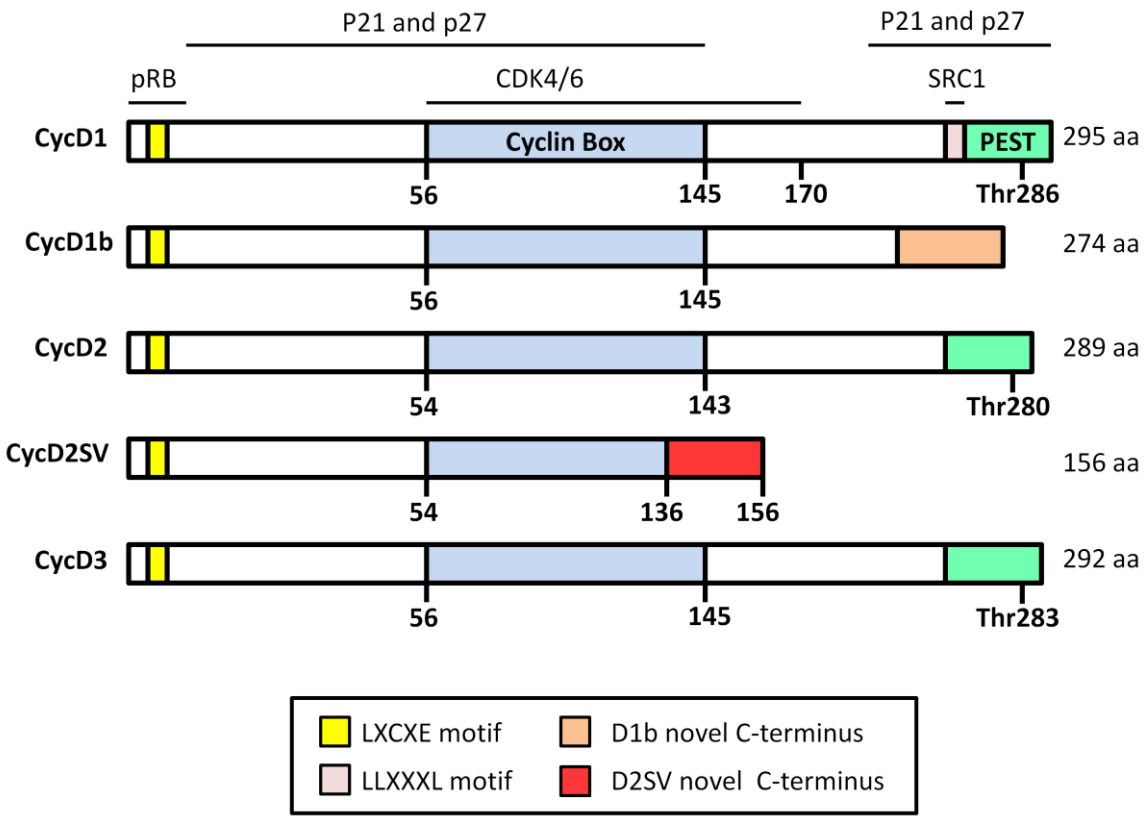
P21 and p27
P21 and p27
pRB
CDK4/6
SRC1
CycD1
Cyclin Box
PEST
295 aa
56
145
170
Thr286
CycD1b
274 aa
56
145
CycD2
289 aa
54
143
Thr280
CycD2SV
156 aa
54
136
156
CycD3
292 aa
56
145
Thr283
LXCXE motif
LLXXXL motif
D1b novel C-terminus
D2SV novel C-terminus

Cip/Kip family, specifically $p27^{Kip1}$ and $p21^{Cip1}$, known repressors of CDK2 (Perez-Roger et al., 1999; Sherr and Roberts, 1995). Binding of $p27^{Kip1}$ and $p21^{Cip1}$ have been shown to promote cycD/CDK association and nuclear import without interfering with the catalytic function of the complex [(Alt et al., 2002; Cheng et al., 1999; LaBaer et al., 1997), see section 1.2.3)].

CycD/CDK4 catalytic function has been demonstrated to impact transcriptional factors, other than E2F, that are involved in cell proliferation and differentiation. Some of these factors include transforming growth factor-β (TGFβ)-responsive transcriptional modulator SMAD3 (Matsuura et al., 2004), members of the RUNX family (Zhang et al., 2008b), GATA4 (Nakajima et al.) and MEF2 family (Lazaro et al., 2002). Another important substrate of cycD/CDK complexes is the BRCA1 gene, which is involved in DNA damage repair (Kehn et al., 2007). CDK4 has also been demonstrated to play a role in mitochondrial function (Wang et al., 2006), cell growth, and processes involved in chromosomal DNA replication and segregation, like centrosome duplication and separation (Adon et al., 2010). CycD/CDK4 activated complexes also regulate cell growth by inducing protein synthesis (Zacharek et al., 2005) and ribosome biogenesis (Ren et al., 2010).

Not all CDK4/CDK6 substrates are involved directly in cell cycle regulation. Some of these substrates are involved in cell motility, cell adhesion and cytoskeletal remodeling (Zhong et al.). In fibroblasts, epithelial cells and macrophages with cycD1 deficiency, a decrease in migration and increase in cell adhesion was observed (Li et al., 2006b; Li et al., 2006c; Neumeister et al., 2003). Fibroblasts and epithelial cells expressing a mutant cycD1 (K112E) lacking the ability to activate CDK4 or CDK6, do

not enhance migration or decrease adhesion, implicating the necessity of CDK activation by cycD1 in these events (Li et al., 2006b; Li et al., 2006c; Musgrove et al., 2011).

1.3.2 D-type Cyclin Regulation

D-type cyclin levels are tightly regulated by ubiquitin mediated degradation and begin to decline at the G1/S-phase boundary (Alao, 2007). CycD1 degradation by the proteasome requires the phosphorylation of a conserved CT threonine, Thr286, by the glycogen synthase kinase 3 beta (GSK-3β) (Diehl et al., 1998; Diehl and Sherr, 1997). Phosphorylation of cycD1 on Thr286 was greatly enhanced by CDK4 association, however, CDK4 binding is not essential for Thr286 phosphorylation (Alao, 2007). During G1, GSK-3β is excluded from the nucleus however is able to enter the nucleus upon S-phase entry. The phosphorylation of cycD1 by GSK-3β is associated with the G1 to S-phase transition in the cell cycle. Studies have demonstrated that GSK-3β access to cycD1 is limited to S-phase due to GSK-3β protein localization (Diehl et al., 1998). GSK-3β enters and exits the nucleus via its interaction with FRAT/GBP (Franca-Koh et al., 2002). Upon entry, GSK-3β gains access to activated cycD1/CDK4 complexes. Phosphorylated cycD1 on Thr286 is recognized by the nuclear exportin CRM1, which transports the cycD1 complex to the cytoplasm. The exported complex is then recognized by E3 ligases, polyubiquitinated and targeted to the 26S proteasome for degradation. Phosphorylation of cycD1 on Thr286 by GSK-3β exports the activated cycD1/CDK4 complexes out of the nucleus where they can no longer influence gene expression. Given that GSK-3β is negatively regulated by the Ras- phosphatidylinositol 3 kinase – Akt

pathway, it explains the increased stability of cycD1 due to mitogenic signals (Gladden and Diehl, 2005).

CycD1 degradation is essential given that the persistent accumulation of cycD1 has been shown to be related with abnormal cell cycle regulation. CycD1 has been shown to associate directly with PCNA, however, it is not clear whether this interaction occurs in the nucleus or the cytoplasm of cells. Essentially, this interaction prevents cells from entering S-phase, effectively inhibiting DNA synthesis (Fukami-Kobayashi and Mitsui, 1999). D-type cyclin accumulation has also been associated with cancer. The cycD1 mutant cycD1-T286A, which can no longer be phosphorylated by GSK-3β remains nuclear during the cell cycle due to reduced association with CRM1. In addition, the continuous expression of cycD1-T286A in a stably transfected murine fibroblast cell line (NIH-3T3) resulted in cellular transformation compared to cycD1 expressing cells. Using a focus formation assay, it was observed that late passage D1-T286A-3T3 cells (18 passages) formed foci whereas D1-3T3 cells did not form foci even after >40 passages. The tumorigenicity of cycD1-T286A was further tested by injecting NIH-3T3 cells in severe combined immunodeficient mice (SCID). Alt *et al.* reported that 7 out of 7 mice injected with D1-T286A-3T3 cells formed tumors by 22 days in contrast to NIH-3T3 and D1-3T3 cells, which were unable to form tumors by 22 days. Characterization of the tumors induced by D1-T286A-3T3 confirmed that the localization of the cycD1 mutant remained nuclear during both G1 and S-phase (Alt et al., 2000).

In addition to GSK-3β, IκB kinase (IKK) α has been demonstrated to regulate cycD1 degradation by Thr286 phosphorylation. IKKα is one of the catalytic subunits of the IKK complex which is involved in NF-κB activation. In addition to activating NF-κB

pathway, IKKα has been shown to play a role in cycD1 protein regulation and cell division (Kwak et al., 2005). Deletion of the CT region of cycD1 followed by specific amino acid mutations identified that IKKα phosphorylates cycD1 on Thr286 located in the PEST domain of cycD1. In addition, cycD1 half life was increased in IKKα$^{-/-}$. These results indicate that IKKα mediated phosphorylation of cycD1 on Thr286 plays a similar role like GSK-3β in cycD1 protein localization and degradation (Kwak et al., 2005). The cellular localization of IKKα in relation to cycD1 has not been examined, however, given the role IKKα plays in cycD1 regulation, one can speculate that IKKα, like GSK-3β, translocates to the nucleus to gain access to activated cycD1 complexes during S-phase.

In addition to the recent discovery of other kinases involved in the regulation of cycD1 localization and degradation by Thr286 phosphorylation, there have been reports questioning the role of GSK-3β in cycD1 regulation. Inhibition of GSK-3β did not interfere with cycD1 phosphorylation or degradation during the cell cycle (Alao, 2007; Guo et al., 2005; Yang et al., 2006a). GSK-3β localization in MCF7 cells did not change during cell division and some cycD1 degradation was occurring when GSK-3β was inhibited (Alao, 2007; Alao et al., 2004; Yang et al., 2006b). In addition, cycD1 ubiquitin mediated degradation has been demonstrated to be independent of cycD1 phosphorylation on Thr286. Gernain *et al.* identified that cycD1 T286A mutants were still susceptible to ubiquitin-mediated proteasomal degradation. In addition, a cycD1 mutant (cycD1-KE) incapable of binding CDK4 also maintained the ability to be degraded by the proteasomal pathway. Based on this evidence, the authors of the study suggest the existence of an alternative ubiquitin mediated pathway, which is independent

of Thr286 phosphorylation, may be responsible for regulating the levels of unbound intracellular cycD1 (Alao, 2007).

Alternatively, Zou *et al.* have identified that in addition to phosphorylation at Thr286, phosphorylation on Thr288 regulates cycD1 stability. Phosphorylation on Thr288 is mediated by the kinase Mirk/Dyrk1b, which is active at the G0 and early G1 phases. The authors demonstrate that the knockdown of Mirk/Dyrk1b by siRNA oligos resulted in the accumulation of cycD1 protein. Furthermore, the use of lithium chloride (LiCl), a GSK-3β inhibitor, did not affect Mirk/Dyrk1b downregulation of cycD1. These results suggest a possible role for Mirk/Dyrk1b in cycD1 degradation (Alao, 2007; Zou et al., 2004).

1.4 D-type Cyclins and CDKs: Redundant or Essential for Life?

In 1989, experiments conducted on budding yeast concluded that any one of the three D-type cyclins was sufficient for normal cell cycle progression, suggesting a redundancy in function of the G1 cyclins (Richardson et al., 1989). Years later, work completed in mice challenged the importance of G1 cyclins in the completion of the cell cycle based on mouse knockout experiments. The first of these experiments were conducted in 1995 where Fatle *et al.* and Sicinski *et al.* demonstrated that mice lacking the cycD1 gene were viable and survived with localized developmental abnormalities in the retina and breast tissues [defective breast lobuloalveolar development during pregnancy; (Fantl et al., 1995; Sicinski et al., 1995)]. These observations supported previous work completed by Matsushime *et al.* where they reported that cycD1 was expressed in distinct cell types (Fantl et al., 1995). In addition to the developmental

abnormalities, cycD1$^{-/-}$ mice were smaller in size, had malformation of the jaw and neurological impairment when compared with littermates carrying the wild type gene (Fantl et al., 1995; Sicinski et al., 1995). Following up on these observations, Sicinski *et al.* generated cycD2$^{-/-}$ and cycD3$^{-/-}$ mice (Sicinska et al., 2003; Sicinski et al., 1996). Male mice lacking cycD2 displayed hypoplastic testes whereas females were found to be sterile as a result of the inability of ovarian granulose cells to proliferate, in response to follicle-stimulating hormone (FSH) (Sicinski et al., 1996). CycD2$^{-/-}$ mice also exhibited thymic hypoplasia and defects in B-lymphocytes and pancreatic cell proliferation (Solvason et al., 2000). In addition, cerebellum abnormalities were observed in cycD2$^{-/-}$ mice whereby granule and stellate interneuron cells were affected. By the second postnatal week, granule cell number decreased significantly in cycD2 deficient mice compared to wild type whereas stellate cell population was nearly non-existent suggesting a vital role for cycD2 in the development of this specific cell type (Huard et al., 1999; Kowalczyk et al., 2004). Mice lacking cycD3 were viable, however, they displayed hypoplastic thymuses resulting in a defect in the normal expansion of immature T-lymphocytes (Sicinska et al., 2003). By interbreeding the single cycD knockout mice, Sicinski *et al.* generated double cycD knockout mice (Ciemerych et al., 2002)(CycD1$^{-/-}$ /D2$^{-/-}$, cycD2$^{-/-}$/D3$^{-/-}$, and cycD1$^{-/-}$/D3$^{-/-}$), and triple cycD knockout mice (Kozar et al., 2004). The double cycD knockout mice developed normally until late gestation. They observed that in double cycD knockout embryos, the remaining cyclin lost tissue specific expression and was upregulated in all tissues to compensate for the lack of the other two D-type cyclins. They concluded that while this compensatory mechanism was sufficient for double knockout embryos to develop to late gestation it was not enough for later stage

development. In double knockouts, mice only expressing cycD1 expressing developed severe megaloblastic anemia, mice only expressing cycD2 suffered neurological abnormalities, and mice only expressing cycD3 suffered impaired cerebellar development (Ciemerych et al., 2002). Surprisingly, triple cycD knockout mice ($D1^{-/-}$, $D2^{-/-}$, and $D3^{-/-}$) were able to develop normally to mid to late gestation (E13.5) (Kozar et al., 2004). Triple cycD knockout embryos died at embryonic day 16.5 due to heart abnormalities and severe anemia. These embryos were also found to have hematopoietic stem cell abnormalities. Since G1 phase requires cycD-CDK4/6 and cycE/CDK2 complexes, Kozar *et al*. concluded that CDK4/6 activity is not necessary for G1 phase progression in early developing mouse embryos. Thus, they hypothesized that CDK2 activity might be sufficient for the cell division in D-type triple knockout mice during early development. They were also able to demonstrate that knocking down CDK2 using retroviruses encoding two independent siRNAs in D-type triple knockdown cells was sufficient to inhibit cellular proliferation compared to wild-type control. Based on these results they concluded that CDK2 was essential for D-type triple knockout cell proliferation and suggested that CDK2/cycE complexes were sufficient for G1/S transition until mid-gestation (Table 2) (Kozar et al., 2004).

In regards to CDKs, the only CDK which is essential for life is CDK1. CDK1 knockout is embryonic lethal at the first cell division, however, with triple knockdown of CDK 4, CDK6, and CDK2 embryos survive until embryonic day 12.5 (Santamaria et al., 2007). CDK2, CDK4 or CDK6 single knockouts were viable, however, they exhibited some localized abnormalities. $CDK2^{-/-}$ mice survived for up to two years with

Table 2. Viability and pathologies of cyclin and CDK knockout mice.

Disrupted Gene(s)	Viability	Pathology	Reference
Cyclin D1	Viable	Abnormalities in retina and breast tissues, malformation of the jaw, and neurological impairment. Mice were smaller compared to wild type littermates.	Fantl et al. (1995), Sicinski et al. (1995)
Cyclin D2	Viable	Hypoplastic testes in male mice but remain fertile and sterility in female mice. Cerebellum abnormalities, hypoplastic thymus and defects in B-lymphocytes and pancreatic cell proliferation.	Sicinski et al. (1996), Huard et al. (1999), Kowalczyk et al. (2004), Solvason et al. (2000)
Cyclin D3	Viable	Impaired T-lymphocyte development	Sicinska et al. (2003)
Cyclin D1 and D2	Viable but die within first three postnatal weeks	Inhibited cerebellar development, small body size and impaired coordination.	Ciemerych et al. (2002)
Cyclin D1 and D3	Non-viable	Neurological abnormalities	Ciemerych et al. (2002)
Cyclin D2 and D3	Non-viable	Develop severe megaloblastic anemia. Embryonic lethal by E18.5.	Ciemerych et al. (2002)
Cyclin D1, D2 and D3	Non-viable	Heart abnormalities and severe anemia (hematopoietic stem cell abnormalities). Develop normally to mid to late gestation (E13.5) and die by E16.5.	Kozar et al. (2004)
CDK1	Non-viable	Embryonic lethal at first cell division	Santamaria et al. (2007)
CDK2	Viable	Survive for two years with no cell division complications except in germ cells. Male and female mice exhibit sterility, small body size, and impaired neural progenitor cell proliferation.	Berthet et al. (2003), Ortega et al. (2003)
CDK4	Viable	Mice exhibit diabetic symptoms (polyuria, hyperglycemia, and ketosis) due to impaired development of β-islet cells. Females are sterile.	Rane et al. (1999), Tsutsui et al (1999), Moons et al. (2002)

CDK6	Viable	Abnormalities in the hematopoietic system	Malumbres et al. (2004)
CDK2 and CDK4	Non-viable	Mice develop to term but die shortly due to heart defects resulting from abnormal embryonic cardiomyocyte development	Berthet et al. (2006) Barriere et al. (2007
CDK2 and CDK6	Viable	Defects in spermatogenesis, oogenesis and hematopoietic cells	Malumbres et al. (2004)
CDK4 and CDK6	Non-viable	Embryonic lethal due to defects in hematopoietic cell proliferation. Some pups survive to birth but die soon after.	Malumbres et al. (2004)
CDK2, CDK4 and CDK6	Non-viable	Cardiac and hematopoietic defects. survive until embryonic day 12.5	Santamaria et al. (2007)

no problems in cell division in most cell types except for germ cells. Mice lacking CDK2 expression were sterile due to a defect in the completion of prophase I during meiotic cell division in male and female germ cells (Berthet et al., 2003; Ortega et al., 2003). $CDK4^{-/-}$ were viable but exhibited decreased growth and development like those observed in $cycD1^{-/-}$ mice. Both male and female $CDK4^{-/-}$ mice were sterile due to defects in spermatogenesis and in corpus luteum formation, respectively (Moons et al., 2002). These mice have impaired development of β-islet cells which are responsible for the synthesis and secretion of insulin (Kulkarni, 2004; Rane et al., 1999). As such, these mice exhibited diabetic symptoms like polyuria, hyperglycemia and ketosis (Rane et al., 1999; Tsutsui et al., 1999). $CDK6^{-/-}$ mostly affects the hematopoietic system as was observed by a decrease in cellularity in the thymus and spleen accompanied by a reduction in circulating red blood cells (Malumbres et al., 2004). These results suggest that CDK2, 4 and 6 are not essential for global cell cycle activity but are important in a specific subset of cells. Double knockdown of any two of CDK2, 4 and 6 enhanced some of the observed defects but did not interfere with global cell cycle activity. $CDK4^{-/-}/CDK6^{-/-}$ double knockouts resulted in embryonic death due to defects in hematopoietic cell proliferation but did not impair G1 entry or progression in other cell types (Malumbres et al., 2004). Elimination of CDK2 and CDK4 resulted in a defect in embryonic cardiomyocyte development. $CDK2^{-/-}/CDK4^{-/-}$ double knockout mice develop to term and die shortly after birth due to cardiac complications. Previously it was thought that CDK2 was capable of compensating for CDK4 knockout in mice, however, these results indicate that CDK2 does not play a compensatory role to CDK4 in any cell types except for embryonic cardiomyocytes (Barriere et al., 2007). Mice lacking the expression of CDK2

and CDK6 are viable and only exhibit abnormalities which were documented in CDK6 and CDK2 single mutant strains (defects in spermatogenesis, oogenesis and hematopoietic cells, Table 2) (Malumbres et al., 2004).

1.5 Cancer, a Cell Cycle Disease: Proto-Oncogenes, Oncogenes and Tumor Suppressors

Cancer is defined as a disease in which somatic or germinal cells gain unregulated proliferative capabilities thereby conferring a survival advantage (Hanahan and Weinberg, 2000). Only 10% of cancer cases occur as a result of germline mutations, whereas 90% of cancers are attributed to somatic mutations and environmental factors (Aggarwal et al., 2009; Sung et al.). There are two types of genes involved in cancer cell formation: oncogenes and tumor suppressor genes. Proto-oncogenes refers to a subset of cellular genes which play a role in promoting cell division, inhibiting cell differentiation and interfering with cell death. Mutations in proto-oncogenes are gain of function mutations, leading to constitutively active oncogenes irresponsive to regulatory elements (Chial, 2008a). An example of such includes mutations which lead to the overexpression of the positive cell cycle regulator cycD1, as discussed in detail in section 1.7. Tumor-suppressor genes are involved in sensing problems affecting proliferation and inhibiting cell division until such problems are addressed. In addition, tumor-suppressor genes are often involved in initiating apoptosis when cell division is compromised. Given the role tumor suppressors play, most of the mutations affecting tumor suppressors are loss of function mutations (Chial, 2008b). As such, both alleles of the tumor suppressor must be mutated for a cancer cell phenotype to arise. This phenomenon was dubbed as the two hit hypothesis and was based on a study conducted on patients with a loss of function

mutation of the tumor suppressor pRb (Knudson, 1971). A loss of function mutation of pRb led to the development of retinoblastoma, a cancer which develops in the cells of the retina.

In an elegant review written by Hanahan and Weinberg, the authors suggest that mutations at the gene level result in the manifestation of six essential alterations in cell physiology which dictate malignant growth: self-sufficiency in growth signals, insensitivity to growth-inhibitory (antigrowth) signals, evasion of programmed cell death (apoptosis), limitless replicative potential, sustained angiogenesis, and tissue invasion and metastasis (Hanahan and Weinberg, 2000). Given that mammalian cells have many fail proof mechanisms to prevent cancer cell formation, it is rare for a single mutation in tumor-suppressor genes or proto-oncogenes to cause cancer cell growth. Only upon multiple synergistic mutations do cells gain the ability to divide uncontrollably.

1.6 Cellular Transformation: Collaboration of H-Ras and c-myc

Ras was first discovered as a viral transforming gene of the Harvey or Kirsten strains of murine sarcoma viruses (Ha-MuSV and Ki-MuSV). The Ras acronym is derived from rat sarcoma based on the observed type of cancer induced in rats (Harvey, 1964; Kirsten and Mayer, 1967). The oncogene associated with the Harvey sarcoma virus was named Ha-Ras whereas that associated with the Kirsten sarcoma virus was named Ki-Ras (Karnoub and Weinberg, 2008). The Ras gene family became a major research interest when they were discovered to play a role in human tumor pathogenesis (Balmain and Pragnell, 1983; Der et al., 1982; Eva and Aaronson, 1983; Guerrero et al., 1984; Parada et al., 1982; Santos et al., 1982; Shimizu et al., 1983; Sukumar et al., 1983). Gene

transfer experiments carried out in NIH-3T3 cells using DNA isolated from human tumor cell lines demonstrated a genetic link to human cancers by causing the transformation of the NIH-3T3 cells (Shih et al., 1981). Confirmation of the existence of such genes was presented when the human transforming genes were cloned from T24 and EJ bladder carcinoma cell lines (Goldfarb et al., 1982; Pulciani et al., 1982; Shih and Weinberg, 1982). DNA isolated from EJ bladder and lung carcinoma cells was later proven to contain genes related to the murine Ras oncogenes by hybridization experiments using probes specific for the viral Ha-Ras and K-Ras (Parada et al., 1982; Santos et al., 1982). Molecular cloning led to the identification of the human Ras genes and were designated as H-Ras and K-Ras. N-Ras, a third member of the Ras family, was later discovered in 1983 and was cloned from neuroblastoma and leukemia cell lines (Hall et al., 1983; Taparowsky et al., 1983).

Ras proto-oncogenes have been demonstrated to bind guanine nucleotides (Scolnick et al., 1979; Shih et al., 1980; Tamanoi et al., 1984; Temeles et al., 1985) and contain intrinsic GTPase activity (Barbacid, 1987; Gibbs et al., 1984; McGrath et al., 1984; Temeles et al., 1985). When bound to guanine triphosphate (GTP) Ras proteins are active whereas when bound to guanine diphosphate (GDP) they are inactive. Guanine-nucleotide exchange factors (GEFs) regulate the activity of Ras proteins by catalyzing the release of GDP molecules bound to Ras. Once GDP is released, GTP is able to bind Ras proteins inducing a conformational change which allows for the interaction and activation of effector proteins necessary for a variety of cellular functions such as endocytosis, cell cycle, motility and apoptosis (Fig. 3) (Ehrhardt et al., 2002; Karnoub and Weinberg, 2008). Negative regulation of Ras proteins is mediated by GTPase activating proteins

(GAPs) which enhances Ras intrinsic GTPase activity effectively hydrolyzing GTP to GDP (Fig. 3) (Rodriguez-Viciana et al., 2005).

Ras signaling induces cycD1 upregulation, which is a strong promoter of G1/S transit (Fig. 3) (Liu et al., 1995). Mutations of the H-*Ras* gene was found in many human cancer cell lines, suggesting that H-*Ras* has proto-oncogenic capablities of transforming cells (Der et al., 1982; Parada et al., 1982; Santos et al., 1982). Comparisons between the sequences of the H-Ras proto-oncogene and oncogene resulted in the discovery of a single point mutation of glycine to valine at the twelfth amino acid of the Ras gene (H-Ras-Val12) (Reddy et al., 1982). This mutation interferes with the association of GAPs with Ras allowing the protein to remain in a constitutively active state. Surprisingly, overexpression of the oncogenic H-Ras-Val12 alone has been shown to inhibit cellular division, a phenomenon dubbed as oncogene-induced senescence (OIS) (Prochownik, 2008). As a protective mechanism, sustained H-Ras activity upregulates the expression of $p15^{INK4b}$, $p16^{INK4a}$, $p19^{ARF}$ and down regulates that of CDK4 to prevent unregulated cellular division and neoplastic growth (Gil and Peters, 2006; Serrano et al., 1997). $p15^{INK4b}$ and $p16^{INK4a}$ are CKIs, which bind to CDK4 and inhibit CDK4/cycD assembly (Fig. 5). $p19^{ARF}$ inhibits the activity of the E3 ubiquitin ligase mdm2, which is involved in p53 degradation (Kim and Sharpless, 2006). By inhibiting mdm2, p53 levels stabilize and induce cell cycle arrest, senescence or apoptosis. One of the targets of p53 is the CDK-inhibitor $p21^{Cip1}$, which inhibits G1/S and G2/M transition by inhibiting CDK4 or CDK2 (He et al., 2005). It was demonstrated that H-Ras-Val12 was only able to transform cells, which have been previously immortalized with carcinogens or transfected with myc, SV40 large T antigen or adenovirus E1A (Land et al., 1983; Ruley,

1983). In case of c-myc, this is thought to be due to the ability of both c-myc and activated H-Ras to perform synergistically overcoming defense mechanisms which prevent cellular transformation (Fig. 7) (Wang et al., 2011).

c-myc is an important transcription factor which plays a role in cell proliferation, survival and differentiation. c-myc protein levels are tightly regulated in cells and are strictly dependent on mitogenic signals. In the absence of mitogenic signals, c-myc mRNA is degraded, decreasing protein levels rapidly. A large number of studies have linked overexpression of c-myc in many types of cancers identifying c-myc as a potent proto-oncogene (Soucek and Evan, 2010). However, like H-Ras, it has been demonstrated that c-myc oncogenic potential is enhanced with collaboration with other genes, such as, activated H-Ras mutant (Bazarov et al., 2001).

The overexpression of c-myc mediates cellular transformation via pathways which overcome the tumor suppressive activity of p53 and the CKI $p15^{INK4b}$ and $p16^{InNK4a}$ (Dang et al., 2006). H-Ras is capable of promoting cycD1 expression but inhibits CDK4 levels by upregulating the CKI $p15^{INK4b}$ and $p16^{INK4a}$. It seems that c-myc upregulation of CDK4 overcomes CDK4 inhibition by H-Ras signaling and cycD1 downregulation by c-myc is compensated for by H-Ras stimulation of cycD1 expression. In addition, c-myc upregulates cycE and induces the activation of CDK2 which counteracts p53 mediated inhibition of the CDK2/cycE complex via $p21^{Cip1}$ and directly downregulates $p21^{Cip1}$ expression (Mitchell and El-Deiry, 1999). Furthermore, c-myc inhibits $p27^{Kip1}$ further stabilizing the CDK2/cycE complex. In addition, c-myc upregulates cycB1, which is down regulated by p53 to induce G2/M arrest, overcoming

Figure 7. A schematic representing Ras and c-myc collaboration in promoting cellular transformation. Ras signaling stimulates the expression of cycD stimulating cell cycle entry and G1/S transition. As a protective mechanism, sustained Ras signaling results in the upregulation of p15, p16, p19 and down regulates the expression of CDK4. p15 and p16 inhibit the activity of cycD/CDK4 complexes and p19 inhibits the activity of mdm2, an E3 ubiquitin ligase, responsible for the degradation of the tumor suppressor p53. By inhibiting mdm2, p19 causes the stabilization of p53 which plays a role in cell cycle arrest, senescence and apoptosis. p53 upregulates p21 expression which is a cyclin dependent kinase inhibitor (CKI) capable of inhibiting cycE/CDK2, cycD/CDK4 among other CDK complexes, effectively inhibiting G1/S and G2/M transition. c-myc is a potent proto-oncogene which has been associated with enhancing Ras tumorigenesis and cellular transformation by overcoming p53, p15 and p16 mediated cell cycle inhibition. c-myc signaling directly counters p53 by upregulating cycB1 and indirectly by inhibiting p21. In addition, c-myc upregulates cycE which is a potent G1/S promoter. c-myc also upregulates CDK4. Figure modified from (Prochownik, 2008).

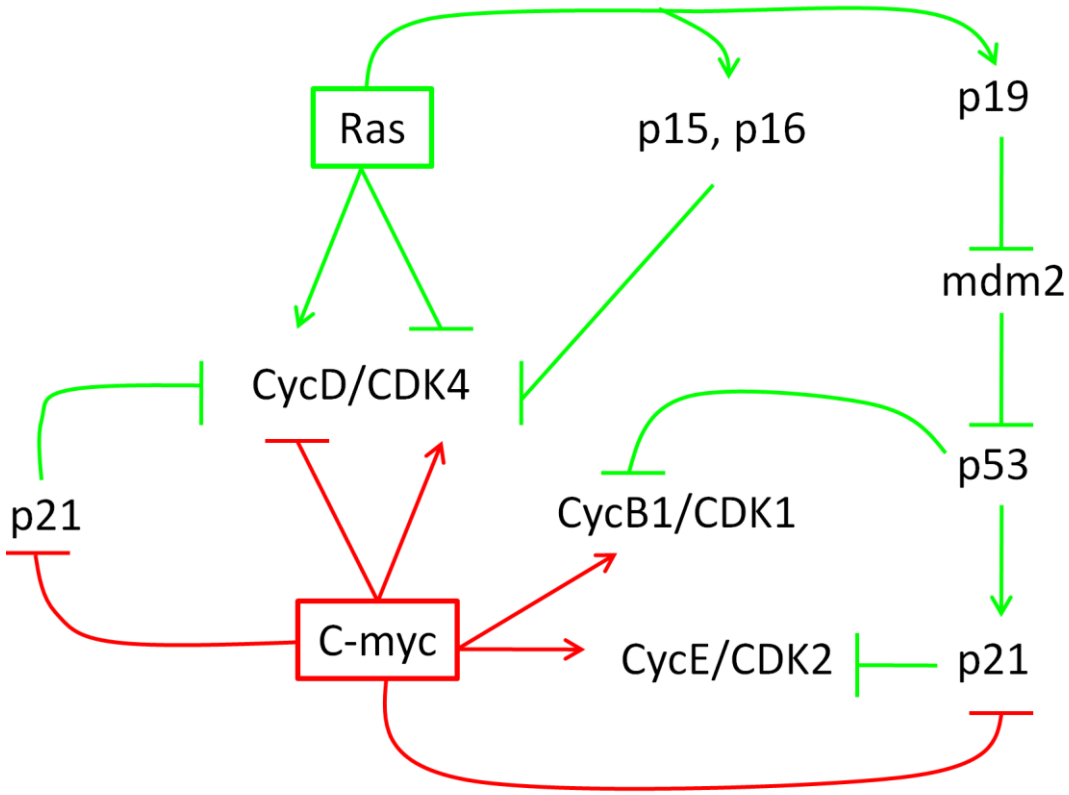
Ras
p15, p16
p19
mdm2
CycD/CDK4
p53
p21
CycB1/CDK1
C-myc
CycE/CDK2
p21

p53 G2/M cell cycle arrest (Innocente et al., 1999; Prochownik, 2008). Mechanistically, these compensatory pathways demonstrate the need for additional oncogene activation to induce Ras oncogene mediated transformation. Indeed, in the absence of other synergistic oncogenes H-Ras oncogene induces cell cycle exit.

1.7 D-type Cyclins, CDKs and Cancer

Given the important role D-type cyclins play in the activation of CDK4/6 and initiating cell cycle and G1/S transit, aberrant expression of D-type cyclins have been associated with multiple types of cancer (Chial, 2008a). *CCND1* gene amplification and overexpression, resulting in cycD1 protein overexpression, plays a role in head and neck squamous cell carcinoma (Hardisson, 2003; Thomas et al., 2005), non-small-cell lung cancer (Gautschi et al., 2007; Santarius et al.), endometrial cancer (Moreno-Bueno et al., 2004; Wu et al., 2006), melanoma (Li et al., 2006a), pancreatic cancer (Garcea et al., 2005), breast cancer (Arnold and Papanikolaou, 2005; Santarius et al.), colorectal cancer (McKay et al., 2000; Toncheva et al., 2004), mantle cell lymphoma (MCL) (Bertoni et al., 2006) and multiple myeloma (Bergsagel and Kuehl, 2005). In these cancer types, the frequency of *CCND1* overexpression and amplification ranges from 0 to over 90% with prevalence being highest in MCL (Bertoni et al., 2006). The translocation of the *CCND1* gene next to the immunoglobulin heavy chain locus (IgH*)* is responsible for 90% of MCLs and is currently used as a diagnostic marker for MCL. Mutation in the F-box 4, an SCF E3 ligase, which is responsible for the degradation of cycD1 can also lead to an increase in cycD1 protein levels and has been attributed to 20% of endometrial cancers

(Barbash et al., 2008). Another example is the gain of function mutations of the potent oncogene Ras (H-Ras-Val12), which leads to the overexpression of cycD1.

In the remaining 10% of MCLs, which do not contain this translocation, *CCND2 or CCND3* gene amplification is observed, resulting in cycD2 and cycD3 protein overexpression, respectively (Bertoni et al., 2006). In comparison to cycD1, cycD2 and cycD3 overexpression is less common in cancer, however, cycD2 overexpression is reported in gastric (Takano et al., 1999) and kidney cancers (Faussillon et al., 2005), whereas cycD3 overexpression has been reported in pancreas (Al-Aynati et al., 2004), colorectal (Watson et al., 1999) and kidney cancers (Hedberg et al., 2002).

Aberrant CDK regulation has been implicated in many types of human cancers. Overexpression of CDK4 has been reported in ovarian (Kusume et al., 1999), urinary bladder (Simon et al., 2002) (amplification), endometrial (Semczuk et al., 2004) and oral (Poomsawat et al.) cancers. A point mutation discovered in CDK4, Arg24Cys, which renders it immune to INK4 regulation has been reported to play a role in melanoma (Goldstein et al., 2002). CDK6 overexpression was found to play a role in oral cancers (Poomsawat et al.). CDK7 and CDK5 have been shown to play a role in breast (Jeon et al.) and lung (Choi et al., 2009) cancer, respectively.

1.8 Splice Variants of D-type Cyclins

1.8.1 Cyclin D1b, a Cyclin D1 Splice Variant

CycD1b is a cycD1 splice variant, which has been identified in multiple cell lines and tissues (Alao, 2007). The alternative splicing event occurs as a result of a known

polymorphism of cycD1, which has been associated with human cancer (Solomon et al., 2003). The A/G polymorphism is present at nucleotide 870 and individuals harboring the A/A genotype have an increased chance of developing specific cancers compared to those with the A/G or G/G genotypes (Solomon et al., 2003). The A-allele has been shown to be associated with the expression of the truncated cycD1 splice variant cycD1b, even though it is a synonomous mutation (Solomon et al., 2003). Compared to the full length cycD1 transcript, which contains exons 1-5, the cycD1b transcript contains exons 1-4, and intron 4 of the cycD1 gene. The alternate splicing results in the synthesis of a 274 amino acid protein with a unique CT region that lacks the CT PEST domain and T286 (Fig. 6) (Alao, 2007). As a result, cycD1b is constitutively nuclear similar to the T286A mutant, as has been discussed earlier. Even though, cycD1b lacks T286, which is involved in the regulation of cycD1 protein degradation, cycD1b half life is only slightly greater than that of cycD1. In addition, cycD1b levels do not accumulate above those observed for cycD1 (Alao, 2007). Surprisingly, cycD1b was demonstrated to be a poor activator of CDK4 and pRb phosphorylation even though it was able to overcome contact inhibition when compared to cycD1 (Alao, 2007; Solomon et al., 2003). In addition, cycD1b stable overexpression in NIH-3T3 cells caused cellular transformation as determined by focus forming assay (Knudsen, 2006). Furthermore, injection of NIH-3T3 cells stably overexpressing cycD1b in SCID mice resulted in the formation of tumors (Knudsen, 2006). Collectively, these results suggest a role for cycD1b in the transformation of cells and tumorigenesis. Indeed cycD1b has been demonstrated to be expressed in esophageal cancers, B-lymphoid malignancies, prostate cancer, colon cancer and breast cancer (Knudsen, 2006).

1.8.2 Splice Variants of Cyclin D2

A splice variant of cycD2 (cycD2SV) was first discovered in mouse tumors induced by Graffi murine leukemia virus and was originally designated "truncated cycD2" (Denicourt et al., 2003). Denicourt *et al.* identified a unique integration site for the Graffi murine leukemia virus and termed it Graffi integration site 1 (Gris1). The viral integration site was mapped to the distal region of mouse chromosome 6 and was identified to be 85 kb upstream of the cycD2 gene (Denicourt et al., 2003). Viral integration at the Gris1 locus induced the expression of a cycD2 splice variant, cycD2SV. The splice variant was encoded by 1.1-kb transcript from the cycD2 gene, resulting in a 17 kDa protein (Denicourt et al., 2003). The cycD2 transcript is composed of exons 1-5 of the cycD2 gene whereas the cycD2SV transcript is composed of exons 1, 2, a read through region from intron 2 and a portion of intron 3 (Denicourt et al., 2003). This new transcript leads to the translation of a truncated 156 amino acid protein compared to cycD2, which is composed of 289 amino acids. The first 136 amino acids of cycD2SV are identical to cycD2; however, the CT 20 amino acids (CT-region) are novel to this protein (Fig. 8). Subsequently, it was shown that cycD2SV was also expressed in normal mouse adult tissues such as brain and ovary (Denicourt et al., 2003). Denicourt *et al.* have demonstrated the transforming capability of cycD2SV when co-expressed with HA-Ras in primary mouse embryonic fibroblasts (MEFs) using focus forming assays. In addition, they were able to demonstrate that cycD2SV mRNA levels were increased in certain tumor types. Surprisingly, even though cycD2SV was able to interact with CDK4, it was unable to activate CDK4 or induce pRb hyperphosphorylation steps necessary for G1/S

Figure 8. Transcriptional and translational steps responsible for the expression of cycD2 and the cycD2 splice variant cycD2SV. CycD2 protein is encoded by exons 1, 2, 3, 4, and 5 whereas cycD2SV is encoded by exons 1 and 2, a read through from intron 2 and a segment from intron 3. As such, when the cycD2 mRNA is translated, a 283 amino acid protein is generated, however, when cycD2SV transcript is translated, a 156 truncated amino acid protein is generated. The first 136 amino acids of cycD2SV are identical to cycD2 however, the last 20 amino acids, termed the CT region, generated from the two intronic sequences in the cycD2SV transcript are novel to this protein.

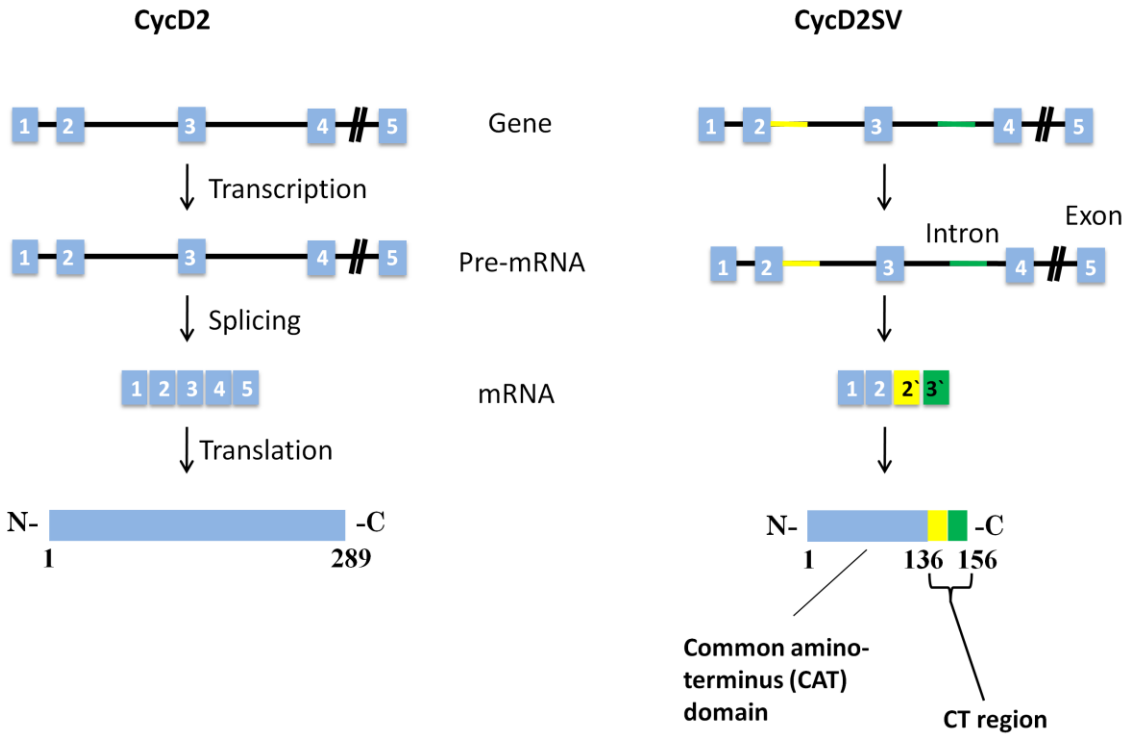
CycD2
CycD2SV
Gene
Transcription
Pre-mRNA
Splicing
mRNA
Translation
Intron
Exon
1 2 3 4 5
1 2 2` 3`
N-
-C
1
289
136
156
Common amino-terminus (CAT) domain
CT region

transition. In addition, the transformation capability of cycD2SV was demonstrated in conjunction with H-Ras (H-Ras-Val12) overexpression and was not established in the absence of the potent oncogene (Denicourt et al., 2008).

1.8.3 Characterization of Expression Profiles of Cyclin D2SV in Embryonic Heart and Postnatal Brain

We have recently established the expression of cycD2SV in mouse embryonic cardiomyocytes. Contrary to data reported by Denicourt *et al.,* we reported a negative role for cycD2SV in cell cycle regulation (Sun et al., 2009). Embryonic cardiomyocytes positive for cycD2SV protein showed decreased mitotic activity compared to those negative for the splice variant as determined by phosphohistone H3 staining. Immunofluorescence staining for cycD2SV on histological sections from E11.5 and E14.5 mouse embryos revealed that the endogenous protein is mostly localized in the ventricular myocardium compared to other tissues. Cardiac sections revealed the accumulation of cycD2SV in the trabecular zone with lower expression in the compact zone. Further examination by confocal microscopy revealed cycD2SV produced micro-aggregates that localized to the cytoplasmic region of cardiomyocytes (Sun et al., 2009).

CycD2SV was also detected in postnatal mouse cerebellum (Kajitani et al., 2010). We examined the expression of cycD2SV in mouse cerebellum at different time points: postnatal day 1 (P1), day 7 (P7), day 14 (P14) and day 28 (P28). Western blot analysis of cerebellar lysates from various postnatal stages with anti-cycD2SV antibodies yielded two bands (20 kDa and 25 kDa). The 20 kDa molecular weight band did not change over developmental stages examined, however, the 25 kDa molecular weight band decreased in intensity whereby at p28 it was 50% the intensity of that determined at P1. In

comparison, cycD2 protein levels peaked at P7 and gradually declined by P28. Localization of cycD2SV and cycD2 protein was determined in cerebellar sections from P7 to P28 by immunohistochemistry. CycD2 levels were detected throughout the cerebellum at P7 but by P28 the signal was limited to the molecular layer of the cerebellum. CycD2SV signal was limited to the Purkinje cell layer from P7 to P28. CycD2SV was localized to the cytoplasm of these cells similar to that observed in embryonic cardiomyocytes (Kajitani et al.). Further experiments are required to determine the functional relevance of cycD2SV expression in Purkinjee cell layer.

1.8.4 Role of Cyclin D2SV in Protein Aggregation, Endoplasmic Reticulum Stress and Cell Cycle Regulation in Cardiomyocytes

To further characterize the role of cycD2SV protein expression and specific role on cardiomyocyte cell cycle regulation, we cloned cycD2SV from mouse embryonic cardiomyocytes and performed overexpression experiments. Upon transfection of cycD2SV in embryonic cardiomyocytes, we observed protein aggregates which were mostly localized to the cytoplasm. Western blot analysis yielded a 20 kDa predominant band accompanied with immunoreactive bands ranging from 32-45 kDa. The presence of higher molecular weight bands in conjunction with the observed protein aggregates by immunohistochemistry suggest possible dimerization, stable intra- or intermolecular disulfide bond formation or polyubiquitination. Overexpression of cycD2SV in mouse embryonic cardiomyocytes led to cell cycle arrest as determined by a 90% reduction in [^{3}H]-thymidine uptake in these cells when compared to vector control or cycD2 transfected cells. Addition of a nuclear localization sequence to cycD2SV did not abolish its negative cell cycle effects and was surprisingly unable to localize the splice variant to

the nucleus. In addition, cycD2SV did not induce apoptosis based on the absence of terminal deoxynucleotidyl transferase mediated dUTP nick end labeling (TUNEL) staining in these cells (Sun et al., 2009).

Given the unique aggregating phenotype of cycD2SV, further experiments were conducted to determine the subcellular localization of the aggregates within the cytoplasmic compartment. Protein aggregation is usually associated with problems in protein folding in the ER. Hence, double-labeling experiments for cycD2SV and markers specific for the ER, Golgi, and lysosomes were conducted on cells transfected with cycD2SV protein. CycD2SV was found to mostly co-localize with ER and lysosomal compartments with a fewer number of cells containing Golgi co-localization. In addition, based on TCRα-GFP, an ER-associated degradation (ERAD) reporter gene, impairment of ERAD was identified to play a role in the accumulation of cycD2SV aggregates (Sun et al., 2009).

Further experiments revealed that cycD2SV aggregation can be abolished using ER stress and cytoskeleton modulating agents. Dynamitin is one of the dynactin subunits (AKA dynein activator complex) and is responsible for linking cargo to the dynein motor complex (Johnston et al., 2002; Sun et al., 2009). Dynein is a motor protein responsible for the transport of various cellular cargos, one of which is aggregation prone proteins, to aggresomes for disposal. Overexpression, of dynamitin has been associated with the disruption of dynein mediated transport of aggregation prone proteins. CHOP is one of the many regulators of ER stress. Co-expression of cycD2SV with either CHOP or dynamitin abolished cycD2SV protein aggregates (Sun et al., 2009).

Mechanistically, cycD2SV does not cause cell cycle exit in embryonic cardiomyocytes as a result of cytotoxic effects or cell death. This is a unique phenomenon which is not shared with other aggregation prone proteins like huntingtin protein which is responsible for neuronal cell death (Bano et al., 2011). Based on immunohistochemistry and co-immunoprecipitation (IP) we concluded that cycD2SV induces cell cycle arrest in embryonic cardiomyocytes by directly sequestering cell cycle proteins such as cycD1, D2, CDK4 and cycB1 (Sun et al., 2009).

1.9 Protein Aggregation, Ubiquitin-Proteasome System, and Autophagy

Protein misfolding occurs as a result of the exposure of hydrophobic residues which are usually hidden by correct protein folding (Goldberg, 2003; Kirkin et al., 2009b). Misfolded proteins are highly susceptible to aggregation, and can lead to the formation of microscopically visible puncta known as inclusion bodies. The buildup of protein aggregates in the cell can interfere with cellular function and as a result, the swift detection and elimination of protein aggregates is important for cell survival (Kopito, 2000). Initially, cells attempt to refold misfolded proteins by recruiting members of the heat shock protein (HSP) family. Once all attempts to correctly fold the protein fail, cells recruit E3 ligases, and the misfolded protein is ubiquitinated and targeted to the proteasome for degradation (Cyr et al., 2002). However, once misfolded proteins form aggregates, proteasomal degradation is no longer sufficient. Aggregated proteins can no longer physically pass through the narrow barrels of proteasomes inactivating the proteasome in the process (Bence et al., 2001; Snyder et al., 2003). Inhibition of the

proteasome activates autophagy as an alternate compensatory mechanism for degradation of the accumulated protein aggregates (Kirkin et al., 2009b).

Autophagy is a catabolic, lysosome-dependent degradation system, by which bulky cytoplasmic substrates (such as organelles) are engulfed and degraded. The main function of autophagy is thought to be supplying amino acids for new protein synthesis and energy during starvation. However, it is also involved in the elimination of toxic macromolecules and damaged organelles, as well as clearing invading microbes (Deretic, 2010; Komatsu and Ichimura, 2010b; Levine and Kroemer, 2009; Mizushima et al., 2008). Autophagy mediated degradation is capable of targeting individual proteins, macromolecular complexes and entire organelles and is essential for cellular homeostasis and survival. Deregulation of autophagy has been implicated in neurodegenerative disease and cancer (Levine and Kroemer, 2009; Ohsumi, 2001; Xie and Klionsky, 2007). The autophagic process involves three processes by which cargo is delivered to the lysosome for degradation: 1) macroautophagy, 2) microautophagy and 3) chaperone-mediated autophagy (Xie and Klionsky, 2007). For the purpose of this document we will be focusing on macroautophagy.

Macroautophagy involves the formation of a crescent-shaped structure, the phagophore, which later expands to form the double membrane autophagosome. During this process, cargo destined for degradation by macroautophagy is recruited to the forming autophagosome. The autophagosome then fuses with lysosomes forming autolysosomes, degrading their contents in the process (Johansen and Lamark, 2011). Macroautophagy was always thought to be a non-selective process by which cells regenerate energy and amino acids during conditions of starvation, however, emerging

evidence has implicated macroautophagy in selective degradation of misfolded aggregating proteins (Komatsu et al., 2007; Pankiv et al., 2007; Rubinsztein, 2006; van der Vaart et al., 2008), organelles (peroxisomes) (Iwata et al., 2006), mitochondria (Geisler et al., ; Narendra et al., 2008; Novak et al., ; Okamoto et al., 2009), ER (Bernales et al., 2006) and ribosomes (Kraft et al., 2008). Autophagic adaptors p62/SQSTM1 (sequestosome1), NBR1 (neighbor of Brca1 gene) and the histone deacetylase 6 (HDAC6) have all been implicated in selective autophagic degradation of protein aggregates (Fig. 9) (Iwata et al., 2005; Kawaguchi et al., 2003; Kirkin et al., 2009a; Pankiv et al., 2007).

1.9.1 p62, NBR1 and Selective Autophagic Degradation of Protein Aggregates

Human p62 is a 440 amino acid protein which contains an NT PB1 domain, a ZZ-type zinc finger domain, nuclear localization signal (NLS), nuclear export signal (NES), LC3 interacting region (LIR), a KEAP1 interacting region (KIR), and a CT ubiquitin-associated domain (UBA) (Johansen and Lamark). The PB1 is a protein-protein interaction domain which enables p62 to interact with various protein kinases, such as NBR1, and to form p62-p62 homopolymers. The UBA domain allows p62 to interact with both mono and polyubiquitin, however, it has a higher affinity to monoubiquitin *in-vitro* (Long et al., 2008; Vadlamudi et al., 1996). p62 was found to accumulate in ubiquitin positive inclusion bodies in some neurodegenerative diseases, such as taupathies and synucleinopathies, as well as hepatic inclusion bodies present in various chronic liver diseases (Kuusisto et al., 2001; Strnad et al., 2008). Bjørkøy *et al.* further

Figure 9. A schematic diagram for the selective autophagic clearance of protein aggregates by p62, NBR1 and HDAC6. A) Protein aggregates are quickly recognized by the cellular machinery and ubiquitinated for degradation. Large protein aggregates can no longer be eliminated by the UPS and are therefore targeted for autophagy mediated degradation. Protein aggregates are recognized by the adapter proteins p62 and NBR1. Both of these proteins contain a ubiquitin binding domain allowing them to bind to ubiquitinated proteins destined for autophagy mediated degradation. In association with NBR1, p62 collects ubiquitin labeled protein aggregates into p62 bodies. p62 and NBR1 target protein aggregates to the autophagosome by associating with LC3. B) When the rate of protein aggregation surpasses the rate of clearance, to minimize toxicity, cells collect all protein aggregates at the MTOC forming aggresomes. HDAC6 binds to ubiquitinated protein aggregates and transports them along the microtubules to the MTOC. Recruitment of p62 to the aggresome assists in the autophagy mediated clearance of the aggregated proteins.

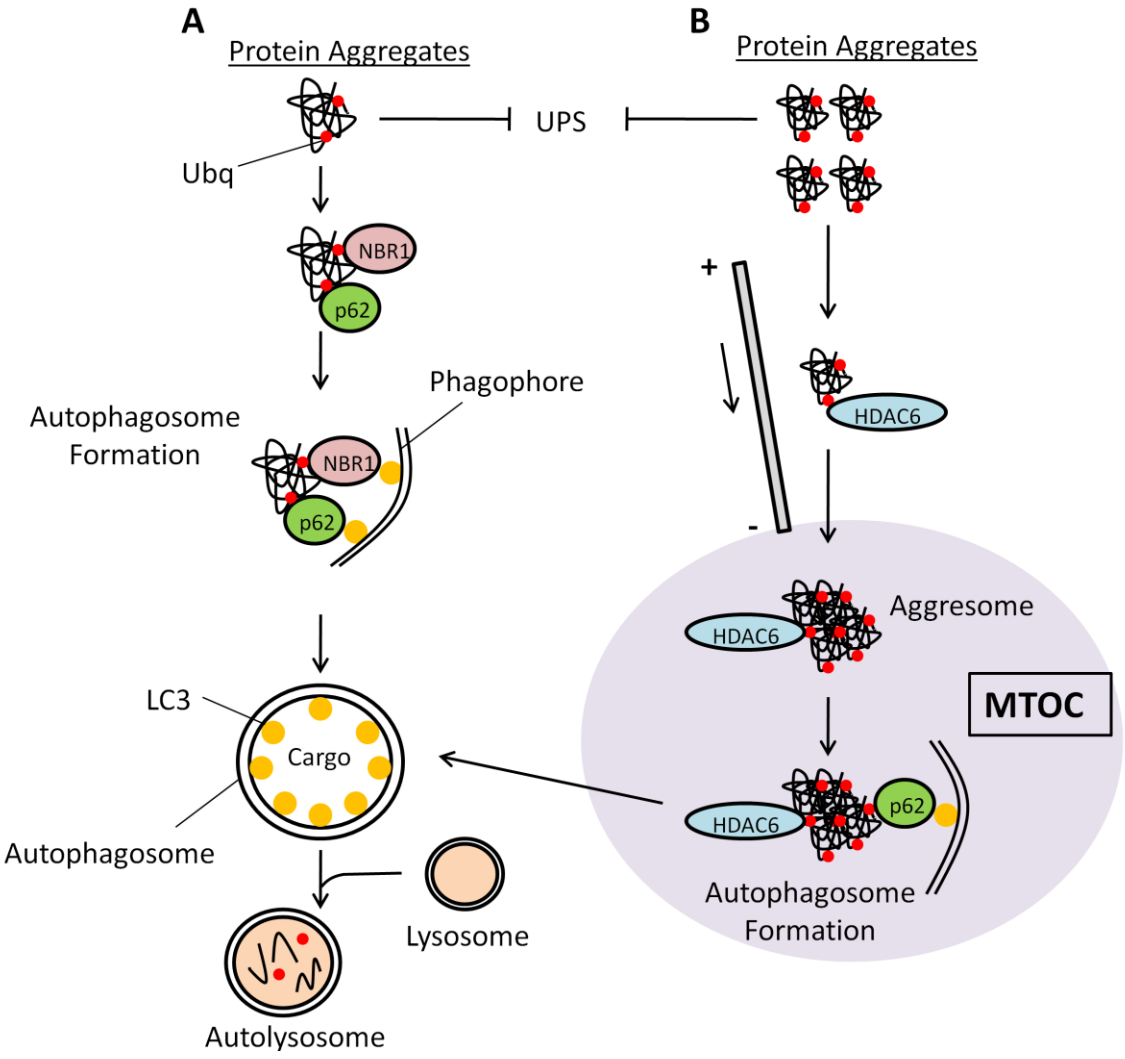
A
Protein Aggregates
Ubq
UPS
NBR1
p62
Phagophore
Autophagosome
Formation
NBR1
p62
LC3
Cargo
Autophagosome
Lysosome
Autolysosome
B
Protein Aggregates
+
HDAC6
-
HDAC6
Aggresome
MTOC
HDAC6
p62
Autophagosome
Formation

demonstrated that the autophagic marker light chain 3 (LC3) colocalized with p62 bodies and co-immunoprecipitated with p62. These experiments suggested a physical interaction between LC3 and p62 linking polyubiquitinated protein aggregates to autophagy (Bjorkoy et al., 2005). In 2007, Pankiv *et al.* for the first time provided evidence of a direct interaction between p62 and the autophagic marker LC3 narrowing down the interaction motif to the 22-amino acid LIR on p62. This study elucidated the mechanism of autophagic mediated degradation of protein aggregates and the role p62 plays in protein aggregate identification and selective targeting to autophagosome. By binding ubiquitin linked aggregated proteins via the UBA domain, polymerizing via the PB1 domain and binding LC3 via the LIR domain, p62 successfully targets aggregated proteins to the autophagosome for degradation (Pankiv et al., 2007).

NBR1 has been identified as another autophagic cargo receptor which is selectively degraded by autophagy. Like p62, NBR1 contains a PB1, UBA and ZZ-type zinc finger domain however it contains two LIR domains (Kirkin et al., 2009a; Kirkin et al., 2009b). The ability of NBR1 to interact with both LC3 and ubiquitin was demonstrated by Waters *et al*. (Waters et al., 2009). NBR1 in collaboration with p62, has been suggested to regulate the packing of polyubiquitinated misfolded proteins, and target them to autophagy mediated degradation (Fig. 9) (Kirkin et al., 2009a; Moscat and Diaz-Meco, 2009).

1.9.2 HDAC6, the Aggresome, and Microtubule Organizing Center

The swift elimination of protein aggregates via autophagy is required in order to minimize cellular stress and toxicity. Generally, protein aggregates are directly

eliminated by p62/NBR1 via autophagy, however, under conditions where the rate of protein aggregation exceeds that of clearance, the multi-ubiquitinated protein aggregates are transported to the microtubule organizing center (MTOC) by HDAC6 where they form the aggresome (Kirkin et al., 2009b). This is thought to be a protective mechanism whereby one large aggregate (aggresome) is less toxic than smaller diffused aggregates (Arrasate et al., 2004). HDAC6 moves soluble ubiquitin tagged aggregates to the MTOC by directly interacting with ubiquitin and the motor protein dynein. HDAC6 has also been shown to transport the autophagy machinery to the aggresome (Iwata et al., 2005). Once the aggresome is formed, recruitment of p62 to the structure targets the polyubiquitinated proteins to the autophagosome (Fig. 9).

1.10 Contact Inhibition

Contact inhibition was first described by Abercrombie and Heaysman as the inhibition of cell movement due to cell-to-cell contact in dense cultures (Abercrombie and Heaysman, 1954). The definition was based on experiments conducted on fibroblast-like cells extracted from chick hearts and neonatal mouse muscle (Abercrombie, 1970). Initial experiments looked at various aspects of cell behavior where fibroblasts were seeded at high densities to ensure cell to cell contact and estimates of cell movement, speed and direction were determined (Abercrombie and Heaysman, 1954). Later experiments using phase contrast cinematography of living cells confirmed that inhibition of cell movement was indeed a consequence of cell to cell contact (Abercrombie and Ambrose, 1958; Stoker and Rubin, 1967).

The term contact inhibition has also been used to refer to inhibition of cellular proliferation in high density cultures as a result of cell-to-cell contact. However, there has been some debate on whether inhibition of cell proliferation is linked to inhibition of cell movement in dense cultures. In a short communication published in Nature in 1967, Stoker and Rubin introduced the term density-dependent inhibition to describe inhibition of proliferation as a result of cell to cell contact. While the authors do not disagree with the idea that cell to cell contact inhibits cell proliferation, they suggest that inhibition of cell movement, contact inhibition, may be mechanistically different from inhibition of proliferation and as such it would be misleading to suggest that the underlying mechanism of both phenomena are the same (Stoker and Rubin, 1967). To avoid confusion for the purpose of this document, when the term contact inhibition is used it will solely refer to growth arrest induced by cell to cell contact in dense cultures.

The idea that cell to cell contact induces growth arrest was based on the observation that primary cells formed monolayers when left to grow to confluence in culture (Stoker and Rubin, 1967). This phenomenon is thought to be very important for organogenesis as well as wound healing. Loss of contact inhibition is often observed in cancer cells where growth is no longer inhibited upon contact, prompting cells to form disorganized multi-layers in culture. To date, the exact mechanism underlying contact inhibition is unknown. It is also not known how cell to cell contact can induce changes in cell cycle events. Cell adhesion molecules (CAMs) have been shown to play a role in this phenomenon (Takai et al., 2008). Nectins and nectin-like (NECL) molecules are immunoglobulin-like cell adhesion molecules which have been implicated in contact inhibition (Takai et al., 2008). Nectin and NECL molecules form homodimers on the cell

membrane surface where they can interact with nectin and NECL molecules on opposing cells. NECL-5 has been directly implicated in the regulation of cellular proliferation as a result of contact inhibition. NECL-5 enhances Ras, Raf and MEK signaling induced by mitogenic signals (growth factors) by inhibiting the activity of a protein termed sprouty2. Sprouty2 is activated in response to mitogenic signals by phosphorylation on a Tyr residue. Once activated, Sprouty2 inhibits Ras signaling stimulated by growth factors. In the absence of cell to cell contact, NECL-5 is present at the cell membrane effectively inhibiting the activation of sprouty2. When cells come into contact, NECL-5 interacts with nectin-3, a member of the nectin family, on the opposing cell membrane resulting in the downregulation of NECL-5 via endocytosis. With the downregulation of NECL-5, sprouty2 is released allowing for its activation which results in the inhibition of growth factor induced activation of Ras and subsequent cell proliferation.

1.11 Project Rationale

According to the Canadian Cancer Society (2011), 40% of Canadian women and 45% of Canadian men will develop cancer at some point during their lifetime. Of those individuals diagnosed with cancer, one out of four will die. As a result, development of new anti-cancer therapies is essential in improving prognosis and quality of life for cancer patients. Cancer cells have the ability to proliferate rapidly while ignoring anti-mitogenic signals. Genomic instability present in tumor cells increases the susceptibility of these cells to further undergo mutations, which in turn enhance proliferative capabilities and tumor aggressiveness (Hanahan and Weinberg, 2000). Some of these

mutations have been linked to alterations in the regulation of cyclins and CDKs either directly or indirectly (von Bergwelt-Baildon et al., 2011).

With the recent understanding that deregulation of CDKs plays a role in a variety of cancer cells, the prospect of targeting these kinases for possible therapeutic benefit has emerged. Currently, two types of scaffold-based CDK-inhibitors are being developed as potential cancer therapies which include ATP-competitive inhibitors and non-ATP competitive inhibitors. ATP competitive inhibitors are small molecule compounds, which are known to compete with ATP binding of CDKs. Since CDKs need ATP to function, binding of the ATP competitive inhibitors interferes with CDK activity (Rizzolio et al., 2010). Most of the CDK-inhibitors developed to date belong to the ATP-competitive group. Although first generation ATP-competitive inhibitors showed promise in preclinical trials, they did not reproduce anticancer activities in cancer patients. The major problem with ATP-competitive inhibitors is caused by the high sequence homology of the ATP pocket shared by all cellular kinases. As a result, most molecules designed to target CDKs are non-specific, and can thereby inhibit other cellular kinases, leading to high toxicity. This limits both the efficacy and dosage of most of the ATP-competitive inhibitors. Due to these limitations, non–ATP competitive inhibitors which target kinase substrates and regulatory binding sites have been developed since protein interactions and binding sites differ between protein kinases. This method allows for higher target specificity which would decrease side effects caused by off target kinase inhibition. Non-ATP competitive inhibitors are mainly divided into three groups: 1) inhibitor derivatives from CDK substrates, 2) inhibitors of CDK/cyclin complexes, and c) inhibitors of the cyclin binding groove (Rizzolio et al., 2010). It must be noted that most

if not all of this new class of drugs are peptide molecules. Peptides have multiple advantages over proteins and antibodies as a therapeutic drug. Some of these advantages include their ability to penetrate into tissues as a result of smaller size (some require fusion sequences to assist in cell entry), less immunogenicity, lower manufacturing costs, and greater stability (can be stored for longer periods of time at room temperature). In addition, when compared to small molecules, peptides exhibit greater specificity without causing any drug-drug interactions or systemic toxicities as a result of their metabolism. Metabolized peptides are broken down into amino acids, which are easily and safely processed by the body compared to various drugs (Vlieghe et al., 2010).

We have recently reported that a splice variant of cycD2, cycD2SV, is able to inhibit cardiomyocyte cell cycle by sequestering positive cell cycle regulators, such as CDK4, cycD2, cycB1, by directing them for ER associated degradation (Sun et al., 2009). Given the characterized function of cycD2SV in primary cells, this protein shows great promise as a template for an anticancer CDK-inhibitor therapeutic peptide. However, the effectiveness of cycD2SV to induce cell cycle exit in immortalized and transformed cell lines is yet to be determined. If cycD2SV is capable of inducing cell cycle exit in immortalized cell lines, further characterization of the cell cycle inhibition domain is necessary to create a therapeutic peptide. To date, it is also not clear whether cycD2SV plays any role in cell cycle regulation during cellular stress conditions, such as confluence and serum starvation.

Based on our previous studies with embryonic cardiomyocytes (Sun et al., 2009), we hypothesized that 1) cycD2SV is capable of inducing cell cycle arrest in transformed and immortalized cell lines and 2) a specific domain of cycD2SV is responsible for cell

cycle exit. Further mapping of this domain would enable us to develop a novel anti-cancer therapeutic peptide.

Work presented in this dissertation investigates the role of cycD2SV in cell cycle regulation using immortalized cell lines. In chapter 2, we characterize the effects of overexpression of cycD2SV mouse cDNA in human (HEK293, MCF7 and T47D) and mouse (NIH-3T3) immortalized cells, identify the mechanisms responsible for splice variant induced cell cycle exit, as well as, attempt to narrow down the cycD2SV cell cycle inhibitory domain by deletion experiments. In chapter 3, we characterize the expression profile of endogenous human cycD2SV in HEK293 cells during states of growth arrest, such as confluence and serum starvation. Additional studies presented in chapter 3 explore the critical role played by cycD2SV in the regulation of cycD2 stability during confluence culture conditions.

Chapter 2: Characterization of Growth Suppressive Function of a Splice Variant of Cyclin D2

2.1 Manuscript Status and Student Contribution

As first author on this manuscript, I performed the majority of experiments, completed all analysis, data interpretation, and statistics. I wrote the manuscript with input and assistance from Dr. Kishore Pasumarthi. This manuscript is currently in preparation for submission to the Journal of Biological Chemistry.

2.2 Abstract

We have recently cloned a novel splice variant of cycD2, termed cycD2SV from mouse embryonic cardiomyocytes. The mouse cycD2SV transcript encodes the first 136 amino acids of mCycD2 followed by a novel 20 amino acid CT region. CycD2SV overexpression in several immortalized cell lines led to formation of ubiquitinated protein aggregates accompanied by a significant decrease in cell proliferation. Secondary structure analysis revealed that the NT α-helix of cycD2SV is not tightly packed with the cyclin box, suggesting a misfolded conformation compared to other cyclins. Deletion analysis suggests that the 1-53 amino acid portion of cycD2SV may be responsible for protein aggregation and the 54-136 amino acid region for mediate cell cycle inhibition. Based on co-immunoprecipitation experiments, we have shown that cycD2SV binds to cycD2 as well as CDK4. In addition, gene expression analysis demonstrated an upregulation in GADD45α and dynamin 2 mRNA levels in cycD2SV overexpressing cells. These two proteins are known to play critical roles in the DNA damage response and apoptosis pathways. TUNEL experiments were negative for apoptosis suggesting that cycD2SV overexpression arrests the cell cycle but does not induce apoptotic cell death. However, cycD2SV expressing cells were more sensitive to cell death induced by external stressors, such as trypsinization. Collectively our results suggest that cycD2SV mediates cell cycle inhibition by sequestering endogenous cell cycle proteins, such as cycD2 and CDK4, targeting them for ubiquitin mediated protein degradation.

2.3 Introduction

Cell cycle progression in mammalian cells is dependent on interactions between cyclins and cyclin dependent kinases (CDKs) (Johnson and Walker, 1999). Specifically, mitogenic signals stimulate the expression of D-type cyclins (cycD1, D2 and D3), which bind to CDK4 and CDK6 (Johnson and Walker, 1999). Upon binding, the complex translocates to the nucleus where it phosphorylates pRb (Johnson and Walker, 1999). In an unphosphorylated state, the pRb protein binds and inactivates the transcription factor E2F (Johnson and Walker, 1999). Once phosphorylated, pRb dissociates from E2F, allowing E2F to upregulate genes necessary for S-phase entry, such as cycE, cycA, and CDK1, among other genes (Johnson and Walker, 1999).

CycD2SV is a recently discovered truncated splice variant of cycD2 that shares the first 136 amino acids of cycD2 with a unique 20 amino acid CT sequence (Denicourt et al., 2003). Given the sequence similarity between cycD2SV and cycD2, it is possible that cycD2SV is also a positive regulator of the cell cycle. In support of this hypothesis, a recent study by Denicourt *et al.* demonstrated that cycD2SV, in conjunction with H-Ras, is a more potent transforming protein as compared to cycD2 (Denicourt et al., 2008). However, they have not directly tested the effects of cycD2SV alone on cell cycle regulation.

We have recently reported that endogenously or exogenously expressed cycD2SV forms protein aggregates, and induces cell cycle arrest in embryonic cardiomyocytes (Sun et al., 2009). Mechanistically, we were able to demonstrate that cycD2SV sequesters cell cycle regulators, such as CDK4, cycD2, cycB1, thereby directing them for ER associated degradation (Sun et al., 2009). While our results with cardiomyocytes suggest that

cycD2SV is a negative cell cycle regulator, studies from Rassart's group clearly suggest a positive role for this protein (Denicourt et al., 2008). It is possible however that differences in cell type account for the discrepancy between these two studies.

In this study, we investigated the function of cycD2SV in multiple immortalized cell lines. Consistent with overexpression results obtained in primary cardiomyocytes, cycD2SV formed protein aggregates and significantly reduced cellular proliferation in T47D, NIH-3T3, HEK293 and MCF7 cells. We demonstrated that cycD2SV is able to bind to cycD2 as well as CDK4 and possibly interfere with their function and/or target them for ubiquitin mediated degradation. Further, cycD2SV expression was associated with impaired ERAD and increased autophagic responses required to eliminate protein aggregates. In addition, we report that the cycD2SV cell cycle inhibition domain is present in the 54-136 sequence of the protein.

2.4 Materials and Methods

2.4.1 Cell Culture and Transient Transfection

HEK293, NIH3T3, MCF-7 and T47D cells were purchased from the American Type Culture Collection (ATCC, Virginia). Cells were cultured in Dulbecco modified Eagle's medium (DMEM, Wisent, Saint-Bruno, Quebec) supplemented with 10% fetal bovine serum (10% FBS-DMEM), 1x antimycotic-antibiotic (AB/AM, 1,000 units penicillin G sodium, 1,000 µg streptomycin sulfate, and 2.5 µg amphotericin B as Fungizone® in 0.85% saline), and 1 mM sodium pyruvate at 37°C in a humidified incubator set at 6% CO_2 (Thermo Fisher Scientific, Nepean, Ontario). Cells were seeded

at 600,000 cells in 100 mm dishes, and at 150,000 in 35 mm dishes at day 0. At day 2, cells were transfected with expression constructs using Lipofectamine™ 2000 according to manufacturer's instructions (Invitrogen, Burlington, Ontario). In brief, media was aspirated, serum free DMEM (Hi-DMEM) was added to the dishes (10 ml/100 mm dish, 2 ml/35 mm dish), and the dishes were returned to the incubator. At 0.5 hours, the lipofectamine-DNA cocktail was prepared, where 500µl of Opti-MEM® (Invitrogen, Burlington, Ontario) was added to two microcentrifuge 1.5ml tubes for 100 mm dish transfections, or 200 µl of Opti-MEM® for 35 mm dish transfection. One tube received the plasmid DNA, while the other tube received Lipofectamine™ 2000 (Invitrogen, Burlington, Ontario). The microcentrifuge tubes were left to stand for 5 minutes then mixed by transferring the contents of the Lipofectamine™ 2000 tube to the DNA microcentrifuge tube. The Lipofectamine™ 2000-DNA cocktail was gently mixed by pipetting, and left to stand for 17 minutes at room temperature. Once the 17 minutes had lapsed, the lipofectamine-DNA cocktail was added to the appropriate dish slowly dropwise and the dishes were returned to the incubator. Cells were incubated with the transfection mixture for 5 hours and were subsequently maintained in freshly added 10% FBS-DMEM for 18 hours post transfection, unless otherwise stated. Transfection efficiency was routinely determined by EGFP-C1 transfections where, on average, it was found to be between 50-60%. To maintain sterility, the transfection protocol was carried out in a ThermoForma class II A2 biological safety cabinet (Thermo Fisher Scientific, Nepean, Ontario). Cells plated in 100 mm dishes received 4 µg of DNA and 10 µl of Lipofectamine™ 2000 reagent, while cells seeded in 35mm dishes received 1.7 µg of DNA and 4.3 µl of Lipofectamine™ 2000 reagent. For co-transfection of two expression

constructs, cells were transfected at a 1:1 ratio of the DNA constructs, such that 100 mm dishes received 2 μg, and 35 mm dishes received 0.425 μg of each construct. All cell culture reagents were purchased from Invitrogen (Burlington, Ontario).

2.4.2 Cloning and Generation of Expression Constructs

To generate the pcDNA-cycD2myc, mouse cycD2 cDNA was PCR amplified from an existing cycD2 construct (Pasumarthi et al., 2005) using the cycD2S and cycD2AS primers (Table 3). Once amplified, the cycD2 fragment was subcloned in to the pcR2.1 vector (Invitrogen, Burlington, Ontario), restriction digested with xho1 and xba1 and ligated into pcDNA 3.1 vector in frame with myc epitope sequence. CycD2SV sequence was amplified from mouse embryonic heart total RNA. Isolated RNA was reverse transcribed with Supercript II reverse transcription kit, and cDNA was amplified using D2ex1S and D2altAS2 primers. PCR amplified sequences were first cloned into pcR2.1 vector (Invitrogen, Burlington, Ontario) and subsequently cloned into pcDNA 3.1 vector and fused in frame with myc. The EGFP-D2SV was generated by amplifying cycD2SV fragment using D2SVS4 and D2altAS primers from pcR2.1-cycD2SV and cloning the fragment in CMV-EGFP-C1 vector (Clontech, Mountain View, California), in frame with EGFP. CycD2SVΔCTmyc and cycD2SV 54-136myc were generated by amplifying 1-136 and 54-136 portion of cycD2SV from TA-cycD2SV construct using D2ex1S and D2 1-136AS-Xba1 or D2 54-136S and D2 136AS-Xba1 primer pairs. The following constructs were received as generous gifts: TCRα-GFP [Dr. John Christianson, Stanford University, (DeLaBarre et al., 2006)], cycB1 [Dr. Karl Riabwol, University of Calgary, (Meyyappan et al., 1998)], mcherry-p62 [Dr. Terje Johansen, University of

Table 3. Primers used for DNA expression construct creation.

Construct	Primer Name	Sequence 5' – 3'
pcDNA-cycD2SV	*D2ex1S*	F AGTGGTGGCCGGCTGGCTATGGAGC
	D2altAS	R CTTACAGTCTTGGTTAGTGTGGCGG
pcDNA-cycD2SVmyc	*D2ex1S*	F AGTGGTGGCCGGCTGGCTATGGAGC
	D2altAS2	R GCCTCTAGAGTGTGGCGGCCTTAGTGTGATGGGG
pEGFP-D2SV	*D2SVS4*	F GCCAGATCTAGTGGTGGCCGGCTGGCTATGGAGC
	D2altAS	R CTTACAGTCTTGGTTAGTGTGGCGG
pcDNA-cycD2SVΔCTmyc	*D2ex1S*	F AGTGGTGGCCGGCTGGCTATGGAGC
	D2 1-136AS-Xba1	R GCTCTAGACAGCAGCTCCTGGGGCTTCAC
pcDNA- cycD2SV 54-136myc	cyc*D2 54-126S*	F CGGCTGGCTATGGAGATGCGCAGGATGGTG
	D2 1-136AS-Xba1	R GCTCTAGACAGCAGCTCCTGGGGCTTCAC
pcDNA- cycD2myc	cyc*D2S*	F GCCCTCGAGATGGAGCTGCTGTGCTGCGAGGTG
	cyc*D2AS*	R GCCTCTAGACAGGTCAACATCCCGCACGTCTGT

F= forward primer; R= reverse primer

Tromsø, (Lamark et al., 2003; Pankiv et al., 2007)], YFP-intersectin [Dr. John P. O'Bryan, University of Illinois, (Mohney et al., 2003)], HA-H-Ras [Dr. Patrick Lee, Dalhousie University, (Leidal et al., 2012)], and HA-ubiquitin (Dr. James Fawcett, Dalhousie University). All subcloning was performed in accordance with standard molecular biology techniques as described in molecular cloning by Mariatis. The fidelity of all constructs was confirmed by DNA sequencing (Robarts Research Institute, London, Ontario).

2.4.3 Immunofluorescence

Cells were plated on coverslips (22x22 mm 0.08-0.13mm thickness, VWR, Mississauga, Ontario) in 35mm dishes, and transfected as described earlier. Cells were fixed in cold methanol for 15 minutes at 4°C, washed in cold phosphate buffered saline (PBS: 0.138 M NaCl, 0.0027 M KCl, pH 7.4), permeabilized in 0.1% Triton X-100 for 5 minutes, and blocked with blocking buffer (1% v/v bovine serum albumin (BSA), 10% v/v goat serum in PBS) for one hour. Cells were probed with primary antibodies raised against myc (sc-40), cycD2SV, HA (sc-805), CDK4 (sc-260), cycB1 (sc-245), cycD2 (sc-593), and γ-tubulin (sc-10732) for one hour at 25°C, followed by a one hour incubation with secondary goat anti-mouse antibodies, conjugated to Alexa Fluor 488 or goat anti-rabbit antibodies conjugated to Alexa Fluor 555 dye (Invitrogen, Burlington, Ontario) for one hour. Subsequently, cells were incubated with 10 mg/ml bisBenzimide H 33342 trihydrochloride (Hoechst 33342) nuclear stain (Sigma-Aldrich, Oakville, Ontario) for five minutes, washed extensively in cold PBS and mounted on glass slides using 1% w/v propyl 3,4,5-trihydroxybenzoate (propyl gallate) in a 1:1 PBS/glycerol solution. Primary

antibodies were diluted 1:50, and secondary antibodies were diluted 1:200 in block buffer unless otherwise stated. Generation of cycD2SV homemade antibodies was previously described, (Sun et al., 2009) and additional details are provided in chapter 3 (See section 3.4.1). All other antibodies were purchased from Santa Cruz Biotechnology Inc. as denoted by the sc present in the catalogue numbers. Images were captured using a Leica DM2500 fluorescence microscope, fitted with a DFC500 digital acquisition system (Leica Microsystems, Concord, Ontario).

2.4.4 [^{3}H]-thymidine labeling and autoradiography

Transfected cells were maintained for twelve hours and pulsed with [^{3}H]-thymidine (GE Healthcare Life Sciences, New Jersey) at a concentration of 1.0 μCi per 1ml of medium for six or twenty-four hours at 37˚C. Cells were fixed in cold methanol for fifteen minutes and processed for immunofluorescence as described earlier. Coverslips were air dried, coated with Kodak autoradiography emulsion type NTB (MarketLINK Scientific, Burlington, Ontario) and placed in a light-tight box at 4°C for 3 days. Coverslips were developed in Kodak-D19 developer (Sigma-Aldrich, Oakville, Ontario) for four minutes, washed in double distilled water (ddH_2O), fixed with Ilford rapid fixer (Polysciences, Pennsylvania) for four minutes, and mounted on glass slides using propyl gallate solution. Cellular morphology was examined under bright field, and nuclei were identified with epi-fluorescence microscopy. Cells containing more than fifteen nuclear silver grains were identified as cells undergoing DNA synthesis.

2.4.5 Protein extraction, Immunoblotting and Immunoprecipitation

Transfected cells were harvested in tumor lysis buffer (1% NP40/Igpal, 5mM EDTA, 50mM Tris HCl pH 8.0, 10mM phenylmethylsulphonyl fluoride (PMSF) and 1mM Aprotinin), sonicated and centrifuged at 13,300 rpm for fifteen minutes at 4°C. The cytosolic fraction was collected, and protein concentration was determined by the Bradford assay (Thermo Fisher Scientific, Nepean, Ontario) as indicated by the manufacturer. Equal amounts of protein (40-60µg) were denatured in Lamelli buffer (62.5 mm Tris-Cl pH 6.8, β-mercaptoethanol, 25% glycerol, 2% SDS, 0.02% bromophenol blue) and resolved in 12.5% polyacrylamide gel [0.375M Tris-HCl, 0.08% SDS, 12.5% acrylamide, 0.2% ammonium persulphate and 20µl tetramethylethylenediamine (TEMED)] at 100 volts. The resolved samples were electrophoretically transferred from the gel to Hybond ECL nitrocellulose membranes (GE Healthcare Life Sciences, New Jersey) by applying a constant current at 100 volts for one hour. The nitrocellulose membrane was stained with napthol blue (1% napthol blue black, 45% methanol and 10% glacial acetic acid) for protein visualization and determination of equal loading. The membrane was rinsed with ddH2O for five minutes and blocked for one hour in PBS containing 0.1% Tween 20, 5% skimmed milk powder and 3% BSA. The blots were incubated for one hour with primary antibodies specific for the following proteins: cycD2SV (1:500), cycD1 (sc-753, 1:500), cycD2 (sc-593, 1:500), p27 (sc-528, 1:500), CDK4 (sc-260, 1:10,000), α-tubulin (sc-8035, 1:5000), and c-myc (sc-40). The blots were washed in 0.1% Tween 20-PBS and incubated with goat-anti rabbit, or goat-anti mouse secondary antibodies conjugated to horse radish peroxidase (HRP) for one hour. Protein bands were detected by ECL Plus Western Blotting

Detection System via the chemiluminescence method according to manufacturer's instructions (GE Healthcare Life Sciences, New Jersey).

For immunoprecipitation, control pcDNA 3.1 vector, cycD2SVmyc, cycD2myc or cycD2myc plus cycD2SV transfected cells were lysed in tumor lysis buffer eighteen hours post transfection. 500µg of protein was incubated with 0.5-1 µg of cycD2SV, cycD2 or myc antibodies for seventeen hours at 4°C, followed by the addition of protein-A-Sepharose beads (GE Healthcare Life Sciences, New Jersey) for one hour at 4°C. Immunocomplexes bound to the beads were collected by centrifugation at 3,000 rpm for one minute, resuspended in Lamelli buffer [0.25 M Tris-Cl pH 6.8, β-mercaptoethanol, 25% glycerol, 2% sodium dodecyl sulfate (SDS), 0.02% bromophenol blue and double distilled water (ddH_2O)] and heated at 95°C for five minutes. The immunoprecipitated samples were resolved on a 12.5% SDS-PAGE gel, electrophoretically transferred to Hybond ECL nitrocellulose membranes and processed for chemiluminescence detection as described earlier.

2.4.6 Apoptosis Assay

Transfected cells seeded on coverslips were fixed with freshly prepared 4% paraformaldehyde in PBS for one hour at room temperature, washed with PBS and permeabilized in 0.1% triton X-100 and 0.1% sodium citrate for two minutes at 4°C. Cells were processed for TUNEL staining according to the manufacturer's instructions (Roche in Situ Cell Death Detection Kit, TMR red). TUNEL positive cells were counted using fluorescence microscopy.

2.4.7 Fluorescence Activated Cell Sorting and QPCR Array Analysis

HEK293 cells were seeded at 600,000 cells per 100mm dish and allowed to grow for 48 hours. Cells were transfected with EGFP-D2SV or EGFP-C1 control plasmid for six hours, and grown under subconfluent conditions. After 48 hours, cells were trypsinized, centrifuged at 2,000 rpm for two minutes, and resuspended in PBS. To eliminate cell clumps, cells were passed through a 40μm mesh filter. To prepare for fluorescence activated cell sorting (FACS), cells were centrifuged again and resuspended in 1ml of sorting buffer (PBS containing 15mM Hepes, 1mM EDTA, 0.5% BSA). Transfected cultures were sorted for EGFP-C1 or EGFP-D2SV cell populations using a BD FACSCanto II flow cytometer. Sorted cells were pelleted by centrifugation at 2,000 rpm for two minutes and cell pellets were processed for RNA extraction using an RNeasy PLUS kit (Qiagen, Mississauga, Ontario). In brief, lysed cells underwent a series of filtration and washing steps in filter columns, where genomic DNA (gDNA) was eliminated and RNA was collected in RNase/DNase free water. RNA samples with an A260/280 ratio of 1.8 to 2.0 were considered pure, and devoid of DNA contamination. Subsequently, RNA samples were analyzed for any changes in transcriptional profile of 84 cell cycle genes by using the Human Cell Cycle RT^2 *ProfilerTM* PCR Array (Qiagen, Mississauga, Ontario).

As recommended by the manufacturer, extracted mRNA was reverse transcribed to cDNA using the RT^2 First Strand Kit (Qiagen, Mississauga, Ontario) prior to loading into the QPCR cell cycle array for gene amplification. QPCR conditions were set on the MX3000P® thermocycler (Stratagene, La Jolla, California) according to the manufacturer's instructions. Gene expression was normalized to five control

housekeeping genes [Glyceraldehyde-3-phosphate dehydrogenase (GAPDH), Beta-2-microglobulin (B2M), Hypoxanthine phosphoribosyltransferase 1 (HPRT1), Ribosomal protein L13a (RPL13a), and Beta Actin (ACTB)] using the $\Delta\Delta C_T$ method (Livak and Schmittgen, 2001). To ensure the reliability and quality of the QPCR data, the PCR arrays also contained gDNA control, reverse transcriptase controls and positive PCR controls.

2.4.8 Trypsinization and Cell Death Experiments

HEK293 cells transfected with EGFP-D2SV or EGFP-C1 control, were trypsinized and reseeded at 30,000 cells in 35 mm dishes with etched grid coverslips (Belko, Vine-land, New Jersey) in accordance with live cell imaging methods, as published by our lab (McMullen et al., 2009). At five hours post plating, the location of 7-20 transfected cells was recorded. Subsequently, cell adherence was recorded at 20, 48, 68 and 80 hours via fluorescence imaging of live cells with a Leica DMIL inverted microscope, fitted with a DFC500 camera.

2.4.9 Electron Microscopy and Sample Preparation

HEK293 transfected with cycD2SVmyc were fixed overnight with 4% paraformaldehyde and 0.5% glutaraldehyde in 0.1 M sodium cacodylate buffer. Cells were scraped and collected in 1.5 ml eppendorf tubes, and dehydrated in a graded series of ethanol. Cells were embedded in LR White resin (Canemco-Marivac) and sectioned in ultrathin 80 nm slices. The sections were placed on nickel grids where they were washed in sodium borohydride followed by 30 mM glycine in 0.1 M borate buffer (pH 9.6).

Sections were then blocked in blotting buffer (5% skimmed milk powder, 3% BSA, 0.1% Tween 20 in PBS) for 45 minutes, incubation with primary cycD2SV antibodies for one hour, followed by secondary anti-rabbit IgG antibodies coupled to 10 nm gold particles (Sigma-Aldrich, Oakville, Ontario) for one hour. After primary and secondary antibody incubations, the sections were washed three times with PBS (five minutes for each wash). Finally, sections were post-fixed in 2.5% glutaraldehyde, washed in PBS, and counterstained with uranyl acetate and lead citrate. For controls, primary cycD2SV antibodies were omitted. Method was adapted based on previous work done in our lab (Zhang and Pasumarthi, 2007).

2.4.10 Statistical Analysis

Unless otherwise stated, all data comparisons were completed using an unpaired two-tail t-test, a one-way or two-way analysis of variance (ANOVA). Date which contained two groups for the measurement variable were analysed by unpaired two-tail t-test whereas data with multiple groups of the measurement variable were analyzed with ANOVA. One-way ANOVA was completed on data sets which contained one nominal variable and one measurable variable (http://udel.edu/~mcdonald/statintro.html). Two-way ANOVA was completed on data sets which contained two nominal variables and one measurable variable. Significance obtained by one-way ANOVA was subjected to a Tukey-Kramer's test for *post-hoc* analysis while a significance obtained by two-way ANOVA was subjected to a Bonferroni *post-hoc* test. Data is expressed as mean ± SEM and was considered statistically significant when the difference in mean values between groups had a P value of 0.05 or less.

2.5 Results

2.5.1 Overexpression of CycD2SV Promotes Intracellular Protein Aggregation in Immortalized Cell Lines

We have previously demonstrated the ability of cycD2SV (mouse cycD2SV) to form aggregates and induce cell cycle exit in mouse embryonic cardiomyocytes (Sun et al., 2009). Based on this observation we sought to investigate the effects of cycD2SV expression in transformed cell lines. Transfection of both myc tagged and untagged (data not shown) cycD2SV in HEK293, NIH-3T3, T47D and MCF-7 cell lines revealed a distinct micro-aggregated staining pattern (Fig. 10A, B; H-M). In-depth quantitative analysis in HEK293 cells revealed that protein aggregates were present in > 90% of HEK293 cells transfected with cycD2SVmyc (Fig. 10G). In contrast, such protein aggregates were undetectable in control cultures not transfected with any plasmid DNA or cultures transfected with cycB1 (Fig. 10E-G). Subcellular localization studies revealed that cycD2SV protein aggregates were localized exclusively in the cytoplasm or nuclear compartments in approximately 75% of transfected cells, whereas 25% of transfected cells contained protein aggregates in both cytoplasmic and nuclear compartments (data not shown). Interestingly, >50% of cells transfected with cycD2 also revealed protein aggregation in these experiments (Fig. 10C, D and G). In contrast to multiple micro-aggregates in McycD2SV transfected cells, cycD2 overexpressing cells frequently contained one large aggregate which localized to nuclear or perinuclear compartments (Fig. 10C, D). We also observed a similar micro-aggregation pattern of endogenous cycD2SV protein in non-transfected HEK293 cells using previously described and well

Figure 10. Characterization of cycD2SV aggregation in immortalized cell lines. HEK293 cells transfected with cycD2SVmyc (A, B), cycD2myc (C, D) and cycB1(Mouse cycB1) (E, F) processed for myc (A, C) and cycB1 (E) immunostaining and nuclear stain (B, D, F). MCF-7 (H, K), T47D (I, K) and NIH-3T3 (J, M) cells transfected with cycD2SVmyc and processed for myc (H, I, J) immunostaining and nuclear stain (K, L, M). The percentage of HEK293 cells positive for protein aggregation was determined for cycD2SVmyc, cycD2myc and cycB1 transfected cells (G). Cells positive for protein aggregates were quantified and expressed as a percent of total counted cells (D). Non-transfected (Non-tf) cells were used as a control for protein aggregation. Values are expressed as mean ± SEM. One way ANOVA, *$p < 0.05$ compared to non-transfected control, approximately 1000 cells were counted for each group from three independent experiments (N=3). Scale bar is 20 μm.

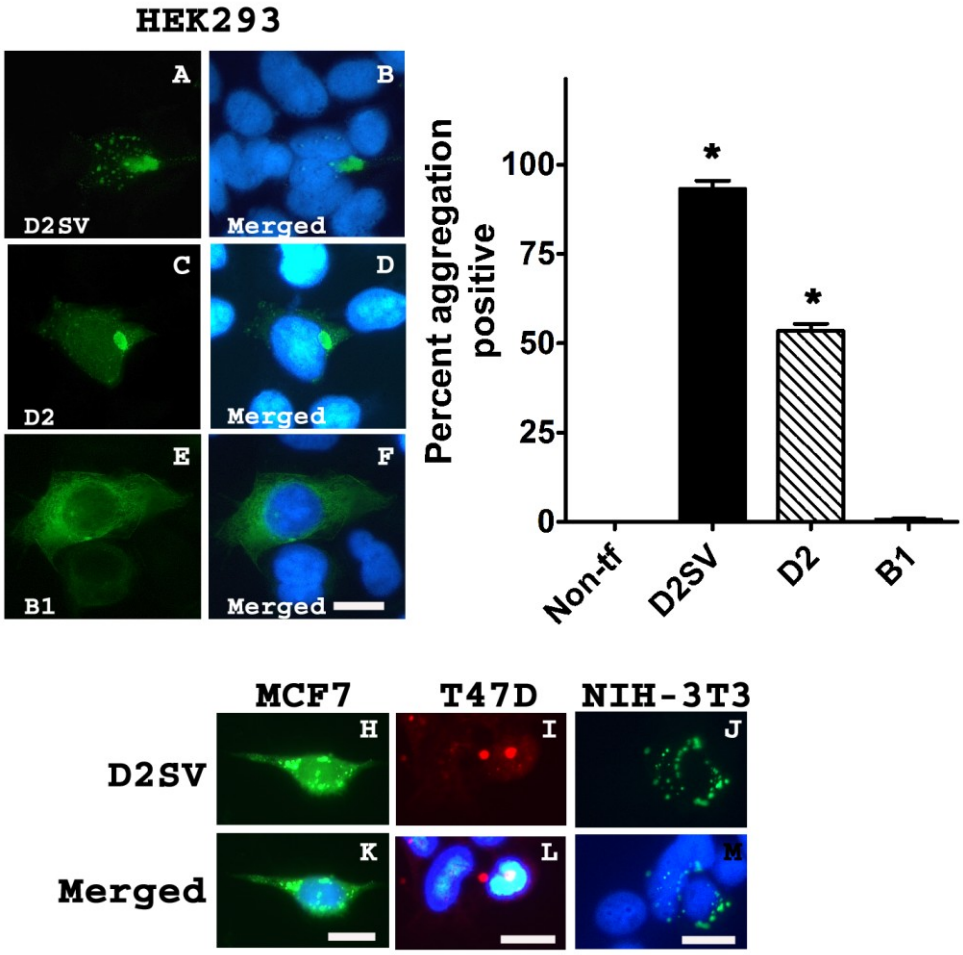
HEK293
A
B
D2SV
Merged
C
D
D2
Merged
E
F
B1
Merged
Percent aggregation positive
100
75
50
25
0
*
*
Non-tf
D2SV
D2
B1
MCF7
T47D
NIH-3T3
D2SV
H
I
J
Merged
K
L
M

characterized polyclonal antibodies [(Sun et al., 2009), Fig. 11A, B, see 3.5.1 to 3.5.3]. In contrast, immunostaining for endogenous cycD2 in HEK293 cells revealed diffuse staining in both nuclear and cytoplasmic compartments, and was rarely associated with any aggregate formation (Fig. 11C, D). Collectively, our results suggest that both endogenous (Human) and overexpressed (Mouse) cycD2SV can form micro-aggregates, whereas only overexpressed cycD2 is subjected for aggregation in immortalized cell lines.

2.5.2 CycD2SV Mediates Cell Cycle Exit in Various Cell Lines

The major focus of this study was to determine whether cycD2SV expression in non-cardiac cell types leads to cell cycle arrest similar to the result that we reported for cardiomyocytes, (Sun et al., 2009), or alternatively causes a proliferative phenotype as suggested by an independent research group (Denicourt et al., 2008). To characterize the effects of cycD2SV on cell cycle activity, we first monitored G1/S-phase transit in HEK293 cells transfected with cycD2SVmyc, cycD2myc, cycB1 or a pcDNA 3.1 vector control. Cells were processed for anti-myc immunostaining and *in situ* [^{3}H]-thymidine autoradiography. The labeling index (LI) was assessed as the proportion of the total number of transfected cells that displayed nuclear [^{3}H]-thymidine silver grains (Fig. 12A-C). Cells transfected with cycD2SV and cycD2 were identified by myc staining, whereas cells expressing cycB1 were identified by cycB1 antibody staining. In the case of pcDNA 3.1 vector transfected control cultures, we monitored the LI using Hoechst 33342 nuclear staining and silver grains. The LI of HEK293 cells overexpressing cycD2SV was significantly lower when compared to that of non-transfected cells or those transfected

Figure 11. Endogenous expression of cycD2SV and cycD2 in HEK293 cells. HEK293 cells were processed for cycD2SV (A) and cycD2 (C) immunostaining and nuclear stain (B, D, and F). Primary antibody was omitted as a control (E, F). Scale bar is 20 μm. End., endogenous; Cont., control.

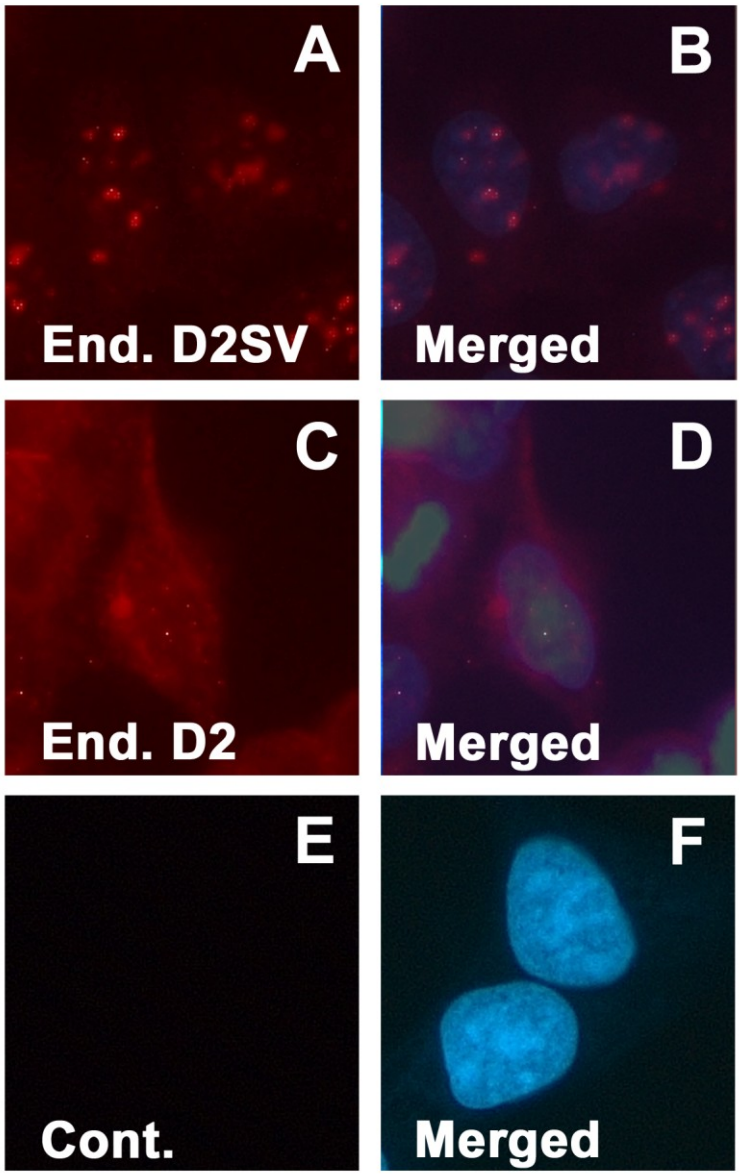
A
End. D2SV
B
Merged
C
End. D2
D
Merged
E
Cont.
F
Merged

with vector alone (8% Vs 45%; approximately five-fold reduction, Fig. 12D). The LIs of cells transfected with cycD2 and cycB1 were also monitored as controls to eliminate the possibility that the observed effects on the cell cycle is due to the general overexpression of cell cycle proteins. While cell cycle activity was significantly elevated in cells expressing cycB1 (approximately 1.3-fold), the G1/S transit rate was significantly decreased in cells expressing cycD2 (approximately 2.5-fold; Fig. 12D). Similar to HEK293, other cell lines (NIH-3T3, T47D and MCF-7) transfected with cycD2SV also showed a significant reduction in [^{3}H]-thymidine labeling when compared to control transfected cells (Approximately 60 to 80-fold**,** Fig.13). These results suggest that overexpression of cycD2SV in non-cardiac cell types also leads to a cell cycle arrest, but not a proliferative phenotype as suggested by an earlier study (Denicourt et al., 2008).

2.5.3 Enforced Expression of CycD2SV and Activated Ras Oncogene does not Increase Cell Cycle Activity or Cellular Transformation

Co-expression of cycD2SV and activated H-Ras (EJ 6.6 construct) was shown to promote transformation of primary mouse embryonic fibroblasts using a focus formation assay by Denicourt *et al* (Denicourt et al., 2008). The oncogenic H-Ras EJ6.6 harbors a single amino acid substitution, leading to the replacement of a glycine to valine residue at amino acid position twelve in the first exon (H-Ras-Val12). The latter is responsible for conversion of the proto-oncogene H-Ras, into an active oncogene (Tabin et al., 1982; Tabin and Weinberg, 1985). To examine whether growth suppressive properties of cycD2SV can be mitigated by activated Ras, we co-transfected HEK293 cells with cycD2SV and H-Ras-Val12 constructs and processed them for double immunostaining and [^{3}H]-thymidine autoradiography. H-Ras-Val12 staining was diffused and frequently

Figure 12. CycD2SV expression decreases the number of cells entering S-phase in HEK293 cultures. Photomicrographs depict examples of [^{3}H]-thymidine labelling assay (A-C). HEK293 cells transfected with cycB1 and labeled with [^{3}H]-thymidine were visualized by cycB1 immunostaining (A), nuclear stain (B) and [^{3}H]-thymidine autoradiography (C). Cells positive for [^{3}H]-thymidine contained nuclear silver grains in the nucleus and were visualized under bright field microscopy (C). Cells positive for [^{3}H]-thymidine were quantified and expressed as a percent of total counted cells (D). pcDNA 3.1 vector transfected cells were used for control (cont). Values are expressed as mean ± SEM. One way ANOVA, *$p < 0.05$ compared to the LI of control cells, approximately 1000 cells were counted for each group from three independent experiments (N=3). Scale bar is 20 μm.

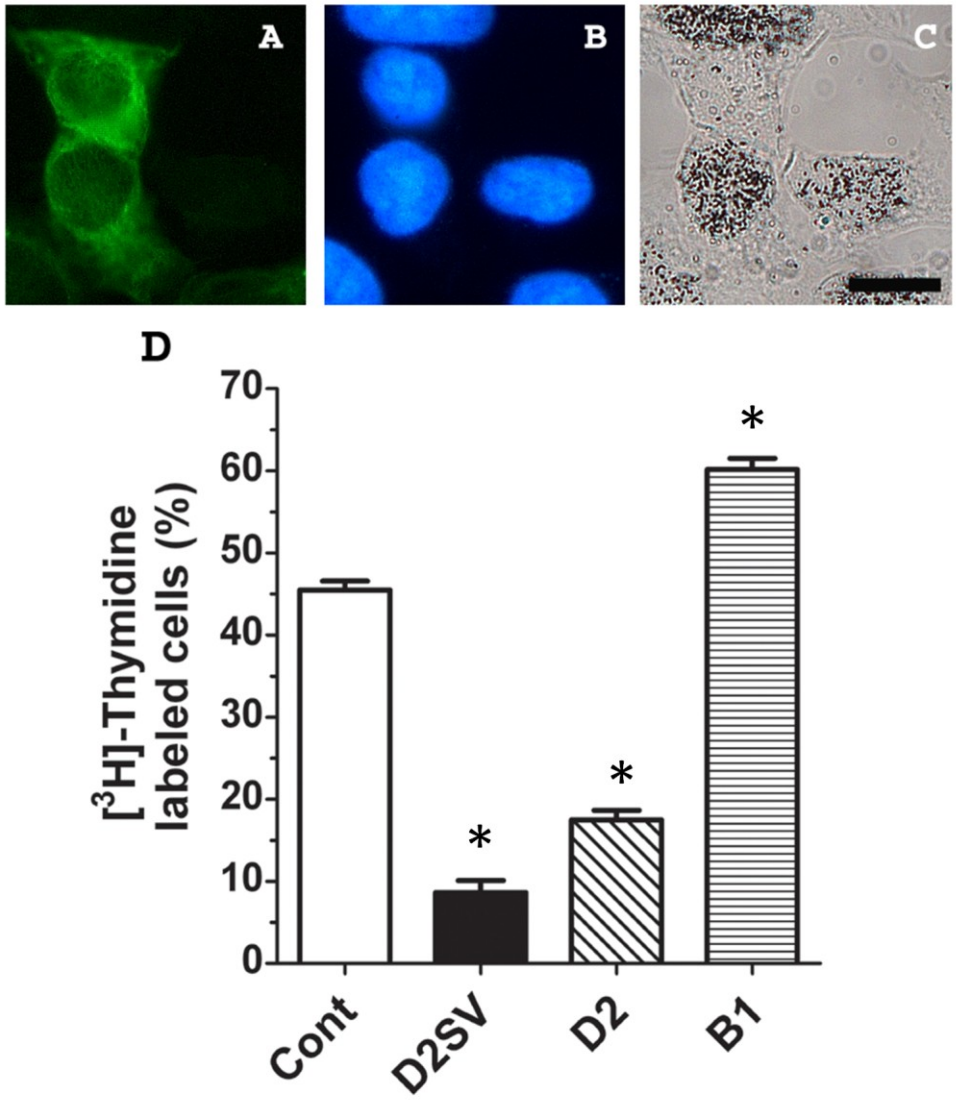
A
B
C
D
[3H]-Thymidine labeled cells (%)
70
60
50
40
30
20
10
0
*
*
*
Cont
D2SV
D2
B1

Figure 13. [^{3}H]-thymidine labeling of NIH-3T3, T47D and MCF-7 transfected with cycD2SVmyc or pcDNA vector (control). Cells positive for [^{3}H]-thymidine were quantified and expressed as a percent of total transfected cells. Cells transfected with pcDNA vector were used for control. Values are expressed as mean ± SEM. Unpaired two-tailed t-test, *$p < 0.05$ compared to respective controls, approximately 1000 cells were counted for each group from three independent experiments (N=3).

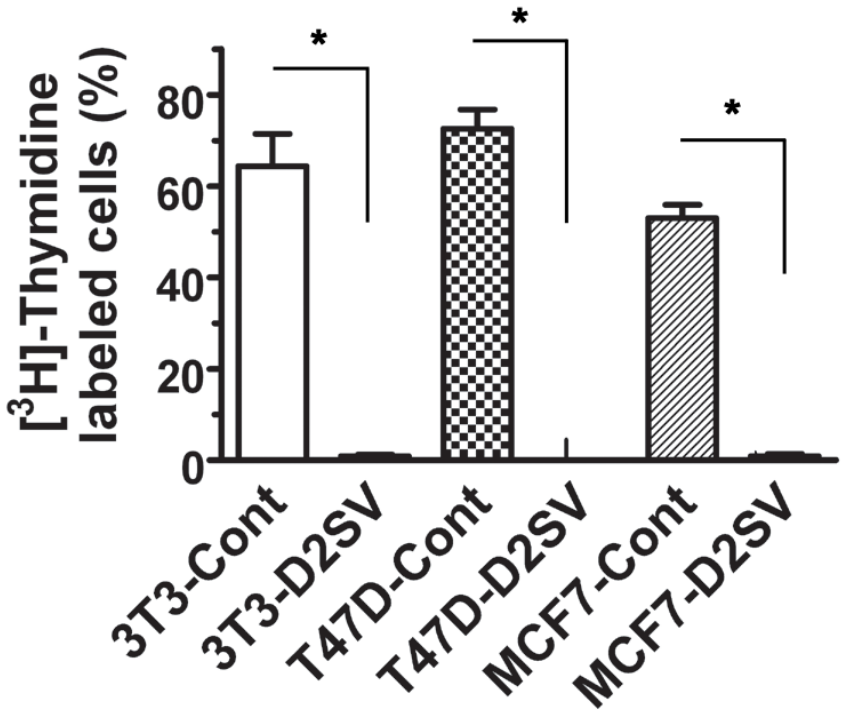
[3H]-Thymidine labeled cells (%)
0
20
40
60
80
*
*
*
3T3-Cont
3T3-D2SV
T47D-Cont
T47D-D2SV
MCF7-Cont
MCF7-D2SV

localized to the cytoplasmic and perinuclear compartments in both single transfected, and co-transfected cells (Fig. 14B). Furthermore, no apparent co-localization of H-Ras and cycD2SV was observed and micro-aggregation pattern of cycD2SV was well preserved in co-transfected cells (Fig. 14A-C). Approximately 9-11% of cells transfected with cycD2SV or H-Ras were positive for [^{3}H]-thymidine incorporation compared to a 30% LI in control transfections (Fig. 14D). When cells were co-transfected with cycD2SV and H-Ras, the [^{3}H]-thymidine incorporation did not change and the LI remained at 10%. To ensure that the expression levels are comparable, protein lysates from transfected cultures were assessed by immunoblotting. Similar amounts of H-Ras or cycD2SV proteins were observed in both single and co-transected cultures (Fig. 14E). These results suggest that activated H-Ras is not sufficient to prevent cycD2SV mediated growth arrest or promote cellular transformation in HEK293 cells.

2.5.4 The 54-136 Amino Acids Region of CycD2SV is Responsible for Cell Cycle Inhibition

To map the sequence domain(s) responsible for cell cycle inhibition and or protein aggregation, we generated two new constructs: cycD2SVΔCT and cycD2SV54-136, which code for truncated versions of cycD2SV (Fig. 15A). The cycD2SVΔCT construct encodes the first 136 amino acids common to both cycD2SV and cycD2, but lacks the 20 amino acid CT-region unique to cycD2SV. In contrast, the cycD2SV54-136 construct codes for amino acids 54-136 common to both cycD2 and cycD2SV proteins. The majority of HEK293 cells transfected with cycD2SVΔCT (approximately 90%) contained aggregates, whereas only 10% of cycD2SV 54-136 transfected cells contained any aggregation (Fig. 15B-F). It was also evident that cycD2SVΔCT protein predominantly

Figure 14. Effects of co-expression of H-Ras and cycD2SV on cell cycle regulation. HEK293 cells co-transfected with cycD2SVmyc and HA tagged H-Ras-Val12 (A-C) were visualized by myc immunostaining (A), HA immunostaining (B) and nuclear stain (C). Scale bar is 20 μm. HEK293 cells transfected with cycD2SV, H-Ras-Val12 or co-transfected with cycD2SV and H-Ras-Val12 were labeled with [^{3}H]-thymidine, processed for immunostaining and [^{3}H]-thymidine autoradiography. Cells positive for [^{3}H]-thymidine were quantified and expressed as a percent of total transfected cells (D). pcDNA transfected cells (Cont) were used for control. Values are expressed as mean ± SEM. One way ANOVA, *$p < 0.05$ compared to control, approximately 1000 cells were counted for each group from three independent experiments (N=3). Western blot performed on HEK293 cells transfected with pcDNA (Cont), cycD2SV, H-Ras-Val12 or cycD2SV co-transfected with H-Ras-Val12 using myc and HA antibodies (E). α-tubulin was used as a protein loading control.

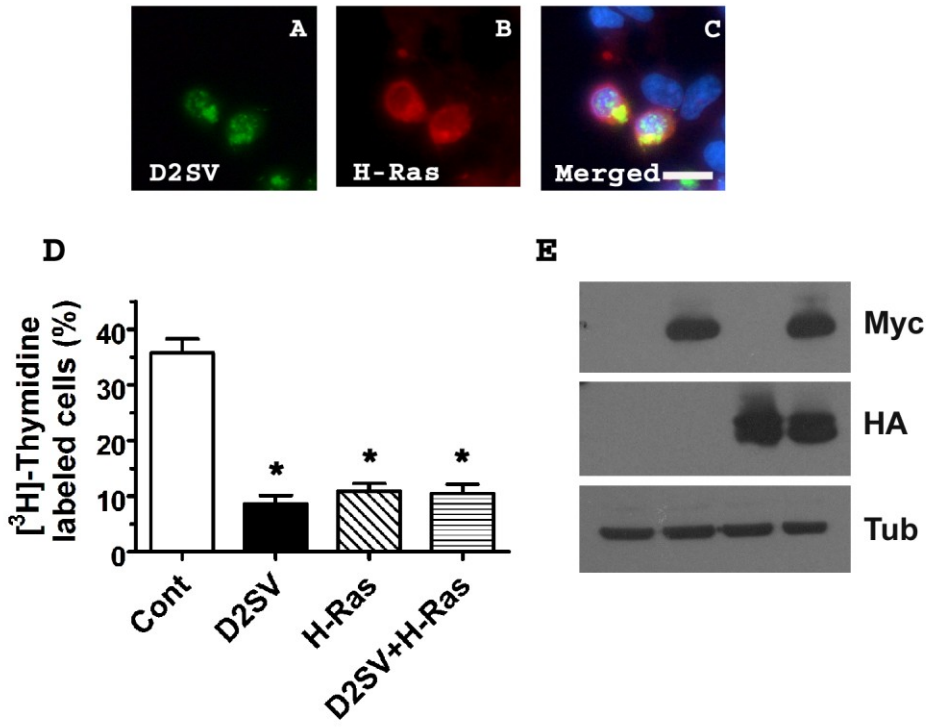
A
B
C
D2SV
H-Ras
Merged
D
E
[3H]-Thymidine labeled cells (%)
40
30
20
10
0
*
*
*
Cont
D2SV
H-Ras
D2SV+H-Ras
Myc
HA
Tub

Figure 15. Effects of cycD2SV 54-136 and cycD2SVΔCT overexpression on cell cycle regulation. A schematic representation of D2SVΔCT and D2SV 54-136 deletions in comparison to full length D2SV (A). Shaded box (136-156 amino acids) in cycD2SV represents the unique CT sequence. HEK293 cells transfected with D2SVΔCTmyc (B, C) and D2SV 54-136myc (D, E) were processed for myc (B, D) immunostaining and nuclear stain (C, E). Scale bar is 20 μm. HEK293 cells transfected with D2SV, D2SVΔCT and D2SV 54-136 were labeled with [^{3}H]-thymidine and processed for immunostaining and [^{3}H]-thymidine autoradiography. The percentage of cells positive for protein aggregation (F) and [^{3}H]-thymidine (G) were quantified and expressed as a percent of total transfected cells. Cells transfected with pcDNA 3.1 vector were used as a control (cont). Values are expressed as mean ± SEM. One way ANOVA, *$p < 0.05$ compared to control, approximately 1000 cells were counted for each group from three independent experiments (N=3).

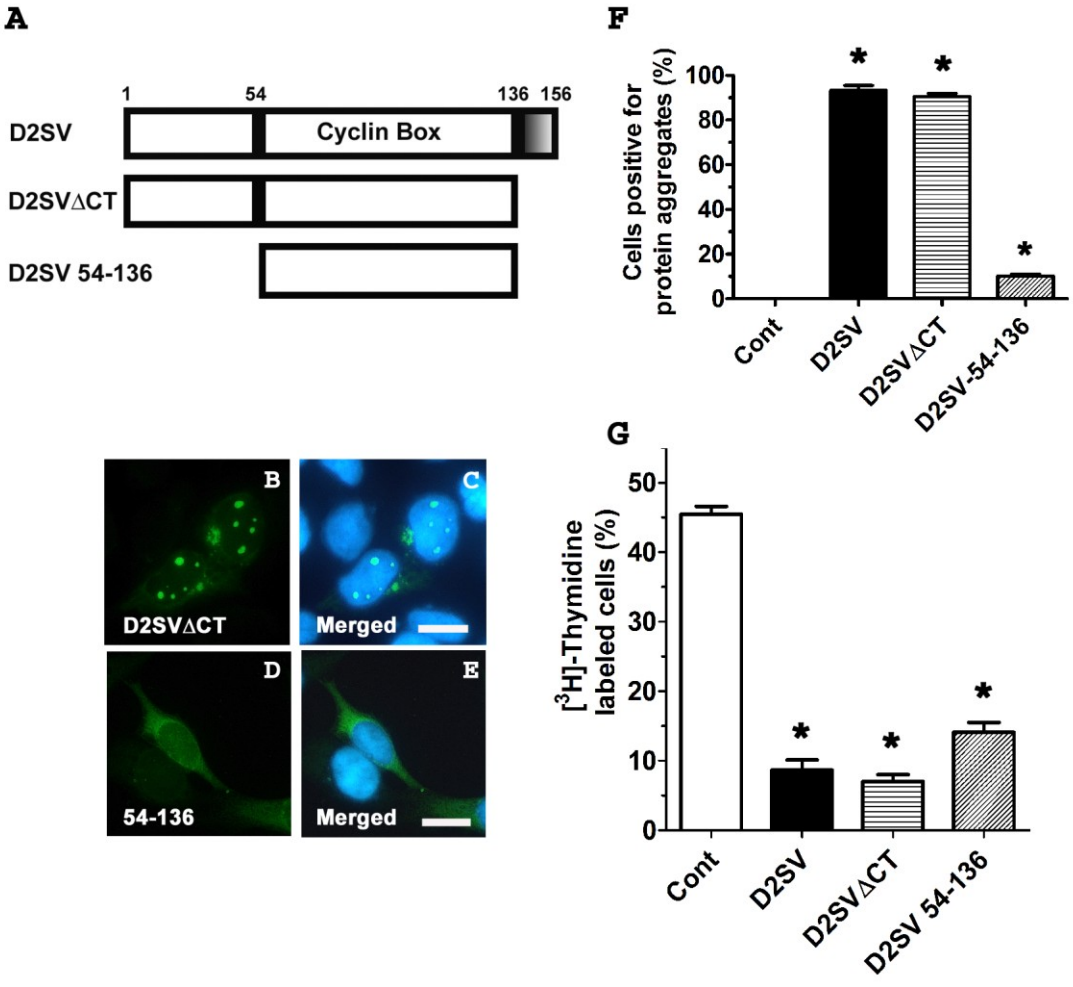
A
1
54
136
156
D2SV
Cyclin Box
D2SVΔCT
D2SV 54-136
B
D2SVΔCT
C
Merged
D
54-136
E
Merged
F
Cells positive for protein aggregates (%)
100
80
60
40
20
0
*
*
*
Cont
D2SV
D2SVΔCT
D2SV-54-136
G
[3H]-Thymidine labeled cells (%)
50
40
30
20
10
0
*
*
*
Cont
D2SV
D2SVΔCT
D2SV 54-136

localized to the nucleus in transfected cells, (Fig. 15B, C) while cycD2SV 54-136 immunostaining was diffuse across both the nuclear and cytoplasmic compartments (Fig. 15D, E). The [^{3}H]-thymidine incorporation was significantly reduced in cycD2SVΔCT transfected cells, similar to the levels observed in cycD2SV transfected cells (Fig. 15G). Similarly, the LI for cells transfected with cycD2SV 54-136 was significantly lower (approximately 3-fold) than that observed in control cells, but was significantly higher (approximately 2-fold) than that observed in cycD2SVΔCT transfected cells (Fig. 15G). Based on these observations, deletion of the unique CT and or 1-53 regions of cycD2SV did not eliminate the cell cycle inhibitory function of cycD2SV protein. However, removal of both 1-53 and the CT region was sufficient to significantly decrease cycD2SV micro-aggregation staining pattern. Collectively, these results suggest that cycD2SV cell cycle inhibitory domain resides in the 54-136 amino acid region, while the 1-53 region may play a major role in cycD2SV aggregation.

2.5.5 CycD2SV Aggregates Participate in Protein-Protein Interactions with CycD2 and CDK4 in HEK293 Cells

The 54-136 amino acid region of the cycD2SV contains the majority of the cyclin box and binding sequences for CDK4 and p21^{Cip1} (Sun et al., 2009; Zwicker et al., 1999). We previously showed that cycD2SV aggregates can sequester various cyclins including cycD2 via an ER stress pathway in embryonic cardiomyocytes (Sun et al., 2009). It is also possible that cycD2SV mediates cell cycle exit in immortalized cell lines by sequestering key cell cycle proteins into aggresomes. Here, we investigated the ability of cycD2SV to physically associate with cycD2 and CDK4 in HEK293 cells using immunostaining and co-IP techniques. Immunostaining experiments demonstrated co-

localization of cycD2SV with endogenous cycD2 in approximately 3-5% of cells transfected with cycD2SV (Fig. 16A-C). In contrast, such co-localization was observed in 100% of cells co-transfected with both cycD2SV and cycD2 constructs (Fig. 16D-F). To confirm whether cycD2SV interacts with cycD2, HEK293 cells were co-transfected with myc-tagged cycD2, and untagged cycD2SV constructs. Protein lysates were immunoprecipitated with myc antibodies and immune complexes were collected using protein A-Sepharose beads. IP and supernatant fractions were subjected to western blot analysis using cycD2SV and D2 antibodies and results indicated that cycD2SV forms a complex with cycD2 (Fig. 17A). To ensure cycD2SV antibodies do not cross-react with cycD2 or vice versa, additional western blotting experiments were performed on lysates from cells transfected with myc-tagged cycD2, cycD2SV and cycD2SVΔCT constructs (Fig. 17B, C). In these experiments, cycD2SV antibodies specifically reacted with cycD2SV, but not with cycD2 or cycD2SVΔCT proteins (Fig. 17B), while cycD2 antibodies exclusively reacted with cycD2, but not with cycD2SV or cycD2SVΔCT proteins (Fig. 17C). While immunostaining experiments did not reveal any co-localization of cycD2SV and endogenous CDK4 in transfected HE293 cells (Fig. 18A-C), IP/western analysis of transfected cells with CDK4 and myc antibodies clearly revealed physical interactions between CDK4 and cycD2SV or cycD2 (Fig. 18D). These results confirm the ability of cycD2SV to bind with both cycD2 and CDK4 in non-cardiac cell types.

Figure 16. Overexpressed cycD2SV co-localizes with endogenous and co-transfected cycD2. HEK293 cells transfected with cycD2SVmyc alone (A-C) or co-transfected with cycD2myc (D-F) were processed for myc (A, E), D2SV (D), cycD2 (B) immunostaining and nuclear stain (C, F). Scale bar is 20 μm. End., endogenous.

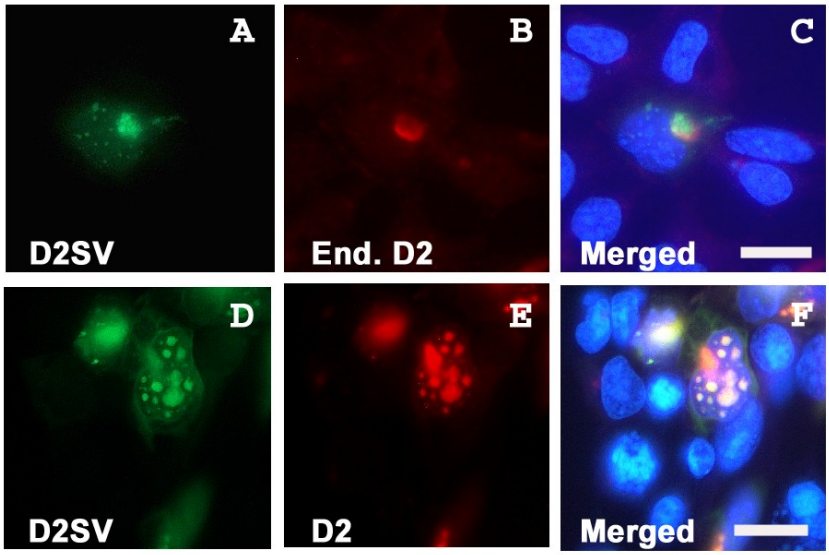
A
D2SV
B
End. D2
C
Merged
D
D2SV
E
D2
F
Merged

Figure 17. Immunoprecipitation (IP) analysis of interactions between cycD2SV and cycD2 (A). Western blot (WB) analysis performed on HEK293 cells transfected with pcDNA, cycD2myc, cycD2SVmyc and cycD2SVΔCTmyc using myc and D2SV antibodies (B) as well as cycD2 and α-tubulin antibodies (C). Results in panels B and C indicate the specificity of cycD2SV and cycD2 antibodies and rule out any cross-reactivity.

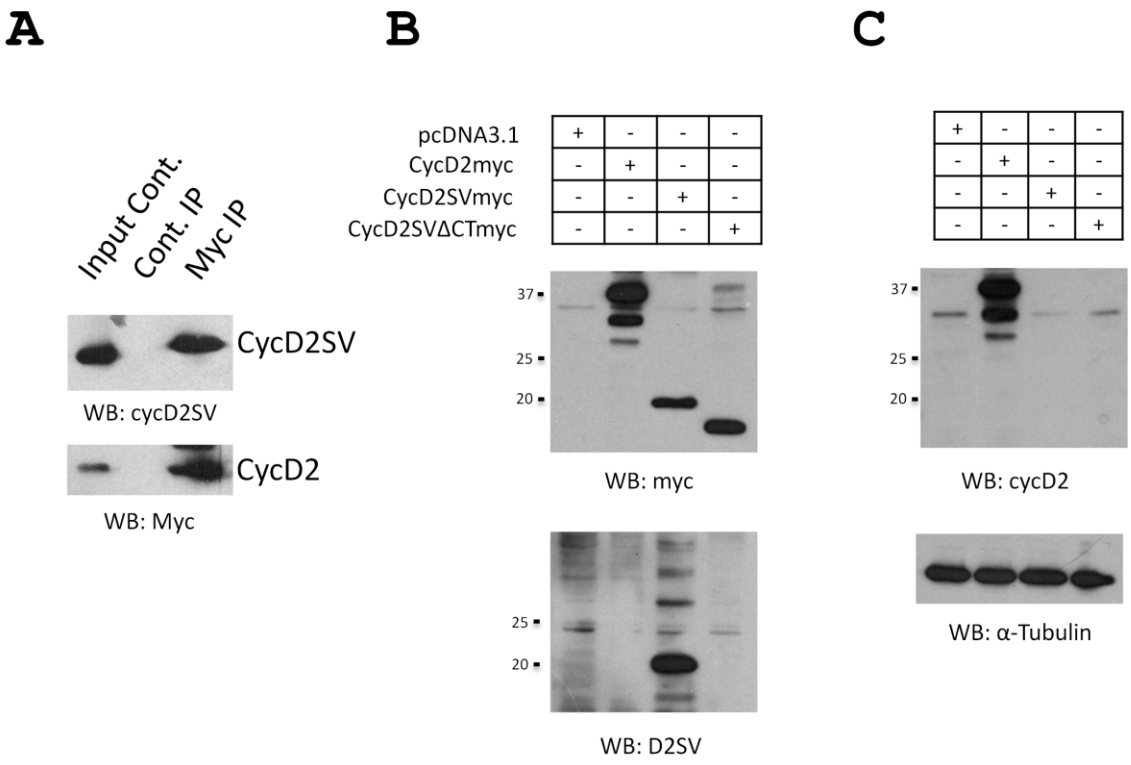
A
B
C
Input Cont.
Cont. IP
Myc IP
CycD2SV
WB: cycD2SV
CycD2
WB: Myc
pcDNA3.1
CycD2myc
CycD2SVmyc
CycD2SVΔCTmyc
37
25
20
WB: myc
25
20
WB: D2SV
37
25
20
WB: cycD2
WB: α-Tubulin

Figure 18. HEK293 cells transfected with cycD2SVmyc (A-C) processed for myc (A), CDK4 (B) immunostaining and nuclear stain (C). Interaction of transfected cycD2SV with endogenous CDK4 was determined by CDK4 immunoprecipitation (D). Endogenous CDK4 was immunoprecipitated from pcDNA (negative control), cycD2myc (positive control) and D2SVmyc transfected cells using CDK4 antibodies. An additional immunoprecipitation negative control was completed using rabbit non-immune serum (RNIS, control) on cycD2SVmyc transfected HEK293 cells. Immunoprecipitated samples were resolved by western blot and the nitrocellulose blot was probed with myc and CDK4 antibodies. Western blot analysis of HEK293 cells transfected with pcDNA (control), empty vector, and D2SVmyc using cycD2SV antibodies (E). IP, immunoprecipitation; WB, western blot; End., endogenous.

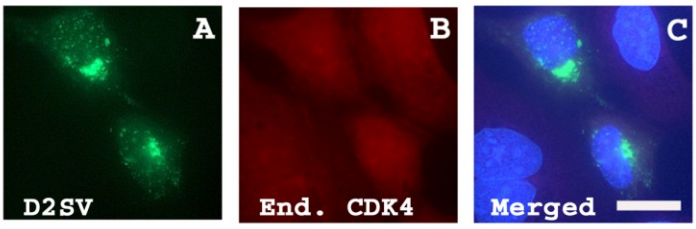
A
D2SV
B
End. CDK4
C
Merged

D

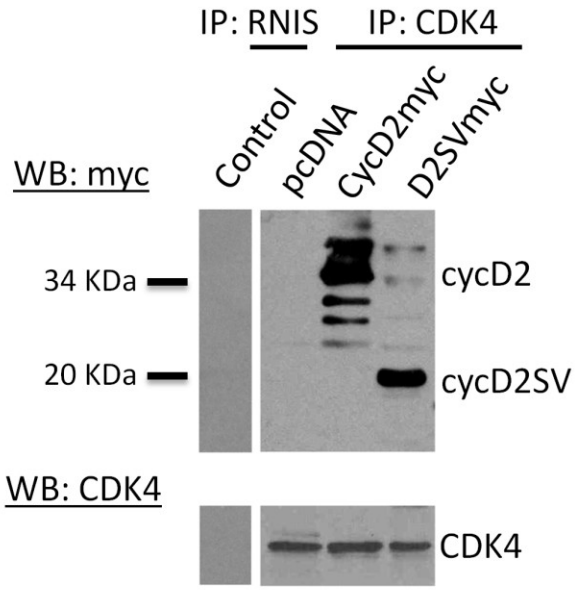
IP: RNIS
IP: CDK4
Control
pcDNA
CycD2myc
D2SVmyc
WB: myc
34 KDa
20 KDa
cycD2
cycD2SV
WB: CDK4
CDK4

E

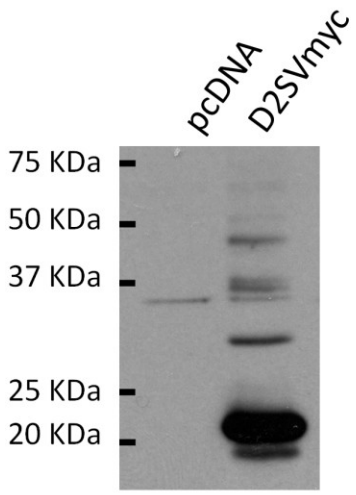
pcDNA
D2SVmyc
75 KDa
50 KDa
37 KDa
25 KDa
20 KDa

2.5.6 CycD2SV Expression Leads to an Impaired ER Stress Associated Protein Degradation and Accumulation of Polyubiquitin Conjugates

Although the predicted molecular weight of mouse cycD2SV is approximately 20 kDa, it has been shown to exist in varying sizes ranging from 20 kDa to 45 kDa in transfected HEK293 cells [(Sun et al., 2009), Fig. 18E] as well as tissue lysates from postnatal cerebellum (Kajitani et al., 2010) or whole embryo extracts (Sun et al., 2009) under denaturing or non-denaturing conditions. However, the precise nature of these high molecular weight immunoreactive cycD2SV bands is not clear. Intracellular accumulation of misfolded proteins has been shown to trigger protein aggregation and subsequent increases in ubiquitin conjugates as a result of impaired ERAD in neurodegenerative model systems (Bence et al., 2001). Next, we examined whether accumulation of cycD2SV aggregates in immortalized cell lines is due to an impairment of ERAD by using a well characterized TCRα-GFP reporter gene system (DeLaBarre et al., 2006). The misfolded TCRα-GFP reporter was readily eliminated in single transfected HEK293 cells as demonstrated by background GFP fluorescence after 24 hrs (data no shown). In contrast, the GFP fluorescence was retained at higher levels in cells co-transfected with TCRα-GFP and cycD2SV, suggesting an impaired ERAD response in cycD2SV expressing cells (Fig. 19A-C).

To examine ubiquitination profiles, HEK293 cells were co-transfected with cycD2SV and HA tagged ubiquitin (HA-Ubq) constructs and processed for double immunostaining. Co-localization of both proteins in all transfected cells (100%) suggests that cycD2SV aggregates are ubiquitinated (100%, Fig. 19D-F). Control cells transfected with HA-Ubq alone showed a diffuse staining with HA antibodies, and did not show any

Figure 19. Co-localization of transfected cycD2SV with markers of ER stress and autophagy. HEK293 cells co-transfected with cycD2SVmyc and TCRα-GFP (A-C), cycD2SVmyc and HA-ubiquitin (D-F), cycD2SVmyc and YFP-intersectin (J-L) and cycD2SV-EGFP and mcherry-p62 (M-O) were processed for myc (A, D, G), HA (E) immunostaining and nuclear stain (C, F, I, L). Co-localization of singly transected cycD2SV aggregates in γ-tubulin positive MTOC (G-I). HEK293 cells transfected with cycD2SVmyc (G-I) processed for myc (G), γ-tubulin (H) immunostaining and nuclear stain (E). Scale bar is 20 μm.

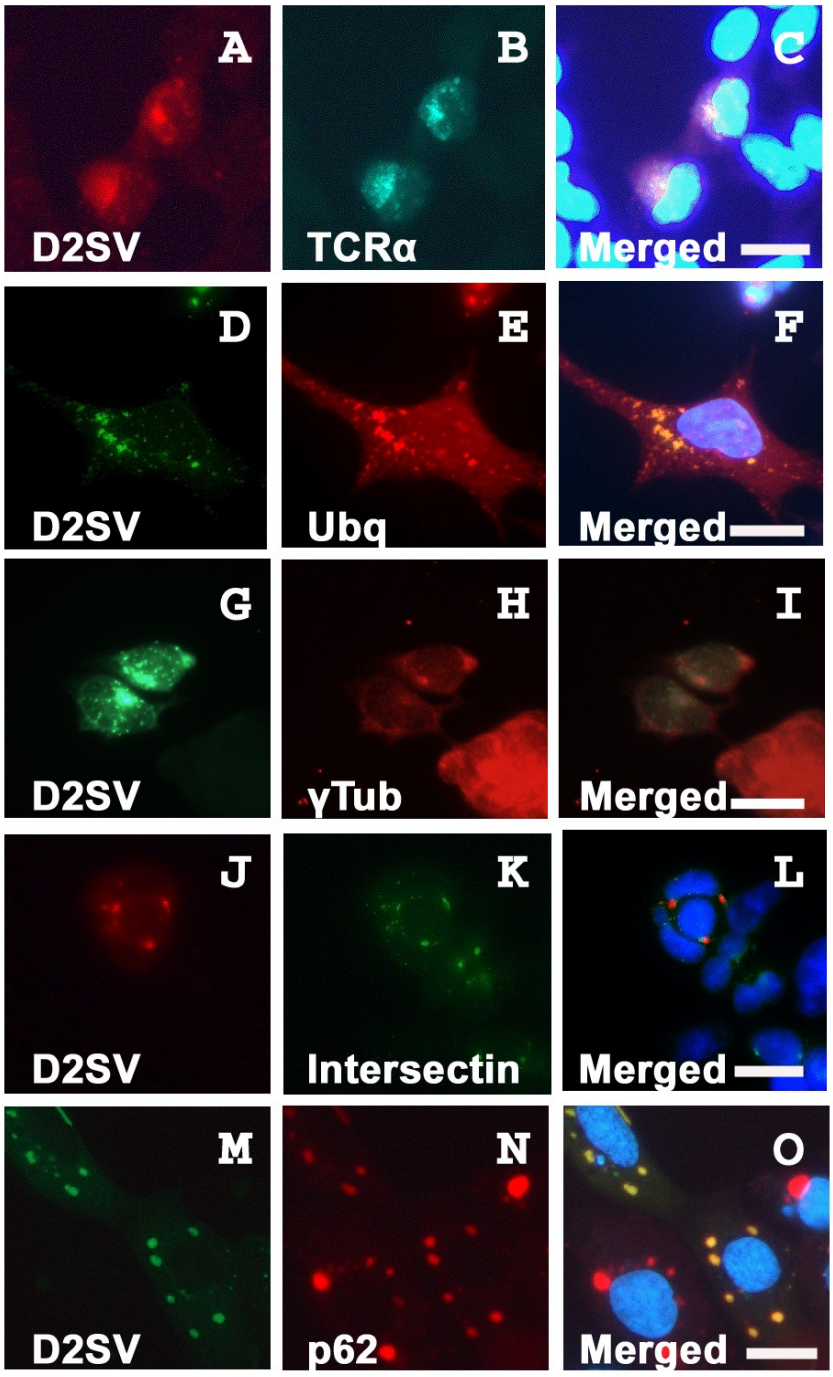
A
D2SV
B
TCRα
C
Merged
D
D2SV
E
Ubq
F
Merged
G
D2SV
H
γTub
I
Merged
J
D2SV
K
Intersectin
L
Merged
M
D2SV
N
p62
O
Merged

ubiquitinated aggregates similar to co-transfected cells (data not shown). Given that cycD2SV induces ER stress which results in the impairment of ERAD, it is likely that cycD2SV ubq positive aggregates may clog the UPS system. Additionally, γ-tubulin staining, a marker of the MTOC, co-localized (Fig. 19G-I) with larger aggregates in 28.4% (± 4.82 SEM) of cells transfected with cycD2SVmyc. The MTOC has been demonstrated to play a role in the autophagic degradation of protein aggregates. When the rate of protein aggregate formation is higher than that of clearance, to minimize toxicity, protein aggregates are shuttled to the MTOC where the aggresome is formed (Kirkin et al., 2009b). The high levels of γ-tubulin co-localization with cycD2SV aggregates suggest that cycD2SV aggregates may have a toxic effect on transfected cells.

2.5.7 CycD2SV Aggregates are Subjected to Autophagosome Mediated Degradation

Presence of polyubiquitinated aggregates, and impaired ERAD response suggest that alternative protein degradation pathways, such as autophagy, may be active in cycD2SV expressing cells. Accordingly, cycD2SV expressing cells were further examined using probes specific for critical components in autophagosome formation (Razi et al., 2009). In these experiments, cycD2SV aggregates were frequently co-localized with markers specific for early or late endosomes (Intersectin-YFP, Fig. 19J-K), and a selective substrate of autophagy (mCherry-p62, Fig. 19M-O). To obtain direct evidence for the presence of cycD2SV in autophagosome, transfected HEK293 cells were processed for EM analysis using cycD2SV antibodies. Presence of anti-cycD2SV related immunogold particles were readily visible in electron-lucent endosomes (data not shown), electron-dense lysosome and autophagosome structures (Fig. 20A). Such unique

Figure 20. Localization of cycD2SV in electron-dense lysosome and autophagosome structures (A, B). HEK293 cells transfected with D2SVmyc (A, B) were fixed, embedded in resin and sectioned (approximately 80nm). Sections were processed for electron microscopy and probed with cycD2SV antibodies (A). As a control primary antibodies were omitted (B). Scale bar is 100 nm.

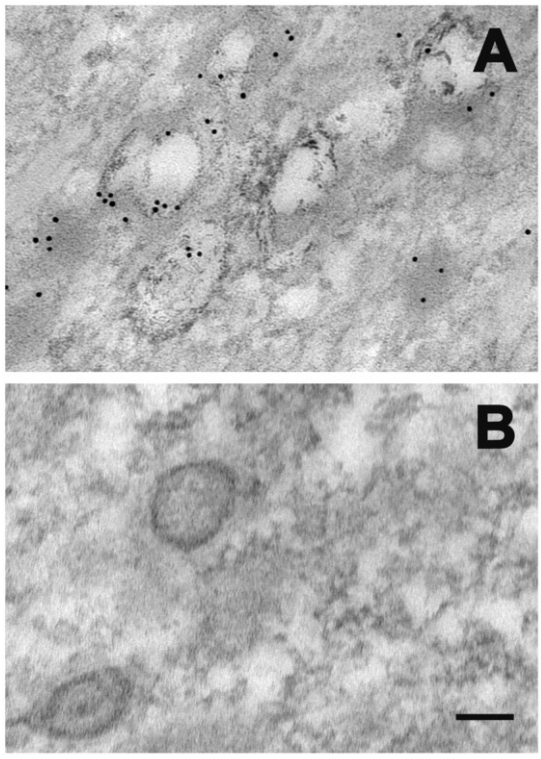
A
B

immunogold labeling pattern was absent in control sections processed by omitting cycD2SV antibodies (Fig. 20B). Collectively, these results suggest that ubiquitin positive cycD2SV aggregates (Fig. 19D-F) can sequester cell cycle proteins, such as cycD2, and CDK4 (Fig. 16A-F, Fig. 17A, Fig. 18D) and target them for autophagosome mediated degradation (Fig. 19M-O, Fig. 20A).

2.5.8 CycD2SV Induced G1/S Cell Cycle Exit May Rely on Transcriptional Changes in G2/M but not G1/S Regulatory Genes

We further sought to determine whether cell cycle exit in cycD2SV expressing cells could result from significant changes in the transcriptional profile of cell cycle genes involved in G1/S and G2/M regulation. For these experiments, total RNA was isolated from FACS sorted cells, expressing EGFP or an EGFP-D2SV fusion protein. Total RNA was reverse transcribed, and cDNA samples were subjected to quantitative PCR analysis using human cell cycle QPCR arrays. This high throughput approach enabled us to simultaneously measure fold changes in the transcriptional profile of 86 cell cycle genes (Fig. 21A-C, Table4). Based on this analysis, there were no significant differences in mRNA levels of the majority of G1/S regulatory genes such as D-type cyclins, CDKs, CKIs and several G1/S check point regulators between control or cycD2SV expressing cells (Table 4). However, we observed a significant increase in the mRNA levels of two G2/M regulatory genes, GADD45α (1.6-fold) and dynamin 2 (1.5-fold, Fig. 21B). GADD45 (growth arrest and DNA-damage inducible protein) α expression is induced by ultraviolet and ionizing radiation, as well as genotoxic stress which subsequently leads to G2/M checkpoint activation, cell cycle arrest, DNA repair,

Figure 21. Cell cycle array analysis on cells expressing EGFP-D2SV. Gating for sorting of HEK293 cells transfected with EGFP-D2SV cells during FACS analysis (A)**.** Relative mRNA levels of GADD45A and dynamitin 2 in EGFP-D2SV FACS sorted cells compared to control EGFP-C1 sorted cells (B). A profile of the fold changes of 86 cell cycle genes completed for EGFP-D2SV FACS sorted cells relative to EGFP-C1 control cells (C). Values are expressed as mean ± SEM. Unpaired two-tail t-test, *$p < 0.05$ compared to EGFP-C1, three separate arrays from three independent experiments were completed (N=3). HEK293 Cells transfected with cycD2SVmyc were processed for immunostaining using myc antibody followed by TUNEL staining. TUNEL positive cells were counted and expressed as a fraction of total cells counted (D). Values are expressed as mean ± SEM. Unpaired two-tail t-test, *$p < 0.05$ compared to control untransfected TUNEL positive cells, approximately 1000 cells were counted for each group from three independent experiments (N=3).

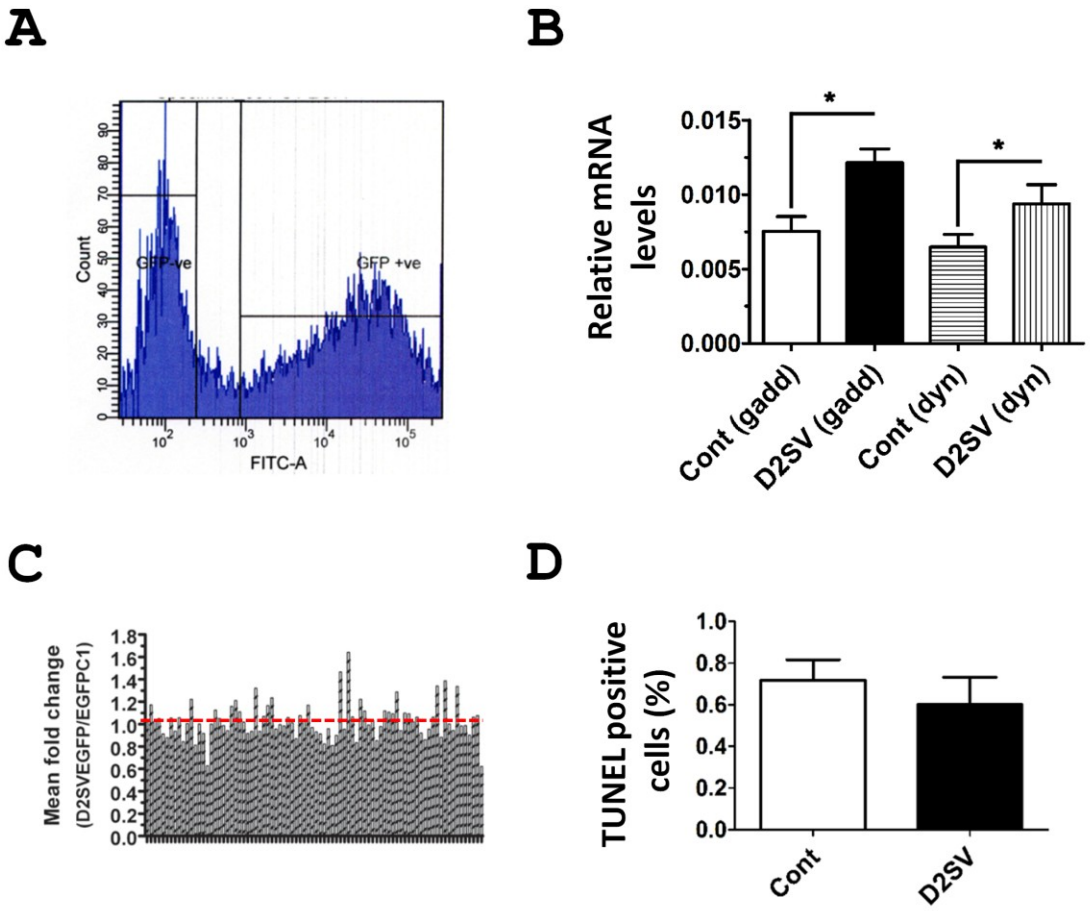
A
Count
GFP -ve
GFP +ve
FITC-A
B
Relative mRNA levels
0.015
0.010
0.005
0.000
*
*
Cont (gadd)
D2SV (gadd)
Cont (dyn)
D2SV (dyn)
C
Mean fold change (D2SVEGFP/EGFPC1)
1.8
1.6
1.4
1.2
1.0
0.8
0.6
0.4
0.2
0.0
D
TUNEL positive cells (%)
1.0
0.8
0.6
0.4
0.2
0.0
Cont
D2SV

Table 4. Cell cycle array completed for C1-EGFP control and D2SV-EGFP sorted cells.

		$2^{-Avg.(\Delta CT)}$			
Gene	**Symbol**	**C1-EGFP**	**D2SV-EGFP**	**Mean of Fold Change**	***p*-Value**
C-abl oncogene 1, receptor tyrosine kinase	ABL1	0.045507	0.046534	1.0226	0.896426
Anaphase promoting complex subunit 2	ANAPC2	0.011429	0.013394	1.1719	0.355643
Anaphase promoting complex subunit 4	ANAPC4	0.014301	0.014657	1.025	0.892721
DIRAS family, GTP-binding RAS-like 3	DIRAS3	0.000178	0.000187	1.0489	0.830631
Ataxia telangiectasia mutated	ATM	0.002082	0.001901	0.9131	0.76961
Ataxia telangiectasia and Rad3 related	ATR	0.014534	0.01276	0.878	0.459864
BCL2-associated X protein	BAX	0.436955	0.460448	1.0538	0.578846
BRCA2 and CDKN1A interacting protein	BCCIP	0.316927	0.296844	0.9366	0.735572
B-cell CLL/lymphoma 2	BCL2	0.004291	0.004532	1.0562	0.771185
Baculoviral IAP repeat-containing 5	BIRC5	0.011091	0.009363	0.8441	0.750298
Breast cancer 1, early onset	BRCA1	0.030372	0.03056	1.0062	0.847403
Breast cancer 2, early onset	BRCA2	0.003753	0.004585	1.2217	0.194956
Cyclin B1	CCNB1	0.875931	0.710929	0.8116	0.347278
Cyclin B2	CCNB2	0.191961	0.192257	1.0015	0.918471
Cyclin C	CCNC	0.120928	0.110934	0.9174	0.584678
Cyclin D1	CCND1	0.018143	0.011394	0.628	0.341384
Cyclin D2	CCND2	0.135424	0.13532	0.9992	0.952798
Cyclin E1	CCNE1	0.054242	0.060978	1.1242	0.264414
Cyclin F	CCNF	0.021726	0.022788	1.0489	0.728108
Cyclin G1	CCNG1	0.51963	0.512081	0.9855	0.884616
Cyclin G2	CCNG2	0.013405	0.012613	0.941	0.69836
Cyclin H	CCNH	0.078503	0.090943	1.1585	0.715719
Cyclin T1	CCNT1	0.05977	0.072349	1.2105	0.244277
Cyclin T2	CCNT2	0.017729	0.019656	1.1087	0.433431
Cell division cycle 16 homolog (S. cerevisiae)	CDC16	0.125482	0.127725	1.0179	0.858039
Cell division cycle 2, G1 to S and G2 to M	CDC2	0.512476	0.470123	0.9174	0.524907
Cell division cycle 20 homolog (S. cerevisiae)	CDC20	0.50309	0.470123	0.9345	0.731918
Cell division cycle 34 homolog (S. cerevisiae)	CDC34	0.015046	0.019884	1.3215	0.208111
Cyclin-dependent kinase 2	CDK2	0.140524	0.131316	0.9345	0.670209
Cyclin-dependent kinase 4	CDK4	0.409581	0.437628	1.0685	0.606063
Cyclin-dependent kinase 5, regulatory subunit 1 (p35)	CDK5R1	0.003494	0.004075	1.1665	0.474335
CDK5 regulatory subunit associated protein	CDK5RAP	0.002141	0.002646	1.2359	0.52246

1	1				
Cyclin-dependent kinase 6	CDK6	0.030023	0.028712	0.9563	0.610107
Cyclin-dependent kinase 7	CDK7	0.05108	0.050805	0.9946	0.995433
Cyclin-dependent kinase 8	CDK8	0.028142	0.02767	0.9832	0.951884
Cyclin-dependent kinase inhibitor 1A (p21Cip1)	CDKN1A	0.182448	0.193148	1.0586	0.770827
Cyclin-dependent kinase inhibitor 1B (p27Kip1)	CDKN1B	0.027948	0.028316	1.0132	0.935082
Cyclin-dependent kinase inhibitor 2A (p16)	CDKN2A	0.127823	0.111191	0.8699	0.472093
Cyclin-dependent kinase inhibitor 2B (p15)	CDKN2B	0.024443	0.026298	1.0759	0.352026
Cyclin-dependent kinase inhibitor 3	CDKN3	0.154844	0.159812	1.0321	0.860987
CHK1 checkpoint homolog (S. pombe)	CHEK1	0.088729	0.103745	1.1692	0.172583
CHK2 checkpoint homolog (S. pombe)	CHEK2	0.057867	0.056112	0.9697	0.701998
CDC28 protein kinase regulatory subunit 1B	CKS1B	0.14717	0.136892	0.9302	0.739475
CDC28 protein kinase regulatory subunit 2	CKS2	0.584614	0.533827	0.9131	0.650498
Cullin 1	CUL1	0.068183	0.056112	0.823	0.615898
Cullin 2	CUL2	0.129608	0.124232	0.9585	0.815363
Cullin 3	CUL3	0.000934	0.000756	0.8098	0.327323
DEAD/H (Asp-Glu-Ala-Asp/His) box polypeptide 11 (CHL1-like helicase homolog, S. cerevisiae)	DDX11	0.014908	0.013394	0.8985	0.944014
Dynamin 2	DNM2	0.006385	0.009363	1.4663	0.044266
E2F transcription factor 4, p107/p130-binding	E2F4	0.030023	0.028645	0.9541	0.695106
Growth arrest and DNA-damage-inducible, alpha	GADD45A	0.00742	0.012184	1.6421	0.042191
General transcription factor IIH, polypeptide 1, 62kDa	GTF2H1	0.127528	0.135633	1.0636	0.589076
G-2 and S-phase expressed 1	GTSE1	0.016089	0.013425	0.8344	0.597626
Hect domain and RLD 5	HERC5	0.024899	0.030419	1.2217	0.054532
HUS1 checkpoint homolog (S. pombe)	HUS1	0.003149	0.003515	1.1164	0.79165
Kinetochore associated 1	KNTC1	0.044777	0.044433	0.9923	0.910348
Karyopherin alpha 2 (RAG cohort 1, importin alpha 1)	KPNA2	0.247509	0.256041	1.0345	0.932005
MAD2 mitotic arrest deficient-like 1 (yeast)	MAD2L1	0.541696	0.461513	0.852	0.50983
MAD2 mitotic arrest deficient-like 2 (yeast)	MAD2L2	0.056939	0.055724	0.9787	0.856011
Minichromosome maintenance complex component 2	MCM2	0.178281	0.199498	1.119	0.418758
Minichromosome maintenance complex component 3	MCM3	0.458679	0.50737	1.1062	0.115046
Minichromosome maintenance complex component 4	MCM4	0.142815	0.155801	1.0909	0.500166
Minichromosome maintenance complex component 5	MCM5	0.084137	0.108401	1.2884	0.419207
Antigen identified by monoclonal antibody Ki-67	MKI67	0.260416	0.245044	0.941	0.752684
Menage a trois homolog 1, cyclin H	MNAT1	0.085115	0.0935	1.0985	0.493612

assembly factor (Xenopus laevis)					
MRE11 meiotic recombination 11 homolog A (S. cerevisiae)	MRE11A	0.007317	0.007983	1.0909	0.925512
Nibrin	NBN	0.00166	0.001694	1.0202	0.696459
Proliferating cell nuclear antigen	PCNA	0.728107	0.772592	1.0611	0.584027
RAD1 homolog (S. pombe)	RAD1	0.03339	0.030701	0.9195	0.630274
RAD17 homolog (S. pombe)	RAD17	0.041298	0.035512	0.8599	0.350128
RAD51 homolog (RecA homolog, E. coli) (S. cerevisiae)	RAD51	0.001429	0.001363	0.9541	0.849772
RAD9 homolog A (S. pombe)	RAD9A	0.026502	0.028121	1.0611	0.699695
Retinoblastoma 1	RB1	0.010813	0.014489	1.34	0.645515
Retinoblastoma binding protein 8	RBBP8	0.052759	0.046534	0.882	0.458713
Retinoblastoma-like 1 (p107)	RBL1	0.052153	0.072349	1.3872	0.095527
Retinoblastoma-like 2 (p130)	RBL2	0.011066	0.011083	1.0015	0.842176
Replication protein A3, 14kDa	RPA3	0.262834	0.247891	0.9431	0.747903
SERTA domain containing 1	SERTAD1	0.014908	0.01993	1.3369	0.420479
S-phase kinase-associated protein 2 (p45)	SKP2	0.335772	0.330131	0.9832	0.927152
SMT3 suppressor of mif two 3 homolog 1 (S. cerevisiae)	SUMO1	0.096203	0.095025	0.9878	0.882802
Transcription factor Dp-1	TFDP1	0.041394	0.037364	0.9026	0.858238
Transcription factor Dp-2 (E2F dimerization partner 2)	TFDP2	0.049798	0.05284	1.0611	0.816079
Tumor protein p53	TP53	0.108484	0.116719	1.0759	0.817862
Ubiquitin-like modifier activating enzyme 1	UBA1	0.121769	0.07577	0.6222	0.284865

cell survival or apoptosis (Liebermann and Hoffman, 2007; Wang et al., 1999; Zhan et al., 1999). In contrast, dynamin 2 plays an important role in mitosis, cytokinesis, endocytosis and membrane trafficking (Evans et al., 1990; Praefcke and McMahon, 2004). Collectively, these results suggest that mRNA levels of the majority of cell cycle genes remain unchanged in cycD2SV overexpressing cells, as compared to those of control cells. Significant increases in two G2/M related gene transcripts suggest that DNA repair and or mitotic process may be compromised in cells positive for cycD2SV protein aggregation, and these results are consistent with lower [^{3}H]-thymidine LI observed in cycD2SV expressing cells.

2.5.9 Intracellular CycD2SV Protein Aggregation Does Not Cause Apoptosis in static cultures but sensitizes cells to mechanical stress and trypsinization induced cell death

In response to stress stimuli, both GADD45α and Dynamin 2 genes have been shown to cause cell cycle arrest and apoptosis in a p53 dependent manner (Fish et al., 2000; Liebermann and Hoffman, 2007). Since these two transcripts are upregulated in cycD2SV expressing cells, we assessed the levels of apoptosis using TUNEL and activated Caspase 3 immunostaining assays. Using these methods, no apoptotic cell death was observed in cells transfected with cycD2SV, or a control plasmid (Fig. 21D).

Furthermore, cycD2SV expressing cells were viable in subconfluent static cultures for more than a week (data not shown). Apoptotic cells can also be identified during light scatter analysis in a flow cytometer by virtue of significant decreases in the forward scatter, (FSC) and side scatter (SSC) assessments (Williams, 2004). Consistent with the results observed in static cultures, the number of viable cells on the FSC vs. SSC

plots during FACS analysis was similar in cells expressing EGFP or EGFP-D2SV fusion proteins (Fig. 22A, B). Based on a significant decrease in cell cycle levels in cycD2SV expressing cells, we reasoned that FACS sorted EGFP-D2SV cells would have a slower growth potential as compared to EGFP expressing control cells. To further examine this notion, equal numbers of FACS sorted cells were plated in new culture dishes for monitoring growth curves over time. Surprisingly, none of the cycD2SV expressing cells survived over a three day subculture period (Fig. 23A-E). In contrast, FACS sorted cells expressing EGFP survived the mechanical stress and trypsinization imposed by the experimental procedure, albeit with initial reductions in cell number (Fig. 23A, F-I). These results suggest that cycD2SV expression may increase cell vulnerability to stress signals.

2.6 Discussion

Based on the observation that cycD2SV was overexpressed in Graffi retrovirus induced leukemias, Rassart's group originally hypothesized that this protein could function as an oncogene (Denicourt et al., 2003). Using an MEF based focus formation assay, it was shown that cycD2SV failed to induce cellular transformation alone or in combination with c-myc, but was able to induce a large number of foci in combination with activated H-Ras (Denicourt et al., 2008). Although previous studies did not directly examine the role of cycD2SV in G1/S transit control of non-cardiac cell types (Denicourt et al., 2008), absence of kinase activity for cycD2SV/CDK4 complex in NIH-3T3 cells (Denicourt et al., 2008) and significant decreases in the LIs of various cell lines expressing cycD2SV in this study are in agreement with a growth suppressive role for

Figure 22. Selection gating for viable cells during FACS sorting for C1-EGFP (A) and D2SV-EGFP (B) transfected cells. Side scatter (SSC) and forward scatter (FSC) plots (A, B) were used to determine predicted viable cells for FACS sorting. Region 1 (R1) contains viable cells whereas region 2 (R2) contains cells in early stages of apoptosis, and region 3 (R3) contains dead cells. Cell shrinkage and nuclear condensations are two of the hallmarks of apoptosis. Cell shrinkage leads to a decrease in forward scatter (FSC) whereas nuclear condensation results in an increase in side scatter (SSC). EGFP-C1 and EGFP-cycD2SV sorted cells roughly contained the same number of cells in regions 2 and 3.

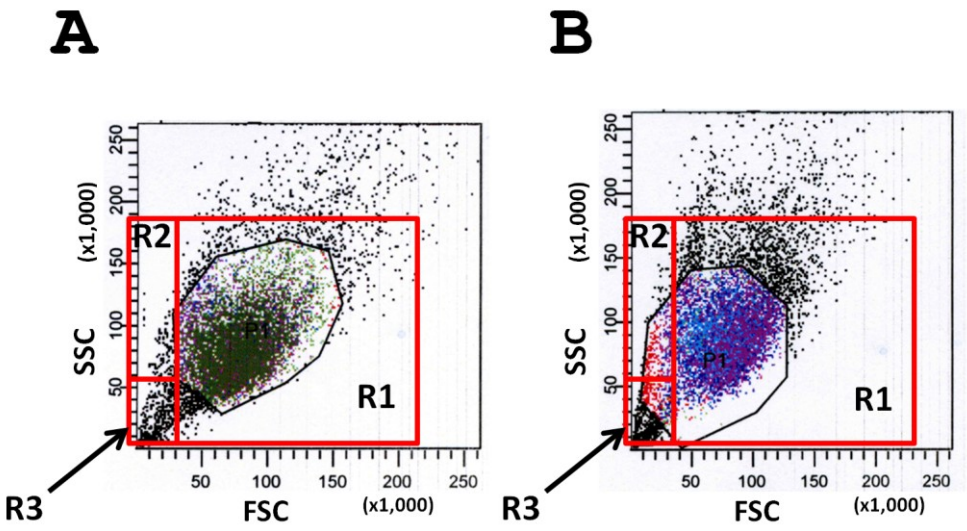
A
B
R2
R1
R3
P1
SSC
(x1,000)
FSC
(x1,000)
50
100
150
200
250

Figure 23. Analysis of D2SV-EGFP induced cell death in collaboration with trypsinization. HEK293 cells transfected with D2SV-EGFP or C1-EGFP were trypsinized and reseeded on gridded coverslips. In each experiment, cells were followed for 80hrs to determine long term cell viability after trypsinization. Surviving cells were quantified and expressed as a percent of total counted cells (D). Values are expressed as mean ± SEM. Two-way ANOVA, *$p < 0.05$, seven to twenty cells were followed from three independent experiments (N=3). Photomicrographs depict examples of D2SV-EGFP (B-E) and C1-EGFP (F-I) cells at 5hrs (B, C, F, G) and 20hrs (D, E, H, I). Note all EGFP-D2SV transfected cells disappeared from culture by 68hrs post trypsinization (A). Examples of cell death in EGFP-D2SV transfected cells as observed in live cultures by fluorescence microscopy (B-E).

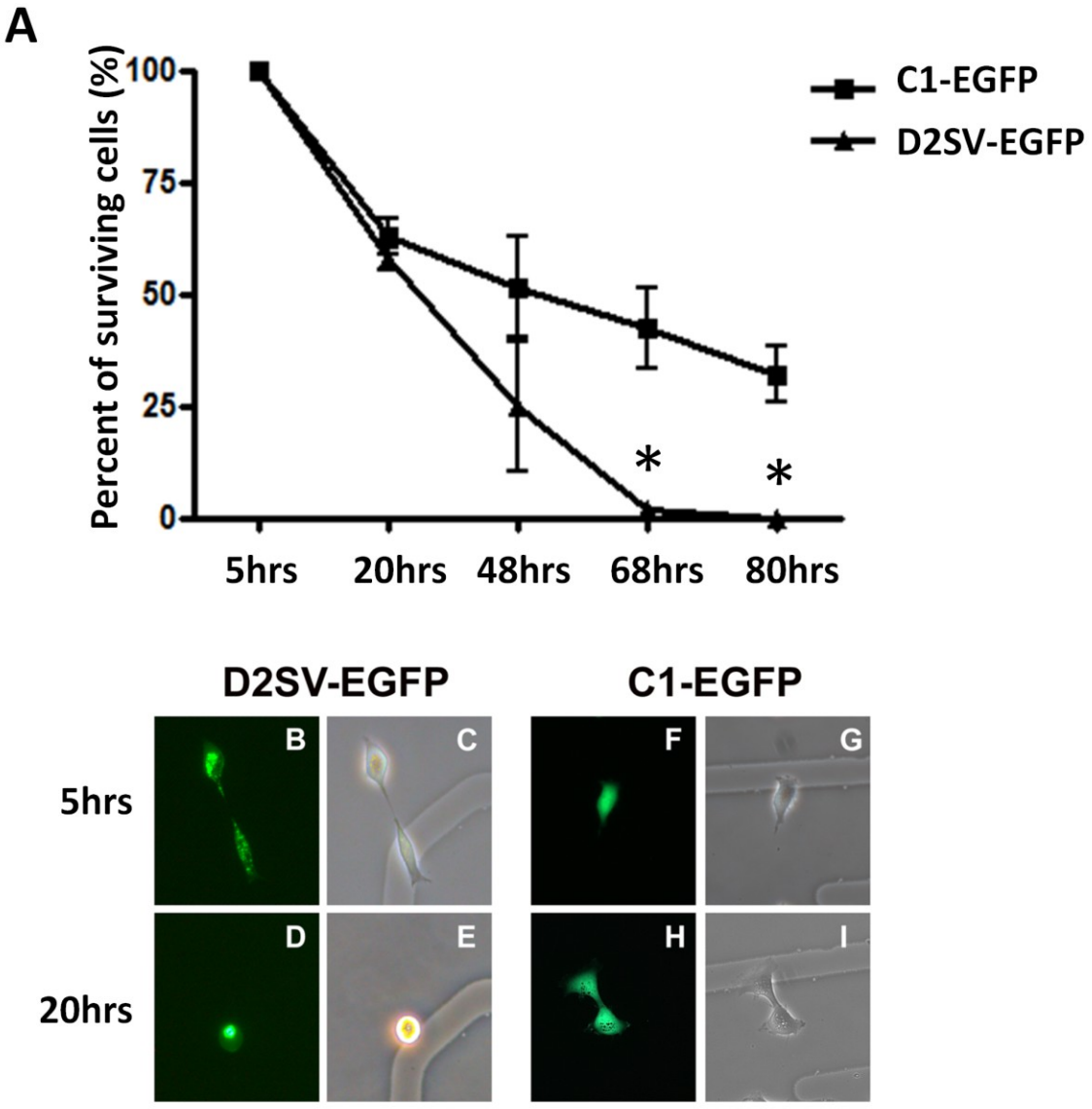
A
Percent of surviving cells (%)
100
75
50
25
0
5hrs
20hrs
48hrs
68hrs
80hrs
C1-EGFP
D2SV-EGFP
*
*
D2SV-EGFP
C1-EGFP
5hrs
20hrs
B
C
F
G
D
E
H
I

cycD2SV in cell cycle regulation. The transforming ability of H-Ras in combination with cycD2SV in primary MEFs (Denicourt et al., 2008) is particularly intriguing since activated H-Ras failed to transform primary fibroblast cells derived from mouse, rat or human sources (Serrano et al., 1997; Wei and Sedivy, 1999). Furthermore, it was shown that immortalization of fibroblasts is a pre-requisite for H-Ras mediated transformation (Newbold and Overell, 1983). Given the inability of H-Ras to rescue cycD2SV mediated cell cycle exit in this study (Fig. 14D), it is unclear how H-Ras and cycD2SV facilitated transformation of MEFs as suggested in Rassart's study (Denicourt et al., 2008). In this study, transfection of H-Ras alone in HEK293 cells significantly decreased cell cycle activity as compared to control transfections (Fig. 14D). This result is in agreement with a previous study which showed that H-Ras expression induces cellular senescence in HEK293 cells (Moumtzi et al., 2010) similar to the phenotype observed in normal fibroblasts (Wei and Sedivy, 1999).

The ability of cycD2SV to form micro aggregates compared to other cyclins, such as cycB1 or cycD2 in immortalized cell lines can be directly attributed to a protein misfolding response as evidenced by increased retention of an ERAD reporter (DeLaBarre et al., 2006) in cycD2SV expressing cells (Fig. 19A-C). Generally protein aggregation occurs as a result of misfolding, (Garcia-Mata et al., 2002) exposed hydrophobic regions, (Wedegaertner, 2002) or insufficient clearance by UPS (Kirkin et al., 2009b). Misfolding of cycD2SV could result from its structural divergence, as compared to a number of G1/S or G2/M cyclins. Mammalian cyclins contain two cyclin folds, each comprised of five alpha helical structures (Fig. 24). The NT cyclin fold provides a CDK binding interface for all cyclins, while the CT cyclin fold is critical for

Figure 24. Sequence alignment of D-type cyclins and cycD2SV identifying important conserved domains. Cyclins in general contain two important cyclin folds, the NT cyclin fold (red box) and the CT cyclin fold (black box), each containing five alpha-helical domains. For clarity, the NT helical domains are labeled as α1-5 and the CT helical domains are labeled as α1'-5'. In general, cyclins also contain two additional NT and CT helical domains (αNT, αCT). However, D-type cyclins appear to lack the αCT domain. The NT cyclin fold also known as the cyclin box is responsible for the association of cyclins with CDKs while the CT cyclin fold is thought to be responsible for binding of CAK and proper folding of the cyclin (GenBank: AAA37519.1). The cycD2SV CT sequence is highlighted in yellow. Helical domains are denoted by blue cylinders. The orange cylinder marks the helical domain (α5sv) present in the cycD2SV unique CT-domain. Asterix (*) denotes amino acids which are identical between all presented sequences. α denotes α-helix.

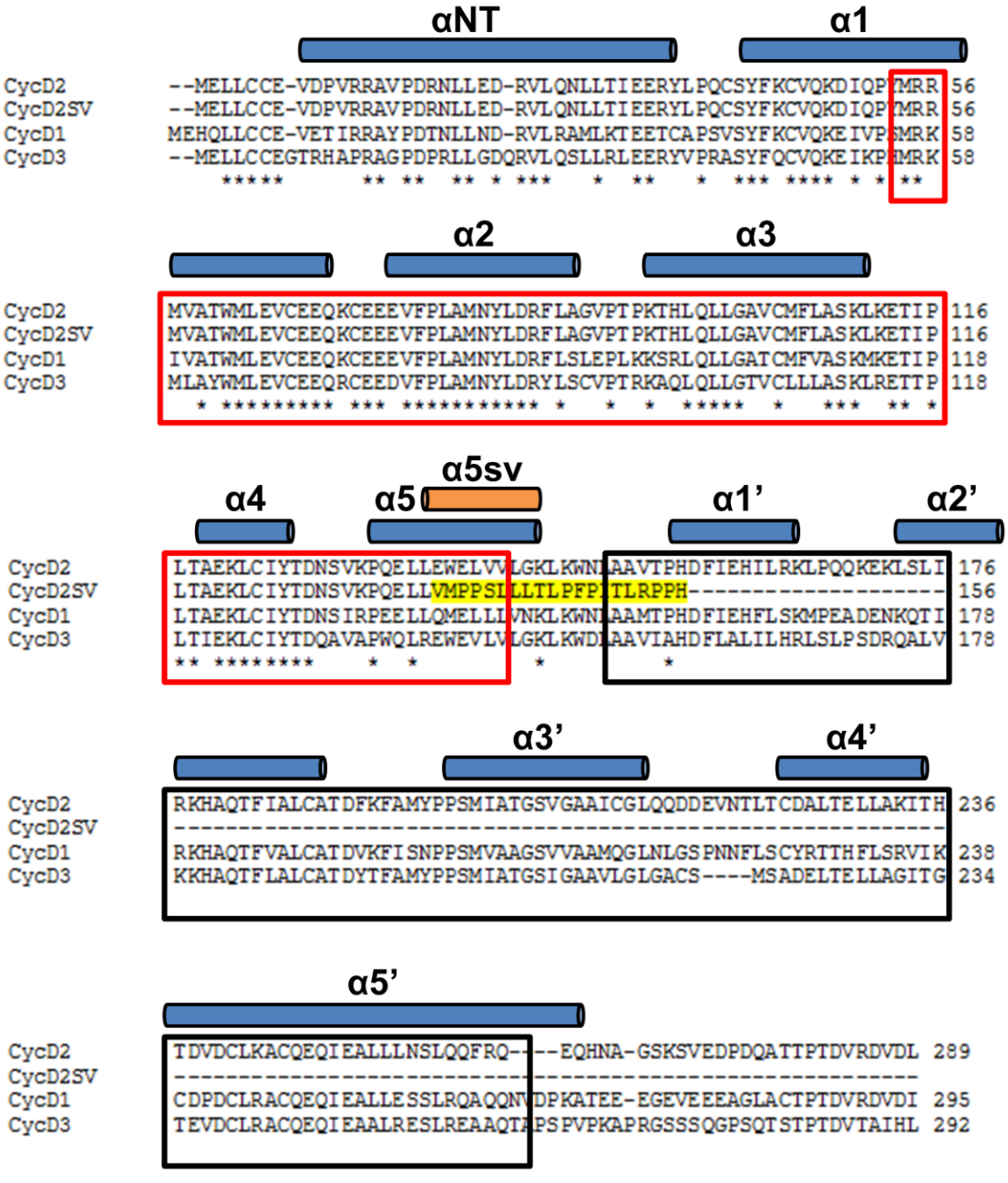
αNT
α1
CycD2 --MELLCCE-VDPVRRAVPDRNLLED-RVLQNLLTIEERYLPQCSYFKCVQKDIQPYMRR 56
CycD2SV --MELLCCE-VDPVRRAVPDRNLLED-RVLQNLLTIEERYLPQCSYFKCVQKDIQPYMRR 56
CycD1 MEHQLLCCE-VETIRRAYPDTNLLND-RVLRAMLKTEETCAPSVSYFKCVQKEIVPSMRK 58
CycD3 --MELLCCEGTRHAPRAGPDPRLLGDQRVLQSLLRLEERYVPRASYFQCVQKEIKPYMRK 58
α2
α3
CycD2 MVATWMLEVCEEQKCEEEVFPLAMNYLDRFLAGVPTPKTHLQLLGAVCMFLASKLKETIP 116
CycD2SV MVATWMLEVCEEQKCEEEVFPLAMNYLDRFLAGVPTPKTHLQLLGAVCMFLASKLKETIP 116
CycD1 IVATWMLEVCEEQKCEEEVFPLAMNYLDRFLSLEPLKKSRLQLLGATCMFVASKMKETIP 118
CycD3 MLAYWMLEVCEEQRCEEDVFPLAMNYLDRYLSCVPTRKAQLQLLGTVCLLLASKLRETTP 118
α5sv
α4
α5
α1'
α2'
CycD2 LTAEKLCIYTDNSVKPQELLEWELVVLGKLKWNLAAVTPHDFIEHILRKLPQQKEKLSLI 176
CycD2SV LTAEKLCIYTDNSVKPQELLVMPPSLLLTLPFPLTLRPPH---------- 156
CycD1 LTAEKLCIYTDNSIRPEELLQMELLLVNKLKWNLAAMTPHDFIEHFLSKMPEADENKQTI 178
CycD3 LTIEKLCIYTDQAVAPWQLREWEVLVLGKLKWDLAAVIAHDFLALILHRLSLPSDRQALV 178
α3'
α4'
CycD2 RKHAQTFIALCATDFKFAMYPPSMIATGSVGAAICGLQQDDEVNTLTCDALTELLAKITH 236
CycD2SV ----------
CycD1 RKHAQTFVALCATDVKFISNPPSMVAAGSVVAAMQGLNLGSPNNFLSCYRTTHFLSRVIK 238
CycD3 KKHAQTFLALCATDYTFAMYPPSMIATGSIGAAVLGLGACS----MSADELTELLAGITG 234
α5'
CycD2 TDVDCLKACQEQIEALLLNSLQQFRQ---EQHNA-GSKSVEDPDQATTPTDVRDVDL 289
CycD2SV ----------
CycD1 CDPDCLRACQEQIEALLESSLRQAQQNVDPKATEE-EGEVEEEAGLACTPTDVRDVDI 295
CycD3 TEVDCLRACQEQIEAALRESLREAAQTAPSPVPKAPRGSSSQGPSQTSTPTDVTAIHL 292

binding of a CAK (Brown et al., 1995; Diehl and Sherr, 1997). In contrast to the majority of mammalian cyclins, cycD2SV contains only the first cyclin fold albeit at partial length (54-136 amino acid region). The fifth helical structure (α5) normally found in the CDK4 binding region of D-type cyclins is replaced in cycD2SV with a shorter helix (α5sv) due to insertion of the unique 20 amino acid CT tail (Fig. 24). Crystal structure studies also indicate that stabilization of a given cyclin molecule depends on extensive hydrophobic packaging interactions between different helices in cyclin folds and also those between the NT helical domain with the first three helices of cyclin fold as well as the CT helical domain (Brown et al., 1995). Since cycD2SV lacks a native structure typically found in other types of cyclins, it is possible that hydrophobic stretches of amino acids (e.g. helix 3) in cycD2SV are exposed unlike cycD2 (Fig. 24, Fig. 25D). As a result of this exposure, cellular machinery involved in protein folding may recognize cycD2SV as a partially folded structure and trigger an ERAD response.

It is generally accepted that some (Anton et al., 1999; Ward et al., 1995) but not all (Johnston et al., 2000) misfolded proteins are subjected to polyubiquitination and presented to the proteasomal system for degradation. In agreement with this notion, our immunostaining experiments with cycD2SV and HA-Ubq co-transfection indicated that cycD2SV aggregates are subjected to polyubiquitination (Fig. 19D-F). Certainly this data offers an explanation for high molecular weight species of cycD2SV observed in native gel electrophoresis of protein lysates from whole embryo and brain lysates or HEK293 cells (Kajitani et al., 2010; Sun et al., 2009). The ubiquitination pattern of cycD2SV is somewhat of an expected result due to the fact that the stability of endogenous D-type

Figure 25. Three-dimensional (3D) protein structure predictions for cycD1 (A), cycD2 (B), cycD3 (C) and cycD2SV (D) as determined by the iterative threading assembly refinement (I-TASSER) server, an internet based 3D protein structure prediction engine. The C-score provided is a confidence score used to estimate the quality of the predicted models and usually lies between -5 and 2. A higher C-score value provides a greater model confidence and C-score values greater than -1.5 have a higher confidence in protein folding. Based on these parameters, the cycD2SV ribbon structure most likely represents the correct folding of the protein. The NT of the presented protein structures is denoted by blue and the CT is denoted by red.

A

cycD1

C-score: 0.83

B

cycD2

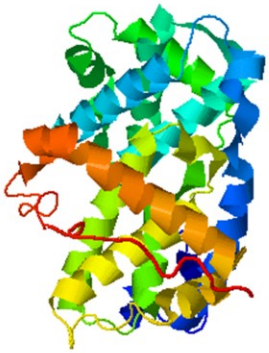

C-score: 0.94

C

cycD3

C-score: 0.51

D

cycD2SV

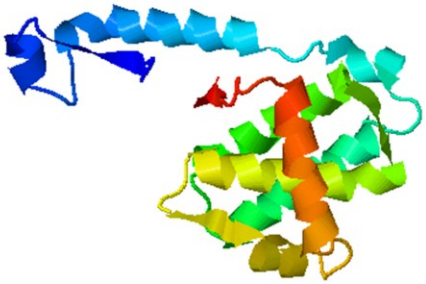

C-score: 0.90

cyclins have been shown to be regulated by UPS degradation (Kida et al., 2007; Lin et al., 2006; Okabe et al., 2006). However, sustained presence of ubiquitin positive aggregates and increased retention of ERAD reporter in cycD2SV expressing cells suggests that overproduction of misfolded proteins may have saturated the ability of UPS system. Consistent with this notion, cycD2SV aggregates were frequently associated with endosomes, lysosomes and autophagosomes, which underscores a critical role for autophagy, a controlled process involving sequestration of certain cytoplasmic contents for lysosomal delivery, where the contents are degraded and recycled (Klionsky, 2010). Indeed, association of cycD2SV in p62 positive vesicles further offers a mechanistic explanation for formation of aggresomal inclusions into autophagosomes. The role of p62 in autophagic clearance of polyubiquitinated protein aggregates has been well documented (Komatsu and Ichimura, 2010a; Moscat and Diaz-Meco, 2009). The carboxy terminal UBA domain of p62 binds to polyubiquitinated proteins, the N-terminal PB1 domain is critical for self-oligomerization and the LRS/LIR domain recruits autophagy regulator LC3/Atg8. It is possible that p62 may link ubiquitinated cycD2SV to the core autophagic protein LC3. However, additional experiments are required to confirm this notion.

In contrast to a high frequency of multiple protein aggregates seen with cycD2SV expression, cycD2 overexpressing cells frequently contained a single large aggregate confined to the perinuclear compartment. Although exogenously expressed cycD2 aggregates were ubiquitinated, they were not positive for markers of autophagy (Data not shown). Absence of such intense perinuclear staining pattern for endogenous cycD2 in HEK293 cells suggests that alternative mechanisms other than ER stress and or

autophagy may be responsible for aggregation of overexpressed cycD2. Misfolding of cycD2 due to fusion with a myc epitope in HEK293 cells can be readily ruled out since exogenous expression of the same cycD2myc fusion protein in embryonic cardiomyocytes did not induce any protein aggregation (Sun et al., 2009). It is possible that high intracellular concentrations of cycD2 may promote dimer or oligomer formation. Consistent with this notion, IP studies using differentially tagged cycD2 constructs (cycD2-DsRed and D2myc) revealed the dimerization possibility of cycD2 molecules either via direct or indirect protein-protein interactions (Zhang and Pasumarthi, unpublished data). Recent studies showed that another cell cycle regulator $p57^{kip2}$ is capable of associating with itself via the NH2 domain to form a homodimeric species, which is a more potent inhibitor of the cycD1/CDK4 complex compared to a single $p57^{kip2}$ molecule (Reynaud et al., 2000). However, it is not known whether homodimers of CKIs such as $p57^{kip2}$ can promote dimerization of cycD/CDK4 heterodimers. Dimerization of CDK4 molecules in two adjacent cycD/CDK4 heterodimers similar to that described for kinase domains of EGF receptors (Zhang et al., 2006) may also offer an explanation for perinuclear cycD2 aggregates. Furthermore, crystal structure studies involving cycD3/CDK4 complex revealed the existence of two copies of cycD3/CDK4 in each crystal and also suggested that the CT cyclin fold may be responsible for dimerization. The cycD3-cycD3 interactions in crystals were thought to be due to the absence of a structured CT tail in cycD3 similar to that found in cycA, B or E that would be expected to shield the surface of the CT cyclin fold (Takaki et al., 2009). Secondary structure analysis via I-Tasser (Roy et al., 2010; Zhang, 2008) also revealed absence of a structured CT tail, distal to the second cyclin fold in cycD2 and cycD1 molecules (Fig. 24

and 25A, B). These structural similarities indeed suggest that cycD2-cycD2 dimerization may be possible through a second cyclin fold similar to that described for cycD3-cycD3 dimerization. In the present study, we have also shown that cycD2SV, which lacks the second cyclin fold can interact with cycD2 by IP or immunolocalization experiments. Interestingly, deletion of 1-53 amino acid NT region of cycD2SV significantly abolished intracellular protein aggregation. This in turn suggests that cycD2-cycD2 or cycD2-cycD2SV dimerization may occur through the structured NT sequence (cycD2SV 1-53) similar to that described for $p57^{kip2}$ (Reynaud et al., 2000). Since cycD2SV 54-136 protein still retains the ability to bind CDK4 (Zhang and Pasumarthi, unpublished data) and exhibits a significant reduction in its tendency for protein aggregation, CDK4-CDK4 interactions may not play a critical role when it comes to cycD2SV aggregation. Collectively, our immunostaining and IP/western studies show for the first time that, under high intracellular concentrations, cycD2 may exist as dimers with cycD2 and or cycD2SV *in vivo*. These results may certainly offer a mechanistic explanation for earlier studies describing cytoplasmic sequestration of endogenous or overexpressed cycD1 in a variety of mammalian cancer cell lines and postmitotic neurons (Alao et al., 2006; Sumrejkanchanakij et al., 2003).

To elucidate the possible mechanism(s) of cycD2SV induced cell cycle exit, we investigated its ability to interact with CDK4 and cycD2 based on the premise that sequestration of these positive cell cycle regulators by cycD2SV, which lacks the CAK binding domain would render them inactive. Consistent with this notion, an earlier study demonstrated that immunocomplexes containing cycD2SV and CDK4 failed to phosphorylate pRb, a critical step required for cells to overcome G1/S restriction point

(Denicourt et al., 2008). Indeed, our results in the present study showed that cycD2SV can sequester CDK4 and cycD2 into p62 positive inclusion bodies and target them for UPS/autophagy mediated degradation. To our knowledge, this is the first report to show that a cyclin variant can directly affect the stability of other cyclins and or CDK complexes. Further deletion analysis suggested that NT 1-53 amino acid region is required for cycD2SV protein aggregation, whereas 54-136 amino acid region is responsible for the majority of cell cycle inhibition (via CDK4 binding).

In this study, we present evidence of the mRNA upregulation of GADD45α and dynamin 2 in response to cycD2SV overexpression. GADD45α is a p53 inducible gene which plays a role in cell cycle arrest in response to double stranded DNA damage (Hollander and Fornace, 2002). Additionally, GADD45α is capable of inducing G2/M arrest by interfering with the formation of cycB/CDK1 complexes (Wang et al., 1999; Zhan et al., 1999). Given the established role of GADD45α, an alternate mechanism by which cycD2SV actuates cell cycle exit might be due to induction of DNA damage. However, based on 53BP1 (p53-binding protein 1) staining, a marker for double stranded DNA breaks, no DNA damage was detected in cycD2SV transfected cells (Data not shown).Overexpression of Dynamin 2 was shown to decrease cell proliferation and cause cell death via p53 pathway (Fish et al., 2000). However, cycD2SV positive cells were negative for apoptosis. Currently, the mechanism by which cycD2SV upregulates these proteins is yet to be elucidated. It would be interesting to investigate whether cycD2SV is able to upregulate these transcripts in a p53 dependent or independent manner.

In a study by Huang *et al*., cell trypsinization was demonstrated to upregulate the pro-apoptotic protein p53 and CKI p21, and down regulate the pro-survival protein Bcl-2

(Huang et al., 2010). Interestingly, cycD2SV transfected cells subjected to trypsinization did not survive in culture 48 hrs post re-plating. While cycD2SV aggregation alone is not enough to induce apoptotic cell death, we believe that cycD2SV expressing cells are sensitized to cell death upon exposure to additional stressors, such as trypsinization. It is possible that cycD2SV toxicity acts synergistically with trypsin induced stress, however, how cycD2SV collaborates with trypsinization is still not known, and perhaps more experimental work is needed to elucidate the mechanism underlying this phenomenon.

Due to a positive regulatory role of D type cyclins in promoting cell cycle progression, aberrant expression of these cyclins have been implicated in various types of cancers (von Bergwelt-Baildon et al., 2011). Alternatively, D type cyclins have also been implicated in cellular senescence, a state of G1 arrest where cells no longer respond to mitogenic signals (Garkavtsev et al., 1998; Han et al., 1999; Meyyappan et al., 1998). Research conducted by Pagano *et al.* demonstrated that microinjection of cycD1 into G1 synchronized or UV exposed human lung IMR-90 fibroblasts dramatically decreased cells entering S-phase by preventing nuclear localization of PCNA (Pagano et al., 1994). PCNA, an auxiliary protein of DNA polymerases δ and ε is required for DNA replication or repair and is known to interact with cycD1 (Matsuoka et al., 1994; Pagano et al., 1994). Pagano *et al* also showed that co-injection of PCNA but not CDK4 or CDK2 expression constructs prevented cycD1 induced replicative arrest. Overexpression of cycD1 was also implicated in cell cycle exit in Hs68 fibroblasts by inactivation of CDK2 kinase activity (Atadja et al., 1995). In the present study, overexpression of cycD2 in HEK293 cells was associated with a significant decrease in S-phase entry, albeit not as effective as cycD2SV. While this result was surprising due to an established role of

cycD2 in cell cycle activation, similar to cycD1, cycD2 has also been implicated in cellular senescence as well as various states of growth arrest (Meyyappan et al., 1998). Both cycD2 mRNA and protein levels were found to be significantly increased in cells subjected to contact inhibition, serum starvation and cellular senescence. Under these conditions, cycD2 was shown to form inactive complexes with CDK2 by preventing its normal association with obligate binding partners such as cycA or cycE (Meyyappan et al., 1998). Collectively, these studies suggest that while D-type cyclins play an important role in cell cycle progression, under certain conditions they may also play a key role in cell cycle exit so as to ensure that cell cycle progression does not occur prematurely.

In this study, we demonstrate the capability of cycD2SV, a splice variant of cycD2, to induce cell cycle arrest in a variety of transformed and immortalized cell lines. We identify both the aggregation domain (1-53) and cell cycle inhibitory domain (54-136) of the protein. We believe the aggregation phenotype of the protein occurs as a result of misfolding due to the truncated CT tail of the protein. We present evidence elucidating possible mechanisms for cycD2SV mediated cell cycle arrest (Fig. 26). CycD2SV is capable of sequestering cell cycle proteins such as cycD2 and CDK4 and targeting them for autophagy mediated degradation. Given the important role of these proteins in G1 phase of the cell cycle we propose that cycD2SV arrests cells at the G1 phase. Additionally, as cycD2SV protein aggregates increase, ER stress is induced, which ultimately leads to the impairment of ERAD. We further demonstrate that cycD2SV aggregates co-localize with the MTOC marker γ-tubulin. Generally, as the rate of protein aggregate formation exceeds that of clearance, protein aggregates are transported to the MTOC where they form the aggresome. As a result of the cellular stress induced by the

Figure 26. Proposed mechanism of action of cycD2SV in cell cycle exit. CycD2SV mediates cell cycle exit by 1) binding important cell cycle proteins, such as cycD2 and CDK4, and targeting them for selective autophagosome degradation and, 2) inducing cellular stress and upregulating a potent G2/M inhibitor, GADD45α.

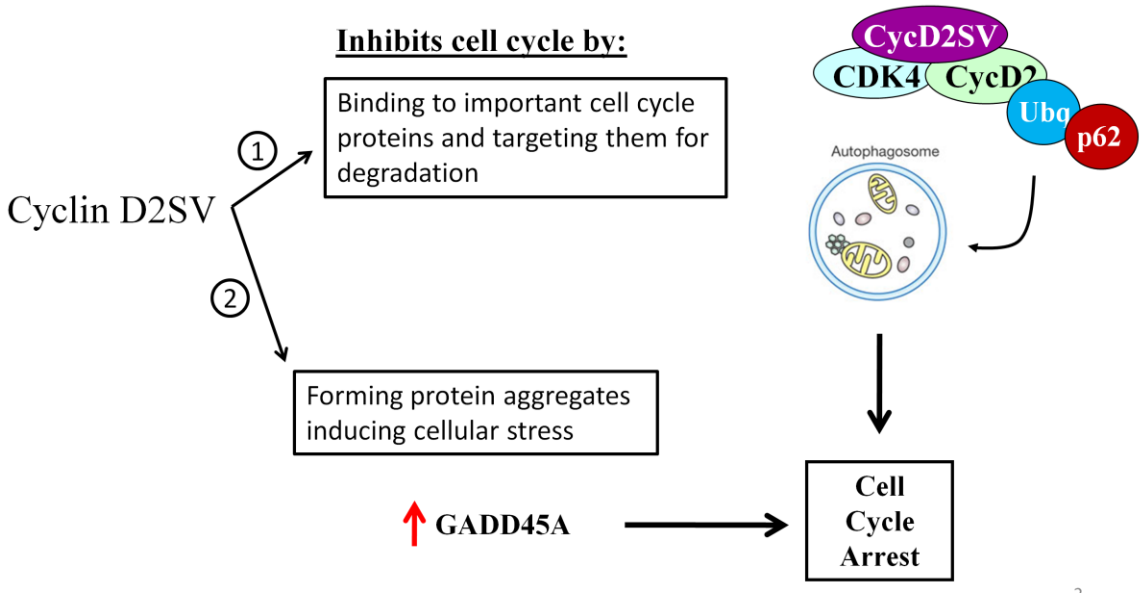
Inhibits cell cycle by:
Binding to important cell cycle proteins and targeting them for degradation
1
Cyclin D2SV
2
Forming protein aggregates inducing cellular stress
GADD45A
Cell Cycle Arrest
CycD2SV
CDK4
CycD2
Ubq
p62
Autophagosome

accumulation of protein aggregates, we believe GADD45α, a G2/M cell cycle inhibitor, is upregulated inducing cell cycle arrest. While cycD2SV aggregation is not sufficient to induce apoptotic cell death, our results indicate that cycD2SV expressing cells are sensitized to cell death when exposed to additional stressors, such as trypsinization. How cycD2SV collaborates with trypsinization is unknown, and perhaps more experimental work is needed to elucidate the mechanism underlying this phenomenon.

Chapter 3: Role of Endogenous Cyclin D2SV in the Regulation of Cyclin D2 Stability during Confluence

3.1 Manuscript Status and Student Contribution

As first author on this manuscript, I performed the majority of experiments, completed all analysis, data interpretation, and statistics. I wrote the manuscript with input and assistance from Dr. Kishore Pasumarthi. This manuscript is currently in preparation for submission to the Journal of Biological Chemistry

3.2 Abstract

CycD2SV is a recently discovered splice variant of cycD2. In this study, we examined the effects of cellular stress on the expression of cycD2SV in human embryonic kidney (HEK293) cells. Under confluence and serum starvation conditions, cycD2SV protein levels increased by 2.5-fold while cycD1, D2, and D3 protein levels significantly decreased. Further investigation by QPCR analysis revealed that cycD2SV mRNA levels remained constant at confluence, while cycD1, D2 and D3 mRNA levels significantly decreased. Collectively, these results suggest that translation efficiency of cycD2SV mRNA may selectively be increased under stress conditions. Furthermore, we showed that transient knockdown of cycD2SV mRNA by shRNA approach can rescue cycD2, but not cycD1 or cycD3 protein levels in confluent cultures. In addition, knock down of cycD2SV mRNA by shRNA increases cell cycle activity as determined by [^{3}H]-thymidine incorporation, further implicating a critical role for cycD2SV in the negative regulation of the cell cycle during cellular stress.

3.3 Introduction

The cell cycle is an integral part of cell division and survival, and, as such, is tightly regulated by numerous proteins (Tessema et al., 2004). Cyclins are a family of regulatory proteins that bind to, and regulate the function of distinct cyclin dependent kinases, which belong to a family of threonine/serine protein kinases (Johnson and Walker, 1999). Upon binding, the cyclin/CDK complex is activated, in turn activating genes necessary for cell cycle progression. To date, sixteen cyclins and eleven CDKs

have been identified, however, not all are involved in the cell cycle (Vermeulen et al., 2003). As the name suggests cyclin protein levels fluctuate during various stages of the cell cycle, whereas CDK levels remain constant and do not change (Vermeulen et al., 2003). Expression of different cyclins at specific time points in cell cycle ensures the activation of the necessary CDKs for proper cell cycle propagation (Tessema et al., 2004).

In response to mitogenic signals, D-type cyclins are the first to be expressed and play a role in initiating the cell cycle (Johnson and Walker, 1999; Tessema et al., 2004; Vermeulen et al., 2003). D-type cyclins can bind to CDK4 or CDK6 and activate them. Once activated, the cyclin/CDK complex phosphorylates pRb, which is bound to the transcription factor, E2F (Johnson and Walker, 1999). When bound to pRb, E2F is inactivated and upon pRb phosphorylation by cyclin D/CDK4 complexes, E2F is released, thereby initiating the transcription of genes required for DNA replication. Given the pivotal role D-type cyclins play in cell cycle initiation, aberrant expression of these cyclins have been linked to many cancers (Tessema et al., 2004). Overexpression of cycD1 has been associated with 90% mantle cell lymphoma, 60% of breast carcinomas, 40% of squamous cell carcinomas of the head and neck, 40% of colorectal cancers, 20% of prostate cancers and in some lung cancers (Tessema et al., 2004). CycD2 overexpression has been reported in gastric and kidney cancers, whereas cycD3 overexpression has been reported in pancreas, colorectal and kidney cancers (von Bergwelt-Baildon et al., 2011). Even alternate splice variants of both cycD1 and cycD2 have been associated with tumorigenic growth (Denicourt et al., 2008; Solomon et al., 2003).

CycD2SV is a recently reported splice variant of cycD2 which was first discovered in a tumor induced by the Graffi Leukemia virus (Denicourt et al., 2003). According to Denicourt *et al.*, overexpression of cycD2SV and HA-H-Ras causes cellular transformation in mouse embryonic fibroblasts as determined by focus forming assay (Denicourt et al., 2008). However, Denicourt *et al* did not provide data to highlight the effects of cycD2SV overexpression in the absence of H-Ras on cell cycle regulation. We have recently reported that overexpression of cycD2SV in primary mouse cardiomyocytes, as well as a multitude of transformed cell lines produced multiple protein aggregates and induced cell cycle arrest [(Sun et al., 2009), see chapter 2]. To elucidate the mechanism by which cycD2SV induced cell cycle exit, we completed co-immunoprecipitation and immunohistochemistry experiments [(Sun et al., 2009), see chapter 2]. We were able to demonstrate that cycD2SV binds to CDK4 and/or cycD2. Furthermore, we showed that cycD2SV aggregates are ubiquitinated, and co-localized with p62, a protein involved in autophagy (See section 2.5.6 and 2.5.7). Additionally, data provided by Denicourt *et al.* demonstrated that CDK4, in complex with cycD2SV, was inactive and was unable to phosphorylate pRb, a step required for cell cycle progression. Collectively, this data suggest that cycD2SV sequesters cycD2/CDK4 complexes, interfering with their function and targeting them for autophagy mediated clearance.

While it is established that overexpression of cycD2SV causes cell cycle exit, it is not yet known whether endogenous cycD2SV plays a similar role. Here, we provide evidence that endogenous cycD2SV plays a role in cell cycle exit induced by contact inhibition and serum starvation in HEK293 cells. We demonstrate that cycD2SV protein

levels are elevated in detergent soluble cytosolic fraction during serum starvation and confluence, while cycD1, D2, and D3 levels decline. Knockdown of cycD2SV mRNA by shRNA approach during confluence rescues cycD2 protein levels, but not those of cycD1 or cycD3. Consistent with decreases in protein levels, mRNA levels of cycD1, D2 and D3 also significantly decrease in confluent cultures.

3.4 Methods

3.4.1 Generation of Cyclin D2SV Polyclonal Antibody

CycD2SV antibody was generated by immunizing New Zealand white rabbits with a short fourteen amino acid (aa) peptide from the CT region of the mouse cycD2SV protein (aa 139-153, LLTLPFPITLRPPH). Rabbits received a series of immunizations until sufficient antibody titer was detected then bled for total serum collection (Sun et al., 2009). The collected serum was affinity purified using a HiTrap™ protein G-Sapharose column for antibody purification (GE Healthcare Life Sciences, New Jersey). The column was first washed with ten column volumes (10 ml) of binding buffer (20mM phosphate pH 7.0). Following the wash, 0.5 ml of the rabbit serum (Female 211) was mixed with binding buffer at a 1:1 ratio, and passed through the column. The column was washed again with ten volumes of binding buffer and subsequently 5 ml of elution buffer (0.1 M glycine HCl pH 2.7) was passed through the column for antibody collection. Upon addition of the elution buffer, the first 1 ml of flow through was discarded, and the column was left to stand for one minute. Later, eluate was collected as 1 ml fractions in four different tubes (designated as fractions one to four) containing 200 µl of neutralizing

buffer (1 M Tris-HCL, pH 9.0). The neutralizing buffer was added to preserve the acid labile IgGs. Finally, the column was washed in five column volumes of elution buffer and stored at 4ºC in 20% ethanol solution (diluted in water). A 10 ml syringe was used for delivery of solutions into the protein G-Sapharose column and solution flow was maintained at 1 ml/minute or slower. A positive meniscus was always maintained when connecting the syringe to the column to avoid injecting air into the column. After injecting the required solution into the column, the syringe was disconnected and the next required solution was added to the syringe before reconnecting it to the column to avoid injecting air into the column. Small aliquots from fractions one to four of eluate were tested for positive immunoreactivity in HEK293 cells transfected with D2SV construct. Usually, fraction one contains the highest titer of affinity purified D2SV antibody. D2SV antibody immunoreactivity was confirmed by immunofluorescence and western blotting as described in chapter 2 with appropriate controls.

3.4.2 Cyclin D2SV Antibody Epitope Mapping and Crossreactivity Study

Synthetic peptides were generated for epitope mapping studies. Peptide sequences coding for the cycD2SV CT (91% peptide purity) domain and a control peptide from the NT (74% peptide purity) region of cycD2 were synthesized (Sigma-Genesis, Oakville, Ontario, Fig. 27A, B). Three peptides, peptide 1, 2 and 3 (79.51%, 95.13% and 80.19% peptide purity respectively), spanning different fragments of the cycD2SV CT domain were also synthesized (Peptide 2.0 Inc, http://www.peptide2.com/index.php, Fig. 27A, B). Peptides were dissolved in ddH_2O and 50 ng, 100 ng, 500 ng and 1 µg were spotted on nitrocellulose membrane, air dried, and probed with affinity purified cycD2SV

Figure 27. Amino acid sequences of the synthesized peptides. Schematic figure depicting the location (A) and sequence (A, B) of the control NT peptide in relation to the cycD2SV amino acid sequence. Additionally, the location (A) and sequence (B) of the CT-peptide and peptides 1-3 are indicated in relation to the cycD2SV CT-domain. Numbers represent amino acid positions relative to the start codon (methionine) (A).

A

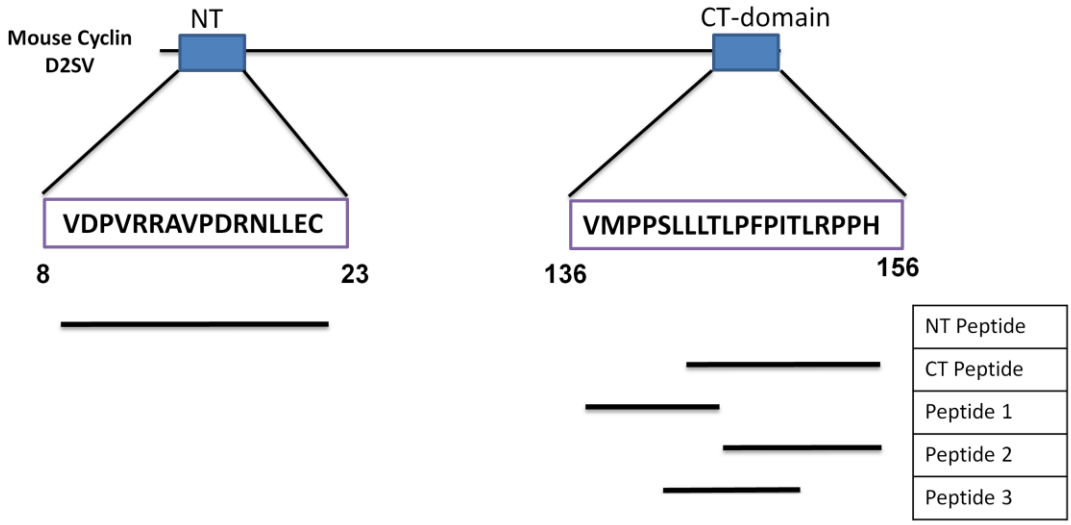

B

Sequence Name	Peptide Sequence
Control Peptide Cyclin D2 N-terminus	VDPVRRAVPDRNLLEC
Cyclin D2SV CT domain	VMPPSLLLTLPFPITLRPPH
Cyclin D2SV C-terminus peptide	LLTLPFPITLRPPH
Peptide 1	VMPPSLLLT
Peptide 2	LPFPITLRPPH
Peptide 3	SLLLTLPFPIT

antibody. For peptide blocking experiments, cycD2SV antibodies were pre-incubated with 200 ng of the test or control peptide for two and a half hours at room temperature prior to probing pcDNA and cycD2SVmyc transfected cell lysates resolved by western blot. Identical conditions, such as peptide concentration and duration of incubation with cycD2SV antibodies, were followed for peptide blocking experiments using immunofluorescence.

3.4.3 Cell Culture Conditions

HEK293 cells purchased from ATCC (Virginia) were cultured in DMEM (Wisent, Saint-Bruno, Quebec) containing 4.5 g/L glucose, L-Glutamine and sodium pyruvate, and supplemented with 10% fetal bovine serum (10% FBS-DMEM), 1x AB/AM (1,000 units penicillin G sodium, 1,000 µg streptomycin sulfate, and 2.5 µg amphotericin B as Fungizone® in 0.85% saline), and 1x mM sodium pyruvate in a humidified incubator set at 6% CO_2 and 37°C (Thermo Fisher Scientific, Nepean, Ontario). All cell culture reagents were purchased from Invitrogen (Burlington, Ontario). For experiments, cells were cultured in 100 mm or 35 mm dishes with square cover glass (22x22 mm 0.08-0.13 mm thickness, VWR, Mississauga, Ontario). Cells cultured in 100 mm dishes were seeded at 600,000 cells per dish and received 10 ml of media, whereas 35 mm dishes were seeded at a density of 150,000 cells per dish, and received 2 ml of media. Unless otherwise stated, media was changed once every two days. For confluence experiments, HEK293 cells were seeded in 100mm dishes and grown to confluence. At days four and six post seeding, the medium was aspirated and fresh medium was added. Protein was extracted on days two, four, six, and eight, whereas RNA was extracted on

days two, four, and six (Fig. 28). For serum starvation experiments, HEK293 cells were seeded in 100mm dishes. For the first two days, cells were left to grow in 10% FBS-DMEM. On the third day, the medium was changed to DMEM containing 0.1% FBS (0.1% FBS-DMEM). On day four, cells were trypsinized and seeded in two new dishes with 0.1% FBS-DMEM. On day six, the cells were trypsinized again and transferred to new dishes. Protein and RNA was extracted (See section 3.4.4 and 3.4.6) on days two, six, and eight (Fig. 29). Samples collected were stored at -80°C until further use.

3.4.4 Protein Extraction and Western Blotting

Cells were lysed by the addition of tumor lysis buffer (1% NP40/Igpal, 5mM EDTA, 50mM Tris HCl pH 8.0, 10mM phenylmethylsulphonyl fluoride (PMSF) and 1mM Aprotinin) directly to the culture dishes. Cells were scraped using a cell scraper, collected in a 1.5 ml eppendorf tube, and subjected to sonication (Sonic Dismembrator, model 100; Thermo Fisher Scientific, Nepean, Ontario; Setting 3.5, duration: 10 seconds x 3). Cell lysates were incubated at 4°C for fifteen minutes. Detergent soluble (cytosol) and detergent insoluble (whole membrane) fractions were collected by high speed centrifugation (13,300 rpm x 15minutes) at 4°C. Aliquots were taken for protein determination by Bradford assay (Thermo Fisher Scientific, Nepean, Ontario) and equivalent amounts of protein (40-60µg) were denatured in Lamelli buffer [62.5 mm Tris-Cl pH 6.8, β-mercaptoethanol, 25% glycerol, 2% sodium dodecyl sulfate (SDS), 0.02% bromophenol blue, and double distilled water (ddH_2O)]. Samples were resolved in a 12.5% SDS-polyacrylamide gel (0.375M Tris-HCl, 0.08% SDS, 10% acrylamide, 0.2% ammonium persulphate and 0.1% v/v TEMED) using a 1x Tris-glycine migration buffer

Figure 28. Experimental timeline for confluence experiments. Cells were seeded at 600,000 cells in 100 mm dishes at day 0 in 10% FBS-DMEM and left to grow to day 8. Media was refreshed at days 2, 4 and 6. Protein was harvested on days 2, 4, 6 and 8 whereas RNA was harvested on days 2, 4 and 6. Day 2 cultures were sparse with no cell to cell contact and as such were designated as control. For shRNA experiments, cells were transfected on day 2 (*) with shRNA constructs and left to grow freely to day 8 where protein was harvested. Media was also refreshed for shRNA constructs on days 2 (following transfection protocol), 4 and 6. Note: See Fig. 31 for additional details on transfection timeline.

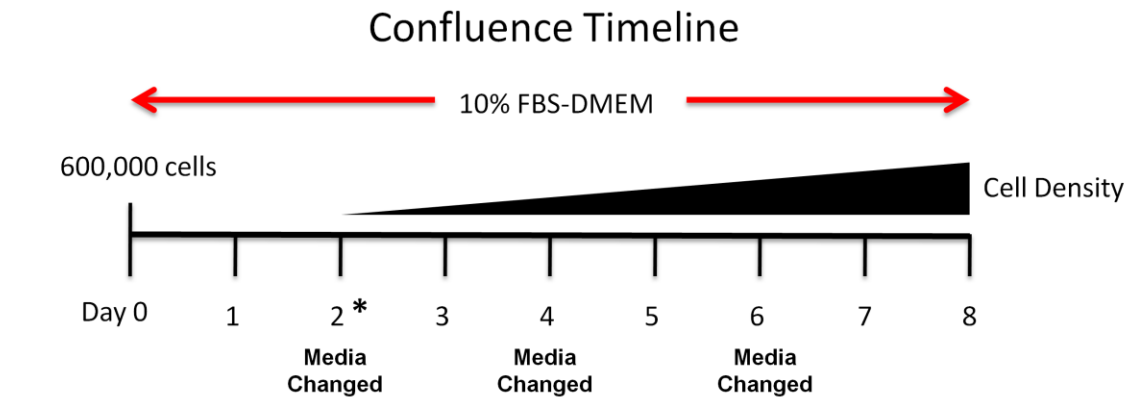
Confluence Timeline
10% FBS-DMEM
600,000 cells
Cell Density
Day 0
1
2 *
3
4
5
6
7
8
Media Changed
Media Changed
Media Changed
Protein
RNA
✓
✓
✓
✓ *
✓
✓
✓

Figure 29. Experimental timeline for serum starvation experiments. Cells were seeded at 600,000 cells in 100 mm dishes at day 0 in 10% FBS-DMEM and left to grow to day 2. At day 2 media was changed to 0.1% FBS-DMEM. At day 4, cells were split to 2 new dishes (1:2) to avoid cell to cell contact. To ensure complete cell cycle arrest due to serum starvation, cells were split once again at day 6 (1:1) and left in culture till day 8. Protein and RNA were harvested at days 2 (control), 6 and 8 time points.

Serum Starvation Time Line

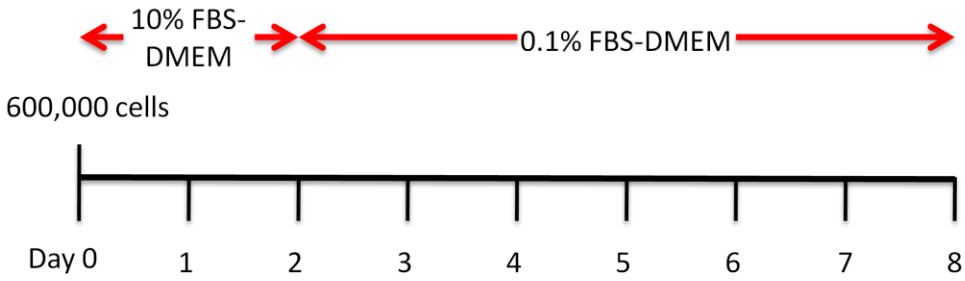

Protein		✓	✓	✓
RNA		✓	✓	✓

(25mM Tris base, 190 mM glycine and 0.1% SDS at 8.3 pH) at 100 volts and transferred to Hybond ECL nitrocellulose membrane (GE Healthcare Life Sciences, New Jersey) by applying a constant current at 100 volts for one hour (Transfer buffer: 25mM Tris base, 190 mM glycine and 20% methanol at 8.3 pH). The membrane was incubated with napthol blue stain (1% napthol blue black, 45% methanol and 10% glacial acetic acid) for protein visualization and determination of protein loading. The membrane was blocked for one hour in blotting buffer (5% skimmed milk powder, 3% BSA, 0.1% Tween 20 in PBS (Sigma-Aldrich, Oakville, Ontario) followed by a one hour primary antibody, and a one hour secondary antibody incubation. Primary antibodies used in this study include: cycD2SV or antibodies purchased from Santa Cruz Biotechnology, California: cycD1 (sc-753), cycD2 (sc-593), p27 (sc-528), CDK4 (sc-260), and α-tubulin (sc-8035). Secondary antibodies include: goat-anti-rabbit (Bio-Rad, Mississauga, Ontario, Catalogue #172-1019) or goat-anti-mouse (Bio-Rad, Mississauga, Ontario, Catalogue #170-6516) antibodies conjugated to horse radish peroxidase. Antibody dilutions were as follows: primary antibody 1:400, secondary goat-anti-rabbit antibody was 1:200 and secondary goat-anti-mouse was 1:1000. Protein bands were detected by ECL Plus Western Blotting Detection System via the chemiluminescence method according to manufacturer's instruction (GE Healthcare Life Sciences, New Jersey).

3.4.5 Band Densitometry for Protein Quantification

For band density analysis, western blot films were scanned and imported into Image J (http://rsbweb.nih.gov/ij/) software. Given that α-tubulin protein level did not change for any of the treatments (confluence and serum starvation), α-tubulin protein

levels were used to normalize any variation in protein loads. Once normalized, experimental band intensity values were represented as fold changes relative to control band intensity values. Statistical analysis was performed using both normalized as well as relative fold changes.

3.4.6 Total RNA Isolation

Total RNA was isolated using the RNeasy mini-kit PLUS according to manufacturer's instructions (Qiagen, Mississauga, Ontario). In brief, samples are lysed in a guanidine-isothiocyanate denaturing buffer and passed through a gDNA eliminator column. In conjunction with a high salt buffer, the gDNA column ensures the total elimination of gDNA. Total RNA concentrations were determined by using the 260 nm absorbance value obtained by a spectrophotometer (SmartSpec^{TM} Plus, Bio-Rad, Mississauga, Ontario). The quality of the RNA was determined by taking the ratio of the absorbance measured at 260 nm to the absorbance measured at 280 nm. A ratio of 1.8 to 2.0 indicates a high level of RNA purity, devoid of DNA contamination. RNA samples with values deviating from these ratios were rejected for further analysis.

3.4.7 Reverse Transcription and Quantitative Real Time Polymerase Chain Reaction

Total RNA extracted from HEK293 cells was reverse transcribed to cDNA using superscript II reverse transcriptase (RT) and random primers (Invitrogen, Burlington, Ontario). The reaction mixture consisted of 1µg of RNA, 1 µl of random primers (0.5 µg/µl, and 1 µl dNTP mix (10 mM each). Subsequently, the final volume of the reaction mixture was adjusted to 12 µl using sterile water. The samples were then heated at 65°C

for five minutes and chilled on ice for five minutes. Finally, 4 µl of 5x superscript first strand buffer, 2 µl 0.1 M DTT, and 1 µl RNaseOUT (40 unites/µl) were added, and the samples were incubated at 25°C for ten minutes before the addition of 1 µl (200 units) of SuperScript II RT . All RT reagents were purchased from Invitrogen (Burlington, Ontario). The samples were mixed by pipetting and incubated at 42°C for fifty minutes, followed by an enzyme inactivation step at 70°C for fifteen minutes. For each new RNA sample, two controls were set up; a no-template control and a no-enzyme control, where sterile water replaced the omitted enzyme or RNA.

The cDNA was amplified by QPCR using the following primers: GAPDH, cycD1, cycD2, cycD3 and cycD2SV (Table 5). The reaction mixture consisted of 2µl of cDNA product, 1µl of the forward and reverse primers (2.5 µM), 10 µl of 2x Brilliant II SYBER Green Master Mix (Stratagene, La Jolla, California), 0.5 µl of 1:1000 Rox reference dye, and 5.5 µl RNase/DNase free dH_2O. QPCR conditions were set on the MX3000P® thermocycler (Stratagene, La Jolla, California) as follows: 95°C for ten minutes, one cycle; 95°C for twenty seconds, 60°C for eighteen seconds and 72°C for thirty seconds, fourty-five cycles. Once the amplification cycles were completed, melting curves were generated by an additional cycle at the following setting: 95°C for one minute, 60°C for thirty seconds and 95°C for thirty seconds. The melting point curve was used to verify the amplification of one gene per primer pair (Fig. 30A). Also, QPCR amplification products were resolved by electrophoresis on a 2.5% agarose gel to verify if the expected amplicon product size was obtained (Fig. 30B). The cycD1, D2 and D3 primers were generated using the NCBI primer-blast software, (http://www.ncbi.nlm.nih.gov/tools/primer-blast/index.cgi?LINK_LOC=BlastNews)

Table 5. Quantitative Real-Time PCR human primer sequences and expected amplicon band sizes.

Gene	Accession Number	Sequence 5' – 3'	Expected Band Size
GAPDH	NM_002046	F ATGGGGAAGGTGAAGGTCG R GGGGTCATTGATGGCAACA	108
Cyclin D1	NM_053056	F CCCTCGGTGTCCTACTTCAA R AGGAAGCGGTCCAGGTAGTT	149
Cyclin D2	NM_001759	F TGGGGAAGTTGAAGTGGAAC R ATCATCGACGGTGGGTACAT	175
Cyclin D3	NM_001760	F GCTGGAGGTATGTGAGGAGC R TGCACAGTTTTTCGATGGTC	185
Cyclin D2SV	AK0079041	F GGCTGGGGTCCCGACTCCGAAG R GATTCCCGCTTTCCCCTGGCCA	204

F= forward primer; R= reverse primer

Figure 30. QPCR primers (GAPDH, cycD1, cycD2, cycD3 and cycD2SV) are specific to their target gene, amplifying only one gene product. Melting curves completed for QPCR primers indicate the presence of only one amplified product for each primer as depicted by a single peak per primer pair (A). Resolved QPCR reactions amplified by the QPCR primers in a 2.5% agarose gel (B). bp, base pairs.

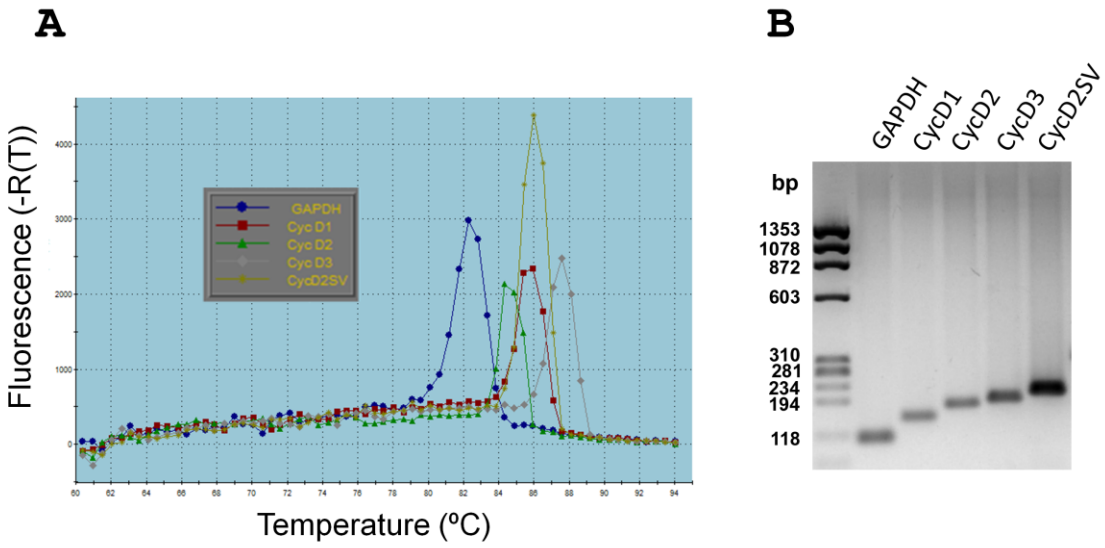
A
B
Fluorescence (-R(T))
Temperature (ºC)
GAPDH
Cyc D1
Cyc D2
Cyc D3
CycD2SV
bp
1353
1078
872
603
310
281
234
194
118
GAPDH
CycD1
CycD2
CycD3
CycD2SV

whereas the primerbank software algorithm (http://pga.mgh.harvard.edu/primerbank/) was used to generate the GAPDH primers. The cycD2SV primer sequences were published previously by Denicourt *et. al.* (Denicourt et al., 2008). Where possible, primers were designed to be exon spanning so as to eliminate gDNA amplification. In addition, gDNA was eliminated using gDNA removal columns provided by the RNeasy mini-kit PLUS during total RNA isolation and samples were tested for gDNA contamination using the SABiosciences (Qiagen, Mississauga, Ontario) QPCR array, which contains a gDNA contamination control well (proprietary intron specific primers). Gene expression was normalized to a control housekeeping gene (GAPDH) using the $\Delta\Delta C_T$ method (Livak and Schmittgen, 2001). In brief, the threshold fluorescence (dRn) was set at 0.1 and the threshold cycle (Ct) values for the amplified genes were collected. The Ct value of an amplified gene refers to the cycle number at which the amplified gene intersects the dRn threshold. Using the Ct values, a series of calculations were executed to determine experimental gene expression relative to control gene expression. First, the ΔCt value for each experimental gene was determined by subtracting the control gene Ct value from the experimental gene Ct value, and the average ΔCt value was calculated. The average ΔCt value was then subtracted from the ΔCt values calculated for each experimental gene yielding the $\Delta\Delta$Ct. The $2^{-\Delta\Delta Ct}$ was calculated using the $\Delta\Delta$Ct values, and the average of the $2^{\Delta\Delta Ct}$ was determined. Finally, the corrected $2^{-\Delta\Delta Ct}$ value was determined for each gene by dividing the $2^{\Delta\Delta Ct}$ values by the $2^{\Delta\Delta Ct}$ average.

3.4.8 Construction of D2SV shRNA Plasmid Constructs

The Block-it^{TM} RNAi designer program (Invitrogen, Burlington, Ontario) was used to design the required single stranded shRNA oligonucleotides specific for human and mouse cycD2SV (Table 6). Human and mouse cycD2SV shRNA sequences were synthesized based on the following guidelines provided by the manufacturer (Invitrogen, Burlington, Ontario): 1) length of the target sequence selected is between 19-29 base pairs, 2) target sequence is preferred to start with a guanine, 3) no nucleotide repeats, 4) low GC content (35-50%), 5) 5' to 3' top strand consists of a CACC leading sequence followed by; target cDNA, a CGAA loop sequence, and the antisense of the target cDNA sequence, 6) the 3' to 5' strand is complementary to the 5' to 3' strand and ends with AAA. The Block-it U6 RNAi Entry Vector Kit was used to generate the mouse and human cycD2SV shRNA constructs according to the manufacturer's instructions (Invitrogen, Burlington, Ontario). Complementary shRNA strands were annealed and ligated into the shRNA-U6-entry vector. The newly formed plasmids were transformed into Transforming One Shot® TOP10 Competent *E.coli* according to manufacturer's instructions, plated on LB agar plates containing 50 µg/ml kanamycin, and incubated overnight at 37°C. The next day, DNA was isolated from two different colonies per plasmid and digested with kpn1 and EcoRV to confirm the presence of our insert. For [^{3}H]-thymidine labeling experiments, the human cycD2SV shRNA plasmid was used to knockdown human cycD2SV, and mouse cycD2SV shRNA was used as a control. Based on the sequence alignment of the mouse and human cycD2SV mRNA coding sequences, the probability of the control mouse cycD2SV shRNA construct knocking down human cycD2SV was determined to be very minimal. Although there was a 50% (14/28 aa)

Table 6.Mouse and human cycD2SV shRNA construct Sequences.

shRNA construct	Sequence 5' – 3'
Human Cyclin D2SV 1	T CACCGCCAGAGCAAATTCTTGGGATCGAAATCCCAAGAATTTGCTCTGGC B AAAAGCCAGAGCAAATTCTTGGGATTTCGATCCCAAGAATTTGCTCTGGC
Human Cyclin D2SV 2	T CACCGCAAATTCTTGGGATCCAGAACGAATTCTGGATCCCAAGAATTTGC B AAAAGCAAATTCTTGGGATCCAGAATTCGTTCTGGATCCCAAGAATTTGC
Mouse Cyclin D2SV	T CACCGCTCCTGACTCTGCCCTTCCCGAAGGAAGGGCAGAGTCAGGAGC B AAAAGCTCCTGACTCTGCCCTTCCTTCGGGAAGGGCAGAGTCAGGAGC
LacZ (Control)	T CACCGCTACACAAATCAGCGATTTCGAAAAATCGCTGATTTGTGTAG B AAAACTACACAAATCAGCGATTTTTCGAAATCGCTGATTTGTGTAGC

T= Top strand; B= Bottom strand

sequence similarity between the mouse cycD2SV shRNA target sequence and human cycD2SV, the homology regions are spread far apart over the human cycD2SV CT-region coding sequence (Fig. 31).

3.4.9 Transient Transfections

For transfections, cells seeded on day zero in 10% FBS-DMEM (600,000 per 100 mm dish or 35,000 cells in 35 mm dish) were left to grow for two days. On day two, the media was aspirated and Hi-DMEM (AB/AM free) was added to the dishes (10 ml/100 mm dish, 2 ml/35 mm dish) and the dishes were returned to the incubator. At the half an hour mark, the lipofectamine-DNA cocktail was prepared according to the manufacturer's instructions. In brief, 500µl of Opti-MEM® (Invitrogen, Burlington, Ontario) was added to each of the two microcentrifuge 1.5ml tubes for 100 mm dish transfections or 200 µl of Opti-MEM® for 35 mm dish transfection. One tube received the plasmid DNA, while the other tube received Lipofectamine™ 2000 (Invitrogen, Burlington, Ontario). The microcentrifuge tubes were left to stand for five minutes, and then mixed by transferring the contents of the Lipofectamine™ 2000 tube to the DNA microcentrifuge tube. The Lipofectamine™ 2000-DNA cocktail was gently mixed by pipetting, and left to stand for seventeen minutes at room temperature. Once the seventeen minutes had lapsed, the lipofectamine-DNA cocktail was added to the appropriate dish dropwise and the dishes were returned to the incubator. After five hours, the Hi-DMEM media containing the transfection cocktail was aspirated, 10% FBS-DMEM was added, and the dishes were returned to the incubator. Transfection efficiency was routinely determined by EGFP-C1 transfections where, on average, it was found to

Figure 31. Comparison of the coding nucleotide sequences of the CT domain of the mouse (M) and human (H) cycD2SV. Identical nucleotide sequences are highlighted in black boxes and the MD2SV shRNA target sequence is indicated by the red line (note the significant mismatched areas between mouse shRNA sequence with the corresponding human D2SV coding region). HD2SV shRNA 1 target sequence is indicated by the green line and the HD2SV shRNA 2 target sequence is indicated by the blue line.

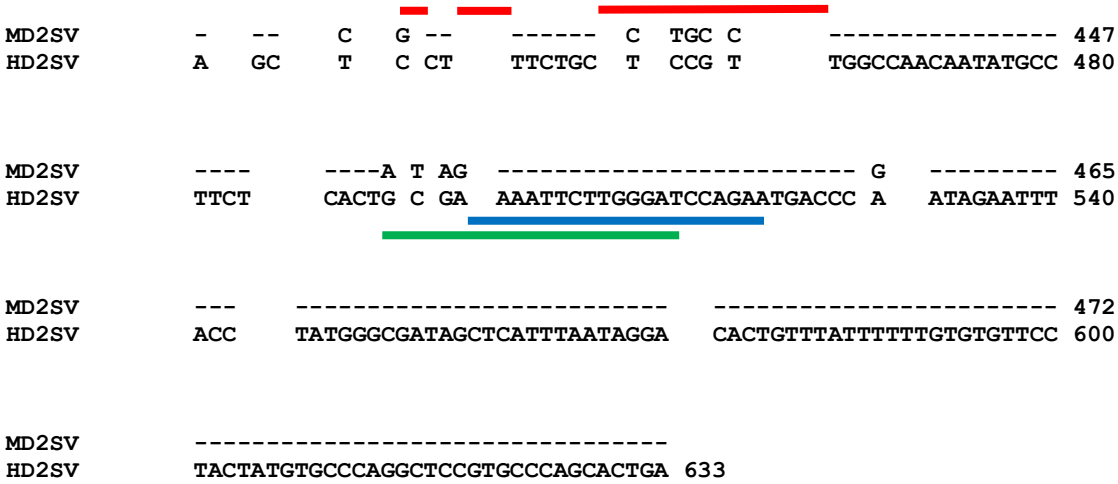
MD2SV - -- C G -- ------ C TGC C ---------- 447
HD2SV A GC T C CT TTCTGC T CCG T TGGCCAACAATATGCC 480
MD2SV ---- ----A T AG ---------- G --------- 465
HD2SV TTCT CACTG C GA AAATTCTTGGGATCCAGAATGACCC A ATAGAATTT 540
MD2SV --- ---------- ---------- 472
HD2SV ACC TATGGGCGATAGCTCATTTAATAGGA CACTGTTTATTTTTTGTGTGTTCC 600
MD2SV ----------
HD2SV TACTATGTGCCCAGGCTCCGTGCCCAGCACTGA 633

be between 50-60%. To maintain sterility, the transfection protocol was carried out in a ThermoForma class II A2 biological safety cabinet (Thermo Fisher Scientific, Nepean, Ontario).

For knockdown of cycD2SV during confluence, cells were transfected, on day two with lacZ shRNA (control), or human cycD2SV construct 1, or a combination of human cycD2SV shRNA constructs 1 and 2 (See Table 6 and Fig. 31). To ensure specificity of the human cycD2SV shRNA constructs, both constructs were designed using the CT region of human cycD2SV (HD2SV shRNA 1: HcycD2SV mRNA 494-514bp, HD2SV shRNA 2: mRNA 499-520bp). In these experiments, cells seeded in 100 mm dishes were transfected with 4 μg of DNA and 10μl of Lipofectamine™ 2000 reagent. For co-transfection of two shRNA plasmids, cells were transfected at a 1:1 ratio of the DNA constructs such that 100 mm dishes received 2 μg of each construct. Subsequently, transfected cells were left to grow to day eight confluence, and were harvested for protein quantification (Fig. 28). CycD2 and cycD2SV levels were determined by western blotting and quantified by densitometry as described under section 3.4.5.

For shRNA knockdown and thymidine labeling experiments, cells were co-transfected in 35 mm dishes with human D2SV shRNA construct 1, or a nonhomologous mouse D2SV shRNA construct, (control; Table 6) and a CMV vector harboring nuclear LacZ sequence [(Soonpaa et al., 1994); Fig. 31]. In these experiments, cells were transfected with two plasmids at a 10:1 ratio (nuclear LacZ to shRNA) with a total plasmid concentration of 0.85 μg of and 2.15 μl of Lipofectamine™ 2000 reagent, and maintained for a total period of 24 hours (Fig. 32). The CMV-nuclear LacZ was used for

Figure 32. Transient transfection timeline. At 0 hour time point media was changed to Hi-DMEM (serum free, AB/AM free). The transfection cocktail was added to the cells in a drop wise fashion at the 1 hour mark. At the 6 hour mark media was changed to 10% FBS-DMEM. For [^{3}H]-thymidine experiments, cells received [^{3}H]-thymidine at 18 hours. At the 24 hour mark cells were either fixed and processed for immunohistochemistry, or X-GAL staining, or protein was harvested. Cells which received [^{3}H]-thymidine were processed for autoradiography after X-GAL staining was completed.

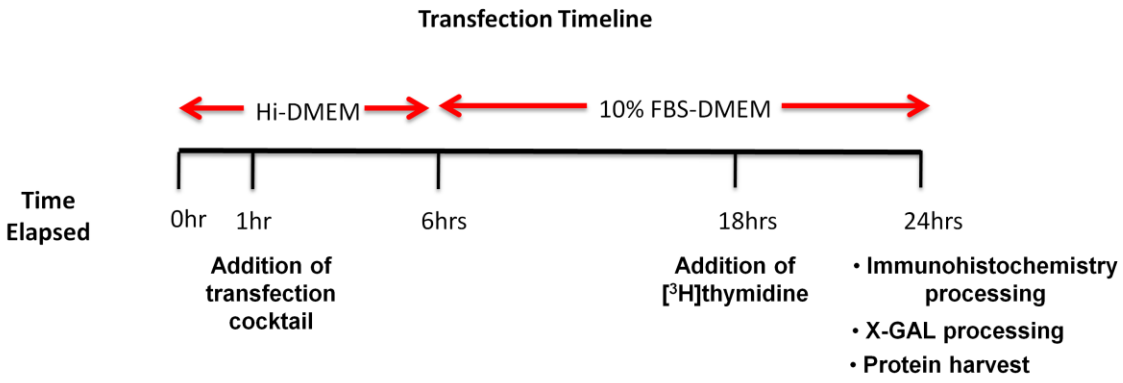
Transfection Timeline
Hi-DMEM
10% FBS-DMEM
Time Elapsed
0hr
1hr
6hrs
18hrs
24hrs
Addition of transfection cocktail
Addition of [3H]thymidine
• Immunohistochemistry processing
• X-GAL processing
• Protein harvest

the visualization of transfected cells in [^{3}H]-thymidine labeling experiments. Transfected cells designated for thymidine incorporation assays were pulsed with 1μCi/ml of [^{3}H]-thymidine (GE Healthcare Life Sciences, New Jersey) six hours prior to cell fixation, and 5-bromo-4-chloro-3-indlyl-β-D-galactopyranoside (X-GAL) staining (Fig. 32). For peptide blocking and immunostaining/western blot experiments, cells seeded in 35 mm or 100 mm dishes were transfected with D2SVmyc or vector control, (See chapter 2, section 2.4.1) and transfected cells were maintained for a total period of 24 hours (Fig. 32).

3.4.10 Immunofluorescence, [^{3}H]-thymidine Autoradiography, Mitotic Index and X-GAL staining

HEK293 cells were fixed with methanol for fifteen minutes at 4°C and blocked with blocking buffer (1% v/v BSA, 10% v/v goat serum in PBS) for one hour. Cells were probed with primary antibody (1:50) followed by a secondary antibody conjugated with Alexa Fluor 488 or 555 dye (1:200) (Invitrogen, Burlington, Ontario) incubation. Subsequently, cells were incubated in 10 mg/ml bisBenzimide H 33342 trihydrochloride (Hoechst 33342) nuclear stain (Sigma-Aldrich, Oakville, Ontario) for five minutes, and mounted on glass slides using 1% w/v propyl gallate in a 1:1 PBS/glycerol solution, Sigma-Aldrich, Oakville, Ontario). In some experiments, post fixation and antibody probing, cells were further processed for [^{3}H]-thymidine autoradiography, where coverslips were air dried, coated with Kodak photographic emulsion, (MarketLINK Scientific, Burlington, Ontario) and placed in a light-tight box at 4°C for three days. Coverslips were developed in Kodak-D19 developer (Sigma-Aldrich, Oakville, Ontario), fixed with Ilford rapid fixer, (Polysciences, Pennsylvania) and mounted using propyl gallate solution. Cellular morphology was examined under bright field, and nuclei were

identified with epifluorescence microscopy. Cells containing more than fifteen nuclear silver grains were considered as cells undergoing DNA synthesis. Mitotic indices were monitored for cells undergoing confluence. A number of cells undergoing mitosis were counted for day two and day eight confluence experiments. Cells undergoing mitosis were determined based on condensed chromosomes, and the presence of mitotic spindles. Images were captured using a Leica DM2500 fluorescence microscope, fitted with a DFC500 digital acquisition system (Leica Microsystems, Concord, Ontario).

For X-GAL staining experiments, cells were fixed in a sodium cacodylate based buffer for thirty minutes at 4˚C, incubated with X-GAL solution at 37˚C and LacZ positive cells were identified by a nuclear blue stain under bright field. The X-GAL solution was prepared according to manufacturer's instructions (Gold Biotechnology, Missouri). In brief, 0.05g of X-GAL powder was added to 2.5 ml of N, N-Dimethyl Formamide (DMF, Sigma-Aldrich, Oakville, Ontario) forming a primary X-GAL solution. Once dissolved, the primary X-GAL solution was added dropwise to a 100 ml PBS solution containing 200 µl of 1M $MgCl_2$ solution, 0.164 g potassium ferricyanide, and 0.212 g potassium ferrocyanide. Subsequent to X-GAL staining, cells were processed for thymidine labeling as described earlier.

3.4.11 Statistical Analysis

Unless otherwise stated, all data comparisons were completed using an unpaired two-tail t-test, or a one-way ANOVA. Significance obtained by ANOVA was further subjected to a Tukey-Kramer's test for *post-hoc* analysis. Data is expressed as mean ±

SEM, and was considered statistically significant when the difference in mean values between groups had a P value of 0.05 or less.

3.5 Results

3.5.1 Characterization of Polyclonal Antibodies Raised Against Mouse Cyclin D2SV

To determine the specificity of our newly raised rabbit polyclonal antibodies to the CT domain of mouse cycD2SV, peptide spotting experiments were conducted. The CT and the NT control peptides were spotted in increasing concentrations (50ng, 100ng, 500ng and 1μg) on a nitrocellulose membrane and left to dry (Fig. 33A). When the nitrocellulose membrane was probed with the newly raised cycD2SV antibody and processed, a signal was detected for the CT peptide but not for the NT control peptide. The CT peptide signal intensity increased with increasing peptide concentration. There was no signal present in the water controls for both the CT peptide and NT peptide (Fig. 33A).

Lysates collected from HEK293 cells transfected with a mouse cycD2SVmyc construct or control vector were resolved by western blot. We detected multiple reactive bands ranging from 20 to 45 kDa (bands: 20, 32, 37, 45) upon probing with cycD2SV antibodies, with the major reactive species at 20 kDa (See section 2.5.6, Fig. 18E). We conducted peptide blocking experiments to determine the specificity of our cycD2SV antibodies. Lysates collected from HEK293 cells transfected with pcDNA 3.1 vector and mouse cycD2SVmyc construct were resolved in duplicates by western blotting. The duplicate blots were separated; one blot was probed with primary antibody, pre-incubated

Figure 33. CycD2SV antibodies detect the mouse CT region of cycD2SV and pre-incubation of antibody with a CT peptide abolishes signals obtained with cycD2SV antibodies. CycD2SV CT and cycD2 control NT peptides were spotted on nitrocellulose membrane in increasing concentrations (50ng-1μg) and subjected to immunoblotting with cycD2SV antibodies (A). Water spots were used for control. Lysates collected from HEK293 cells transfected with cycD2SVmyc or pcDNA 3.1 vector control were resolved by western blot (B). The nitrocellulose blot was probed with either cycD2SV antibodies pre-incubated with cycD2SV CT peptide or cycD2 control NT peptide. Note the 25kD endogenous human protein (putative human D2SV) is also blocked in the presence of CT peptide (open arrowhead).

A

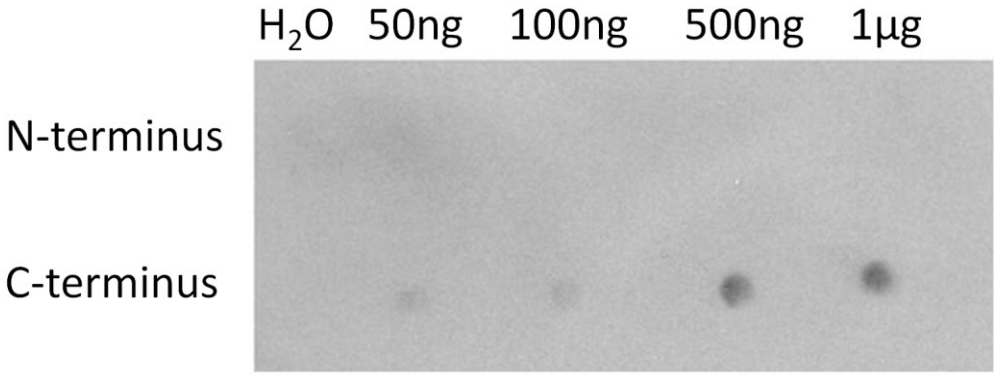
H2O
50ng
100ng
500ng
1µg
N-terminus
C-terminus

B

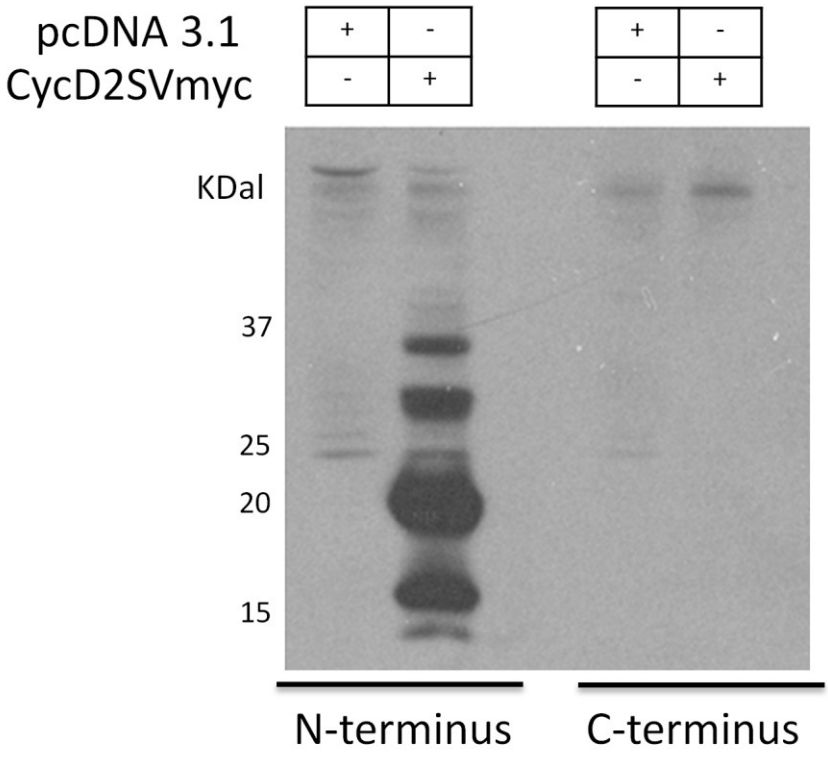
pcDNA 3.1
CycD2SVmyc
+
-
-
+
+
-
-
+
KDal
37
25
20
15
N-terminus
C-terminus

with the NT peptide, while the second blot was probed with antibody pre-incubated with the CT peptide. In contrast, all bands (14-34 kDa) in the cycD2SVmyc transfected lane disappeared when probed with the antibodies pre-incubated with the CT peptide, indicating that all detected bands were specific to cycD2SV antibody immunoreactivity (Fig. 33B). In addition, we observed the disappearance of a 25 kDa band in the control pcDNA transfected lane when the cycD2SV antibodies were pre-incubated with CT peptide. This led us to believe that the cycD2SV antibodies may have been crossreacting with endogenous cycD2SV protein present in HEK293 cells (Fig. 33B).

3.5.2 Epitope Mapping for Cyclin D2SV Antibodies

The cycD2SV antibodies were raised against amino acids 143-156 (LLTLPFPITLRPPH), a fourteen amino acid stretch from the mouse cycD2SV CT-region. To narrow down the cycD2SV antibody reactive region, we designed three shorter peptides that spanned the fourteen amino acid sequence to which our antibodies were raised against (Fig. 27A, B). All three peptides were spotted on a nitrocellulose membrane and probed with cycD2SV antibody (Fig. 34A). The cycD2SV antibody was unable to detect peptides one and three, but was able to detect peptide two. A positive signal was obtained with peptide two concentrations ranging from 50 ng, 100 ng, 500 ng and 1 μg peptide spots, with no signal for the control spot. As expected, the signal intensity increased with increased peptide concentrations. In addition, cycD2SV protein was detected in transfected cells probed with antibodies pre-incubated with peptide one, (Fig. 34B-D) but was not detected in coverslips probed with antibody pre-incubated with peptide two (Fig. 34E-G). These results would suggest that the cycD2SV antibody

Figure 34. CycD2SV antibodies detect the cycD2SV CT sequence present in peptide 2 but not those present in peptide 1 or 3. Peptide 1, peptide 2 and peptide 3 were spotted on nitrocellulose membrane in increasing concentrations (50ng-1μg) and probed with cycD2SV antibodies (A). HEK293 cells transfected with cycD2SVmyc or pcDNA 3.1 were processed for immunohistochemistry and probed with cycD2SV antibodies pre-incubated with either peptide 1 (B-D) or peptide 2 (E-G). Scale bars are 20 μm.

A

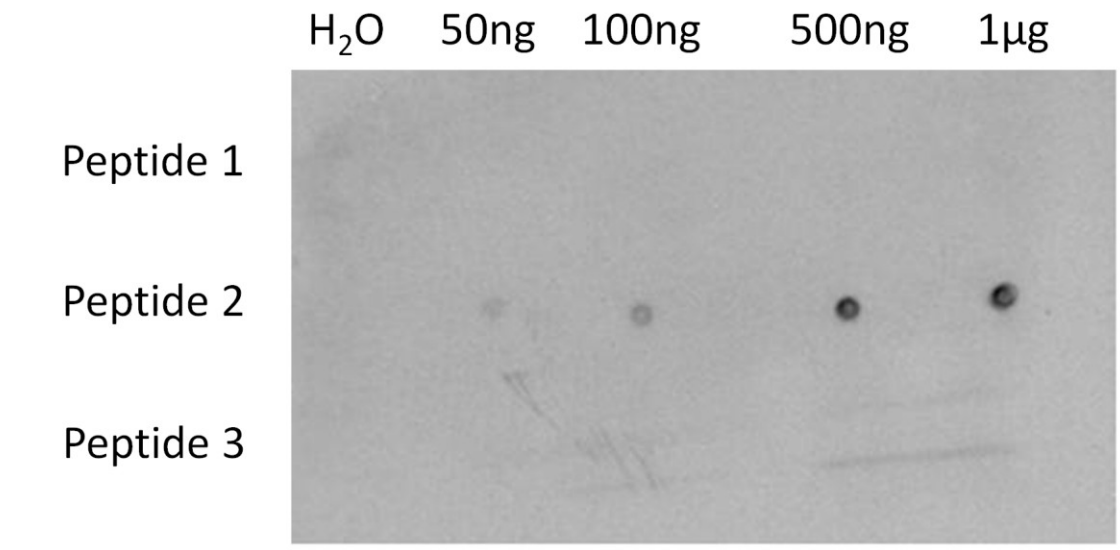
H_2O
50ng
100ng
500ng
1µg
Peptide 1
Peptide 2
Peptide 3

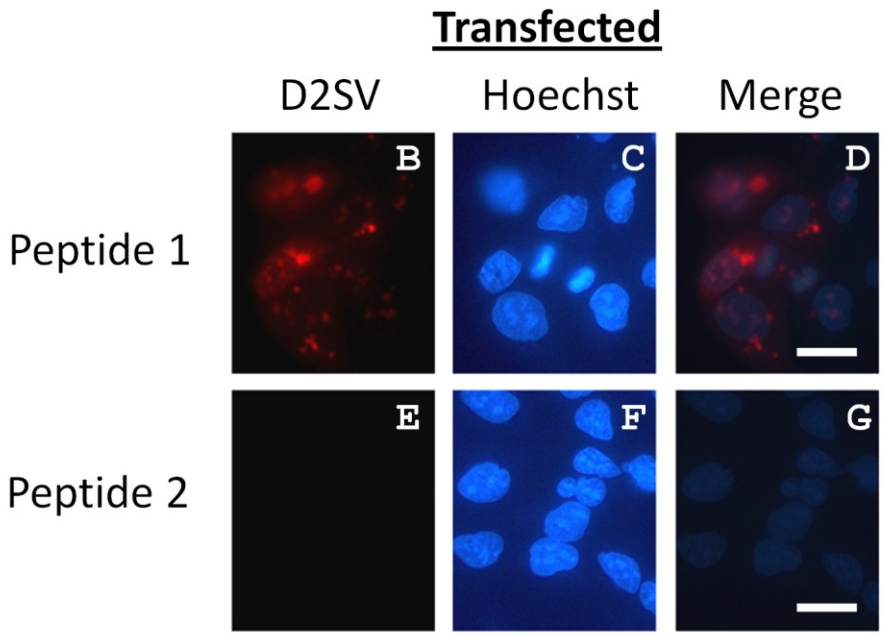
Transfected
D2SV
Hoechst
Merge
Peptide 1
Peptide 2
B
C
D
E
F
G

reactive domain is located in peptide two.

Based on the peptide spotting experiments using three newly synthesized peptides, we were able to narrow down the specific amino acid sequence recognized by the cycD2SV antibodies. Since peptide three shares the amino acid sequence LPFPIT with peptide two, and our cycD2SV antibodies do not recognize peptide three, it is likely that our antibodies detect the LRPPH sequence present in peptide two (Fig. 27A, B). However, it is possible that cycD2SV antibodies may require the entire peptide two sequence, LPFPITLRPPH, for protein recognition. When we compared the mouse CT domain with the human CT domain (Fig. 27A, B), we found that there was a 60% sequence similarity in the LRPPH domain, and a 54% sequence similarity in the LPFPITLRPPH domain between species (Fig. 35). The first two amino acids, lysine and arginine, as well as the last amino acid, histidine, of the LRPPH sequence were conserved in both mouse and human. In the human sequence, the two prolines were substituted with an alanine and glutamine. In the LPFPITLRPPH domain, six out of eleven amino acid residues are conserved in both mouse and human. Based on the sequence similarity between the cycD2SV mouse and human sequences, we believe the antibody can recognize either the LRXXH or the LXFPXXLRXXH domain of the CT region. However, given that the human cycD2SV LXFPXX sequence is separated from the LPXXH domain by 51 amino acids, (Fig. 35) and that our mouse cycD2SV antibodies do not react with peptide three, which contains the LXFPXX portion of the LXFPXXLRXXH domain, it is most likely that our antibodies detect the LRXXH domain.

Figure 35. Comparison of the amino acid sequences of mouse and human cycD2SV (Denicourt et al., 2003). Identical amino acids are indicated by highlighted areas in black. The CT region of the mouse and human cycD2SV sequence is indicated by the red line. Conserved LXFPXX and LRXXH domains between species are indicated. These domains are relevant to D2SV antibody epitope mapping studies. MD2SV, mouse D2SV; HD2SV, human D2SV.


HD2SV MELLCHEVDPVRRAVRDRNLLRDDRVLQNLLTIEERYLPQCSYFKCVQKDIQPYMRRMVA 60
MD2SV TWMLEV-CEEQKCEEEVFPLAMNYLDRFLAGVPTPKTHLQLLGAVCMFLASKLKETIPLT 118
HD2SV TWMLEVVCEEQKCEEEVFPLAMNYLDRFLAGVPTPKSHLQLLGAVCMFLASKLKETSPLT 120
MD2SV AEKLCIYTDNSVKPQELLVMP-PSLLLTLPFEIT---------- 151
HD2SV AEKLCIYTDNSIKPQELLVMTGPFLPSFLRFELSPGQQYAFYHHCQSKFLGSRMTPPIEF 180
LXFPXX
MD2SV ----------LRPPH 156
HD2SV THLWAIAHLIGNHCLFFVCSYYVPRLRAQH 210
LRXXH

3.5.3 Human Cyclin D2SV is Detected by Polyclonal Antibodies Raised Against Mouse Cyclin D2SV and is Expressed Endogenously in HEK293 Cells

Immunohistochemistry staining completed on the untransfected human cell line, HEK293, by anti-cycD2SV antibodies detected small punctate bodies (See section 2.5.1, Fig 11A, B). Although, these punctate bodies were not as large as those observed in cells transfected with the mouse cycD2SVmyc construct, the cellular localization of these bodies was consistent with that observed in transfected cells. The punctate bodies localized mostly to the perinuclear zone of cells. In addition, western blotting completed on untransfected HEK293 cells yielded a 25 kDa band (Fig. 18E) which is the predicted molecular weight for the human cycD2SV protein sequence, (Denicourt et al., 2003) as determined by the protein molecular weight calculator provided by EnCor Biotechnology Inc. (http://www.encorbio.com/protocols/Prot-MW.htm) Based on these observations, and the high sequence similarity between mouse and human cycD2SV in the CT region, it is likely that mouse cycD2SV antibodies detect endogenous human cycD2SV protein in HEK293 cells.

To confirm that endogenous cycD2SV signal obtained with immunohistochemistry using cycD2SV antibodies was not an artifact, we conducted a peptide blocking experiment using peptide one as a control, and peptide two (Fig. 36A-F) on untransfected HEK293. HEK293 cells were probed with cycD2SV antibodies, which have been pre- incubated with either peptide one or peptide two. No signal was detected for untransfected HEK293 cells probed with cycD2SV antibodies pre-incubated with peptide two (Fig. 36D-F) whereas cells probed with cycD2SV antibodies pre-incubated with the control peptide one (Fig. 36A-C) exhibited antibody reactivity. These results

Figure 36. CycD2SV antibodies detect endogenous cycD2SV protein in the human cell line HEK293. Untransfected HEK293 cells were processed for immunohistochemistry and probed with cycD2SV antibodies pre-incubated with either peptide 1 (A-C) or peptide 2 (D-E). Absence of punctuate bodies in cells probed with antibodies pre-incubated with peptide 2 indicates that immunoreactive epitope is localized in this peptide sequence. Scale bar is 20 μm.

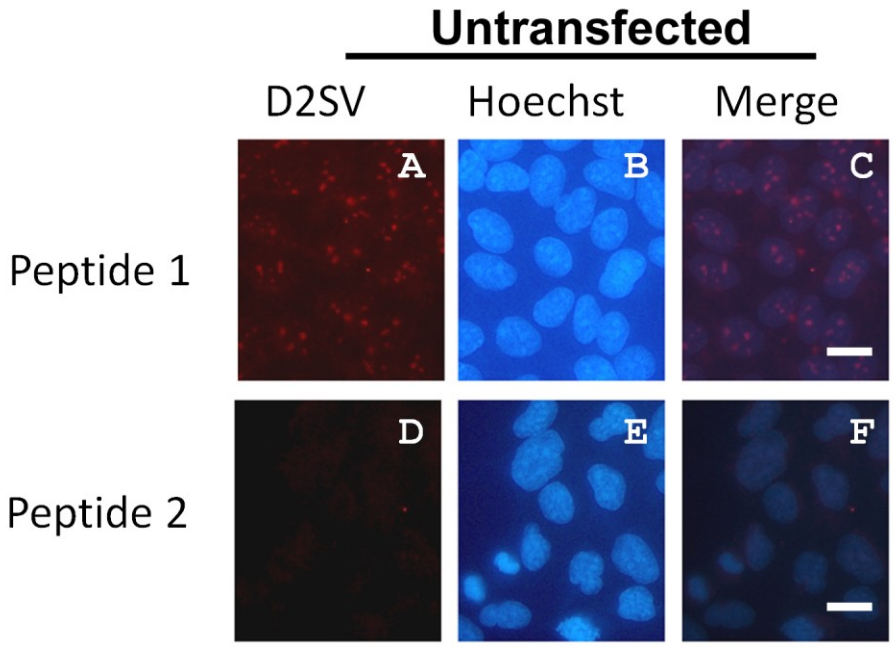
Untransfected
D2SV
Hoechst
Merge
Peptide 1
Peptide 2
A
B
C
D
E
F

suggest that the cycD2SV antibodies raised against the mouse cycD2SV CT region are also capable of detecting human cycD2SV.

3.5.4 Cyclin D2SV Protein Levels are Elevated During Contact Inhibition Induced Cell Cycle Arrest in Confluent Cultures

While it is established that overexpression of cycD2SV causes cell cycle exit, it is not yet known whether endogenous cycD2SV plays a similar role. To this end, we decided to investigate the role of endogenous cycD2SV in known states of cell cycle arrest, specifically during confluence and serum starvation. HEK293 cells subjected to confluence over a period of eight days showed a 2.5-fold increase of cycD2SV protein expression when compared to day two non-confluent cells as determined by western blot analysis (Fig. 37C, D). This increase in cycD2SV protein expression was accompanied with a decreased expression of important cell cycle proteins: cycD1 (-8.3-fold, Fig. 37A, D) and cycD2 (-6.66-fold, Fig. 37B, D). However, CDK4 levels did not significantly fluctuate during confluence. $p27^{Kip1}$ protein levels were monitored as a control, since it has been reported that $p27^{Kip1}$ levels increase significantly when cells undergo confluence (Kato et al., 1997; Polyak et al., 1994a). $p27^{Kip1}$ levels were elevated (ten to twenty fold in three different experiments) by day eight confluence (Fig. 37D). Relative protein levels were first corrected for any variation in protein loading using α-tubulin and normalized to day two control protein levels. Mitotic figures were also counted in cells exposed to confluence conditions as an indication of the number of cells undergoing cellular division. Mitotic index (MI) percentage was decreased by 3.5-fold in confluent cultures compared to non-confluent cultures (MI for non-confluent cultures = 3.107% ± 0.3472 vs. MI for confluent cultures = 0.8863% ± 0.1800, Fig. 38A-C). Collectively, these

Figure 37. CycD2SV protein levels are elevated during contact inhibition. Lysates collected from HEK293 cells subjected to confluence were resolved by western blot and probed with α-tubulin, cycD1, cycD2, cycD2SV and p27 antibodies (D). Cells were collected on days 2, 4, 6 and 8 where day 2 represents control non-confluent cultures. Relative protein expression was quantified using band densitometry and values were expressed as mean ± SEM (A-C). One-way ANOVA, *$p < 0.05$, compared to day 2 levels, N = 3-4 independent experiments.

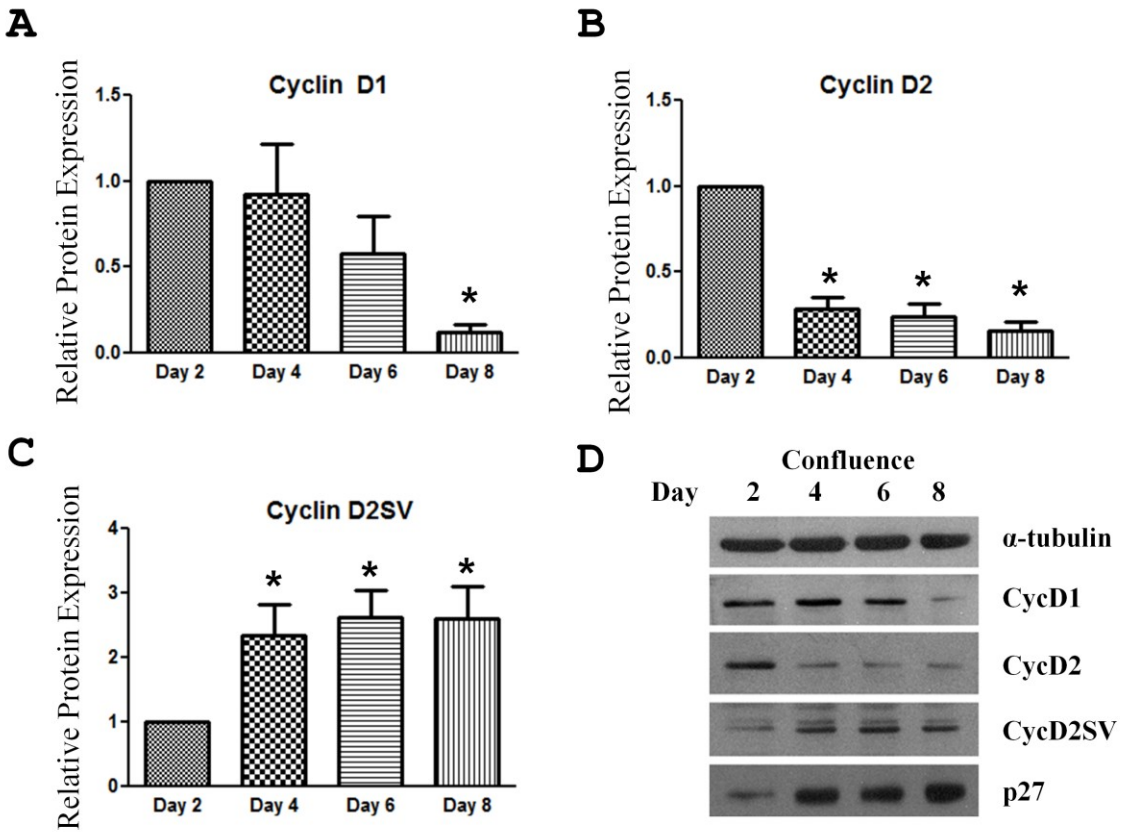
A
Cyclin D1
Relative Protein Expression
1.5
1.0
0.5
0.0
Day 2
Day 4
Day 6
Day 8
*
B
Cyclin D2
Relative Protein Expression
1.5
1.0
0.5
0.0
Day 2
Day 4
Day 6
Day 8
*
*
*
C
Cyclin D2SV
Relative Protein Expression
4
3
2
1
0
Day 2
Day 4
Day 6
Day 8
*
*
*
D
Confluence
Day 2 4 6 8
α-tubulin
CycD1
CycD2
CycD2SV
p27

Figure 38. Mitotic index of HEK293 cells decreases during confluence as a result of contact inhibition. HEK293 cells were seeded on glass coverslips in 35 mm dishes, fixed on either day 2 or day 8 and the mitotic index was determined for both time points. Cells on day 2 represent control non-confluent cultures (A) whereas day 8 cells demonstrate crowding confluent cultures (B). Values are expressed as mean ± SEM. Unpaired two-tail t-test, *$p < 0.05$, N = 3. 300-500 cells counted per N. Scale bar is 20 μm.

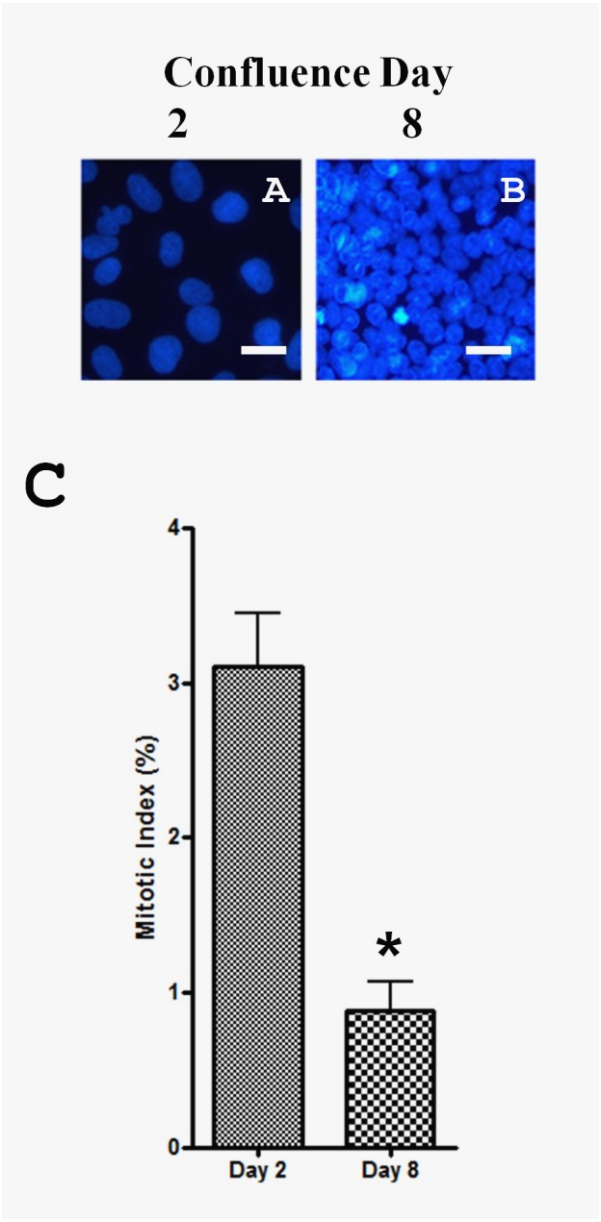
Confluence Day
2
8
A
B
C
Mitotic Index (%)
4
3
2
1
0
*
Day 2
Day 8

results suggest that cycD2SVprotein levels are significantly elevated in confluent cultures.

3.5.5 Serum Deprivation Induces Cyclin D2SV Protein Expression

In addition to confluence, cycD2SV levels were also assessed during serum starvation. Cells subjected to serum starvation are also known to downregulate cell cycle and cellular division (Shin et al., 2008; Won et al., 1992). Similar to confluence conditions, cycD2SV protein levels increased by 2-fold (Fig. 39C, D) and cycD1 and cycD2 protein levels decreased by 3.3-fold (Fig. 39A, D) and 3.8-fold (Fig. 39B, D), respectively in cells exposed to serum starvation, and harvested on day eight. However, CDK4 levels did not fluctuate. $p27^{Kip1}$ protein levels were also observed to increase dramatically under these serum starvation conditions (ten to twenty fold in three different experiments, Fig. 39D).

3.5.6 CycD2SV mRNA Levels do not Fluctuate in Confluent Cultures

To assess whether cycD2SV protein upregulation during confluence is due to increased gene transcription, cycD2SV mRNA expression was analyzed. Total RNA extracted from HEK293 cells harvested at various stages of confluence (Day two - non confluent control, day four, and day six; Fig. 28) were analyzed for cycD2SV, as well as cycD1, D2 and D3 transcripts using QPCR analysis (Fig. 40A-D). ΔΔCT method was used to calculate fold changes, and samples were adjusted for load variations using GAPDH, a house keeping gene with transcript levels which did not fluctuate during confluence. CycD2SV mRNA expression did not significantly change during confluence

Figure 39. CycD2SV protein is upregulated in response to serum starvation. Lysates collected from HEK293 cells subjected to serum starvation were resolved by western blot and probed with α-tubulin, cycD1, cycD2, cycD2SV and p27 antibodies (D). Cells were subjected to 0.1% FBS-DMEM starting at day 2 and lysates were collected on day 6 and day 8. Control cells were collected at day 2 prior to serum starvation. Relative protein expression was quantified using band densitometry and values were expressed as mean ± SEM (A-C). One-way ANOVA, *$p < 0.05$, compared to day 2, $N = 4$ independent experiments.

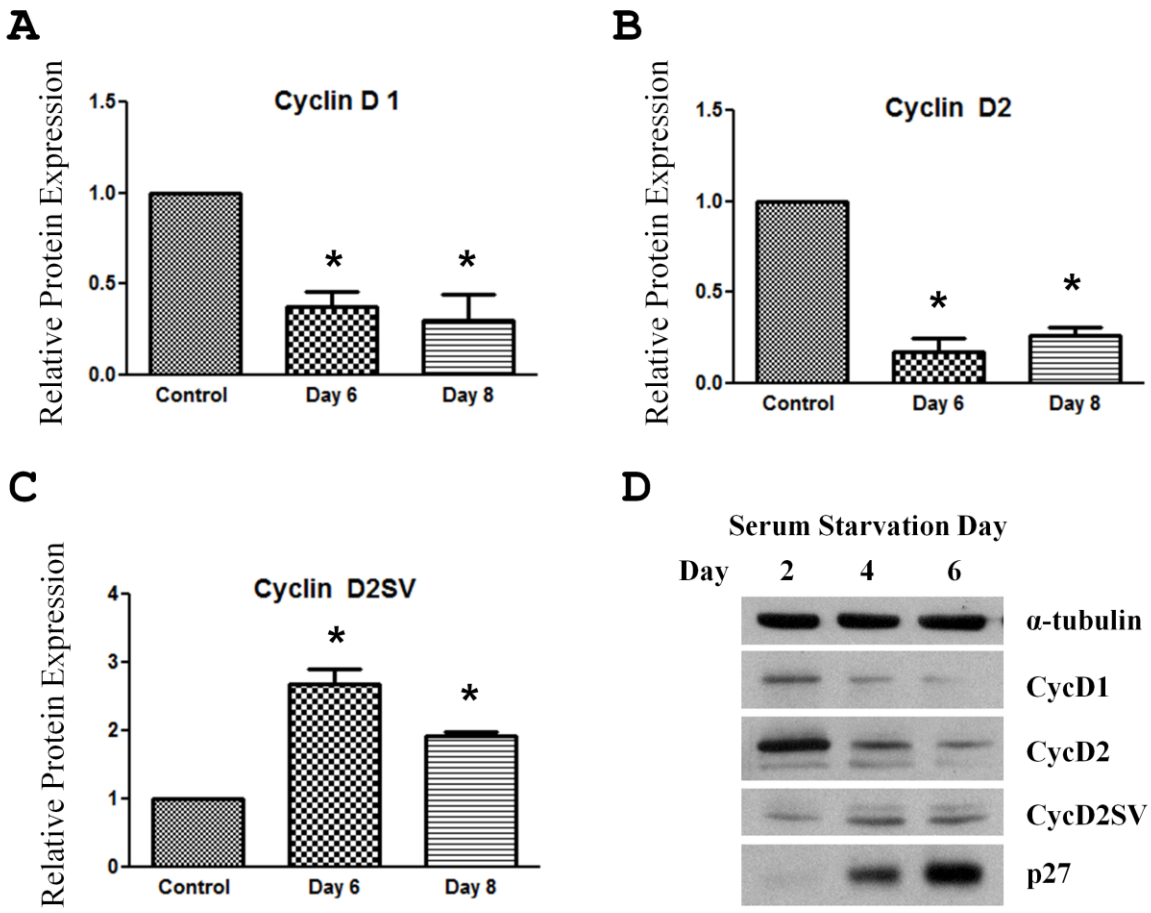
A
Cyclin D 1
Relative Protein Expression
1.5
1.0
0.5
0.0
*
*
Control
Day 6
Day 8
B
Cyclin D2
Relative Protein Expression
1.5
1.0
0.5
0.0
*
*
Control
Day 6
Day 8
C
Cyclin D2SV
Relative Protein Expression
4
3
2
1
0
*
*
Control
Day 6
Day 8
D
Serum Starvation Day
Day 2 4 6
α-tubulin
CycD1
CycD2
CycD2SV
p27

Figure 40. CycD2SV gene expression does not change during confluence where as cycD1, D2 and D3 gene expression decreases. Total RNA was collected on day 2, 4 and 6 where day 2 represented control non-confluent cultures. The cDNA amplification was completed using cycD1 (A), D2 (B), D3 (C) and D2SV (D) primer pairs. Relative mRNA expression values were expressed as mean ± SEM. One-way ANOVA, *$p < 0.05$, compared to day 2, N = 3 independent experiments.

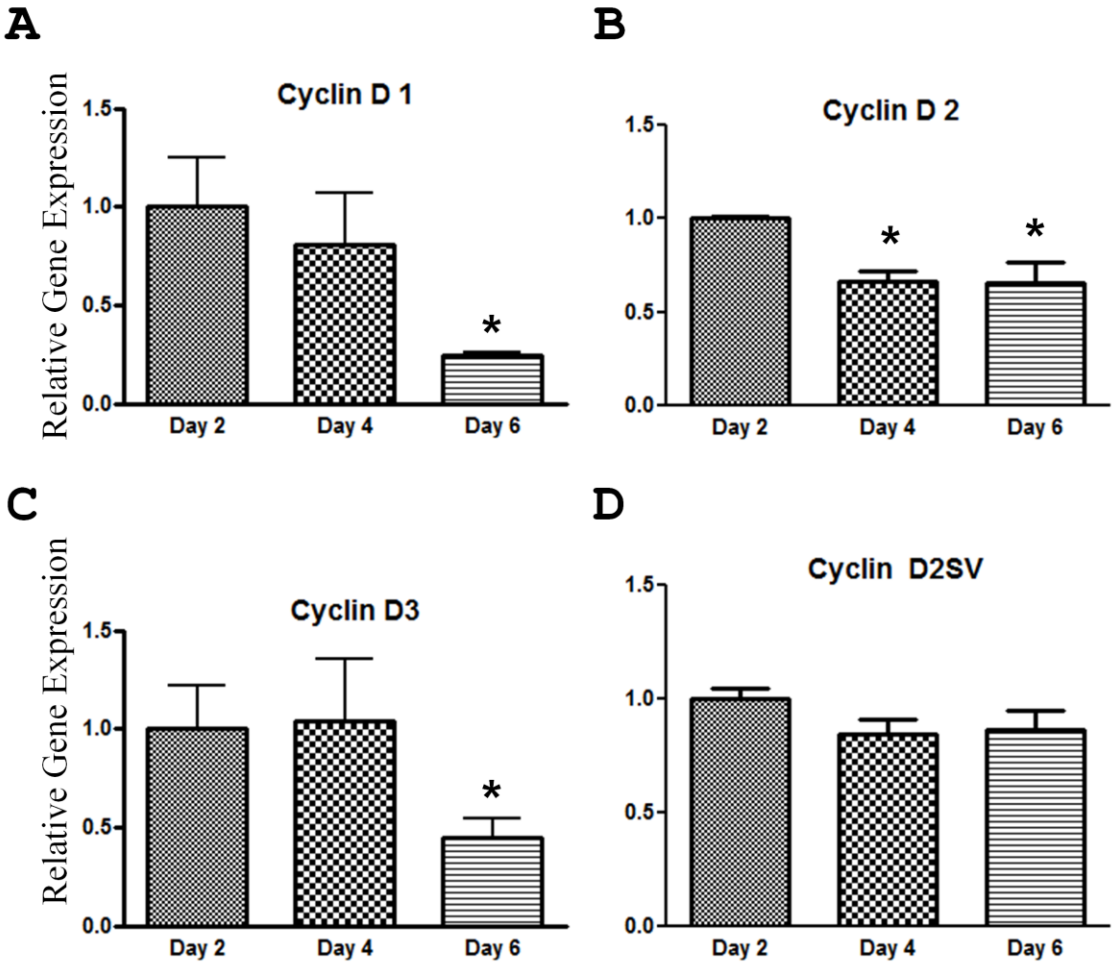
A
Cyclin D 1
Relative Gene Expression
1.5
1.0
0.5
0.0
*
Day 2
Day 4
Day 6
B
Cyclin D 2
1.5
1.0
0.5
0.0
*
*
Day 2
Day 4
Day 6
C
Cyclin D3
Relative Gene Expression
1.5
1.0
0.5
0.0
*
Day 2
Day 4
Day 6
D
Cyclin D2SV
1.5
1.0
0.5
0.0
Day 2
Day 4
Day 6

(Fig. 40D) however, cycD1, cycD2 and cycD3 mRNA levels decreased significantly (Fig. 40A-C). CycD1 mRNA levels decreased by up to 80% at day six confluence, whereas cycD2 and cycD3 mRNA levels decreased by 40% and 55% by day six confluence, respectively.

3.5.7 shRNA Knock Down of CycD2SV Rescues CyclinD2 Levels During Confluence

Mechanisms uncovering cycD2SV overexpression mediated cell cycle exit suggest a direct role for cycD2SV in the sequestration of cycD2 protein, and targeting it for ubiquitin mediated degradation. To investigate whether cycD2SV has a direct role on cycD2 levels during confluence, we knocked down cycD2SV by transient transfections using two shRNA constructs (Table 6). On day two, cells were transfected with a control LacZ shRNA, or HD2SV shRNA construct 1, or a combination of HD2SV shRNA constructs 1 and 2. Cells were left to grow to day eight confluence, and were then harvested for protein quantification. Cells transfected with control LacZ shRNA construct showed an upregulation of cycD2SV protein expression, and a down regulation of cycD2 protein expression reflecting the normal expression patterns observed during confluence (Fig. 41C). Transfection of HD2SV shRNA constructs resulted in a two-fold decrease in cycD2SV protein expression at day eight confluence (Fig. 41B). In addition, knock down of cycD2SV was able to increase cycD2 protein levels by 3.5-fold at day eight confluence, as compared to control (Fig. 41A; as mentioned earlier, both control and HD2SV shRNA transfected cells were harvested at day eight confluence). This result suggests a direct role for cycD2SV in the regulation of cycD2 protein levels since

Figure 41. CycD2SV knockdown during confluence rescues cycD2 protein levels but not cycD1 or cycD3. HEK293 cells were transfected with either HD2SV shRNA 1 (labeled HSVshRNA1) or a combination of HD2SV shRNA 1 and HD2SV shRNA 2 (labeled HSVshRNA1+2) at day 2. Control cells were transfected with LacZ shRNA construct. Cells were left to grow to confluence where they were harvested on day 8. Collected lysates were resolved by western blot and probed with α-tubulin, cycD1, cycD2, cycD3, cycD2SV, CDK4 and CDK2 antibodies (C). Relative protein expression was quantified using band densitometry and values were expressed as mean ± SEM (A-B). One-way ANOVA, *$p < 0.05$, compared to control, N = 3 independent experiments.

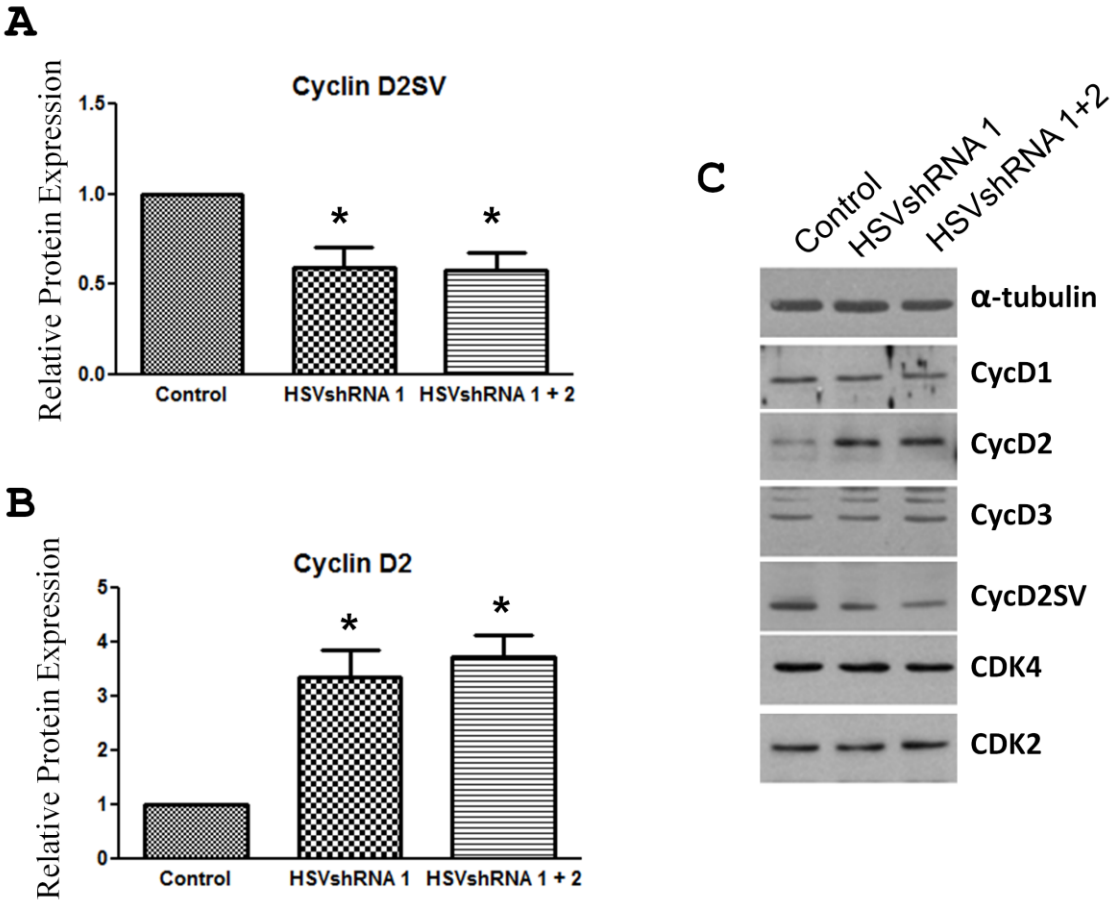
A
Cyclin D2SV
Relative Protein Expression
1.5
1.0
0.5
0.0
*
*
Control
HSVshRNA 1
HSVshRNA 1 + 2
B
Cyclin D2
Relative Protein Expression
5
4
3
2
1
0
*
*
Control
HSVshRNA 1
HSVshRNA 1 + 2
C
Control
HSVshRNA 1
HSVshRNA 1+2
α-tubulin
CycD1
CycD2
CycD3
CycD2SV
CDK4
CDK2

knocking down cycD2SV prevents downregulation of cycD2 protein during confluence (Fig. 41A-C). CycD2SV knockdown had no effect on cycD1, cycD3, CDK4 or CDK2 protein levels.

3.5.8 shRNA Knock Down of CycD2SV Increases Percentage of Cells Entering S-phase

HEK293 cells were co-transfected with CMV-nuclear LacZ reporter gene, and either a cycD2SV shRNA construct against mouse (control) or human cycD2SV. The mouse shRNA construct was used as a control. The CMV-nuclear LacZ was used as a marker for tracking transfected cells which were visualized using X-GAL staining. LacZ positive cells were identified by a nuclear blue signal visible under bright field microscopy. Given the 10 to 1 shRNA to nuclear LacZ gene transfection ratio, any cell transfected with nuclear LacZ is ten times more likely to be transfected with the shRNA construct. Cells transfected with human cycD2SV shRNA construct had a significantly increased [^{3}H]-thymidine LI compared to control mouse cycD2SV shRNA transfected cells (1.68-fold increase, Fig. 42A-C). Cells transfected with the human cycD2SV shRNA construct yielded a 42% [^{3}H]-thymidine LI, whereas control cells transfected with the mouse cycD2SV shRNA yielded a 25% [^{3}H]-thymidine LI.

3.6 Discussion

After performing several peptide spotting and blocking experiments, we successfully demonstrate that in house cycD2SV antibodies detect mouse, as well as human cycD2SV. Peptide mapping experiments revealed that the domain recognized by the antibodies was limited to the LRXXH domain present in the CT-region of cycD2SV.

Figure 42. CycD2SV knockdown increases S-phase entry in HEK293 cells as determined by [3H]-thymidine labeling. HEK293 cells were transfected with either control mouse (M) D2SV shRNA or human (H) D2SV shRNA constructs. In addition to the cycD2SV shRNA constructs, cells were co-transfected with a nuclear LacZ expressing construct at a LacZ to shRNA construct ratio of 10:1. Prior to cell fixation cells were incubated with 1μCi/ml of [^{3}H]-thymidine for six hours. After fixation, cells were subjected to XGAL staining to visualize transfected cells and processed for [^{3}H]-thymidine autoradiography. Unpaired two-tail t-test, *$p < 0.05$, $N = 3$ independent experiments. 300 cells counted per group in each experiment. Scale bar is 20 μm.

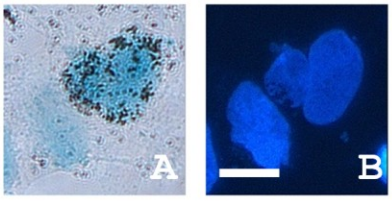
A
B

C

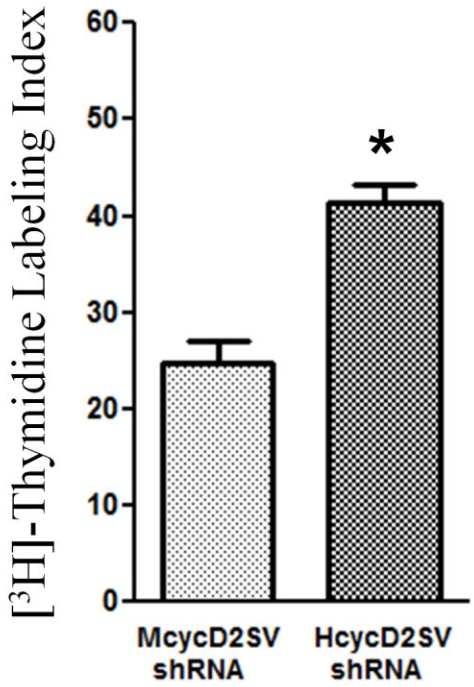
[3H]-Thymidine Labeling Index
60
50
40
30
20
10
0
*
McycD2SV shRNA
HcycD2SV shRNA

Sequence comparisons revealed a high sequence similarity between mouse and human cycD2SV sequences in the LRXXH domain, suggesting the antibodies may detect human cycD2SV. Western blots completed with lysates collected from HEK293 cells using cycD2SV antibodies, detected a 25 kDa band, the predicted molecular weight for human cycD2SV protein. In addition, immunohistochemistry completed on untransfected HEK293 cells using cycD2SV antibodies detected small punctuate bodies. Peptide two containing LRXXH epitope abolished endogenous cycD2SV signal obtained by cycD2SV antibodies. These results confirm that our in-house mouse cycD2SV antibodies can also detect human cycD2SV. Furthermore, a blast search was completed using the cycD2SV CT sequence to eliminate the possibility of crossreaction with other endogenous protein. While the blast search yielded very few proteins which contain a similar LRXXH domain, none of the proteins had a predicted molecular weight of 25 kDa. In addition, the presence of cycD2SV in human tissue has been previously documented whereby cycD2SV transcript was detected in human brain samples. However, to our knowledge, this is the first reported protein expression of cycD2SV in a human cell type.

In order for cyclins to stimulate cell cycle progression they must first: 1) bind to CDKs to form an activated kinase complex, and 2) translocate to the nucleus where the complex can upregulate genes necessary for cell cycle progression. Once the cyclin complex exerts its required effect, the complex is exported to the cytoplasm where the regulatory cyclin subunit is targeted for degradation. Controlling the cellular location, activation and degradation of cyclins allows cells to tightly regulate cell cycle entry as well as transition between phases. For example, in response to mitogenic signals, D-type

cyclins are produced and complex with CDK4 or CDK6, forming an activated kinase complex. The newly formed complex translocates to the nucleus and upregulates genes necessary for G1/S transit. Once cells transition past the G1/S-phase, the activity of cycD/CDK4 or CDK6 complexes is no longer necessary, and D-type cyclins are transported out of the nucleus to the cytoplasm for degradation.

Cyclins are also down regulated during various states of growth arrest, namely during confluence and serum starvation. Here, we demonstrate that cycD1, D2 and D3 protein and mRNA levels all decrease in response to confluence and serum starvation. These results are consistent with previously published literature (Won et al., 1992). In addition, we have observed an increase in cycD2SV expression, a protein which has been previously linked with cell cycle inhibition in overexpression studies [(Sun et al., 2009), see chapter 2]. These results underscore the significance of endogenous cycD2SV in cell cycle regulation during stress conditions such as contact inhibition, and serum starvation. Interestingly, cycD2SV knockdown during confluence resulted in the rescue of only cycD2 protein levels, and had no effect on cycD1, cycD3, CDK4 or CDK2 protein levels, suggesting a direct role for cycD2SV in the downregulation of cycD2 during confluence. Cells have been shown to possess the ability to post-translationally regulate D-type cyclins independent of each other. During DNA damage, cycD1 is specifically degraded whereas cycD2 and D3 levels are maintained (Agami and Bernards, 2000). Additionally, retinoic acid stimulates the expression of cycD2, but downregulates the expression of cycD1 and cycD3 (Ma et al., 2005). Thus, cycD2SV protein expression in response to confluence is perhaps a cellular strategy to specifically down regulate cycD2 levels to achieve cell cycle exit.

Our previous results indentified the ability of cycD2SV to directly interact with co-transfected or endogenous cycD2, as well as HA-Ubq by co-immunoprecipitation and subcellular immunolocalization experiments. In addition, we demonstrated that cycD2SV co-localizes with p62, a protein involved in the clearance of toxic aggregating proteins via autophagy (Rusten and Stenmark, 2010). Specifically, p62 is able to identify ubiquitinated aggregated proteins and target them for autophagy mediated clearance (Rusten and Stenmark, 2010). CycD2 is mainly regulated at the transcriptional level, (Sherr and Roberts, 1999; Murray, 2004) however, it is also regulated at the post-translational level via ubiquitin mediated proteasomal degradation. Like cycD1, cycD2 has been demonstrated to be subject to GSK-3β regulation. Once phosphorylated on Thr280, cycD2 is ubiquitinated and flagged for proteasome-dependent degradation (Kida et al., 2007). Based on the results from our studies, we propose a novel mechanism where cycD2SV sequesters cycD2 and/or CDK4 and targets them for autophagy mediated degradation, and we believe that cycD2SV might be playing a similar role during confluence and serum starvation. However, given the smaller size of endogenous cycD2SV puncta as compared to those of transfected cycD2SV, the proteasomal system might be sufficient for degradation of the sequestered complexes in untransfected cells. Endogenous cycD2SV protein mostly localizes to the cytoplasm, and, as such, we propose that during confluence and serum starvation, cycD2SV sequesters cycD2 in the cytoplasm. By restricting cycD2 to the cytoplasm, cycD2SV: 1) effectively inhibits the ability of cycD2/CDK complexes from upregulating genes necessary for G1/S transition, and 2) provides access of the complex to the degradation machinery.

It has been noted that cycD2 levels are the first to be upregulated from the D-type cyclins in response to mitogenic signals, suggesting an important and necessary role for cycD2 in G1/S transition. During G0/G1, the degradation of p27 is required for successful progression of the cell cycle. CycD2 has been shown to bind to p27 and facilitate nuclear export, where p27 is targeted for proteolysis by the ubiquitin ligase, Kip1 ubiquitination-promoting complex (KPC) (Hara et al., 2005; Susaki et al., 2007). Once upregulated, cycD2 sequesters p27, interfering with the ability of p27 to inhibit CDKs. This mechanism allows cyclin/CDK complexes to activate cell cycle progression without interference from p27. Just as it is important for cells to upregulate cycD2 levels in response to mitogenic signals, we believe it is also important for cells to down regulate cycD2 levels rapidly in response to anti-mitogenic signals. This is supported by evidence provided in this paper. In response to contact inhibition, cycD2 levels were downregulated more rapidly as compared to cycD1 levels (Fig. 37A, B, Fig. 40A, B). The same was observed for cycD2 mRNA levels, where they were significantly downregulated at an earlier time point as compared to cycD1 and cycD3 mRNA levels. By downregulating cycD2, p27 is no longer sequestered, and is free to bind to CDKs, effectively inhibiting the cell cycle. As a result, it comes as no surprise that HEK293 cells would introduce special regulatory mechanisms to ensure cycD2 protein levels are rapidly degraded in response to anti-mitogenic signals. Thus, we believe that cycD2SV may serve an important role in neutralizing cycD2 activity and targeting it for rapid degradation during states of growth arrest (Fig. 43). Indeed, knockdown of cycD2SV increased HEK293 S-phase entry, further demonstrating the important role cycD2SV plays in regulating the cell cycle via cycD2 downregulation.

Figure 43. Proposed role for cycD2SV mediated cell cycle exit during confluent culture conditions. A) In non-confluent culture conditions, cycD2SV protein levels are downregulated. During G1, cycD2 levels are elevated and cycD2 plays a role in 1) exporting p27 from the nucleus to the cytoplasm where it is degraded and, 2) binding CDK4, influencing the activation of the transcription factor E2F and subsequent upregulation of genes required for G1/S transition. B) During confluent conditions, cycD2SV levels are upregulated interfering with the activity of 1) CDK4/cycD complex activity and, 2) cycD2 mediated sequestration and degradation of p27. By binding to CDK4/cycD complexes and interfering with their function, E2F activation is inhibited and genes required for cell cycle progression are no longer upregulated. Additionally, we believe cycD2SV may directly interact with cycD2 in early G1 interfering with p27 nuclear export and degradation. As such, p27 protein stability is increased, contributing to increased p27 protein levels observed during confluent culture conditions and inhibition of cell cycle progression.

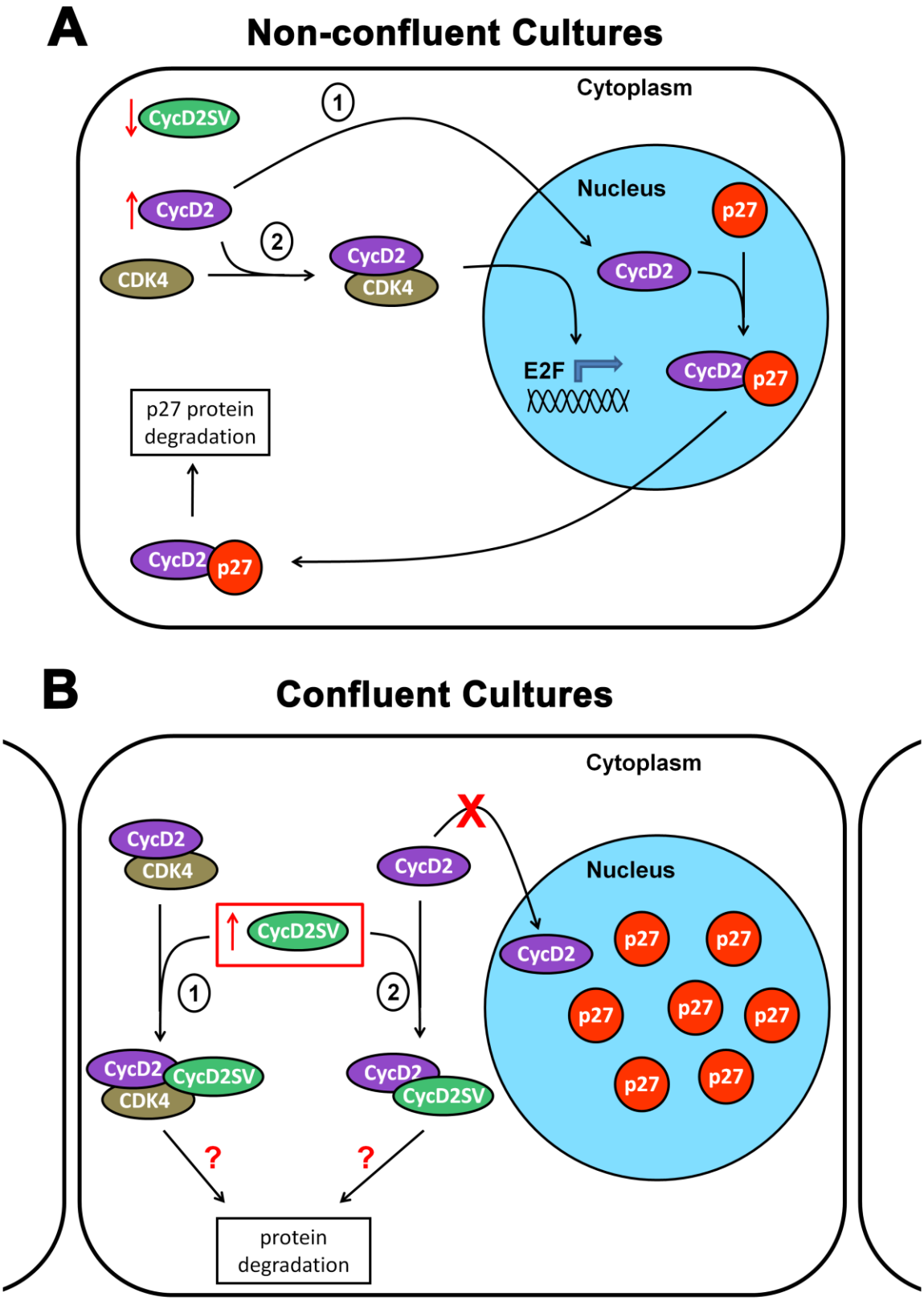
A
Non-confluent Cultures
Cytoplasm
CycD2SV
CycD2
CDK4
1
2
CycD2
CDK4
Nucleus
p27
CycD2
E2F
CycD2
p27
p27 protein
degradation
CycD2
p27
B
Confluent Cultures
Cytoplasm
CycD2
CDK4
X
CycD2
Nucleus
CycD2SV
CycD2
p27
p27
p27
p27
p27
p27
p27
1
2
CycD2
CycD2SV
CDK4
CycD2
CycD2SV
?
?
protein
degradation

While we report a negative regulatory role for cycD2SV, contrary to our findings, cycD2SV was originally reported to have transforming capabilities in MEFs when co-transfected with the oncogene H-Ras. In addition, cycD2SV mRNA levels were shown to be elevated in multiple human brain cancers, suggesting an oncogenic role for the splice variant (Denicourt et al., 2008). Here, we demonstrate the upregulation of cycD2SV levels during normal cellular events, such as confluence and serum starvation, suggesting a negative cell cycle regulatory role for cycD2SV. These results are in agreement with our previous results, where we reported that overexpression of cycD2SV resulted in cell cycle exit. Although, cycD2SV is the first reported D-type splice variant implicated in the negative regulation of the cell cycle, it is not the first cyclin splice variant to possess such a role. In a study by Zschemisch et al., three isoforms of cycE1 (IN3, Δ4, and Δ5) were shown to associate with retarded tumor growth. They also reported the expression of a new cycE1 isoform, Δ3/8, in nonproliferating murine hepatocytes (Zschemisch et al., 2006). Mechanistically, the authors provide evidence of the association of the Δ3/8 isoform with CDK2, and suggest a possible dominant negative role for the splice variant. Additionally, a novel splice variant of cycB (CBsv) was also implicated in negative cell cycle regulation. CBsv was discovered in sea urchin oocytes and embryos by Lozano *et al*., and was demonstrated to be overexpressed in growing oocytes during vitellogenesis when G2 arrest occurs. Due to the low affinity of CBsv for cdc2 (CDK1), the authors suggest that it is unlikely that CBsv functions as a dominant negative molecule. Alternatively, they suggest a possible interaction between CBsv and the phosphatase CDC25 is responsible for the negative cell cycle effects of the splice variant (Lozano et al., 1998). CDC25 phosphatase plays an important role in M-phase entry by de-

phosphorylating cycB1/CDK1 complexes, thus, inhibition of the activity of CDC25 would interfere with M-phase entry. However, it is possible that cycD2SV may play distinct roles in different cell types which would explain the contradictory roles reported for cycD2SV.

Contradictory roles for cyclins have been previously reported where in some cell types cyclins can induce cell cycle exit. CycD1 has been shown to play a role in cellular senescence, where cycD1 protein levels were elevated in IMR90 human lung fibroblasts during cellular senescence by up to fifteen-fold (Han et al., 1999). Additionally, Meyyappan *et al.* have demonstrated that both cycD2 mRNA, and protein are upregulated in primary human diploid and murine fibroblasts during cell cycle exit induced by serum starvation, and contact inhibition. They also demonstrated that cycD2 is down regulated in cells released from contact inhibition and serum starvation, overall suggesting a negative cell cycle regulatory function of cycD2 during conditions of cell cycle arrest (Meyyappan et al., 1998). Alternatively, *CCND2* promoter has been reported to be methylated leading to a loss of function in pancreatic (Matsubayashi et al., 2003), breast (Evron et al., 2001) and prostate cancer (Padar et al., 2003) thereby suggesting a possible tumor suppressor function, as opposed to an oncogenic function of cycD2 (Musgrove et al., 2011).

In this study, we presented evidence that endogenous cycD2SV behaves as a negative cell cycle regulator modulating cycD2 levels during states of growth arrest. We demonstrated that during confluence and serum starvation conditions, cycD1, D2 and D3 protein levels decrease, while cycD2SV protein levels increase. A similar pattern was observed for cycD1, cycD2 and cycD3 mRNA levels during confluence, however,

cycD2SV mRNA levels did not fluctuate. Knock down of cycD2SV during confluence was able to rescue cycD2 protein levels but not those of cycD1 or cycD3, and had no effect on CDK4 or CDK2 protein levels. In addition, cycD2SV knockdown increased S-phase entry in HEK293 cells. Cumulatively, these results suggest a direct involvement of cycD2SV in the down regulation of cycD2, and possibly increasing the efficacy of p27 in CDK inhibition during confluent culture condition. Collectively, these results advance our current knowledge of cell cycle exit mechanisms mediated by cell-to-cell contact inhibition. It is not yet clear however, whether cycD2SV binds to monomeric cycD2 or cycD2 complexed with CDK4. Our previous results, along with results reported by Denicourt *et al.* would suggest that cycD2SV is capable of binding both cycD2 and CDK4, targeting them for UPS/autophagy degradation. However, knockdown of cycD2SV experiment in this study suggests that cycD2SV during confluence may only be modulating cycD2 levels, and not those of CDK4. Alternatively, cyclin dependent kinases have been shown to be stable throughout the cell cycle and perhaps CDK4 clearance as part of a cycD2/CDK4 complex, could be compensated for by transcriptional or translational upregulation. In addition, due to the high sequence similarity between cycD2SV and D-type cyclins, how cycD2SV specifically recognizes and sequesters only cycD2 is yet to be determined. Furthermore, it would be interesting to determine whether cycD2SV flags cycD2 for proteasomal degradation by promoting GSK3β Thr280 phosphorylation of cycD2 or provides an alternative unique degradation pathway independent of GSK3β phosphorylation.

Chapter 4. Discussion

With the understanding that CDKs play an essential role in cell cycle progression, the idea of inhibiting CDKs has emerged as a possible anti-cancer therapeutic target. Currently, there are two types of scaffold-based CDK-inhibitors: ATP competitive inhibitors and non ATP competitive inhibitors. ATP competitive inhibitors compete with ATP binding to CDKs. Since CDKs need ATP to function, binding of the ATP competitive inhibitors interferes with CDK activity. Most of the CDK-inhibitors developed to date belong to the ATP competitive inhibitors, however, in recent years there has been a rise in non ATP CDK-inhibitors due to the limited clinical efficacy and toxicity issues related to ATP competitive inhibitors. Non ATP competitive inhibitors are usually therapeutic peptides which are modeled based on: 1) CDK substrates, 2) inhibitors of CDK/cyclin complexes, and c) inhibitors of the cyclin binding groove (Rizzolio et al., 2010).

In the studies presented here, we demonstrate the ability of cycD2SV to form protein aggregates and inhibit cell division in a variety of immortalized and transformed cell lines. Mechanistically, we provide evidence that cycD2SV sequesters cycD2 and CDK4 and targets them for selective autophagic degradation via the adaptor protein p62. We believe that narrowing down the cell cycle inhibitory (CCI) domain of cycD2SV could lead to an effective anti-cancer therapeutic peptide. Deletion experiments revealed that the first 53 amino acids of cycD2SV are responsible for protein aggregation. Surprisingly, amino acids 54-136 of cycD2SV were capable of inhibiting cell cycle, albeit not as potently as full length cycD2SV, even though there was no protein aggregation present. This result led us to conclude that while the 54-136 amino acid

sequence lacked the aggregation domain, it contained the cell cycle inhibitory domain. The 54-136 amino acid sequence stands at 84 amino acids just over the 76 amino acids size recommended for therapeutic peptides. As such, deletions from the CT and NT are needed to further narrow down the cell cycle inhibitory domain, especially given the need of the addition of accessory sequence(s) to the peptide to assist in cell targeting and cell entry.

The field of cancer treatment is moving slowly towards personalized care, where the paradigm of one-fits-all is slowly being phased out. While cancers fall into distinct classifications such as breast, stomach, and colon cancers, etc., cancers belonging to the same group can be different at the molecular level. An example of such is in breast cancer, where breast cancer cells in some, but not all, patients are positive for human epidermal growth factor receptor 2 (HER2) (Slamon et al., 1989). The discovery of the HER2 led to the development of drugs such as trastuzumab and lapatinib, which inhibit the HER2 receptor (Burris, 2004; Hudis, 2007). This development has allowed us to treat HER2 positive breast cancers in a more effective way (Tsang and Finn, 2012). As such, characterizing cancers at the molecular level would enable us to pick the most effective agents to use for treatments. However, it is also essential to understand the mechanism of action of the various therapeutic agents available to us to allow for maximum efficacy. Furthermore, a therapeutic peptide designed based on the CCI of cycD2SV would be most useful in cancers with D-type cyclin overexpression or CDK4 overactivation. However, based on knockout experiments, one could infer that (theoretically) a cycD2SV CCI based therapeutic would be most effective in gonadal cancers, brain cancers, Non-Hodgkin lymphoma, and pancreatic cancer. This deduction is based on the essential role

cycD2 and CDK4 play in the proliferation of these cell types (See section 1.4, Table 2). Other cell types have developed compensatory mechanisms where D-type cyclins and CDK4 are no longer essential for cellular proliferation. As such, inhibition of CDK4 and cycD2 function within these cell types might not be enough to cause cell cycle arrest. Also, cancers with pRb inactivation would be immune to such an approach.

Additional obstacles for the use of cycD2SV as a therapeutic peptide stem from the limitations of peptides when used as a therapeutic agent. The major limitations of therapeutic peptides are: low bioavailability and half-life due to proteolytic digestion by gastric enzymes, high clearance by the liver and kidneys (hepatic and renal clearance), and poor membrane penetration as a result of their hydrophilicity (Talmadge, 1998; Vlieghe et al., 2010). However, some of these limitations can be overcome by following therapeutic peptide optimization protocols (Ladner et al., 2004; Witt and Davis, 2006; Witt et al., 2001). Many modifications, such as the use of cyclic peptides and pseudo-peptides, have been recently reported to help peptides resist degradation and elimination, and improve their overall bioavailability without jeopardizing their biological activity (Vlieghe et al., 2010).

Based on data provided in this dissertation, we demonstrate that cycD2SV overexpression, while capable of inducing cell cycle arrest, does not cause apoptosis. Initial experiments completed on cells overexpressing cycD2SV demonstrated that cells expressing this protein survived for up to one week in culture (Data not shown). Additional experiments completed using TUNEL staining did not reveal any apoptotic cell death in HEK293 cells overexpressing cycD2SV (See section 2.5.9, Fig. 21D). These results suggested that while cycD2SV inhibited cell cycle progression, it did not induce

apoptotic cell death. As such, we propose the use of cycD2SV as a cytostatic agent which can be administered in between rounds of chemotherapy or radiation treatment. According to the Log Kill hypothesis, anti-cancer drugs follow a log kill kinetic where a given dose of the drug kills a constant proportion of cancer cells, as opposed to a constant number of cells (Dy and Adjei, 2008; Skipper et al., 1964). Thus, if the initial tumor load is 10^{12} cells, and a drug kills three logs of cells per round of treatment, the tumor burden would decrease by 10^3 cells every round of treatment. However, given the non-specificity of chemotherapeutic drugs which cause severe side-effects, in between treatment rounds a rest period is given to allow for normal cells to recover. Unfortunately, during this time a portion of cancer cells recover as well. By administering cycD2SV peptide during the rest period, we could potentially halt cancer cell recovery. This would lead to the overall decrease of the total number of chemotherapy rounds, which in turn would improve patient quality of life, as well as decrease medical costs.

We are aware that once the CCI is narrowed down, further experiments to assess the function and ascertain the *in vivo* success of the peptide are necessary. To test the effectiveness of the therapeutic peptide, one could test the ability of the peptides to bind and inhibit the activation of CDK4 in the presence of cycD2 and CAK. *In vitro* phosphorylation experiments could be performed by adding various peptides to a test tube with recombinant CDK4, cycD2 and CAK proteins in the presence or absence of gamma ^{32}P-ATP. Following a thirty minute incubation at 30ºC, an aliquot from each reaction would be resolved by western blot. Autoradiographic exposure of the resolved gel should reveal the status of CDK4 phosphorylation. Tubes with biologically active CCI peptides should have little or no CDK4 phosphorylation, while tubes with

biologically inactive peptides should have high levels of CDK4 phosphorylation [Method adapted from (Denicourt et al., 2008)]. Experiments should also be conducted to test for the effectiveness of the therapeutic peptide in an i*n vivo* setting. Addition of the HIV TAT-1 sequence (RRRQRRKKRG) will facilitate peptide entry through the plasma membrane of living cells (Fischer et al., 2005; Tunnemann et al., 2006; Zorko and Langel, 2005). The efficacy of the cycD2SV CCI peptide can be tested in human cancer xenograft models. For example, human breast cancer cells such as MCF-7 cells can be injected into the lower mammary fat pad of SCID mice. When tumor size reaches 100 mm^3, mice can be treated with an intratumor peptide injection (control scrambled peptide vs. CCI peptide) as described earlier (Du et al., 2007; Paine-Murrieta et al., 1997). Relative tumor growth can be assessed over a period of 40-50 days. One can expect that mice receiving the CCI peptide injections will have retarded tumor growth compared to mice receiving control scramble peptide injections.

In this dissertation, we demonstrate that elevated levels of cycD2SV, whether by overexpression (transient transfection) or upregulation during states of growth arrest, induces cell cycle exit. As such, in addition to using cycD2SV as a therapeutic peptide, an alternative method of exploiting cycD2SV-induced cell cycle arrest could be achieved by attempting to elevate endogenous cycD2SV levels in cancer cells with various agents. For example, the cardiac glycoside digoxin, which has been used to treat heart failure, is known to modulate splicing (Stoilov et al., 2008). Interestingly, digoxin was shown to inhibit tumor growth while its mechanism of action is debated (Lopez-Lazaro, 2009; Zhang et al., 2008a). If digoxin administration is capable of altering cycD2 splicing to

favor cycD2SV expression, it could offer a new mechanism by which digoxin can induce cell cycle exit in cancer cells.

Cells have developed many mechanisms in order to deal with stress induced by a variety of conditions such as cellular confluence, nutrient deprivation and protein aggregation. Given that protein aggregates usually occur as a result of protein misfolding, the response developed by cells to handle protein aggregates, such as cycD2SV, is referred to as the unfolded protein response (UPR) (Brewer and Diehl, 2000). Evidence provided for cycD2SV misfolding includes TCRα reporter retention in HEK293 cells, co-transfected with cycD2SV, and the presence of high molecular weight bands when lysates from HEK293 cells were resolved in native gels under non-denaturing conditions (Sun et al., 2009). Also, the analysis of the 3D structure of cycD2SV revealed an overhanging NT domain. We believe that as a result of the truncation of cycD2SV and the absence of the CT domain present in other D-type cyclins, the NT is no longer folded correctly, resulting in protein aggregation. Once the UPR is stimulated, cells either overcome the protein aggregates via clearance or undergo apoptosis if the problem is unresolved (Niwa and Walter, 2000). As discussed earlier, cycD2SV is cytostatic and does not induce apoptosis. However, HEK293 cells overexpressing cycD2SV did not survive in culture after subjecting them to trypsinization and replating. Huang *et al.* reported that trypsinization can induce a stress response in cultured cells (Huang et al., 2010). Specifically, trypsinization led to the downregulation of the cell survival protein, Bcl-2, and the upregulation of the proapoptotic protein p53 and the CKI, p21. While cycD2SV mediated UPR is not sufficient in the induction of apoptotic cell death, our results indicate that cycD2SV expressing cells are sensitized to cell death when exposed

to additional stressors such as trypsinization. How cycD2SV collaborates with trypsinization is still not known and perhaps more experimental work is needed to elucidate the mechanism underlying this phenomenon.

In preliminary studies, we observed that cells overexpressing cycD2SV contained higher levels of p53 when compared with control untransfected cells (data not shown). This observation was consistent with our earlier findings, where cycD2SV overexpression induced the GADD45α gene expression, a p53-inducible gene. p53 is a tumor suppressor gene which is capable of inducing cellular senescence, cell cycle arrest, or apoptosis (Jin and Levine, 2001). One of the well studied mechanisms for p53 activation is its role in DNA damage. In response to DNA damage caused by ionizing radiation or ultraviolet light, ATM activates the checkpoint kinases Chk1 and Chk2 which in turn cause activation of p53 via phosphorylation at Ser20 (Borras et al., 2011). 53BP1 is a DNA double strand break (DSB) sensor which is recruited to sites of DSBs. As such, cells containing DSBs stained with 53BP1 exhibit visible nuclear foci which are used to identify DNA damage (Rappold et al., 2001; Schultz et al., 2000; Wang et al., 2002) . Based on 53BP1 staining completed on HEK293 cells overexpressing cycD2SV, cycD2SV does not seem to induce DNA damage (data not shown). However, based on upregulation of p53 and sensitization of cycD2SV expressing cells to trypsin induced cell death, it would be interesting to further examine whether D2SV expression also sensitizes cells to a variety of anticancer agents.

In summary, we identified a splice variant of cycD2, cycD2SV, which is capable of inducing cell cycle arrest in a variety of transformed and immortalized cell lines. We provided a mechanism whereby cycD2SV sequesters important cell cycle proteins such

as cycD2 and CDK4, and targets them for selective autophagic degradation. We also propose the upregulation of the tumor suppressor protein, p53, as a possible additional mechanism by which cycD2SV induces cell cycle exit. However, it is not clear whether cycD2SV sequestration of cell cycle proteins and p53 upregulation are events which are capable of independently inducing cell cycle arrest or if they are synergistic in nature. By sequestering important G1 proteins, such as cycD and CDK4, and targeting them for degradation we believe that cycD2SV induces cell cycle arrest at the G1 phase of the cell cycle. However, if cycD2SV does indeed assist in the upregulation, activation and stabilization of p53, in addition to inducing a G1 arrest, cycD2SV might be capable of inducing G2 phase arrest. We have narrowed down the cell cycle inhibitory domain, however, further deletion studies are required to design a peptide which is usable as a therapeutic peptide. We identified that cycD2SV is capable of inducing cell death in cells exposed to stressors such as trypsinization, and it would be interesting to determine whether cycD2SV is capable of sensitizing cancer cells to a variety of anti-cancer agents.

4.1 Major Conclusions

Based on overexpression experiments we conclude that cycD2SV mediates cell cycle exit via two mechanisms: 1) by binding important cell cycle proteins, such as cycD2 and CDK4, and targeting them for selective autophagosome degradation and, 2) by inducing cellular stress and upregulating a potent G2/M inhibitor, GADD45α, (Fig. 26). In this dissertation we demonstrate that cycD2SV is capable of binding both CDK4 and cycD2 in immunoprecipitation experiments. Whether cycD2SV, is capable of binding to CDK4 or cycD2 separately or in complex is yet to be determined. However,

once cycD2SV is bound to CDK4, cycD2 or CDK4/cycD2 complexes, we believe that cycD2SV sequesters these proteins in the cytoplasm where they are targeted for selective autophagosome degradation. We believe that a misfolded structure of cycD2SV which differs significantly from the conventional cyclin structure, increases its propensity for intracellular aggregation. These aggregates may occur as a result of self association or oligomerziation, similar to those processes described for cycD3 or p57, and/or in association with other cell cycle proteins such as cycD2 and CDK4. The creation of these aggregated masses induces ER stress resulting in impaired ERAD. In addition, the cellular stress induced by cycD2SV protein aggregation results in the upregulation of a G2/M inhibitor, GADD45α. However, the exact mechanism for GADD45α upregulation by cycD2SV protein aggregation is yet to be elucidated.

Additionally, based on the evidence presented in this dissertation, endogenous cycD2SV plays a critical role in cell cycle exit. Experiments completed on confluent and serum deprived HEK293 cells demonstrate the upregulation of cycD2SV protein levels suggesting a role for the splice variant during states of growth arrest. Knocking down of cycD2SV during confluence specifically rescued cycD2 protein levels but had no effect on other cell cycle protein levels such as cycD1, cycD3, CDK4 and CDK2. Additionally, knockdown of cycD2SV upregulates S-phase entry in HEK293 cells further implicating cycD2SV in cell cycle arrest. In addition to the known role of cycD2 in pRb phosphorylation, during early G1 cycD2 has been shown to sequester the CKI p27 in the cytoplasm and interfere with its negative cell cycle regulatory function. Given that early upregulation of cycD2 during G1 phase is necessary to ensure the sequestration of p27 to allow for G1 transition, we propose that during states of growth arrest cycD2SV

upregulation may be responsible for alleviating p27 inhibition by cycD2. Once cycD2 is sequestered by cycD2SV, p27 is free to translocate to the nucleus where it inhibits cyclin/CDK complexes and interferes with G1 progression (Fig. 43).

References

Abercrombie, M. (1970). Contact inhibition in tissue culture. In Vitro *6*, 128-142.

Abercrombie, M., and Ambrose, E. J. (1958). Interference microscope studies of cell contacts in tissue culture. Exp Cell Res *15*, 332-345.

Abercrombie, M., and Heaysman, J. E. (1954). Observations on the social behaviour of cells in tissue culture. II. Monolayering of fibroblasts. Exp Cell Res *6*, 293-306.

Adon, A. M., Zeng, X., Harrison, M. K., Sannem, S., Kiyokawa, H., Kaldis, P., and Saavedra, H. I. (2010). Cdk2 and Cdk4 regulate the centrosome cycle and are critical mediators of centrosome amplification in p53-null cells. Mol Cell Biol *30*, 694-710.

Agami, R., and Bernards, R. (2000). Distinct initiation and maintenance mechanisms cooperate to induce G1 cell cycle arrest in response to DNA damage. Cell *102*, 55-66.

Aggarwal, B. B., Vijayalekshmi, R. V., and Sung, B. (2009). Targeting inflammatory pathways for prevention and therapy of cancer: short-term friend, long-term foe. Clin Cancer Res *15*, 425-430.

Akoulitchev, S., Chuikov, S., and Reinberg, D. (2000). TFIIH is negatively regulated by cdk8-containing mediator complexes. Nature *407*, 102-106.

Alao, J. P. (2007). The regulation of cyclin D1 degradation: roles in cancer development and the potential for therapeutic invention. Mol Cancer *6*, 24.

Alao, J. P., Gamble, S. C., Stavropoulou, A. V., Pomeranz, K. M., Lam, E. W., Coombes, R. C., and Vigushin, D. M. (2006). The cyclin D1 proto-oncogene is sequestered in the cytoplasm of mammalian cancer cell lines. Mol Cancer *5*, 7.

Alao, J. P., Lam, E. W., Ali, S., Buluwela, L., Bordogna, W., Lockey, P., Varshochi, R., Stavropoulou, A. V., Coombes, R. C., and Vigushin, D. M. (2004). Histone deacetylase inhibitor trichostatin A represses estrogen receptor alpha-dependent transcription and promotes proteasomal degradation of cyclin D1 in human breast carcinoma cell lines. Clin Cancer Res *10*, 8094-8104.

Al-Aynati, M. M., Radulovich, N., Ho, J., and Tsao, M. S. (2004). Overexpression of G1-S cyclins and cyclin-dependent kinases during multistage human pancreatic duct cell carcinogenesis. Clin Cancer Res *10*, 6598-6605.

Alt, J. R., Cleveland, J. L., Hannink, M., and Diehl, J. A. (2000). Phosphorylation-dependent regulation of cyclin D1 nuclear export and cyclin D1-dependent cellular transformation. Genes Dev *14*, 3102-3114.

Alt, J. R., Gladden, A. B., and Diehl, J. A. (2002). p21(Cip1) Promotes cyclin D1 nuclear accumulation via direct inhibition of nuclear export. J Biol Chem *277*, 8517-8523.

Anton, L. C., Schubert, U., Bacik, I., Princiotta, M. F., Wearsch, P. A., Gibbs, J., Day, P. M., Realini, C., Rechsteiner, M. C., Bennink, J. R., and Yewdell, J. W. (1999). Intracellular localization of proteasomal degradation of a viral antigen. J Cell Biol *146*, 113-124.

Arnold, A., and Papanikolaou, A. (2005). Cyclin D1 in breast cancer pathogenesis. J Clin Oncol *23*, 4215-4224.

Arrasate, M., Mitra, S., Schweitzer, E. S., Segal, M. R., and Finkbeiner, S. (2004). Inclusion body formation reduces levels of mutant huntingtin and the risk of neuronal death. Nature *431*, 805-810.

Atadja, P., Wong, H., Veillette, C., and Riabowol, K. (1995). Overexpression of cyclin D1 blocks proliferation of normal diploid fibroblasts. Exp Cell Res *217*, 205-216.

Averous, J., Fonseca, B. D., and Proud, C. G. (2008). Regulation of cyclin D1 expression by mTORC1 signaling requires eukaryotic initiation factor 4E-binding protein 1. Oncogene *27*, 1106-1113.

Bagella, L., Giacinti, C., Simone, C., and Giordano, A. (2006). Identification of murine cdk10: association with Ets2 transcription factor and effects on the cell cycle. J Cell Biochem *99*, 978-985.

Balmain, A., and Pragnell, I. B. (1983). Mouse skin carcinomas induced in vivo by chemical carcinogens have a transforming Harvey-ras oncogene. Nature *303*, 72-74.

Bano, D., Zanetti, F., Mende, Y., and Nicotera, P. (2011). Neurodegenerative processes in Huntington's disease. Cell Death Dis *2*, e228.

Barbacid, M. (1987). ras genes. Annu Rev Biochem *56*, 779-827.

Barbash, O., Zamfirova, P., Lin, D. I., Chen, X., Yang, K., Nakagawa, H., Lu, F., Rustgi, A. K., and Diehl, J. A. (2008). Mutations in Fbx4 inhibit dimerization of the SCF(Fbx4) ligase and contribute to cyclin D1 overexpression in human cancer. Cancer Cell *14*, 68-78.

Barriere, C., Santamaria, D., Cerqueira, A., Galan, J., Martin, A., Ortega, S., Malumbres, M., Dubus, P., and Barbacid, M. (2007). Mice thrive without Cdk4 and Cdk2. Mol Oncol *1*, 72-83.

Bazarov, A. V., Adachi, S., Li, S. F., Mateyak, M. K., Wei, S., and Sedivy, J. M. (2001). A modest reduction in c-myc expression has minimal effects on cell growth and apoptosis but dramatically reduces susceptibility to Ras and Raf transformation. Cancer Res *61*, 1178-1186.

Belmont, A. S. (2006). Mitotic chromosome structure and condensation. Curr Opin Cell Biol *18*, 632-638.

Bence, N. F., Sampat, R. M., and Kopito, R. R. (2001). Impairment of the ubiquitin-proteasome system by protein aggregation. Science *292*, 1552-1555.

Bergsagel, P. L., and Kuehl, W. M. (2005). Molecular pathogenesis and a consequent classification of multiple myeloma. J Clin Oncol *23*, 6333-6338.

Bernales, S., McDonald, K. L., and Walter, P. (2006). Autophagy counterbalances endoplasmic reticulum expansion during the unfolded protein response. PLoS Biol *4*, e423.

Berthet, C., Aleem, E., Coppola, V., Tessarollo, L., and Kaldis, P. (2003). Cdk2 knockout mice are viable. Curr Biol *13*, 1775-1785.

Bertoni, F., Rinaldi, A., Zucca, E., and Cavalli, F. (2006). Update on the molecular biology of mantle cell lymphoma. Hematol Oncol *24*, 22-27.

Bjorkoy, G., Lamark, T., Brech, A., Outzen, H., Perander, M., Overvatn, A., Stenmark, H., and Johansen, T. (2005). p62/SQSTM1 forms protein aggregates degraded by autophagy and has a protective effect on huntingtin-induced cell death. J Cell Biol *171*, 603-614.

Blow, J. J., and Hodgson, B. (2002). Replication licensing--defining the proliferative state? Trends Cell Biol *12*, 72-78.

Borras, C., Gomez-Cabrera, M. C., and Vina, J. (2011). The dual role of p53: DNA protection and antioxidant. Free Radic Res *45*, 643-652.

Borriello, A., Cucciolla, V., Oliva, A., Zappia, V., and Della Ragione, F. (2007). p27Kip1 metabolism: a fascinating labyrinth. Cell Cycle *6*, 1053-1061.

Bowman, G. D., O'Donnell, M., and Kuriyan, J. (2004). Structural analysis of a eukaryotic sliding DNA clamp-clamp loader complex. Nature *429*, 724-730.

Brewer, J. W., and Diehl, J. A. (2000). PERK mediates cell-cycle exit during the mammalian unfolded protein response. Proc Natl Acad Sci U S A *97*, 12625-12630.

Brooks, C. L., and Gu, W. (2011). p53 regulation by ubiquitin. FEBS Lett *585*, 2803-2809.

Brown, N. R., Noble, M. E., Endicott, J. A., Garman, E. F., Wakatsuki, S., Mitchell, E., Rasmussen, B., Hunt, T., and Johnson, L. N. (1995). The crystal structure of cyclin A. Structure *3*, 1235-1247.

Burris, H. A., 3rd (2004). Dual kinase inhibition in the treatment of breast cancer: initial experience with the EGFR/ErbB-2 inhibitor lapatinib. Oncologist *9 Suppl 3*, 10-15.

Carnero, A., and Hannon, G. J. (1998). The INK4 family of CDK inhibitors. Curr Top Microbiol Immunol *227*, 43-55.

Castro, A., Bernis, C., Vigneron, S., Labbe, J. C., and Lorca, T. (2005). The anaphase-promoting complex: a key factor in the regulation of cell cycle. Oncogene *24*, 314-325.

Chang, L., and Karin, M. (2001). Mammalian MAP kinase signalling cascades. Nature *410*, 37-40.

Chaturvedi, P., Eng, W. K., Zhu, Y., Mattern, M. R., Mishra, R., Hurle, M. R., Zhang, X., Annan, R. S., Lu, Q., Faucette, L. F.*, et al.* (1999). Mammalian Chk2 is a downstream effector of the ATM-dependent DNA damage checkpoint pathway. Oncogene *18*, 4047-4054.

Cheng, M., Olivier, P., Diehl, J. A., Fero, M., Roussel, M. F., Roberts, J. M., and Sherr, C. J. (1999). The p21(Cip1) and p27(Kip1) CDK 'inhibitors' are essential activators of cyclin D-dependent kinases in murine fibroblasts. Embo J *18*, 1571-1583.

Chial, H. (2008a). Proto-oncogenes to oncogenes to cancer. Nature Education *1*.

Chial, H. (2008b). Tumor Suppressor (TS) Genes and the Two-Hit Hypothesis. Nature Education *1*.

Choi, H. S., Lee, Y., Park, K. H., Sung, J. S., Lee, J. E., Shin, E. S., Ryu, J. S., and Kim, Y. H. (2009). Single-nucleotide polymorphisms in the promoter of the CDK5 gene and lung cancer risk in a Korean population. J Hum Genet *54*, 298-303.

Ciemerych, M. A., Kenney, A. M., Sicinska, E., Kalaszczynska, I., Bronson, R. T., Rowitch, D. H., Gardner, H., and Sicinski, P. (2002). Development of mice expressing a single D-type cyclin. Genes Dev *16*, 3277-3289.

Coulonval, K., Kooken, H., and Roger, P. P. (2011). Coupling of T161 and T14 phosphorylations protects cyclin B-CDK1 from premature activation. Mol Biol Cell *22*, 3971-3985.

Cruz, J. C., and Tsai, L. H. (2004). A Jekyll and Hyde kinase: roles for Cdk5 in brain development and disease. Curr Opin Neurobiol *14*, 390-394.

Cyr, D. M., Hohfeld, J., and Patterson, C. (2002). Protein quality control: U-box-containing E3 ubiquitin ligases join the fold. Trends Biochem Sci *27*, 368-375.

Dang, C. V., O'Donnell, K. A., Zeller, K. I., Nguyen, T., Osthus, R. C., and Li, F. (2006). The c-Myc target gene network. Semin Cancer Biol *16*, 253-264.

De Bondt, H. L., Rosenblatt, J., Jancarik, J., Jones, H. D., Morgan, D. O., and Kim, S. H. (1993). Crystal structure of cyclin-dependent kinase 2. Nature *363*, 595-602.

DeLaBarre, B., Christianson, J. C., Kopito, R. R., and Brunger, A. T. (2006). Central pore residues mediate the p97/VCP activity required for ERAD. Mol Cell *22*, 451-462.

Denicourt, C., and Dowdy, S. F. (2004). Cip/Kip proteins: more than just CDKs inhibitors. Genes Dev *18*, 851-855.

Denicourt, C., Kozak, C. A., and Rassart, E. (2003). Gris1, a new common integration site in Graffi murine leukemia virus-induced leukemias: overexpression of a truncated cyclin D2 due to alternative splicing. J Virol *77*, 37-44.

Denicourt, C., Legault, P., McNabb, F. A., and Rassart, E. (2008). Human and mouse cyclin D2 splice variants: transforming activity and subcellular localization. Oncogene *27*, 1253-1262.

Der, C. J., Krontiris, T. G., and Cooper, G. M. (1982). Transforming genes of human bladder and lung carcinoma cell lines are homologous to the ras genes of Harvey and Kirsten sarcoma viruses. Proc Natl Acad Sci U S A *79*, 3637-3640.

Deretic, V. (2010). Autophagy in infection. Curr Opin Cell Biol *22*, 252-262.

Devault, A., Martinez, A. M., Fesquet, D., Labbe, J. C., Morin, N., Tassan, J. P., Nigg, E. A., Cavadore, J. C., and Doree, M. (1995). MAT1 ('menage a trois') a new RING finger

protein subunit stabilizing cyclin H-cdk7 complexes in starfish and Xenopus CAK. Embo J *14*, 5027-5036.

Dhariwala, F. A., and Rajadhyaksha, M. S. (2008). An unusual member of the Cdk family: Cdk5. Cell Mol Neurobiol *28*, 351-369.

Diehl, J. A., Cheng, M., Roussel, M. F., and Sherr, C. J. (1998). Glycogen synthase kinase-3beta regulates cyclin D1 proteolysis and subcellular localization. Genes Dev *12*, 3499-3511.

Diehl, J. A., and Sherr, C. J. (1997). A dominant-negative cyclin D1 mutant prevents nuclear import of cyclin-dependent kinase 4 (CDK4) and its phosphorylation by CDK-activating kinase. Mol Cell Biol *17*, 7362-7374.

Du, W., Hattori, Y., Yamada, T., Matsumoto, K., Nakamura, T., Sagawa, M., Otsuki, T., Niikura, T., Nukiwa, T., and Ikeda, Y. (2007). NK4, an antagonist of hepatocyte growth factor (HGF), inhibits growth of multiple myeloma cells: molecular targeting of angiogenic growth factor. Blood *109*, 3042-3049.

Duan, Y., He, X., Yang, H., Ji, Y., Tao, T., Chen, J., Hu, L., Zhang, F., Li, X., Wang, H., *et al.* (2010). Cyclin D3/CDK11(p58) complex involved in Schwann cells proliferation repression caused by lipopolysaccharide. Inflammation *33*, 189-199.

Dufner, A., and Thomas, G. (1999). Ribosomal S6 kinase signaling and the control of translation. Exp Cell Res *253*, 100-109.

Dy, G. K., and Adjei, A. A. (2008). Systemic cancer therapy: evolution over the last 60 years. Cancer *113*, 1857-1887.

Ehrhardt, A., Ehrhardt, G. R., Guo, X., and Schrader, J. W. (2002). Ras and relatives--job sharing and networking keep an old family together. Exp Hematol *30*, 1089-1106.

el-Deiry, W. S., Tokino, T., Velculescu, V. E., Levy, D. B., Parsons, R., Trent, J. M., Lin, D., Mercer, W. E., Kinzler, K. W., and Vogelstein, B. (1993). WAF1, a potential mediator of p53 tumor suppression. Cell *75*, 817-825.

Eva, A., and Aaronson, S. A. (1983). Frequent activation of c-kis as a transforming gene in fibrosarcomas induced by methylcholanthrene. Science *220*, 955-956.

Evans, D. L., Harris, D. T., and Jaso-Friedmann, L. (1990). Effects of phorbol esters and calcium ionophore on nonspecific cytotoxic cells. Dev Comp Immunol *14*, 223-230.

Evron, E., Umbricht, C. B., Korz, D., Raman, V., Loeb, D. M., Niranjan, B., Buluwela, L., Weitzman, S. A., Marks, J., and Sukumar, S. (2001). Loss of cyclin D2 expression in the majority of breast cancers is associated with promoter hypermethylation. Cancer Res *61*, 2782-2787.

Fantl, V., Stamp, G., Andrews, A., Rosewell, I., and Dickson, C. (1995). Mice lacking cyclin D1 are small and show defects in eye and mammary gland development. Genes Dev *9*, 2364-2372.

Faussillon, M., Monnier, L., Junien, C., and Jeanpierre, C. (2005). Frequent overexpression of cyclin D2/cyclin-dependent kinase 4 in Wilms' tumor. Cancer Lett *221*, 67-75.

Fesquet, D., Labbe, J. C., Derancourt, J., Capony, J. P., Galas, S., Girard, F., Lorca, T., Shuttleworth, J., Doree, M., and Cavadore, J. C. (1993). The MO15 gene encodes the catalytic subunit of a protein kinase that activates cdc2 and other cyclin-dependent kinases (CDKs) through phosphorylation of Thr161 and its homologues. Embo J *12*, 3111-3121.

Fischer, R., Fotin-Mleczek, M., Hufnagel, H., and Brock, R. (2005). Break on through to the other side-biophysics and cell biology shed light on cell-penetrating peptides. Chembiochem *6*, 2126-2142.

Fish, K. N., Schmid, S. L., and Damke, H. (2000). Evidence that dynamin-2 functions as a signal-transducing GTPase. J Cell Biol *150*, 145-154.

Fisher, R. P. (2005). Secrets of a double agent: CDK7 in cell-cycle control and transcription. J Cell Sci *118*, 5171-5180.

Fisher, R. P., Jin, P., Chamberlin, H. M., and Morgan, D. O. (1995). Alternative mechanisms of CAK assembly require an assembly factor or an activating kinase. Cell *83*, 47-57.

Fisher, R. P., and Morgan, D. O. (1994). A novel cyclin associates with MO15/CDK7 to form the CDK-activating kinase. Cell *78*, 713-724.

Flores-Rozas, H., Kelman, Z., Dean, F. B., Pan, Z. Q., Harper, J. W., Elledge, S. J., O'Donnell, M., and Hurwitz, J. (1994). Cdk-interacting protein 1 directly binds with proliferating cell nuclear antigen and inhibits DNA replication catalyzed by the DNA polymerase delta holoenzyme. Proc Natl Acad Sci U S A *91*, 8655-8659.

Franca-Koh, J., Yeo, M., Fraser, E., Young, N., and Dale, T. C. (2002). The regulation of glycogen synthase kinase-3 nuclear export by Frat/GBP. J Biol Chem *277*, 43844-43848.

Fukami-Kobayashi, J., and Mitsui, Y. (1999). Cyclin D1 inhibits cell proliferation through binding to PCNA and cdk2. Exp Cell Res *246*, 338-347.

Garcea, G., Neal, C. P., Pattenden, C. J., Steward, W. P., and Berry, D. P. (2005). Molecular prognostic markers in pancreatic cancer: a systematic review. Eur J Cancer *41*, 2213-2236.

Garcia-Mata, R., Gao, Y. S., and Sztul, E. (2002). Hassles with taking out the garbage: aggravating aggresomes. Traffic *3*, 388-396.

Garkavtsev, I., Hull, C., and Riabowol, K. (1998). Molecular aspects of the relationship between cancer and aging: tumor suppressor activity during cellular senescence. Exp Gerontol *33*, 81-94.

Garriga, J., and Grana, X. (2004). Cellular control of gene expression by T-type cyclin/CDK9 complexes. Gene *337*, 15-23.

Gautier, J., Solomon, M. J., Booher, R. N., Bazan, J. F., and Kirschner, M. W. (1991). cdc25 is a specific tyrosine phosphatase that directly activates p34cdc2. Cell *67*, 197-211.

Gautschi, O., Ratschiller, D., Gugger, M., Betticher, D. C., and Heighway, J. (2007). Cyclin D1 in non-small cell lung cancer: a key driver of malignant transformation. Lung Cancer *55*, 1-14.

Geisler, S., Holmstrom, K. M., Skujat, D., Fiesel, F. C., Rothfuss, O. C., Kahle, P. J., and Springer, W. (2010). PINK1/Parkin-mediated mitophagy is dependent on VDAC1 and p62/SQSTM1. Nat Cell Biol *12*, 119-131.

Gibbs, J. B., Sigal, I. S., Poe, M., and Scolnick, E. M. (1984). Intrinsic GTPase activity distinguishes normal and oncogenic ras p21 molecules. Proc Natl Acad Sci U S A *81*, 5704-5708.

Gil, J., and Peters, G. (2006). Regulation of the INK4b-ARF-INK4a tumour suppressor locus: all for one or one for all. Nat Rev Mol Cell Biol *7*, 667-677.

Girard, F., Strausfeld, U., Fernandez, A., and Lamb, N. J. (1991). Cyclin A is required for the onset of DNA replication in mammalian fibroblasts. Cell *67*, 1169-1179.

Gladden, A. B., and Diehl, J. A. (2005). Location, location, location: the role of cyclin D1 nuclear localization in cancer. J Cell Biochem *96*, 906-913.

Goldberg, A. L. (2003). Protein degradation and protection against misfolded or damaged proteins. Nature *426*, 895-899.

Goldfarb, M., Shimizu, K., Perucho, M., and Wigler, M. (1982). Isolation and preliminary characterization of a human transforming gene from T24 bladder carcinoma cells. Nature *296*, 404-409.

Goldstein, A. M., Chidambaram, A., Halpern, A., Holly, E. A., Guerry, I. D., Sagebiel, R., Elder, D. E., and Tucker, M. A. (2002). Rarity of CDK4 germline mutations in familial melanoma. Melanoma Res *12*, 51-55.

Gopinathan, L., Ratnacaram, C. K., and Kaldis, P. (2011). Established and novel Cdk/cyclin complexes regulating the cell cycle and development. Results Probl Cell Differ *53*, 365-389.

Guerrero, I., Calzada, P., Mayer, A., and Pellicer, A. (1984). A molecular approach to leukemogenesis: mouse lymphomas contain an activated c-ras oncogene. Proc Natl Acad Sci U S A *81*, 202-205.

Guo, Y., Yang, K., Harwalkar, J., Nye, J. M., Mason, D. R., Garrett, M. D., Hitomi, M., and Stacey, D. W. (2005). Phosphorylation of cyclin D1 at Thr 286 during S phase leads to its proteasomal degradation and allows efficient DNA synthesis. Oncogene *24*, 2599-2612.

Hall, A., Marshall, C. J., Spurr, N. K., and Weiss, R. A. (1983). Identification of transforming gene in two human sarcoma cell lines as a new member of the ras gene family located on chromosome 1. Nature *303*, 396-400.

Han, E. K., Ng, S. C., Arber, N., Begemann, M., and Weinstein, I. B. (1999). Roles of cyclin D1 and related genes in growth inhibition, senescence and apoptosis. Apoptosis *4*, 213-219.

Hanahan, D., and Weinberg, R. A. (2000). The hallmarks of cancer. Cell *100*, 57-70.

Hannon, G. J., Casso, D., and Beach, D. (1994). KAP: a dual specificity phosphatase that interacts with cyclin-dependent kinases. Proc Natl Acad Sci U S A *91*, 1731-1735.

Hara, T., Kamura, T., Kotoshiba, S., Takahashi, H., Fujiwara, K., Onoyama, I., Shirakawa, M., Mizushima, N., and Nakayama, K. I. (2005). Role of the UBL-UBA protein KPC2 in degradation of p27 at G1 phase of the cell cycle. Mol Cell Biol *25*, 9292-9303.

Hardisson, D. (2003). Molecular pathogenesis of head and neck squamous cell carcinoma. Eur Arch Otorhinolaryngol *260*, 502-508.

Harper, J. W., Adami, G. R., Wei, N., Keyomarsi, K., and Elledge, S. J. (1993). The p21 Cdk-interacting protein Cip1 is a potent inhibitor of G1 cyclin-dependent kinases. Cell *75*, 805-816.

Harper, J. W., Burton, J. L., and Solomon, M. J. (2002). The anaphase-promoting complex: it's not just for mitosis any more. Genes Dev *16*, 2179-2206.

Harvey, J. J. (1964). An Unidentified Virus Which Causes the Rapid Production of Tumours in Mice. Nature *204*, 1104-1105.

He, G., Siddik, Z. H., Huang, Z., Wang, R., Koomen, J., Kobayashi, R., Khokhar, A. R., and Kuang, J. (2005). Induction of p21 by p53 following DNA damage inhibits both Cdk4 and Cdk2 activities. Oncogene *24*, 2929-2943.

Hedberg, Y., Roos, G., Ljungberg, B., and Landberg, G. (2002). Cyclin D3 protein content in human renal cell carcinoma in relation to cyclin D1 and clinico-pathological parameters. Acta Oncol *41*, 175-181.

Hershko, A. (1983). Ubiquitin: roles in protein modification and breakdown. Cell *34*, 11-12.

Hoeller, D., and Dikic, I. (2009). Targeting the ubiquitin system in cancer therapy. Nature *458*, 438-444.

Hollander, M. C., and Fornace, A. J., Jr. (2002). Genomic instability, centrosome amplification, cell cycle checkpoints and Gadd45a. Oncogene *21*, 6228-6233.

Hotchkiss, A., Robinson, J., MacLean, J., Feridooni, T., WAFA, K. and Pasumarthi, K.B. (2012). Role of D-type cyclins in heart development and disease. Can J Physiol Pharmacol *In Press*.

Huang, H. L., Hsing, H. W., Lai, T. C., Chen, Y. W., Lee, T. R., Chan, H. T., Lyu, P. C., Wu, C. L., Lu, Y. C., Lin, S. T.*, et al.* (2010). Trypsin-induced proteome alteration during cell subculture in mammalian cells. J Biomed Sci *17*, 36.

Huard, J. M., Forster, C. C., Carter, M. L., Sicinski, P., and Ross, M. E. (1999). Cerebellar histogenesis is disturbed in mice lacking cyclin D2. Development *126*, 1927-1935.

Hubscher, U. (2009). DNA replication fork proteins. Methods Mol Biol *521*, 19-33.

Hudis, C. A. (2007). Trastuzumab--mechanism of action and use in clinical practice. N Engl J Med *357*, 39-51.

Innocente, S. A., Abrahamson, J. L., Cogswell, J. P., and Lee, J. M. (1999). p53 regulates a G2 checkpoint through cyclin B1. Proc Natl Acad Sci U S A *96*, 2147-2152.

Iwata, A., Riley, B. E., Johnston, J. A., and Kopito, R. R. (2005). HDAC6 and microtubules are required for autophagic degradation of aggregated huntingtin. J Biol Chem *280*, 40282-40292.

Iwata, J., Ezaki, J., Komatsu, M., Yokota, S., Ueno, T., Tanida, I., Chiba, T., Tanaka, K., and Kominami, E. (2006). Excess peroxisomes are degraded by autophagic machinery in mammals. J Biol Chem *281*, 4035-4041.

Jeffrey, P. D., Russo, A. A., Polyak, K., Gibbs, E., Hurwitz, J., Massague, J., and Pavletich, N. P. (1995). Mechanism of CDK activation revealed by the structure of a cyclinA-CDK2 complex. Nature *376*, 313-320.

Jeon, S., Choi, J. Y., Lee, K. M., Park, S. K., Yoo, K. Y., Noh, D. Y., Ahn, S. H., and Kang, D. (2010). Combined genetic effect of CDK7 and ESR1 polymorphisms on breast cancer. Breast Cancer Res Treat *121*, 737-742.

Jin, J., Cardozo, T., Lovering, R. C., Elledge, S. J., Pagano, M., and Harper, J. W. (2004). Systematic analysis and nomenclature of mammalian F-box proteins. Genes Dev *18*, 2573-2580.

Jin, S., and Levine, A. J. (2001). The p53 functional circuit. J Cell Sci *114*, 4139-4140.

Johansen, T., and Lamark, T. (2011). Selective autophagy mediated by autophagic adapter proteins. Autophagy *7*, 279-296.

Johnson, D. G., and Walker, C. L. (1999). Cyclins and cell cycle checkpoints. Annu Rev Pharmacol Toxicol *39*, 295-312.

Johnston, J. A., Dalton, M. J., Gurney, M. E., and Kopito, R. R. (2000). Formation of high molecular weight complexes of mutant Cu, Zn-superoxide dismutase in a mouse model for familial amyotrophic lateral sclerosis. Proc Natl Acad Sci U S A *97*, 12571-12576.

Johnston, J. A., Illing, M. E., and Kopito, R. R. (2002). Cytoplasmic dynein/dynactin mediates the assembly of aggresomes. Cell Motil Cytoskeleton *53*, 26-38.

Jorgensen, P., Nishikawa, J. L., Breitkreutz, B. J., and Tyers, M. (2002). Systematic identification of pathways that couple cell growth and division in yeast. Science *297*, 395-400.

Kajitani, K., Wafa, K., Pasumarthi, K. B., and Robertson, G. S. (2010). Developmental expression of the cyclin D2 splice variant in postnatal Purkinje cells of the mouse cerebellum. Neurosci Lett *477*, 100-104.

Kaldis, P. (1999). The cdk-activating kinase (CAK): from yeast to mammals. Cell Mol Life Sci *55*, 284-296.

Karnoub, A. E., and Weinberg, R. A. (2008). Ras oncogenes: split personalities. Nat Rev Mol Cell Biol *9*, 517-531.

Kato, A., Takahashi, H., Takahashi, Y., and Matsushime, H. (1997). Contact inhibition-induced inactivation of the cyclin D-dependent kinase in rat fibroblast cell line, 3Y1. Leukemia *11 Suppl 3*, 361-362.

Kato, J. Y., Matsuoka, M., Strom, D. K., and Sherr, C. J. (1994). Regulation of cyclin D-dependent kinase 4 (cdk4) by cdk4-activating kinase. Mol Cell Biol *14*, 2713-2721.

Kawaguchi, Y., Kovacs, J. J., McLaurin, A., Vance, J. M., Ito, A., and Yao, T. P. (2003). The deacetylase HDAC6 regulates aggresome formation and cell viability in response to misfolded protein stress. Cell *115*, 727-738.

Kehn, K., Berro, R., Alhaj, A., Bottazzi, M. E., Yeh, W. I., Klase, Z., Van Duyne, R., Fu, S., and Kashanchi, F. (2007). Functional consequences of cyclin D1/BRCA1 interaction in breast cancer cells. Oncogene *26*, 5060-5069.

Kelly, T. J., and Brown, G. W. (2000). Regulation of chromosome replication. Annu Rev Biochem *69*, 829-880.

Kesavapany, S., Li, B. S., Amin, N., Zheng, Y. L., Grant, P., and Pant, H. C. (2004). Neuronal cyclin-dependent kinase 5: role in nervous system function and its specific inhibition by the Cdk5 inhibitory peptide. Biochim Biophys Acta *1697*, 143-153.

Kida, A., Kakihana, K., Kotani, S., Kurosu, T., and Miura, O. (2007). Glycogen synthase kinase-3beta and p38 phosphorylate cyclin D2 on Thr280 to trigger its ubiquitin/proteasome-dependent degradation in hematopoietic cells. Oncogene *26*, 6630-6640.

Kim, W. Y., and Sharpless, N. E. (2006). The regulation of INK4/ARF in cancer and aging. Cell *127*, 265-275.

Kirkin, V., Lamark, T., Sou, Y. S., Bjorkoy, G., Nunn, J. L., Bruun, J. A., Shvets, E., McEwan, D. G., Clausen, T. H., Wild, P.*, et al.* (2009a). A role for NBR1 in autophagosomal degradation of ubiquitinated substrates. Mol Cell *33*, 505-516.

Kirkin, V., McEwan, D. G., Novak, I., and Dikic, I. (2009b). A role for ubiquitin in selective autophagy. Mol Cell *34*, 259-269.

Kirsten, W. H., and Mayer, L. A. (1967). Morphologic responses to a murine erythroblastosis virus. J Natl Cancer Inst *39*, 311-335.

Klionsky, D. J. (2010). The autophagy connection. Dev Cell *19*, 11-12.

Knudsen, K. E. (2006). The cyclin D1b splice variant: an old oncogene learns new tricks. Cell Div *1*, 15.

Knudson, A. G., Jr. (1971). Mutation and cancer: statistical study of retinoblastoma. Proc Natl Acad Sci U S A *68*, 820-823.

Koff, A., Ohtsuki, M., Polyak, K., Roberts, J. M., and Massague, J. (1993). Negative regulation of G1 in mammalian cells: inhibition of cyclin E-dependent kinase by TGF-beta. Science *260*, 536-539.

Koh, J., Enders, G. H., Dynlacht, B. D., and Harlow, E. (1995). Tumour-derived p16 alleles encoding proteins defective in cell-cycle inhibition. Nature *375*, 506-510.

Komatsu, M., and Ichimura, Y. (2010a). Physiological significance of selective degradation of p62 by autophagy. FEBS Lett *584*, 1374-1378.

Komatsu, M., and Ichimura, Y. (2010b). Selective autophagy regulates various cellular functions. Genes Cells *15*, 923-933.

Komatsu, M., Waguri, S., Koike, M., Sou, Y. S., Ueno, T., Hara, T., Mizushima, N., Iwata, J., Ezaki, J., Murata, S.*, et al.* (2007). Homeostatic levels of p62 control cytoplasmic inclusion body formation in autophagy-deficient mice. Cell *131*, 1149-1163.

Kopito, R. R. (2000). Aggresomes, inclusion bodies and protein aggregation. Trends Cell Biol *10*, 524-530.

Kowalczyk, A., Filipkowski, R. K., Rylski, M., Wilczynski, G. M., Konopacki, F. A., Jaworski, J., Ciemerych, M. A., Sicinski, P., and Kaczmarek, L. (2004). The critical role of cyclin D2 in adult neurogenesis. J Cell Biol *167*, 209-213.

Kozar, K., Ciemerych, M. A., Rebel, V. I., Shigematsu, H., Zagozdzon, A., Sicinska, E., Geng, Y., Yu, Q., Bhattacharya, S., Bronson, R. T.*, et al.* (2004). Mouse development and cell proliferation in the absence of D-cyclins. Cell *118*, 477-491.

Kraft, C., Deplazes, A., Sohrmann, M., and Peter, M. (2008). Mature ribosomes are selectively degraded upon starvation by an autophagy pathway requiring the Ubp3p/Bre5p ubiquitin protease. Nat Cell Biol *10*, 602-610.

Krek, W., and Nigg, E. A. (1991). Differential phosphorylation of vertebrate p34cdc2 kinase at the G1/S and G2/M transitions of the cell cycle: identification of major phosphorylation sites. Embo J *10*, 305-316.

Kulkarni, R. N. (2004). The islet beta-cell. Int J Biochem Cell Biol *36*, 365-371.

Kusume, T., Tsuda, H., Kawabata, M., Inoue, T., Umesaki, N., Suzuki, T., and Yamamoto, K. (1999). The p16-cyclin D1/CDK4-pRb pathway and clinical outcome in epithelial ovarian cancer. Clin Cancer Res *5*, 4152-4157.

Kuusisto, E., Salminen, A., and Alafuzoff, I. (2001). Ubiquitin-binding protein p62 is present in neuronal and glial inclusions in human tauopathies and synucleinopathies. Neuroreport *12*, 2085-2090.

Kwak, Y. T., Li, R., Becerra, C. R., Tripathy, D., Frenkel, E. P., and Verma, U. N. (2005). IkappaB kinase alpha regulates subcellular distribution and turnover of cyclin D1 by phosphorylation. J Biol Chem *280*, 33945-33952.

LaBaer, J., Garrett, M. D., Stevenson, L. F., Slingerland, J. M., Sandhu, C., Chou, H. S., Fattaey, A., and Harlow, E. (1997). New functional activities for the p21 family of CDK inhibitors. Genes Dev *11*, 847-862.

Ladner, R. C., Sato, A. K., Gorzelany, J., and de Souza, M. (2004). Phage display-derived peptides as therapeutic alternatives to antibodies. Drug Discov Today *9*, 525-529.

Lamark, T., Perander, M., Outzen, H., Kristiansen, K., Overvatn, A., Michaelsen, E., Bjorkoy, G., and Johansen, T. (2003). Interaction codes within the family of mammalian Phox and Bem1p domain-containing proteins. J Biol Chem *278*, 34568-34581.

Land, H., Parada, L. F., and Weinberg, R. A. (1983). Tumorigenic conversion of primary embryo fibroblasts requires at least two cooperating oncogenes. Nature *304*, 596-602.

Larminie, C. G., Cairns, C. A., Mital, R., Martin, K., Kouzarides, T., Jackson, S. P., and White, R. J. (1997). Mechanistic analysis of RNA polymerase III regulation by the retinoblastoma protein. Embo J *16*, 2061-2071.

Lazaro, J. B., Bailey, P. J., and Lassar, A. B. (2002). Cyclin D-cdk4 activity modulates the subnuclear localization and interaction of MEF2 with SRC-family coactivators during skeletal muscle differentiation. Genes Dev *16*, 1792-1805.

Lee, M. H., Reynisdottir, I., and Massague, J. (1995). Cloning of p57KIP2, a cyclin-dependent kinase inhibitor with unique domain structure and tissue distribution. Genes Dev *9*, 639-649.

Lehner, C. F., and O'Farrell, P. H. (1989). Expression and function of Drosophila cyclin A during embryonic cell cycle progression. Cell *56*, 957-968.

Leidal, A. M., Cyr, D. P., Hill, R. J., Lee, P. W., and McCormick, C. (2012). Subversion of Autophagy by Kaposi's Sarcoma-Associated Herpesvirus Impairs Oncogene-Induced Senescence. Cell Host Microbe *11*, 167-180.

Levine, B., and Kroemer, G. (2009). Autophagy in aging, disease and death: the true identity of a cell death impostor. Cell Death Differ *16*, 1-2.

Li, W., Sanki, A., Karim, R. Z., Thompson, J. F., Soon Lee, C., Zhuang, L., McCarthy, S. W., and Scolyer, R. A. (2006a). The role of cell cycle regulatory proteins in the pathogenesis of melanoma. Pathology *38*, 287-301.

Li, Y., Dowbenko, D., and Lasky, L. A. (2002). AKT/PKB phosphorylation of p21Cip/WAF1 enhances protein stability of p21Cip/WAF1 and promotes cell survival. J Biol Chem *277*, 11352-11361.

Li, Z., Jiao, X., Wang, C., Ju, X., Lu, Y., Yuan, L., Lisanti, M. P., Katiyar, S., and Pestell, R. G. (2006b). Cyclin D1 induction of cellular migration requires p27(KIP1). Cancer Res *66*, 9986-9994.

Li, Z., Wang, C., Jiao, X., Lu, Y., Fu, M., Quong, A. A., Dye, C., Yang, J., Dai, M., Ju, X.*, et al.* (2006c). Cyclin D1 regulates cellular migration through the inhibition of thrombospondin 1 and ROCK signaling. Mol Cell Biol *26*, 4240-4256.

Liang, Y., Lin, S. Y., Brunicardi, F. C., Goss, J., and Li, K. (2009). DNA damage response pathways in tumor suppression and cancer treatment. World J Surg *33*, 661-666.

Liebermann, D. A., and Hoffman, B. (2007). Gadd45 in the response of hematopoietic cells to genotoxic stress. Blood Cells Mol Dis *39*, 329-335.

Lin, D. I., Barbash, O., Kumar, K. G., Weber, J. D., Harper, J. W., Klein-Szanto, A. J., Rustgi, A., Fuchs, S. Y., and Diehl, J. A. (2006). Phosphorylation-dependent ubiquitination of cyclin D1 by the SCF(FBX4-alphaB crystallin) complex. Mol Cell *24*, 355-366.

Lindqvist, A., Rodriguez-Bravo, V., and Medema, R. H. (2009). The decision to enter mitosis: feedback and redundancy in the mitotic entry network. J Cell Biol *185*, 193-202.

Liu, J. J., Chao, J. R., Jiang, M. C., Ng, S. Y., Yen, J. J., and Yang-Yen, H. F. (1995). Ras transformation results in an elevated level of cyclin D1 and acceleration of G1 progression in NIH 3T3 cells. Mol Cell Biol *15*, 3654-3663.

Livak, K. J., and Schmittgen, T. D. (2001). Analysis of relative gene expression data using real-time quantitative PCR and the 2(-Delta Delta C(T)) Method. Methods *25*, 402-408.

Lolli, G., and Johnson, L. N. (2005). CAK-Cyclin-dependent Activating Kinase: a key kinase in cell cycle control and a target for drugs? Cell Cycle *4*, 572-577.

Lolli, G., Lowe, E. D., Brown, N. R., and Johnson, L. N. (2004). The crystal structure of human CDK7 and its protein recognition properties. Structure *12*, 2067-2079.

Long, J., Gallagher, T. R., Cavey, J. R., Sheppard, P. W., Ralston, S. H., Layfield, R., and Searle, M. S. (2008). Ubiquitin recognition by the ubiquitin-associated domain of p62 involves a novel conformational switch. J Biol Chem *283*, 5427-5440.

Long, X., Ortiz-Vega, S., Lin, Y., and Avruch, J. (2005). Rheb binding to mammalian target of rapamycin (mTOR) is regulated by amino acid sufficiency. J Biol Chem *280*, 23433-23436.

Lopez-Lazaro, M. (2009). Digoxin, HIF-1, and cancer. Proc Natl Acad Sci U S A *106*, E26; author reply E27.

Loyer, P., Trembley, J. H., Grenet, J. A., Busson, A., Corlu, A., Zhao, W., Kocak, M., Kidd, V. J., and Lahti, J. M. (2008). Characterization of cyclin L1 and L2 interactions with CDK11 and splicing factors: influence of cyclin L isoforms on splice site selection. J Biol Chem *283*, 7721-7732.

Lozano, J. C., Schatt, P., Marques, F., Peaucellier, G., Fort, P., Feral, J. P., Geneviere, A. M., and Picard, A. (1998). A presumptive developmental role for a sea urchin cyclin B splice variant. J Cell Biol *140*, 283-293.

Lu, L., Ladinsky, M. S., and Kirchhausen, T. (2009). Cisternal organization of the endoplasmic reticulum during mitosis. Mol Biol Cell *20*, 3471-3480.

Lukas, J., Herzinger, T., Hansen, K., Moroni, M. C., Resnitzky, D., Helin, K., Reed, S. I., and Bartek, J. (1997). Cyclin E-induced S phase without activation of the pRb/E2F pathway. Genes Dev *11*, 1479-1492.

Ma, Y., Feng, Q., Sekula, D., Diehl, J. A., Freemantle, S. J., and Dmitrovsky, E. (2005). Retinoid targeting of different D-type cyclins through distinct chemopreventive mechanisms. Cancer Res *65*, 6476-6483.

Malumbres, M., and Barbacid, M. (2001). To cycle or not to cycle: a critical decision in cancer. Nat Rev Cancer *1*, 222-231.

Malumbres, M., and Barbacid, M. (2005). Mammalian cyclin-dependent kinases. Trends Biochem Sci *30*, 630-641.

Malumbres, M., and Barbacid, M. (2009). Cell cycle, CDKs and cancer: a changing paradigm. Nat Rev Cancer *9*, 153-166.

Malumbres, M., Sotillo, R., Santamaria, D., Galan, J., Cerezo, A., Ortega, S., Dubus, P., and Barbacid, M. (2004). Mammalian cells cycle without the D-type cyclin-dependent kinases Cdk4 and Cdk6. Cell *118*, 493-504.

Matsubayashi, H., Sato, N., Fukushima, N., Yeo, C. J., Walter, K. M., Brune, K., Sahin, F., Hruban, R. H., and Goggins, M. (2003). Methylation of cyclin D2 is observed frequently in pancreatic cancer but is also an age-related phenomenon in gastrointestinal tissues. Clin Cancer Res *9*, 1446-1452.

Matsuoka, S., Edwards, M. C., Bai, C., Parker, S., Zhang, P., Baldini, A., Harper, J. W., and Elledge, S. J. (1995). p57KIP2, a structurally distinct member of the p21CIP1 Cdk inhibitor family, is a candidate tumor suppressor gene. Genes Dev *9*, 650-662.

Matsuoka, S., Yamaguchi, M., and Matsukage, A. (1994). D-type cyclin-binding regions of proliferating cell nuclear antigen. J Biol Chem *269*, 11030-11036.

Matsuura, I., Denissova, N. G., Wang, G., He, D., Long, J., and Liu, F. (2004). Cyclin-dependent kinases regulate the antiproliferative function of Smads. Nature *430*, 226-231.

McGrath, J. P., Capon, D. J., Goeddel, D. V., and Levinson, A. D. (1984). Comparative biochemical properties of normal and activated human ras p21 protein. Nature *310*, 644-649.

McKay, J. A., Douglas, J. J., Ross, V. G., Curran, S., Murray, G. I., Cassidy, J., and McLeod, H. L. (2000). Cyclin D1 protein expression and gene polymorphism in colorectal cancer. Aberdeen Colorectal Initiative. Int J Cancer *88*, 77-81.

McMullen, N. M., Zhang, F., Hotchkiss, A., Bretzner, F., Wilson, J. M., Ma, H., Wafa, K., Brownstone, R. M., and Pasumarthi, K. B. (2009). Functional characterization of

cardiac progenitor cells and their derivatives in the embryonic heart post-chamber formation. Dev Dyn *238*, 2787-2799.

Medema, R. H., Herrera, R. E., Lam, F., and Weinberg, R. A. (1995). Growth suppression by p16ink4 requires functional retinoblastoma protein. Proc Natl Acad Sci U S A *92*, 6289-6293.

Meyyappan, M., Wong, H., Hull, C., and Riabowol, K. T. (1998). Increased expression of cyclin D2 during multiple states of growth arrest in primary and established cells. Mol Cell Biol *18*, 3163-3172.

Mitchell, K. O., and El-Deiry, W. S. (1999). Overexpression of c-Myc inhibits p21WAF1/CIP1 expression and induces S-phase entry in 12-O-tetradecanoylphorbol-13-acetate (TPA)-sensitive human cancer cells. Cell Growth Differ *10*, 223-230.

Mizushima, N., Levine, B., Cuervo, A. M., and Klionsky, D. J. (2008). Autophagy fights disease through cellular self-digestion. Nature *451*, 1069-1075.

Mohney, R. P., Das, M., Bivona, T. G., Hanes, R., Adams, A. G., Philips, M. R., and O'Bryan, J. P. (2003). Intersectin activates Ras but stimulates transcription through an independent pathway involving JNK. J Biol Chem *278*, 47038-47045.

Moldovan, G. L., Pfander, B., and Jentsch, S. (2007). PCNA, the maestro of the replication fork. Cell *129*, 665-679.

Moons, D. S., Jirawatnotai, S., Parlow, A. F., Gibori, G., Kineman, R. D., and Kiyokawa, H. (2002). Pituitary hypoplasia and lactotroph dysfunction in mice deficient for cyclin-dependent kinase-4. Endocrinology *143*, 3001-3008.

Moreno-Bueno, G., Rodriguez-Perales, S., Sanchez-Estevez, C., Marcos, R., Hardisson, D., Cigudosa, J. C., and Palacios, J. (2004). Molecular alterations associated with cyclin D1 overexpression in endometrial cancer. Int J Cancer *110*, 194-200.

Morgan, D. O. (1995). Principles of CDK regulation. Nature *374*, 131-134.

Morgan, D. O., and De Bondt, H. L. (1994). Protein kinase regulation: insights from crystal structure analysis. Curr Opin Cell Biol *6*, 239-246.

Moscat, J., and Diaz-Meco, M. T. (2009). p62 at the crossroads of autophagy, apoptosis, and cancer. Cell *137*, 1001-1004.

Moumtzi, S. S., Roberts, M. L., Joyce, T., Evangelidou, M., Probert, L., Frillingos, S., Fotsis, T., and Pintzas, A. (2010). Gene expression profile associated with oncogenic ras-

induced senescence, cell death, and transforming properties in human cells. Cancer Invest *28*, 563-587.

Musacchio, A., and Salmon, E. D. (2007). The spindle-assembly checkpoint in space and time. Nat Rev Mol Cell Biol *8*, 379-393.

Musgrove, E. A., Caldon, C. E., Barraclough, J., Stone, A., and Sutherland, R. L. (2011). Cyclin D as a therapeutic target in cancer. Nat Rev Cancer *11*, 558-572.

Nakajima, K., Inagawa, M., Uchida, C., Okada, K., Tane, S., Kojima, M., Kubota, M., Noda, M., Ogawa, S., Shirato, H.*, et al.* (2011). Coordinated regulation of differentiation and proliferation of embryonic cardiomyocytes by a jumonji (Jarid2)-cyclin D1 pathway. Development *138*, 1771-1782.

Nakayama, K. I., and Nakayama, K. (2005). Regulation of the cell cycle by SCF-type ubiquitin ligases. Semin Cell Dev Biol *16*, 323-333.

Nakayama, K. I., and Nakayama, K. (2006). Ubiquitin ligases: cell-cycle control and cancer. Nat Rev Cancer *6*, 369-381.

Narendra, D., Tanaka, A., Suen, D. F., and Youle, R. J. (2008). Parkin is recruited selectively to impaired mitochondria and promotes their autophagy. J Cell Biol *183*, 795-803.

Neumeister, P., Pixley, F. J., Xiong, Y., Xie, H., Wu, K., Ashton, A., Cammer, M., Chan, A., Symons, M., Stanley, E. R., and Pestell, R. G. (2003). Cyclin D1 governs adhesion and motility of macrophages. Mol Biol Cell *14*, 2005-2015.

Newbold, R. F., and Overell, R. W. (1983). Fibroblast immortality is a prerequisite for transformation by EJ c-Ha-ras oncogene. Nature *304*, 648-651.

Niida, H., and Nakanishi, M. (2006). DNA damage checkpoints in mammals. Mutagenesis *21*, 3-9.

Nishitani, H., and Lygerou, Z. (2002). Control of DNA replication licensing in a cell cycle. Genes Cells *7*, 523-534.

Niwa, M., and Walter, P. (2000). Pausing to decide. Proc Natl Acad Sci U S A *97*, 12396-12397.

Noda, A., Ning, Y., Venable, S. F., Pereira-Smith, O. M., and Smith, J. R. (1994). Cloning of senescent cell-derived inhibitors of DNA synthesis using an expression screen. Exp Cell Res *211*, 90-98.

Novak, I., Kirkin, V., McEwan, D. G., Zhang, J., Wild, P., Rozenknop, A., Rogov, V., Lohr, F., Popovic, D., Occhipinti, A.*, et al.* (2010). Nix is a selective autophagy receptor for mitochondrial clearance. EMBO Rep *11*, 45-51.

O'Connor, C. (2008). Cell Division: Stages of Mitosis. Nature Education *1*.

Ohsumi, Y. (2001). Molecular dissection of autophagy: two ubiquitin-like systems. Nat Rev Mol Cell Biol *2*, 211-216.

Okabe, H., Lee, S. H., Phuchareon, J., Albertson, D. G., McCormick, F., and Tetsu, O. (2006). A critical role for FBXW8 and MAPK in cyclin D1 degradation and cancer cell proliferation. PLoS One *1*, e128.

Okamoto, K., Kondo-Okamoto, N., and Ohsumi, Y. (2009). Mitochondria-anchored receptor Atg32 mediates degradation of mitochondria via selective autophagy. Dev Cell *17*, 87-97.

Ortega, S., Prieto, I., Odajima, J., Martin, A., Dubus, P., Sotillo, R., Barbero, J. L., Malumbres, M., and Barbacid, M. (2003). Cyclin-dependent kinase 2 is essential for meiosis but not for mitotic cell division in mice. Nat Genet *35*, 25-31.

Padar, A., Sathyanarayana, U. G., Suzuki, M., Maruyama, R., Hsieh, J. T., Frenkel, E. P., Minna, J. D., and Gazdar, A. F. (2003). Inactivation of cyclin D2 gene in prostate cancers by aberrant promoter methylation. Clin Cancer Res *9*, 4730-4734.

Pagano, M., Theodoras, A. M., Tam, S. W., and Draetta, G. F. (1994). Cyclin D1-mediated inhibition of repair and replicative DNA synthesis in human fibroblasts. Genes Dev *8*, 1627-1639.

Paine-Murrieta, G. D., Taylor, C. W., Curtis, R. A., Lopez, M. H., Dorr, R. T., Johnson, C. S., Funk, C. Y., Thompson, F., and Hersh, E. M. (1997). Human tumor models in the severe combined immune deficient (scid) mouse. Cancer Chemother Pharmacol *40*, 209-214.

Pan, Z. Q., Reardon, J. T., Li, L., Flores-Rozas, H., Legerski, R., Sancar, A., and Hurwitz, J. (1995). Inhibition of nucleotide excision repair by the cyclin-dependent kinase inhibitor p21. J Biol Chem *270*, 22008-22016.

Pankiv, S., Clausen, T. H., Lamark, T., Brech, A., Bruun, J. A., Outzen, H., Overvatn, A., Bjorkoy, G., and Johansen, T. (2007). p62/SQSTM1 binds directly to Atg8/LC3 to facilitate degradation of ubiquitinated protein aggregates by autophagy. J Biol Chem *282*, 24131-24145.

Parada, L. F., Tabin, C. J., Shih, C., and Weinberg, R. A. (1982). Human EJ bladder carcinoma oncogene is homologue of Harvey sarcoma virus ras gene. Nature *297*, 474-478.

Parker, L. L., and Piwnica-Worms, H. (1992). Inactivation of the p34cdc2-cyclin B complex by the human WEE1 tyrosine kinase. Science *257*, 1955-1957.

Pasumarthi, K. B., Nakajima, H., Nakajima, H. O., Soonpaa, M. H., and Field, L. J. (2005). Targeted expression of cyclin D2 results in cardiomyocyte DNA synthesis and infarct regression in transgenic mice. Circ Res *96*, 110-118.

Pateras, I. S., Apostolopoulou, K., Niforou, K., Kotsinas, A., and Gorgoulis, V. G. (2009). p57KIP2: "Kip"ing the cell under control. Mol Cancer Res *7*, 1902-1919.

Perez-Roger, I., Kim, S. H., Griffiths, B., Sewing, A., and Land, H. (1999). Cyclins D1 and D2 mediate myc-induced proliferation via sequestration of p27(Kip1) and p21(Cip1). Embo J *18*, 5310-5320.

Pickart, C. M. (2001). Mechanisms underlying ubiquitination. Annu Rev Biochem *70*, 503-533.

Pines, J. (2011). Cubism and the cell cycle: the many faces of the APC/C. Nat Rev Mol Cell Biol *12*, 427-438.

Polyak, K., Kato, J. Y., Solomon, M. J., Sherr, C. J., Massague, J., Roberts, J. M., and Koff, A. (1994a). p27Kip1, a cyclin-Cdk inhibitor, links transforming growth factor-beta and contact inhibition to cell cycle arrest. Genes Dev *8*, 9-22.

Polyak, K., Lee, M. H., Erdjument-Bromage, H., Koff, A., Roberts, J. M., Tempst, P., and Massague, J. (1994b). Cloning of p27Kip1, a cyclin-dependent kinase inhibitor and a potential mediator of extracellular antimitogenic signals. Cell *78*, 59-66.

Poomsawat, S., Buajeeb, W., Khovidhunkit, S. O., and Punyasingh, J. (2010). Alteration in the expression of cdk4 and cdk6 proteins in oral cancer and premalignant lesions. J Oral Pathol Med *39*, 793-799.

Poon, R. Y., and Hunter, T. (1995). Dephosphorylation of Cdk2 Thr160 by the cyclin-dependent kinase-interacting phosphatase KAP in the absence of cyclin. Science *270*, 90-93.

Poon, R. Y., Yamashita, K., Adamczewski, J. P., Hunt, T., and Shuttleworth, J. (1993). The cdc2-related protein p40MO15 is the catalytic subunit of a protein kinase that can activate p33cdk2 and p34cdc2. Embo J *12*, 3123-3132.

Potapova, T. A., Sivakumar, S., Flynn, J. N., Li, R., and Gorbsky, G. J. (2011). Mitotic progression becomes irreversible in prometaphase and collapses when Wee1 and Cdc25 are inhibited. Mol Biol Cell *22*, 1191-1206.

Praefcke, G. J., and McMahon, H. T. (2004). The dynamin superfamily: universal membrane tubulation and fission molecules? Nat Rev Mol Cell Biol *5*, 133-147.

Prochownik, E. V. (2008). c-Myc: linking transformation and genomic instability. Curr Mol Med *8*, 446-458.

Pulciani, S., Santos, E., Lauver, A. V., Long, L. K., Robbins, K. C., and Barbacid, M. (1982). Oncogenes in human tumor cell lines: molecular cloning of a transforming gene from human bladder carcinoma cells. Proc Natl Acad Sci U S A *79*, 2845-2849.

Pyronnet, S., and Sonenberg, N. (2001). Cell-cycle-dependent translational control. Curr Opin Genet Dev *11*, 13-18.

Rane, S. G., Dubus, P., Mettus, R. V., Galbreath, E. J., Boden, G., Reddy, E. P., and Barbacid, M. (1999). Loss of Cdk4 expression causes insulin-deficient diabetes and Cdk4 activation results in beta-islet cell hyperplasia. Nat Genet *22*, 44-52.

Rappold, I., Iwabuchi, K., Date, T., and Chen, J. (2001). Tumor suppressor p53 binding protein 1 (53BP1) is involved in DNA damage-signaling pathways. J Cell Biol *153*, 613-620.

Raught, B., and Gingras, A.C. (2007). Signaling to translation initiation (NY, CSHL Press, Cold Spring Harbor).

Razi, M., Chan, E. Y., and Tooze, S. A. (2009). Early endosomes and endosomal coatomer are required for autophagy. J Cell Biol *185*, 305-321.

Reddy, E. P., Reynolds, R. K., Santos, E., and Barbacid, M. (1982). A point mutation is responsible for the acquisition of transforming properties by the T24 human bladder carcinoma oncogene. Nature *300*, 149-152.

Ren, J., Wang, Y., Liang, Y., Zhang, Y., Bao, S., and Xu, Z. (2010). Methylation of ribosomal protein S10 by protein-arginine methyltransferase 5 regulates ribosome biogenesis. J Biol Chem *285*, 12695-12705.

Ren, S., and Rollins, B. J. (2004). Cyclin C/cdk3 promotes Rb-dependent G0 exit. Cell *117*, 239-251.

Reynaud, E. G., Guillier, M., Leibovitch, M. P., and Leibovitch, S. A. (2000). Dimerization of the amino terminal domain of p57Kip2 inhibits cyclin D1-cdk4 kinase activity. Oncogene *19*, 1147-1152.

Richardson, H. E., Wittenberg, C., Cross, F., and Reed, S. I. (1989). An essential G1 function for cyclin-like proteins in yeast. Cell *59*, 1127-1133.

Rizzolio, F., Tuccinardi, T., Caligiuri, I., Lucchetti, C., and Giordano, A. (2010). CDK inhibitors: from the bench to clinical trials. Curr Drug Targets *11*, 279-290.

Roberti, A., Macaluso, M. and Giordano, A. (2009). Alterations in Cell Cycle Regulatory Genes in Breast Cancer. In Current Clinical Oncology: Breast Cancer in the Post-Genomic Era, A. a. N. Giordano, N., ed. (Humana Press).

Rodriguez-Viciana, P., Tetsu, O., Oda, K., Okada, J., Rauen, K., and McCormick, F. (2005). Cancer targets in the Ras pathway. Cold Spring Harb Symp Quant Biol *70*, 461-467.

Rogers, S., Wells, R., and Rechsteiner, M. (1986). Amino acid sequences common to rapidly degraded proteins: the PEST hypothesis. Science *234*, 364-368.

Rosenwald, I. B., Rhoads, D. B., Callanan, L. D., Isselbacher, K. J., and Schmidt, E. V. (1993). Increased expression of eukaryotic translation initiation factors eIF-4E and eIF-2 alpha in response to growth induction by c-myc. Proc Natl Acad Sci U S A *90*, 6175-6178.

Rossig, L., Jadidi, A. S., Urbich, C., Badorff, C., Zeiher, A. M., and Dimmeler, S. (2001). Akt-dependent phosphorylation of p21(Cip1) regulates PCNA binding and proliferation of endothelial cells. Mol Cell Biol *21*, 5644-5657.

Roy, A., Kucukural, A., and Zhang, Y. (2010). I-TASSER: a unified platform for automated protein structure and function prediction. Nat Protoc *5*, 725-738.

Rubinsztein, D. C. (2006). The roles of intracellular protein-degradation pathways in neurodegeneration. Nature *443*, 780-786.

Ruley, H. E. (1983). Adenovirus early region 1A enables viral and cellular transforming genes to transform primary cells in culture. Nature *304*, 602-606.

Russo, A. A., Jeffrey, P. D., and Pavletich, N. P. (1996). Structural basis of cyclin-dependent kinase activation by phosphorylation. Nat Struct Biol *3*, 696-700.

Rusten, T. E., and Stenmark, H. (2010). p62, an autophagy hero or culprit? Nat Cell Biol *12*, 207-209.

Sanchez, Y., Wong, C., Thoma, R. S., Richman, R., Wu, Z., Piwnica-Worms, H., and Elledge, S. J. (1997). Conservation of the Chk1 checkpoint pathway in mammals: linkage of DNA damage to Cdk regulation through Cdc25. Science *277*, 1497-1501.

Santamaria, D., Barriere, C., Cerqueira, A., Hunt, S., Tardy, C., Newton, K., Caceres, J. F., Dubus, P., Malumbres, M., and Barbacid, M. (2007). Cdk1 is sufficient to drive the mammalian cell cycle. Nature *448*, 811-815.

Santarius, T., Shipley, J., Brewer, D., Stratton, M. R., and Cooper, C. S. (2010). A census of amplified and overexpressed human cancer genes. Nat Rev Cancer *10*, 59-64.

Santos, E., Tronick, S. R., Aaronson, S. A., Pulciani, S., and Barbacid, M. (1982). T24 human bladder carcinoma oncogene is an activated form of the normal human homologue of BALB- and Harvey-MSV transforming genes. Nature *298*, 343-347.

Satyanarayana, A., and Kaldis, P. (2009). Mammalian cell-cycle regulation: several Cdks, numerous cyclins and diverse compensatory mechanisms. Oncogene *28*, 2925-2939.

Schultz, L. B., Chehab, N. H., Malikzay, A., and Halazonetis, T. D. (2000). p53 binding protein 1 (53BP1) is an early participant in the cellular response to DNA double-strand breaks. J Cell Biol *151*, 1381-1390.

Scolnick, E. M., Papageorge, A. G., and Shih, T. Y. (1979). Guanine nucleotide-binding activity as an assay for src protein of rat-derived murine sarcoma viruses. Proc Natl Acad Sci U S A *76*, 5355-5359.

Scott, M. T., Morrice, N., and Ball, K. L. (2000). Reversible phosphorylation at the C-terminal regulatory domain of p21(Waf1/Cip1) modulates proliferating cell nuclear antigen binding. J Biol Chem *275*, 11529-11537.

Scott, P. H., Cairns, C. A., Sutcliffe, J. E., Alzuherri, H. M., McLees, A., Winter, A. G., and White, R. J. (2001). Regulation of RNA polymerase III transcription during cell cycle entry. J Biol Chem *276*, 1005-1014.

Semczuk, A., Miturski, R., Skomra, D., and Jakowicki, J. A. (2004). Expression of the cell-cycle regulatory proteins (pRb, cyclin D1, p16INK4A and cdk4) in human endometrial cancer: correlation with clinicopathological features. Arch Gynecol Obstet *269*, 104-110.

Serrano, M., Lin, A. W., McCurrach, M. E., Beach, D., and Lowe, S. W. (1997). Oncogenic ras provokes premature cell senescence associated with accumulation of p53 and p16INK4a. Cell *88*, 593-602.

Sheaff, R. J. (1997). Regulation of mammalian cyclin-dependent kinase 2. Methods Enzymol *283*, 173-193.

Sherr, C. J., and Roberts, J. M. (1995). Inhibitors of mammalian G1 cyclin-dependent kinases. Genes Dev *9*, 1149-1163.

Shih, C., Padhy, L. C., Murray, M., and Weinberg, R. A. (1981). Transforming genes of carcinomas and neuroblastomas introduced into mouse fibroblasts. Nature *290*, 261-264.

Shih, C., and Weinberg, R. A. (1982). Isolation of a transforming sequence from a human bladder carcinoma cell line. Cell *29*, 161-169.

Shih, T. Y., Papageorge, A. G., Stokes, P. E., Weeks, M. O., and Scolnick, E. M. (1980). Guanine nucleotide-binding and autophosphorylating activities associated with the p21src protein of Harvey murine sarcoma virus. Nature *287*, 686-691.

Shimizu, K., Goldfarb, M., Perucho, M., and Wigler, M. (1983). Isolation and preliminary characterization of the transforming gene of a human neuroblastoma cell line. Proc Natl Acad Sci U S A *80*, 383-387.

Shin, J. S., Hong, S. W., Lee, S. L., Kim, T. H., Park, I. C., An, S. K., Lee, W. K., Lim, J. S., Kim, K. I., Yang, Y.*, et al.* (2008). Serum starvation induces G1 arrest through suppression of Skp2-CDK2 and CDK4 in SK-OV-3 cells. Int J Oncol *32*, 435-439.

Sicinska, E., Aifantis, I., Le Cam, L., Swat, W., Borowski, C., Yu, Q., Ferrando, A. A., Levin, S. D., Geng, Y., von Boehmer, H., and Sicinski, P. (2003). Requirement for cyclin D3 in lymphocyte development and T cell leukemias. Cancer Cell *4*, 451-461.

Sicinski, P., Donaher, J. L., Geng, Y., Parker, S. B., Gardner, H., Park, M. Y., Robker, R. L., Richards, J. S., McGinnis, L. K., Biggers, J. D.*, et al.* (1996). Cyclin D2 is an FSH-responsive gene involved in gonadal cell proliferation and oncogenesis. Nature *384*, 470-474.

Sicinski, P., Donaher, J. L., Parker, S. B., Li, T., Fazeli, A., Gardner, H., Haslam, S. Z., Bronson, R. T., Elledge, S. J., and Weinberg, R. A. (1995). Cyclin D1 provides a link between development and oncogenesis in the retina and breast. Cell *82*, 621-630.

Silvera, D., Formenti, S. C., and Schneider, R. J. (2010). Translational control in cancer. Nat Rev Cancer *10*, 254-266.

Simon, R., Struckmann, K., Schraml, P., Wagner, U., Forster, T., Moch, H., Fijan, A., Bruderer, J., Wilber, K., Mihatsch, M. J., *et al.* (2002). Amplification pattern of 12q13-q15 genes (MDM2, CDK4, GLI) in urinary bladder cancer. Oncogene *21*, 2476-2483.

Skipper, H. E., Schabel, F. M., Jr., and Wilcox, W. S. (1964). Experimental Evaluation of Potential Anticancer Agents. Xiii. On the Criteria and Kinetics Associated with "Curability" of Experimental Leukemia. Cancer Chemother Rep *35*, 1-111.

Slamon, D. J., Godolphin, W., Jones, L. A., Holt, J. A., Wong, S. G., Keith, D. E., Levin, W. J., Stuart, S. G., Udove, J., Ullrich, A., and et al. (1989). Studies of the HER-2/neu proto-oncogene in human breast and ovarian cancer. Science *244*, 707-712.

Snyder, H., Mensah, K., Theisler, C., Lee, J., Matouschek, A., and Wolozin, B. (2003). Aggregated and monomeric alpha-synuclein bind to the S6' proteasomal protein and inhibit proteasomal function. J Biol Chem *278*, 11753-11759.

Solomon, D. A., Wang, Y., Fox, S. R., Lambeck, T. C., Giesting, S., Lan, Z., Senderowicz, A. M., Conti, C. J., and Knudsen, E. S. (2003). Cyclin D1 splice variants. Differential effects on localization, RB phosphorylation, and cellular transformation. J Biol Chem *278*, 30339-30347.

Solomon, M. J., Lee, T., and Kirschner, M. W. (1992). Role of phosphorylation in p34cdc2 activation: identification of an activating kinase. Mol Biol Cell *3*, 13-27.

Solvason, N., Wu, W. W., Parry, D., Mahony, D., Lam, E. W., Glassford, J., Klaus, G. G., Sicinski, P., Weinberg, R., Liu, Y. J., *et al.* (2000). Cyclin D2 is essential for BCR-mediated proliferation and CD5 B cell development. Int Immunol *12*, 631-638.

Soonpaa, M. H., Koh, G. Y., Klug, M. G., and Field, L. J. (1994). Formation of nascent intercalated disks between grafted fetal cardiomyocytes and host myocardium. Science *264*, 98-101.

Soucek, L., and Evan, G. I. (2010). The ups and downs of Myc biology. Curr Opin Genet Dev *20*, 91-95.

Stevenson, A. L., and McCarthy, J. E. (2008). Found in translation: another RNA helicase function. Mol Cell *32*, 755-756.

Stewart, M. P., Helenius, J., Toyoda, Y., Ramanathan, S. P., Muller, D. J., and Hyman, A. A. (2009). Hydrostatic pressure and the actomyosin cortex drive mitotic cell rounding. Nature *469*, 226-230.

Stewart, M. P., Helenius, J., Toyoda, Y., Ramanathan, S. P., Muller, D. J., and Hyman, A. A. (2011). Hydrostatic pressure and the actomyosin cortex drive mitotic cell rounding. Nature *469*, 226-230.

Stoilov, P., Lin, C. H., Damoiseaux, R., Nikolic, J., and Black, D. L. (2008). A high-throughput screening strategy identifies cardiotonic steroids as alternative splicing modulators. Proc Natl Acad Sci U S A *105*, 11218-11223.

Stoker, M. G., and Rubin, H. (1967). Density dependent inhibition of cell growth in culture. Nature *215*, 171-172.

Strnad, P., Zatloukal, K., Stumptner, C., Kulaksiz, H., and Denk, H. (2008). Mallory-Denk-bodies: lessons from keratin-containing hepatic inclusion bodies. Biochim Biophys Acta *1782*, 764-774.

Sukumar, S., Notario, V., Martin-Zanca, D., and Barbacid, M. (1983). Induction of mammary carcinomas in rats by nitroso-methylurea involves malignant activation of H-ras-1 locus by single point mutations. Nature *306*, 658-661.

Sumrejkanchanakij, P., Tamamori-Adachi, M., Matsunaga, Y., Eto, K., and Ikeda, M. A. (2003). Role of cyclin D1 cytoplasmic sequestration in the survival of postmitotic neurons. Oncogene *22*, 8723-8730.

Sun, Q., Zhang, F., Wafa, K., Baptist, T., and Pasumarthi, K. B. (2009). A splice variant of cyclin D2 regulates cardiomyocyte cell cycle through a novel protein aggregation pathway. J Cell Sci *122*, 1563-1573.

Sung, B., Prasad, S., Yadav, V. R., Lavasanifar, A., and Aggarwal, B. B. (2011). Cancer and diet: How are they related? Free Radic Res *45*, 864-879.

Susaki, E., Nakayama, K., and Nakayama, K. I. (2007). Cyclin D2 translocates p27 out of the nucleus and promotes its degradation at the G0-G1 transition. Mol Cell Biol *27*, 4626-4640.

Suzuki, A., Tsutomi, Y., Akahane, K., Araki, T., and Miura, M. (1998). Resistance to Fas-mediated apoptosis: activation of caspase 3 is regulated by cell cycle regulator p21WAF1 and IAP gene family ILP. Oncogene *17*, 931-939.

Tabin, C. J., Bradley, S. M., Bargmann, C. I., Weinberg, R. A., Papageorge, A. G., Scolnick, E. M., Dhar, R., Lowy, D. R., and Chang, E. H. (1982). Mechanism of activation of a human oncogene. Nature *300*, 143-149.

Tabin, C. J., and Weinberg, R. A. (1985). Analysis of viral and somatic activations of the cHa-ras gene. J Virol *53*, 260-265.

Takai, Y., Miyoshi, J., Ikeda, W., and Ogita, H. (2008). Nectins and nectin-like molecules: roles in contact inhibition of cell movement and proliferation. Nat Rev Mol Cell Biol *9*, 603-615.

Takaki, T., Echalier, A., Brown, N. R., Hunt, T., Endicott, J. A., and Noble, M. E. (2009). The structure of CDK4/cyclin D3 has implications for models of CDK activation. Proc Natl Acad Sci U S A *106*, 4171-4176.

Takano, Y., Kato, Y., Masuda, M., Ohshima, Y., and Okayasu, I. (1999). Cyclin D2, but not cyclin D1, overexpression closely correlates with gastric cancer progression and prognosis. J Pathol *189*, 194-200.

Talmadge, J. E. (1998). Pharmacodynamic aspects of peptide administration biological response modifiers. Adv Drug Deliv Rev *33*, 241-252.

Tamanoi, F., Walsh, M., Kataoka, T., and Wigler, M. (1984). A product of yeast RAS2 gene is a guanine nucleotide binding protein. Proc Natl Acad Sci U S A *81*, 6924-6928.

Taparowsky, E., Shimizu, K., Goldfarb, M., and Wigler, M. (1983). Structure and activation of the human N-ras gene. Cell *34*, 581-586.

Tee, A. R., and Blenis, J. (2005). mTOR, translational control and human disease. Semin Cell Dev Biol *16*, 29-37.

Temeles, G. L., Gibbs, J. B., D'Alonzo, J. S., Sigal, I. S., and Scolnick, E. M. (1985). Yeast and mammalian ras proteins have conserved biochemical properties. Nature *313*, 700-703.

Tessema, M., Lehmann, U., and Kreipe, H. (2004). Cell cycle and no end. Virchows Arch *444*, 313-323.

Thomas, G. R., Nadiminti, H., and Regalado, J. (2005). Molecular predictors of clinical outcome in patients with head and neck squamous cell carcinoma. Int J Exp Pathol *86*, 347-363.

Toncheva, D., Petrova, D., Tzenova, V., Dimova, I., Yankova, R., Yordanov, V., Damjanov, D., Todorov, T., and Zaharieva, B. (2004). Tissue microarray analysis of cyclin D1 gene amplification and gain in colorectal carcinomas. Tumour Biol *25*, 157-160.

Toyoshima, H., and Hunter, T. (1994). p27, a novel inhibitor of G1 cyclin-Cdk protein kinase activity, is related to p21. Cell *78*, 67-74.

Tsang, R. Y., and Finn, R. S. (2012). Beyond trastuzumab: novel therapeutic strategies in HER2-positive metastatic breast cancer. Br J Cancer *106*, 6-13.

Tsutsui, T., Hesabi, B., Moons, D. S., Pandolfi, P. P., Hansel, K. S., Koff, A., and Kiyokawa, H. (1999). Targeted disruption of CDK4 delays cell cycle entry with enhanced p27(Kip1) activity. Mol Cell Biol *19*, 7011-7019.

Tunnemann, G., Martin, R. M., Haupt, S., Patsch, C., Edenhofer, F., and Cardoso, M. C. (2006). Cargo-dependent mode of uptake and bioavailability of TAT-containing proteins and peptides in living cells. Faseb J *20*, 1775-1784.

Vadlamudi, R. K., Joung, I., Strominger, J. L., and Shin, J. (1996). p62, a phosphotyrosine-independent ligand of the SH2 domain of p56lck, belongs to a new class of ubiquitin-binding proteins. J Biol Chem *271*, 20235-20237.

van der Vaart, A., Mari, M., and Reggiori, F. (2008). A picky eater: exploring the mechanisms of selective autophagy in human pathologies. Traffic *9*, 281-289.

Vermeulen, K., Van Bockstaele, D. R., and Berneman, Z. N. (2003). The cell cycle: a review of regulation, deregulation and therapeutic targets in cancer. Cell Prolif *36*, 131-149.

Vervoorts, J., and Luscher, B. (2008). Post-translational regulation of the tumor suppressor p27(KIP1). Cell Mol Life Sci *65*, 3255-3264.

Vidal, A., and Koff, A. (2000). Cell-cycle inhibitors: three families united by a common cause. Gene *247*, 1-15.

Vlieghe, P., Lisowski, V., Martinez, J., and Khrestchatisky, M. (2010). Synthetic therapeutic peptides: science and market. Drug Discov Today *15*, 40-56.

von Bergwelt-Baildon, M. S., Kondo, E., Klein-Gonzalez, N., and Wendtner, C. M. (2011). The cyclins: a family of widely expressed tumor antigens? Expert Rev Vaccines *10*, 389-395.

Waga, S., Hannon, G. J., Beach, D., and Stillman, B. (1994). The p21 inhibitor of cyclin-dependent kinases controls DNA replication by interaction with PCNA. Nature *369*, 574-578.

Walczak, C. E., Cai, S., and Khodjakov, A. (2010). Mechanisms of chromosome behaviour during mitosis. Nat Rev Mol Cell Biol *11*, 91-102.

Walker, D. H., and Maller, J. L. (1991). Role for cyclin A in the dependence of mitosis on completion of DNA replication. Nature *354*, 314-317.

Wang, B., Matsuoka, S., Carpenter, P. B., and Elledge, S. J. (2002). 53BP1, a mediator of the DNA damage checkpoint. Science *298*, 1435-1438.

Wang, C., Li, Z., Lu, Y., Du, R., Katiyar, S., Yang, J., Fu, M., Leader, J. E., Quong, A., Novikoff, P. M., and Pestell, R. G. (2006). Cyclin D1 repression of nuclear respiratory factor 1 integrates nuclear DNA synthesis and mitochondrial function. Proc Natl Acad Sci U S A *103*, 11567-11572.

Wang, C., Lisanti, M. P., and Liao, D. J. (2011). Reviewing once more the c-myc and Ras collaboration: converging at the cyclin D1-CDK4 complex and challenging basic concepts of cancer biology. Cell Cycle *10*, 57-67.

Wang, X. W., Zhan, Q., Coursen, J. D., Khan, M. A., Kontny, H. U., Yu, L., Hollander, M. C., O'Connor, P. M., Fornace, A. J., Jr., and Harris, C. C. (1999). GADD45 induction of a G2/M cell cycle checkpoint. Proc Natl Acad Sci U S A *96*, 3706-3711.

Warbrick, E., Lane, D. P., Glover, D. M., and Cox, L. S. (1995). A small peptide inhibitor of DNA replication defines the site of interaction between the cyclin-dependent kinase inhibitor p21WAF1 and proliferating cell nuclear antigen. Curr Biol *5*, 275-282.

Ward, C. L., Omura, S., and Kopito, R. R. (1995). Degradation of CFTR by the ubiquitin-proteasome pathway. Cell *83*, 121-127.

Waters, S., Marchbank, K., Solomon, E., Whitehouse, C., and Gautel, M. (2009). Interactions with LC3 and polyubiquitin chains link nbr1 to autophagic protein turnover. FEBS Lett *583*, 1846-1852.

Watson, D. S., Brotherick, I., Shenton, B. K., Wilson, R. G., Angus, B., Varma, J. S., and Campbell, F. C. (1999). Cyclin D3 expression, cell proliferation and pathological stage of human primary colorectal cancer. Oncology *56*, 66-72.

Wedegaertner, P. B. (2002). Characterization of subcellular localization and stability of a splice variant of G alpha i2. BMC Cell Biol *3*, 12.

Wei, S., and Sedivy, J. M. (1999). Expression of catalytically active telomerase does not prevent premature senescence caused by overexpression of oncogenic Ha-Ras in normal human fibroblasts. Cancer Res *59*, 1539-1543.

Williams, O. (2004). Apoptosis Methods and Protocols, Vol 282 (Totowa, NJ, Humana Press Inc.).

Witt, K. A., and Davis, T. P. (2006). CNS drug delivery: opioid peptides and the blood-brain barrier. Aaps J *8*, E76-88.

Witt, K. A., Gillespie, T. J., Huber, J. D., Egleton, R. D., and Davis, T. P. (2001). Peptide drug modifications to enhance bioavailability and blood-brain barrier permeability. Peptides *22*, 2329-2343.

Won, K. A., Xiong, Y., Beach, D., and Gilman, M. Z. (1992). Growth-regulated expression of D-type cyclin genes in human diploid fibroblasts. Proc Natl Acad Sci U S A *89*, 9910-9914.

Wu, W., Slomovitz, B. M., Soliman, P. T., Schmeler, K. M., Celestino, J., Milam, M. R., and Lu, K. H. (2006). Correlation of cyclin D1 and cyclin D3 overexpression with the loss of PTEN expression in endometrial carcinoma. Int J Gynecol Cancer *16*, 1668-1672.

Wurzenberger, C., and Gerlich, D. W. (2011). Phosphatases: providing safe passage through mitotic exit. Nat Rev Mol Cell Biol *12*, 469-482.

Xie, Z., and Klionsky, D. J. (2007). Autophagosome formation: core machinery and adaptations. Nat Cell Biol *9*, 1102-1109.

Yang, K., Guo, Y., Stacey, W. C., Harwalkar, J., Fretthold, J., Hitomi, M., and Stacey, D. W. (2006a). Glycogen synthase kinase 3 has a limited role in cell cycle regulation of cyclin D1 levels. BMC Cell Biol *7*, 33.

Yang, K., Hitomi, M., and Stacey, D. W. (2006b). Variations in cyclin D1 levels through the cell cycle determine the proliferative fate of a cell. Cell Div *1*, 32.

Zaal, K. J., Smith, C. L., Polishchuk, R. S., Altan, N., Cole, N. B., Ellenberg, J., Hirschberg, K., Presley, J. F., Roberts, T. H., Siggia, E.*, et al.* (1999). Golgi membranes are absorbed into and reemerge from the ER during mitosis. Cell *99*, 589-601.

Zacharek, S. J., Xiong, Y., and Shumway, S. D. (2005). Negative regulation of TSC1-TSC2 by mammalian D-type cyclins. Cancer Res *65*, 11354-11360.

Zerbini, L. F., Wang, Y., Correa, R. G., Cho, J. Y., and Libermann, T. A. (2005). Blockage of NF-kappaB induces serine 15 phosphorylation of mutant p53 by JNK kinase in prostate cancer cells. Cell Cycle *4*, 1247-1253.

Zhan, Q., Antinore, M. J., Wang, X. W., Carrier, F., Smith, M. L., Harris, C. C., and Fornace, A. J., Jr. (1999). Association with Cdc2 and inhibition of Cdc2/Cyclin B1 kinase activity by the p53-regulated protein Gadd45. Oncogene *18*, 2892-2900.

Zhang, F., and Pasumarthi, K. B. (2007). Ultrastructural and immunocharacterization of undifferentiated myocardial cells in the developing mouse heart. J Cell Mol Med *11*, 552-560.

Zhang, H., Qian, D. Z., Tan, Y. S., Lee, K., Gao, P., Ren, Y. R., Rey, S., Hammers, H., Chang, D., Pili, R.*, et al.* (2008a). Digoxin and other cardiac glycosides inhibit HIF-1alpha synthesis and block tumor growth. Proc Natl Acad Sci U S A *105*, 19579-19586.

Zhang, L., Fried, F. B., Guo, H., and Friedman, A. D. (2008b). Cyclin-dependent kinase phosphorylation of RUNX1/AML1 on 3 sites increases transactivation potency and stimulates cell proliferation. Blood *111*, 1193-1200.

Zhang, X., Gureasko, J., Shen, K., Cole, P. A., and Kuriyan, J. (2006). An allosteric mechanism for activation of the kinase domain of epidermal growth factor receptor. Cell *125*, 1137-1149.

Zhang, Y. (2008). I-TASSER server for protein 3D structure prediction. BMC Bioinformatics *9*, 40.

Zhong, Z., Yeow, W. S., Zou, C., Wassell, R., Wang, C., Pestell, R. G., Quong, J. N., and Quong, A. A. (2010). Cyclin D1/cyclin-dependent kinase 4 interacts with filamin A and affects the migration and invasion potential of breast cancer cells. Cancer Res *70*, 2105-2114.

Zorko, M., and Langel, U. (2005). Cell-penetrating peptides: mechanism and kinetics of cargo delivery. Adv Drug Deliv Rev *57*, 529-545.

Zou, Y., Ewton, D. Z., Deng, X., Mercer, S. E., and Friedman, E. (2004). Mirk/dyrk1B kinase destabilizes cyclin D1 by phosphorylation at threonine 288. J Biol Chem *279*, 27790-27798.

Zschemisch, N. H., Liedtke, C., Dierssen, U., Nevzorova, Y. A., Wustefeld, T., Borlak, J., Manns, M. P., and Trautwein, C. (2006). Expression of a cyclin E1 isoform in mice is correlated with the quiescent cell cycle status of hepatocytes in vivo. Hepatology *44*, 164-173.

Zwicker, J., Brusselbach, S., Jooss, K. U., Sewing, A., Behn, M., Lucibello, F. C., and Muller, R. (1999). Functional domains in cyclin D1: pRb-kinase activity is not essential for transformation. Oncogene *18*, 19-25.

Zwijsen, R. M., Buckle, R. S., Hijmans, E. M., Loomans, C. J., and Bernards, R. (1998). Ligand-independent recruitment of steroid receptor coactivators to estrogen receptor by cyclin D1. Genes Dev *12*, 3488-3498.

Appendix I: Copyright Permission

Authors' rights[2]

As of 2009, copyright in all articles in NRC Research Press journals remains with the authors. All articles published previously are copyright Canadian Science Publishing (which operates as NRC Research Press) or its licensors (also see our Copyright information).

Under the terms of the license granted to NRC Research Press, authors retain the following rights:

1. To post a copy of their submitted manuscript (pre-print) on their own Web site, an institutional repository, or their funding body's designated archive.
2. To post a copy of their accepted manuscript (post-print) on their own Web site, an institutional repository, or their funding body's designated archive. Authors who archive or self-archive accepted articles must provide a hyperlink from the manuscript to the Journal's Web site.
3. They and any academic institution where they work at the time may reproduce their manuscript for the purpose of course teaching.
4. To reuse all or part of their manuscript in other works created by them for noncommercial purposes, provided the original publication in an NRC Research Press journal is acknowledged through a note or citation.

These authors' rights ensure that NRC Research Press journals are compliant with open access policies of top international granting bodies, including the Canadian Institutes of Health Research, US National Institutes of Health, the Wellcome Trust, the UK Medical Research Council, the Institut national de la santé et de la recherche médicale in France, and others.

The above rights do not extend to copying or reproduction of the full article for commercial purposes. Authorization to do so may be obtained by clicking on the "Reprints and Permissions" link in the Article Tools Box of the article in question or under license by Access©. The Article Tool Box is accessible through the full-text article or abstract page.

In support of authors who wish or need to sponsor open access to their published research articles, NRC Research Press also offers an OpenArticle option.

[2] As appears on the NRC Research Press website
http://www.nrcresearchpress.com/page/authors/information/rights